Vibrational Behaviour of Plane Frame Structures composed of Prismatic and Tapered Sections

Paul Kin Sang LAM

A thesis submitted for the degree of Doctor of Philosophy

Department of Civil Engineering
The University of Aston in Birmingham

September, 1979

Vibrational Behaviour of
Plane Frame Structures
composed of
Prismatic and Tapered Sections

Paul Kin Sang LAM

A thesis submitted for the degree of
Doctor of Philosophy

September, 1979

Summary

The dynamic analysis of prismatic structures is further developed to include structures with members of different forms of taper. The mass, static stiffness and dynamic stiffness matrices are formulated for two assumed displacement functions — polynomial and quasi-exact, the latter giving an exact solution for prismatic structures. Both functions give an exact solution with finer subdivisions of the elements. The methods of subdivision are compared for their effectiveness. The formulation of the property matrices, for both functions in both prismatic and tapered sections,are fully documentated and are proved to be valid in the analyses.

The solution methods described give natural frequencies, the modal shapes and the analysis of dynamic response. The matrix iteration methods are developed to solve the linear eigensystems which are derived from the polynomial expressions. Nonlinear eigensystems,developed from the quasi-exact function, are studied by means of the count algorithm. This algorithm identifies a root with the concept of the Sturm sequence and the isolation of the singularity. It also serves as a powerful tool in dealing with abnormalities.

The behaviour of plane frame structures, both of prismatic and tapered section, is studied with a wide variety of examples. Certain special features are noted : the convergence tests ; the extensional mode in flexural vibration ; the discontinuities in sectional properties ; the optimisation of structures and the half-structuring analysis at the plane of symmetry. The analytical results obtained are supported by experimental evidence.

DYNAMIC, FRAME, PRISMATIC, TAPERED, FINITE-ELEMENT

Acknowledgements

The author wishes to express his thanks to Professor M. Holmes, B.Sc., Ph.D., D.Sc., C.Eng., FICE , FIStructE , FIMunE , and to Mr. D.J. Just, B.Sc., Ph.D., C.Eng., MICE, under whose supervision this project was carried out, for their continual advice, encouragement and guidance.

The author also wishes to thank Professor E. Downham of the Department of Mechanical Engineering of the University and his technical staff for the valuable help given in the experimental work.

Finally, the author is indebted to his wife, Helen , for her continual support and for typing the manuscript.

To My Mother

TABLE OF CONTENT

Chapter 8 Dynamic Response

Chapter 9 Techniques & Computer Aids

Chapter 10 Discussion & Conclusion

NOMENCLATURE

Roman alphabet

a	Haunch length
a_i	Arbitrary constants, i=1,2,3,....
a_r	Scalar multiplier
A	Cross-sectional area
AP	Asymptotic pole
b	Breadth of a rectangular section
b_r	Unknown coefficient
c	Damping coefficient
C_c	Critical damping coefficient
CA	Count algorithm
d	Depth of a rectangular section
D-f	Determinant-frequency curve
DFP	Dimensionless frequency parameter
E	Young's modulus
EI	Flexural rigidity
EA	Extensional rigidity
f	Frequency in HZ(cycles per second)
$f(x)$	Function in the Sturm sequence
H	Height of a frame
I	Second moment of area
L	(i) length of an element (ii) span length of a frame (iii) span length between supports of beam structures
m	Depth ratio
m'	Optimised depth ratio
$m(x)$	Linearly varying section function of depth $(1+\frac{m-1}{L}x)$

M Bending moment

n (i) number of degrees of freedom
(ii) breadth ratio

$n(x)$ Linearly varying section function of breadth $(1+\frac{n-1}{L}x)$

p Transformation ratio of the depth of the equivalent uniform section (E.U.S.)

P Axial force

q Transformation ratio of the breadth of the E.U.S.

$q(x)$ Quotient in the Sturm sequence

r_f Frame aspect ratio

r_g Radius of gyration

r_s Slenderness ratio

R_ξ Rayleigh quotient

$s\langle J\rangle$ Sign count in the count algorithm

S_e A count in the extensional asymptotic pole algorithm

S_f A count in the flexural asymptotic pole algorithm

S (i) Total count in the count algorithm
(ii) Shear force

t time

u Axial displacement

U Axial displacement amplitude, $U=u\sin(\omega t+\phi')$

v Response amplitude coefficient

w Transverse displacement

W Transverse displacement amplitude, $W=w\sin(\omega t+\phi')$

x (i) distance measured along the abscissa
(ii) Abscissa in the local coordinate system

X Abscissa in the global coordinate system

y (i) distance measured along the ordinate
(ii) Ordinate in the local coordinate system

Y Ordinate in the global coordinate system

Greek alphabet

α	Flexural dimensionless frequency parameter (λL)
β	Extensional dimensionless frequency parameter (λL)
γ	Extensional frequency parameter, $\gamma^2 = \frac{\rho}{E}\omega^2$
δ_{ij}	Kronecker delta
δx	Elemental length
ζ	Damping ratio
θ	Slope displacement
θ'	Angle of rotation in unitary transformation
λ	Flexural frequency parameter, $\lambda^4 = \frac{\rho A}{EI}\omega^2$
μ	Eigenvalue for a standard eigensystem
ξ	Shape function
π	Constant, (=3.14159....)
ρ	Density in Kg/m^3
ϕ	An angle through which an element rotates from local to global system
φ	A variable in the Bessel function transformation (eq.5.47)
ψ	A variable in the Bessel function transformation (eq.5.48)
ω	Angular frequency in radians per second
Ω	Forcing frequency

Matrices

[A]	Portion of total matrix for deriving static stiffness matrix
[C]	Constraint matrix
[D]	Rigidity matrix
[G]	Non-singular matrix with zero-elements above the diagonal
[I]	Unit matrix
[J]	Dynamic stiffness matrix
$[\bar{J}]$	Square matrix for standard eigensystem ($[K]^{-1}[M]$)
[K]	Static stiffness matrix

$[M]$ Mass matrix

$[N]$ Portion of total matrix for deriving mass matrix

$[O]$ Null matrix

$[P]$ Orthogonal matrix

$[T]$ Displacement transformation matrix

$[X]$ Total matrix for deriving dynamic stiffness matrix (e.g. $EI[A]^T[A]-\rho A\omega^2[N]^T[N]$)

Vectors

$\{a\}$ Constants vector

$\{d\}$ Response amplitude vector

$\{f\}$ Distributed force vector

$\{F\}$ (i) External force vector
(ii) Driving force amplitude vector

$\{P(t)\}$ Applied load vector

$\{W\}$ Axial deformation vector

$\{x\}$ (i) Arbitrary vector for iteration
(ii) Response vector

$\{y\}$ Arbitrary vector for iteration

$\{\delta\}$ Displacement vector

$\{\varepsilon\}$ Strain vector

$\{\sigma\}$ Stress vector

Suffices

e Extensional vibration

f Flexural vibration

g Global system

k Static stiffness matrix

l lower bound

m mass matrix

o Equivalent uniform section

u upper bound

Chapter 1

Introduction

CHAPTER 1

INTRODUCTION

§1.1 Historical Review

During recent years, the dynamic analysis of structures has become increasingly important in civil engineering structural mechanics. The increase in emphasis on dynamic behaviour can be attributed largely to two aspects — an increasing demand and an expanding capability. There is now a demand for engineers to become familiar with dynamic analysis procedures, and to apply them to the study of structural systems which are of extreme complexity and/or non-uniformity, and an expanding capability that has made possible the dynamic analysis of large structures has been provided by modern large scale digital computers operating on finite element formulations of problems.

As is often the case with original development, it is rather difficult to quote an exact date on which the finite element method was formulated. Important original contributions have been presented by Turner et.al[1]., Argyris & Kelsey[2], and Clough[3] by whom the term "finite element" was first introduced. Initially developed on a physical basis for the analysis of problems in structural mechanics, it is now recognised that the finite element method may be applied to many other fields in physics and engineering.

The problems on the vibration of solid bodies were first investigated by Euler and Bernoulli in the 18th Century when the differential equation of elastic vibration of the beam was developed. Theorems on mechanical vibration were established during the time of Rayleigh (1842-1919), and since then, the theory has been extended to the analysis of plates and shells.[4,5,6] Preliminary work on beams of variable section, carried out by Cranch and Adler[7], was applied to beams with certain particular boundary conditions. The natural frequencies of beams with a wider range of boundary conditions has been presented by Gorman.[8]

The finite element technique applied to vibration problems is now becoming well-known, and the study of the vibrational behaviour of large plane frame structures is assuming a greater demand. Further, although non-prismatic sections are becoming more common, either for economic or aesthetic reasons, relatively little work appears to have been carried out into the vibrational behaviour of structures composed of such elements.

It is with the vibrational study of plane frameworks, composed of both prismatic and variable sections, that this thesis is concerned. Before this study is presented, however, a brief review of the theory of vibrations and of the method of finite elements, as applied to vibration problems, is presented.

§1.2 Fundamental Theory of Vibration

The two kinds of vibration that a structure can undergo are free vibration and forced vibration.[9-17] In free vibration a structure undergoes oscillatory motion while free of any external forces, whereas in forced vibration the structure responds to a system of time-varying external forces. An understanding of the free vibrations of any structure is virtually a prerequisite to the understanding of its response in forced vibration. Furthermore, it is found that in the majority of design problems, once a solution for free vibration is obtained, the need for solving the more complicated problem of forced vibration response is obviated.

§1.2.1 Governing differential equations for free vibration

(a) Flexural vibration

The differential equation governing the free vibration of beams is discussed in most texts on vibration.[9-17] Consider a small beam element of length δx, as shown in fig.1.2.1b, where bending moments and shear forces act on the ends of the element. Considering the beam displacements and associated slopes to be sufficiently small, and equating the net transverse force acting on the element to the product of its mass and acceleration the equation in its general form becomes

$$\frac{\partial^2}{\partial x^2}\left(EI\frac{\partial^2 w}{\partial x^2}\right) + \rho A\frac{\partial^2 w}{\partial t^2} = 0 \qquad 1.2.1$$

This equation applies to both prismatic and non-prismatic elements. For prismatic elements the equation simplifies to

$$EI\frac{d^4W}{dx^4} - \rho A\omega^2 W = 0 \qquad 1.2.2$$

where $w = W\sin(\omega t + \phi')$, i.e. oscillatory motion, W being a function of x only, and ω & ϕ' being the angular frequency and phase angle respectively.

(b) Extensional vibration

The forces in the axial direction acting on a small beam element of length δx are indicated in fig.1.2.2c. The differential equation for extensional vibration is thus

$$\frac{\partial}{\partial x}\left(EA\,\frac{\partial u}{\partial x}\right) = A\frac{\partial^2 u}{\partial t^2} \qquad 1.2.3$$

For prismatic elements this reduces to

$$\frac{d^2U}{dx^2} + \frac{\rho}{E}\omega^2 U = 0 \qquad 1.2.4$$

where $u = U\sin(\omega t + \phi')$, i.e. oscillatory motion, U being a function of x only.

The method of setting up the equations for forced vibration follows a similar procedure.

§1.2.2 Limitation

In considering the equilibrium of forces for the governing differential equations of free vibration, the effects of shear strain and rotary inertia have been neglected. In special cases in which these assumptions are not permitted, further consultation should be made to the literature[15] on this subject.

§1.3 Finite Element Method

This method, originating with the slope-deflection equations, is a development of the matrix displacement method, and has been described in many texts.[19-24] However for completeness and for cross-reference purposes, the method as applied to free vibration problems is outlined with equations and formulae forming a sequence of operations. The formulations of element matrices in the following chapters will follow this procedure.

§1.3.1 The displacement function

Due to the fact that elements are only connected at nodes, the number of degrees of freedom assumed in each element is dependent on the number of nodes it possesses. For this reason, the distribution of the displacements throughout the element must, in general, also be assumed, the number of terms being determined by the number of degrees of freedom. The assumption should describe the deflected shape of an element as closely as possible, and a commonly employed function is one that is polynomial in nature. The polynomial displacement function for an one-dimensional element is of the form

$$W = \sum a_i x^{i-1} \qquad 1.3.1$$

where a_i are arbitrary constant coefficients & $i = 1,2,3,\ldots\ldots n$, the number of degrees of freedom. The directions of W & x are indicated in fig.1.2.1a .

The nodal displacements $\{\delta\}$ may then be obtained in terms of the arbitrary constants $\{a\}$ by

$$\{\delta\} = [C]\{a\} \qquad 1.3.2$$

and the inverse manipulation yields

$$\{a\} = [C]^{-1}\{\delta\} \qquad 1.3.3$$

As can be inferred from eqs.1.2.1 to 1.2.4, element matrices for vibration problems will be composed of two portions

(a) the static stiffness matrix,

(b) the mass matrix,

which is dependent on the density of the material of the element.

§1.3.2 Formulation of static stiffness matrix

This matrix, relating the nodal forces to the corresponding displacements, is constructed from the following steps:-

(a) Strain-displacement relationship

The strain-displacement relationship is given in matrix form as

$$\{\varepsilon\} = [A]\{a\} \qquad 1.3.4$$

and the substitution of equation 1.3.3 gives

$$\{\varepsilon\} = [A][C]^{-1}\{\delta\} \qquad 1.3.5$$

(b) Stress-strain relationship

This relationship between stress and strain given by Hooke's Law is expressed in matrix form as

$$\{\sigma\} = [D]\{\varepsilon\} \qquad 1.3.6$$

and the substitution of equation 1.3.5 gives

$$\{\sigma\} = [D][A][C]^{-1}\{\delta\} \qquad 1.3.7$$

where $[D]$ is EI in a beam element and EA in a bar element.

(c) Static stiffness matrix

The element matrices are obtained from the application of either virtual work or unit displacement methods. Without repeating the procedures of derivation which are discussed in many textbooks,[19-24] the static stiffness matrix is given as transversely,

$$[K] = EI\,[C^{-1}]^{T} \cdot \int_0^L [A]^{T}[A]\,dx \cdot [C]^{-1} \qquad 1.3.8$$

longitudinally,

$$[K] = EA\,[C^{-1}]^{T} \cdot \int_0^L [A]^{T}[A]\,dx \cdot [C]^{-1} \qquad 1.3.9$$

where here the matrices $[A]$ are respectively the transverse and longitudinal portions of the total matrix given in eq.1.3.4 .

§1.3.3 Formulation of mass matrix

This matrix relates the nodal forces to the nodal accelerations and may be constructed as follows,

(a) Displacement and constant vectors

The assumed displacement function is rewritten in the following matrix form,

$$\{W\} = [N]\{a\} \qquad 1.3.10$$

and the substitution of equation 1.3.3 gives

$$\{W\} = [N][C]^{-1}\{\delta\} \qquad 1.3.11$$

(b) Force and acceleration

As the body force is associated with the volume of the element, the distributed force per unit length is expressed as,

$$[f] = \rho A\{\ddot{W}\} \qquad 1.3.12$$

and the substitution of equation 1.3.11 gives

$$[f] = \rho A[N][C]^{-1}\{\ddot{\delta}\} \qquad 1.3.13$$

(c) Mass matrix

With the consideration of the total virtual work done by the distributed forces, it is possible to express the nodal acceleration in terms of the equivalent external nodal forces as

$$[F] = [M]\{\ddot{\delta}\} \qquad 1.3.14$$

where $[M] = \rho A \cdot [C^{-1}]^T \cdot \int_0^L [N]^T[N]dx \cdot [C]^{-1}$ 1.3.15

this being the mass matrix.

§1.3.4 Dynamic stiffness matrix

The combination of the static stiffness matrix and the mass matrix results in the dynamic stiffness matrix[25-31], [J], the form of which is

$$[J] = [K] - \omega^2[M] \qquad 1.3.16$$

Combining the expressions for [K] and [M] yields the matrix [J] in the form

Transversely,

$$[J] = [C^{-1}]^T \cdot \int_0^L (EI[A]^T[A] - \omega^2 \rho A[N]^T[N])\,dx \cdot [C]^{-1} \qquad 1.3.17$$

Longitudinally,

$$[J] = [C^{-1}]^T \cdot \int_0^L (EA[A]^T[A] - \omega^2 \rho A[N]^T[N])\,dx \cdot [C]^{-1} \qquad 1.3.18$$

§1.4 Scope of Work

Although non-prismatic members can be approximated by a number of stepped prismatic elements, such an approximation does not always give a satisfactory result, and hence the motivation to obtain stiffness matrices for non-prismatic elements is obvious in static as well as in dynamic analysis.

An understanding of prismatic members is a prerequisite to the understanding of non-prismatic members, and therefore a general study on the vibration of prismatic structures is first presented. Apart from the formulation of element matrices for prismatic members, a survey of methods of solution of eigen-problems is given. A wide range of examples then describes the many important features, and comparisons and convergence tests to exact solutions are given.

In the investigation into the behaviour of non-prismatic structures two forms of displacement function are used. Due to the complexity of functions for non-prismatic members, certain difficulties were encountered in the solution routines, and the interpretation of the difficulties arising, especially the asymptotic poles which are roots of a clamped-clamped member, are described. The investigation of the vibrational behaviour of non-prismatic structures is systematically built up by analysing several comprehensive examples. Supporting experi-mental work is described with details of instrumentation.

The knowledge of free vibrational behaviour is extended to the dynamic response of structures. For exciting forces of sinusoidal form, two methods are introduced — frequency response and mode superposition methods which are illustrated with examples. For exciting forces of non-harmonic motion, a step-by-step integration method is outlined. Structures with both prismatic and non-prismatic sections are considered.

Apart from the documentation of several main programs which are used throughout the thesis, the development of other useful routines which have been compiled into a set of library subroutines is also described, and some of the techniques used for the efficient programming of solution routines are presented.

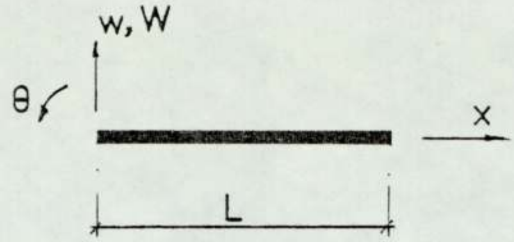

Fig.1.2.1a Sign convention

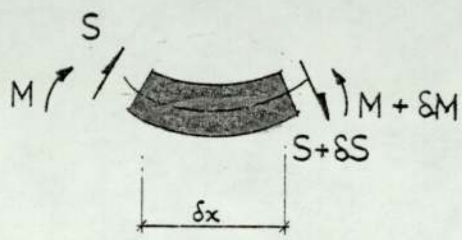

Fig.1.2.1b Beam element

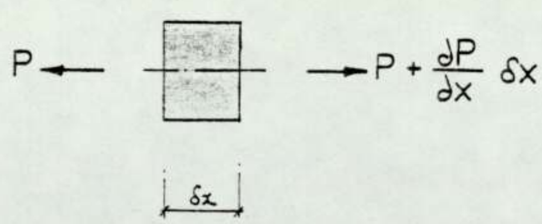

Fig.1.2.1c Bar element

Chapter 2

Formulation of matrices

CHAPTER 2

FORMULATION OF MATRICES

§2.1 Discretisation & Equilibrium

§2.1.1 Equation of motion

The finite element method provides a means for discretisation of the continuum problem by expressing its displacements as a finite series of displacement functions. The amplitude serves as the generalised co-ordinates of the system. The time-varying displacements of a linear system which is represented by w(x,t) may be expressed as follows:

$$w(x,t) = \sum_{n=1}^{n} \xi n(x) Wn(t) \qquad 2.1.1$$

where $\xi n(x)$ are independent shape functions which satisfy the boundary conditions and Wn(t) represents the time-varying amplitude of these shapes.

The equation of motion of the discretised continuum expresses the equilibrium of the forces corresponding to the generalised co-ordinates of the system. Thus, if the nodal displacements in eq.2.1.1 are represented by the displacement vector $\{\delta\}$, the equilibrium relationships of the forces corresponding with $\{\delta\}$ may be written as:

$$\{F_S\} + \{F_I\} + \{F_D\} = \{P(t)\} \qquad 2.1.2$$

in which the terms on the left hand side represent the elastic force, inertia force and damping force vectors respectively and the right hand side is the applied dynamic load vector. In matrix notation, this is represented as:

$$[K]\{x\} + [M]\{\ddot{x}\} + [C]\{\dot{x}\} = \{P(t)\} \qquad 2.1.3$$

If the damping matrix $[c]$ is neglected, the general formulation for an undamped system is in the form of

$$[K]\{x\} + [M]\{\ddot{x}\} = \{P(t)\} \qquad 2.1.4$$

For steady state sinusoidal motion, $\{x\}$ is assumed in the form of

$$\{x\} = \mathcal{R}\{\delta e^{i\omega t}\} \qquad 2.1.5$$

where $\{\delta\}$ is a column vector of nodal displacements

ω is the unknown frequency

$i = \sqrt{-1}$

and $\mathcal{R}\{\,\}$ signifies "the real part of".

Substituting for $\{x\}$ into eq.2.1.4, a more generalised form of representing the dynamic equilibrium of an undamped system is

$$[K]\{\delta\} - \omega^2[M]\{\delta\} = \{P(t)\} \qquad 2.1.6$$

§2.1.2 Free vibration & resonance

The free vibration properties of the finite-element idealisation may be evaluated by considering the equation of motion, eq.2.1.6, for the special case in which external loads vanish, i.e.,

$$[K]\{\delta\} - \omega^2[M]\{\delta\} = 0 \qquad 2.1.7$$

This is immediately recognised as a typical eigenvalue problem. Different values of angular frequency, ω, which are generated are referred to as natural frequencies of the system.

A resonant frequency is defined as the frequency for which the response is a maximum. It is reported[17] that the peak values of displacement, velocity and acceleration response of a system occur at slightly different forcing frequencies. The difference, which is a result of damping considerations, is negligible for the degree of damping usually embodied in physical systems. The frequency at which resonance occurs is generally taken as

$$\text{resonant frequency} \quad = \omega\sqrt{(1-\gamma)^2} \qquad 2.1.8$$

where the damping ratio $\gamma = c/c_c$

c = damping coefficient

c_c = critical damping coefficient.

§2.1.3 Displacement functions

As previously mentioned, in most finite element analyses the manner in which the element deforms must be assumed. These assumptions should incorporate the following principles;-

(a) The displacement function must have the same number of arbitrary coefficients as the number of degrees of freedom of the element.

(b) The deflected shape is described as nearly as possible without any preferred direction of displacement.

(c) No internal strain is experienced within an element which undergoes rigid body movement.

(d) A tendency to constant stress and strain conditions occurs as the size of the element is reduced.

(e) The compatibility of displacements along the boundaries with adjacent elements should be satisfied.

The most commonly employed type of displacement function used is polynomial in nature. As this function is frequency-independent, the formulated dynamic stiffness matrix is taken as a linear eigenvalue problem.

For elements formulated using the polynomial displacement function, a further simplification may be made by concentrating equivalent portions of the total mass at the nodal points. The most important advantage of using this lumped mass representation is that the mass matrix is diagonal and the numerical operations are greatly reduced.

However the more accurate representation is to consider the mass to be distributed over the element, and to use the mass matrix given in eq.1.3.15 to produce this effect. The polynomial functions are themselves approximations to the true shape of the deflected curve of the vibration problem, and hence only approximate results will be attained using matrices based on these functions. The true shape of the deflection curve may be obtained for elements where the deflection is a function of one variable only by solving the governing differential equation, and matrices formed using these functions will be exact in as much as results obtained from them will be independent of any element subdivision. These various functions and the matrices so formed are now described

§2.2 Dynamic Stiffness Matrices Formed from a Polynomial Displacement Function

§2.2.1 Static stiffness matrix

It is convenient for the formulation of matrices if the positive directions of the forces and displacements are defined. A set of local axes for an element is shown in fig.2.2.1 where x is the distance measured along the p-axis from node 1 to node 2. The positive directions of displacements u, w & θ corresponding to forces P, S & M respectively are shown.

(a) The displacement function

An assumed displacement function which has been introduced in §1.3 is polynomial in nature. For a beam with four transverse and two axial degrees of freedom, this form of function will be written:-

for transverse displacement,

$$W = a_1 + a_2x + a_3x^2 + a_4x^3 \qquad 2.2.1$$

and for longitudinal displacement,

$$U = a_5 + a_6x \qquad 2.2.2$$

where a_1 to a_6 are arbitrary constants.

The chosen displacement functions, eqs.2.2.1 & 2.2.2, indicate that the transverse and longitudinal displacements are mutually independent of each other. It is noted that the differentiation of eq.2.2.1 gives the slope displacement, thus,

$$\frac{dW}{dx} = a_2 + 2a_3x + 3a_4x^2 \qquad 2.2.3$$

Substituting the end conditions, x = 0 for node 1 and x = L for node 2, into eqs.2.2.1 to 2.2.3 gives

$$\begin{bmatrix} W_1 \\ \theta_1 \\ W_2 \\ \theta_2 \\ u_1 \\ u_2 \end{bmatrix} = \left[\begin{array}{cccc|cc} 1 & 0 & 0 & 0 & & \\ 0 & 1 & 0 & 0 & \multicolumn{2}{c}{[0]} \\ 1 & L & L^2 & L^3 & & \\ 0 & 1 & 2L & 3L^2 & & \\ \hline & & & & 1 & 0 \\ \multicolumn{4}{c|}{[0]} & 1 & L \end{array}\right] \begin{bmatrix} a_1 \\ a_2 \\ a_3 \\ a_4 \\ a_5 \\ a_6 \end{bmatrix} \qquad 2.2.4$$

or more concisely

$$\{\delta\} = [C]\{a\} \qquad 2.2.5$$

The inverse of eq.2.2.5 gives

$$\{a\} = [C]^{-1}\{\delta\} \qquad 2.2.6$$

where

$$[C]^{-1} = \frac{1}{L^3}\left[\begin{array}{cccc|cc} L^3 & 0 & 0 & 0 & & \\ 0 & L^3 & 0 & 0 & \multicolumn{2}{c}{[0]} \\ -3L & -2L^2 & 3L & -L^2 & & \\ 2 & L & -2 & L & & \\ \hline & & & & L^3 & 0 \\ \multicolumn{4}{c|}{[0]} & -1 & L^3 \end{array}\right] \qquad 2.2.7$$

(b) <u>The strain-displacement relationship</u>

Differentiating eqs.2.2.2 & 2.2.3 with respect to x yields

$$\frac{dU}{dx} = a_6 \qquad 2.2.8$$

and $$\frac{d^2W}{dx^2} = 2a_3 + 6a_4x \qquad 2.2.9$$

which represent the axial strain and curvature of the element respectively. Substituting into eq.1.3.4 gives

$$\begin{bmatrix} \varepsilon_e \\ \varepsilon_f \end{bmatrix} = \left[\begin{array}{cccc|cc} 0 & 0 & 0 & 0 & 0 & 1 \\ \hline 0 & 0 & 2 & 6x & 1 & 0 \end{array}\right] \begin{bmatrix} a_1 \\ a_2 \\ a_3 \\ a_4 \\ a_5 \\ a_6 \end{bmatrix} \qquad 2.2.10$$

or more concisely

$$\{\varepsilon\} = [A]\{a\} \qquad 2.2.11$$

(c) <u>The stress-strain relationship</u>

For elastic material which obeys Hooke's law, the forces are related to the strains as follow:-

for axial force,

$$P = EA \cdot \varepsilon_e \qquad 2.2.12$$

and for bending moment,

$$M = EI \cdot \varepsilon_f \qquad 2.2.13$$

Eqs.2.2.12 & 2.2.13 may be rewritten in matrix form as:-

$$\begin{bmatrix} P \\ M \end{bmatrix} = \begin{bmatrix} EA & 0 \\ 0 & EI \end{bmatrix} \begin{bmatrix} \varepsilon_e \\ \varepsilon_f \end{bmatrix} \qquad 2.2.14$$

or more concisely

$$\{\sigma\} = [D]\{\varepsilon\} \qquad 2.2.15$$

Substituting eqs.2.2.10 into 2.2.15 gives

$$\{\sigma\} = [D][A]\{\delta\} \qquad 2.2.16$$

(d) <u>The stiffness terms</u>

If matrices $[C]^{-1}$ of eq.2.2.7 and $[A]$ of eq.2.2.11 are substituted into eqs.1.3.8 & 1.3.9, and the integration and triple matrix multiplication performed, the static stiffness matrix $[K]$ in its general form will be as given in eq.2.2.17.

$$[K]\{\delta\} = \frac{EI}{L^3} \left[\begin{array}{cccc|cc} 12 & 6L & -12 & 6L & & \\ & 4L^2 & -6L & 2L^2 & & [0] \\ & & 12 & -6L & & \\ & & & 4L^2 & & \\ \hline \text{Symmetrical} & & & & \frac{AL^2}{I} & -\frac{AL^2}{I} \\ & & & & & \frac{AL^2}{I} \end{array} \right] \begin{bmatrix} w_1 \\ \theta_1 \\ w_2 \\ \theta_2 \\ u_1 \\ u_2 \end{bmatrix} \qquad 2.2.17$$

It may be pointed out that the polynomial form gives exact functions for a static prismatic beam, the transverse function producing the standard slope deflection equations in matrix form. The functions are obtained by solving

$$EI\frac{d^4W}{dx^4} = 0 \qquad \& \qquad EA\frac{d^2U}{dx^2} = 0 \qquad 2.2.18$$

these being the transverse and longitudinal differential equations for an end-loaded beam.

§2.2.2 Lumped mass matrix

If the distributed mass is lumped into two equal portions at the nodal points of an element, the representation of the lumped mass is as given in eq.2.2.19

$$[M]\{\delta\} = \rho AL \begin{bmatrix} \frac{1}{2} & 0 & 0 & 0 & & \\ & 0 & 0 & 0 & \multicolumn{2}{c}{[0]} \\ & & \frac{1}{2} & 0 & & \\ & & & 0 & & \\ \multicolumn{4}{c}{\text{Symmetrical}} & \frac{1}{2} & 0 \\ & & & & & \frac{1}{2} \end{bmatrix} \begin{bmatrix} w_1 \\ \theta_1 \\ w_2 \\ \theta_2 \\ u_1 \\ u_2 \end{bmatrix} \qquad 2.2.19$$

Substituting eqs.2.2.17 & 2.2.19 into eqs.1.3.17 & 1.3.18 gives the dynamic stiffness matrix [J] shown in equation 2.2.20.

$$[J]\{\delta\} = \frac{EI}{L^3} \begin{bmatrix} 12-\frac{1}{2}\alpha^4 & 6L & -12 & 6L & & \\ & 4L^2 & -6L & 2L^2 & \multicolumn{2}{c}{[0]} \\ & & 12-\frac{1}{2}\alpha^4 & -6L & & \\ & & & 4L^2 & & \\ \multicolumn{4}{c}{\text{Symmetrical}} & \frac{AL^2}{I}-\frac{\alpha^4}{2} & -\frac{AL^2}{I} \\ & & & & & \frac{AL^2}{I}-\frac{\alpha^4}{2} \end{bmatrix} \begin{bmatrix} w_1 \\ \theta_1 \\ w_2 \\ \theta_2 \\ u_1 \\ u_2 \end{bmatrix} \qquad 2.2.20$$

where $\alpha^4 = \frac{\rho A}{EI}\omega^2 L^4$

§2.2.3 Consistent mass matrix

The assumed displacement function (eqs.2.2.1 & 2.2.2) may be expressed in matrix form as

$$\begin{bmatrix} W \\ U \end{bmatrix} = \left[\begin{array}{cccc|cc} 1 & x & x^2 & x^3 & 0 & 0 \\ \hline 0 & 0 & 0 & 0 & 1 & x \end{array}\right] \begin{bmatrix} a_1 \\ a_2 \\ a_3 \\ a_4 \\ a_5 \\ a_6 \end{bmatrix} \qquad 2.2.21$$

It has been mentioned that the transverse and longitudinal displacements are mutually independent of each other, and hence the shape function matrix may be rewritten as:-

for extensional vibration,

$$[N] = [\,0 \quad 0 \quad 0 \quad 0 \quad 1 \quad x\,] \qquad 2.2.22$$

and for flexural vibration,

$$[N] = [\,1 \quad x \quad x^2 \quad x^3 \quad 0 \quad 0\,] \qquad 2.2.23$$

Substituting $[C]^{-1}$ of eq.2.2.7 and $[N]$ of eq.2.2.22 & eq.2.2.23 into eq.1.3.15, and again carrying out the integration and triple matrix multiplication, the mass matrix in its general form becomes as shown in eq.2.2.24.

$$[M]\{\delta\} = \frac{\rho AL}{420} \left[\begin{array}{cccc|cc} 156 & 22L & 54 & -13L & & \\ & 4L^2 & 13L & -3L^2 & & [0] \\ & & 156 & -22L & & \\ & & & 4L^2 & & \\ \hline & & & & 210 & 70 \\ & \text{Symmetrical} & & & & 210 \end{array}\right] \begin{bmatrix} w_1 \\ \theta_1 \\ w_2 \\ \theta_2 \\ u_1 \\ u_2 \end{bmatrix}$$

2.2.24

If now the matrices [K] of eq.2.2.17 and [M] of eq.2.2.24 are substituted into the expression, $[J] = [K] - \omega^2[M]$, the dynamic stiffness matrix is as given in eq.2.2.25.

Eq.2.2.25 on P.25

With regard to the polynomial functions, it may be observed that the maximum number of eigenvalues that can be solved from a [J] matrix is equal to the number of degrees of freedom in the structure, i.e. the order of the matrix. The greater the number of elements in a structure the more accurate become the results and also the greater become the number of eigenvalues that can be obtained. As an example, the maximum number of eigenvalues obtainable in the structures shown in figs.2.2.2a & b are respectively two and five.

Eq.2.2.25 Dynamic stiffness matrix for polynomial function

$$[J]\{\delta\} = \frac{EI}{420L^3}\begin{bmatrix} (420r_s^2-210\alpha^4) & 0 & 0 & (-420r_s^2-70\alpha) & 0 & 0 \\ & (5040-156\alpha^4) & (2520-22\alpha^4)L & 0 & -(5040+54\alpha^4) & (2520+13\alpha^4)L \\ & & (1680-4\alpha^4)L^2 & 0 & -(2520+13\alpha^4)L & (840+3\alpha^4)L^2 \\ & & & (420r-210\alpha) & 0 & 0 \\ & \text{Symmetrical} & & & (5040-156\alpha^4) & -(2520-22\alpha^4)L \\ & & & & & (1680-4\alpha^4)L^2 \end{bmatrix}\begin{bmatrix} u_1 \\ w_1 \\ \theta_1 \\ u_2 \\ w_2 \\ \theta_2 \end{bmatrix}$$

where slenderness ratio, $r_s = \sqrt{(AL^2/I)}$

dimensionless frequency parameter, $\alpha = \lambda L$

$= \sqrt[4]{(\omega^2 \rho A/EI)}\,.L$

§2.3 Dynamic Stiffness Matrix Formed from Solution of Governing Differential Equations

§2.3.1 The exact displacement function

The setting up of the governing differential equations for a beam undergoing free vibration has been given in §1.2 and the equations are rewritten here as:-

(a) for transverse displacement, or flexural vibration,

$$\frac{\partial^2}{\partial x^2}\left(EI\frac{\partial^2 w}{\partial x^2}\right) + \frac{\partial^2}{\partial t^2}(\rho A w) = 0 \qquad 2.3.1$$

(b) for longitudinal displacement, or extensional vibration,

$$\frac{\partial^2}{\partial x^2}(EAu) - \frac{\partial^2}{\partial t^2}(\rho A u) = 0 \qquad 2.3.2$$

Since for a uniform section, the flexural rigidity (EI) and mass per unit length (ρA) are constants, eqs.2.3.1 & 2.3.2 are respectively simplified to

$$EI\frac{\partial^4 w}{\partial x^4} + \rho A\frac{\partial^2 w}{\partial t^2} = 0 \qquad 2.3.3$$

and

$$EA\frac{\partial^2 u}{\partial x^2} - \rho A\frac{\partial^2 u}{\partial t^2} = 0 \qquad 2.3.4$$

Now letting $w = W\sin(\omega t + \phi')$ and $u = U\sin(\omega t + \phi')$, these equations may be expressed as

$$EI\frac{d^4 W}{dx^4} - \omega^2 \rho A W = 0 \qquad 2.3.5$$

and

$$EA\frac{d^2 U}{dx^2} + \omega^2 \rho A U = 0 \qquad 2.3.6$$

The general solution of eq.2.3.5 gives, for flexural vibration,

$$W = a_1 \sin\lambda x + a_2 \cos\lambda x + a_3 \sinh\lambda x + a_4 \cosh\lambda x \qquad 2.3.7$$

where $\lambda^4 = \rho A \omega^2 / EI$

and the general solution of eq.2.3.6 gives, for extensional vibration,

$$U = a_5 \sin\gamma x + a_6 \cos\gamma x \qquad 2.3.8$$

where $\gamma^2 = \rho A \omega^2 / EA$

These two equations are defined as exact displacement functions, and results obtained from them will be independent of element subdivision. The displacement at any point distance x from node 1 (fig.2.2.1) is evaluated in terms of circular and hyperbolic expressions, a_1 to a_6 being arbitrary constants. It may also be noted that the transverse and longitudinal displacements are mutually independent of each other, but the relationship between the two frequency parameters is

$$\gamma = \lambda^2 \sqrt{(I/A)} \qquad 2.3.9$$

§2.3.2 The static stiffness matrix

The equation for the slope at any point in the element is obtained by differentiating eq.2.3.5, thus

$$\frac{dW}{dx} = \lambda\,(a_1\cos\lambda x - a_2\sin\lambda x + a_3\cosh\lambda x + a_4\sinh\lambda x) \qquad 2.3.10$$

Substituting the boundary conditions, x = 0 at node 1 and x = L at node 2, into eqs.2.3.5, 2.3.8 & 2.3.10 gives

$$\begin{bmatrix} w_1 \\ \theta_1 \\ w_2 \\ \theta_2 \\ u_1 \\ u_2 \end{bmatrix} = \left[\begin{array}{cccc|cc} 0 & 1 & 0 & 0 & & \\ \lambda & 0 & \lambda & 0 & \multicolumn{2}{c}{[0]} \\ s & c & sh & ch & & \\ \lambda c & -\lambda s & \lambda ch & \lambda sh & & \\ \hline & \multicolumn{2}{c}{[0]} & & 0 & 1 \\ & & & & \sin\gamma L & \cos\gamma L \end{array}\right] \begin{bmatrix} a_1 \\ a_2 \\ a_3 \\ a_4 \\ a_5 \\ a_6 \end{bmatrix} \qquad 2.3.11$$

where

$$\begin{aligned} s &= \sin\lambda L \\ c &= \cos\lambda L \\ sh &= \sinh\lambda L \\ ch &= \cosh\lambda L \end{aligned}$$

This may be written more concisely as

$$\{\delta\} = [C]\{a\} \qquad 2.3.12$$

To express the arbitrary constants in terms of the nodal displacements, the inverse manipulation of eq.2.3.12 is carried out, thus

$$\{a\} = [C]^{-1}\{\delta\} \qquad 2.3.13$$

$[C]^{-1}$ being written in full as

$$[C]^{-1} = \begin{bmatrix} C_f & 0 \\ 0 & C_e \end{bmatrix} \qquad 2.3.14$$

where

$$[C_f] = \frac{1}{2\lambda(1-cch)}\begin{bmatrix} -\lambda(sch+csh) & (1-ssh-cch) & \lambda(s+sh) & (c-ch) \\ \lambda(1+ssh-cch) & (sch-csh) & \lambda(c-ch) & -(s-sh) \\ \lambda(sch+csh) & (1+ssh-cch) & -\lambda(s+sh) & -(c-ch) \\ \lambda(1-ssh-cch) & -(sch-csh) & -\lambda(c-ch) & (s-sh) \end{bmatrix} \qquad 2.3.15$$

and

$$[C_e] = \frac{1}{\sin\gamma L}\begin{bmatrix} -\cos\gamma L & 1 \\ \sin\gamma L & 0 \end{bmatrix} \qquad 2.3.16$$

To obtain the curvature and axial strain, eqs.2.3.10 & 2.3.8 are differentiated with respect to x, thus

$$\frac{d^2W}{dx^2} = \lambda^2(-a_1\sin\lambda x \ -a_2\cos\lambda x \ +a_3\sinh\lambda x \ +a_4\cosh\lambda x \ ) \qquad 2.3.17$$

$$\frac{dU}{dx} = \gamma(\ a_5\cos\gamma x \ -a_6\sin\gamma x \ ) \qquad 2.3.18$$

Matrix notation for the strain-displacement relationship gives

$$\{\varepsilon\} = [A]\,\{a\} \qquad 2.3.19$$

and the substitution of eqs.2.3.27 & 2.3.18 gives

$$\begin{bmatrix} \varepsilon_f \\ \varepsilon_e \end{bmatrix} = \left[\begin{array}{cccc|cc} -\lambda^2\sin\lambda x & -\lambda^2\cos\lambda x & \lambda^2\sinh\lambda x & \lambda^2\cosh\lambda x & 0 & 0 \\ \hline 0 & 0 & 0 & 0 & \gamma\cos\gamma x & -\gamma\sin\gamma x \end{array}\right]\begin{bmatrix} a_1 \\ a_2 \\ a_3 \\ a_4 \\ a_5 \\ a_6 \end{bmatrix}$$

2.3.20

The stress-strain relationship is the same as that used in §2.2 for polynomial functions. Manipulating this together with $[A]$ and $[C]^{-1}$, the formulation of the static stiffness matrix may then be carried out by the integration and triple multiplication. This is shown in eqs.2.3.21 to 2.3.23.

Eqs.2.3.21 to 2.3.23 on P.30

$$[K] = \left[\begin{array}{c:c} [K_f] & 0 \\ \hdashline 0 & [K_e] \end{array}\right]\left[\begin{array}{c} w_1 \\ \theta_1 \\ w_2 \\ \theta_2 \\ u_1 \\ u_2 \end{array}\right] \qquad \text{Eq.2.3.21}$$

Eq.2.3.22

$$[K_f] = \lambda EI \left[\begin{array}{c|c|c|c} \frac{\lambda^2(c-ch)^2\lambda L}{4(1-cch)^2}+\frac{\lambda^2(sch+csh)}{4(1-cch)} & \frac{\lambda(s-sh)(c-ch)\lambda L}{4(1-cch)^2}+\frac{\lambda ssh}{2(1-cch)} & \frac{\lambda^2(c-ch)ssh\lambda L}{4(1-cch)^2}-\frac{\lambda^2(s+sh)}{4(1-cch)} & -\frac{\lambda(s-sh)ssh\lambda L}{4(1-cch)^2}-\frac{\lambda(c-ch)}{2(1-cch)} \\ \hline & \frac{(s-sh)^2\lambda L}{4(1-cch)^2}+\frac{3(sch-csh)}{4(1-cch)} & \frac{\lambda(s-sh)ssh\lambda L}{4(1-cch)^2}+\frac{\lambda(c-ch)}{2(1-cch)} & \frac{(2(c-ch)+ssh(c+ch))\lambda L}{4(1-cch)^2}-\frac{3(s-sh)}{4(1-cch)} \\ \cline{2-4} & \text{Symmetrical} & \frac{\lambda^2(c-ch)^2\lambda L}{4(1-cch)^2}+\frac{\lambda^2(sch+csh)}{4(1-cch)} & \frac{\lambda(s-sh)(c-ch)\lambda L}{4(1-cch)^2}\ \frac{\lambda ssh}{2(1-cch)} \\ \cline{3-4} & & & \frac{(s-sh)\lambda L}{4(1-cch)^2}+\frac{3(sch-csh)}{4(1-cch)} \end{array}\right]$$

$$[K_e] = \gamma EA \left[\begin{array}{c|c} \frac{\gamma}{2\sin^2\gamma L}+\frac{\cos\gamma L}{2\sin\gamma L} & -\frac{\gamma^2\cos\gamma L}{2\sin^2\gamma L}-\frac{1}{2\sin\gamma L} \\ \hline \text{Symmetrical} & \frac{\gamma}{2\sin^2\gamma L}+\frac{\cos\gamma L}{2\sin\gamma L} \end{array}\right] \qquad \text{Eq.2.3.23}$$

§2.3.3 Mass matrix

The exact displacement functions may be expressed in matrix notation as

$$\{\delta\} = [N]\{a\} \qquad 2.3.24$$

where $\{a\} = [a_1 \ a_2 \ a_3 \ a_4 \ a_5 \ a_6]^T$, and the displacement shape function matrix is

(a) for flexural vibration

$$[N] = [\sin\lambda x \quad \cos\lambda x \quad \sinh\lambda x \quad \cosh\lambda x \quad 0 \quad 0] \qquad 2.3.25$$

(b) for extensional vibration

$$[N] = [\ 0 \quad 0 \quad 0 \quad 0 \quad \sin\gamma x \quad \cos\gamma x] \qquad 2.3.26$$

Substituting for $[N]$ and $[C]^{-1}$ of eq.2.3.14 into eq.1.3.15, the mass matrix may be expressed as shown in eqs.2.3.27 to 2.3.29.

Eq.2.3.27 to 2.3.29 on P.32

It may be observed that, for each element term, $[K]$ and $[M]$ possess similar expressions, and in the combination of $[K]$ and $[M]$ to form the dynamic stiffness matrix $[K] - \omega^2[M]$, these similarities enable the direct formulation of this matrix to be obtained in very simple terms.

$$[M] = \begin{bmatrix} [M_f] & 0 \\ 0 & [M_e] \end{bmatrix} \begin{bmatrix} w_1 \\ \theta_1 \\ w_2 \\ \theta_2 \\ u_1 \\ u_2 \end{bmatrix} \qquad \text{Eq.2.3.27}$$

Eq.2.3.28

$$[M_f] = \lambda EI \begin{bmatrix} \frac{\lambda^2(c-ch)^2\lambda L}{4(1-cch)^2} - \frac{3\lambda^2(sch+csh)}{4(1-cch)} & \frac{\lambda(s-sh)(c-ch)\lambda L}{4(1-cch)^2} - \frac{\lambda ssh}{2(1-cch)} & \frac{\lambda^2(c-ch)ssh\lambda L}{4(1-cch)^2} + \frac{3\lambda^2(s+sh)}{4(1-cch)} & -\frac{\lambda(s-sh)ssh\lambda L}{4(1-cch)^2} + \frac{\lambda(c-ch)}{2(1-cch)} \\ & \frac{(s-sh)^2\lambda L}{4(1-cch)^2} - \frac{sch-csh}{4(1-cch)} & \frac{\lambda(s-sh)ssh\lambda L}{4(1-cch)^2} - \frac{\lambda(c-ch)}{2(1-cch)} & \frac{(2(c-ch)+ssh(c+ch))\lambda L}{4(1-cch)^2} + \frac{s-sh}{4(1-cch)} \\ \text{Symmetrical} & & \frac{(c-ch)^2\lambda L}{4(1-cch)^2} - \frac{3\lambda^2(sch+csh)}{4(1-cch)} & \frac{\lambda(s-sh)(c-ch)\lambda L}{4(1-cch)^2} + \frac{\lambda ssh}{2(1-cch)} \\ & & & \frac{(s-sh)\lambda L}{4(1-cch)^2} - \frac{sch-csh}{4(1-cch)} \end{bmatrix}$$

$$[M_e] = EA \begin{bmatrix} \frac{\gamma}{2\sin^2\gamma L} - \frac{\cos\gamma L}{2\sin\gamma L} & -\frac{\gamma^2\cos\gamma L}{2\sin^2\gamma L} + \frac{1}{2\sin\gamma L} \\ \text{Symmetrical} & \frac{\gamma}{2\sin^2\gamma L} - \frac{\cos\gamma L}{2\sin\gamma L} \end{bmatrix} \qquad \text{Eq.2.3.29}$$

§2.3.4 Dynamic stiffness matrix

The formation of this matrix as $[K] - \omega^2[M]$ gives

Eq.2.3.30 to 2.3.32 on P.35

It can be seen that the elements of the dynamic stiffness matrix are far simpler than those of its constituent components $[K]$ & $[M]$, showing the advantage of employing derived displacement functions. Furthermore, this simplication can be executed at an earlier stage of the formulation. If $[K]$ & $[M]$ of eqs.1.3.8, 1.3.9 & 1.3.15 are substituted into $[J] = [K] - \omega^2[M]$, $[J]$ is given as:-

$$[J] = [C^{-1}]^T \cdot \int_0^L [X]dx \cdot [C]^{-1} \qquad 2.3.33$$

$$\text{where } [X] = D[A]^T[A] - \rho A\omega^2[N]^T[N] \qquad 2.3.34$$

& where $D = EI$ for a beam and
EA for a bar

Substituting $[A]$ of eq.2.3.20 and $[N]$ of eqs.2.3.25 & 2.3.26 into $[X]$ gives

$$[X] = EI\lambda^4 \left[\begin{array}{cccc|cc} 0 & 0 & X_{13} & X_{14} & & \\ & 0 & X_{23} & X_{24} & \multicolumn{2}{c}{[0]} \\ & & 0 & 0 & & \\ & & & 0 & & \\ \hline & \text{Sym.} & & & X_{55} & X_{56} \\ & & & & & X_{66} \end{array}\right] \qquad 2.3.35$$

where
$X_{13} = -2\sin\lambda x \sinh\lambda x$
$X_{14} = -2\sin\lambda x \cosh\lambda x$
$X_{23} = -2\cos\lambda x \sinh\lambda x$
$X_{24} = -2\cos\lambda x \cosh\lambda x$

$X_{55} = \cos 2\gamma x$
$X_{56} = -\sin 2\gamma x$
$X_{66} = -\cos 2\gamma x$

The integration of [X], and afterwards the triple matrix multiplication, will directly produce the dynamic stiffness matrix. The advantage is to by-pass the formulation of the complicated [K] & [M] matrices. Following the modified procedure, one set of integrations and triple matrix multiplications is necessary, and a further simplification occurs with the formation of zero element terms.

$$[J] = \begin{bmatrix} [J_f] & 0 \\ 0 & [J_e] \end{bmatrix} \begin{bmatrix} w_1 \\ \theta_1 \\ w_2 \\ \theta_2 \\ u_1 \\ u_2 \end{bmatrix} \qquad \text{Eq.2.3.30}$$

Eq.2.3.31

$$[J_f] = \frac{\lambda EI}{1-cch} \begin{bmatrix} \lambda^2(sch+csh) & \lambda ssh & -\lambda^2(s+sh) & -\lambda(c-ch) \\ & (sch-csh) & \lambda(c-ch) & -(s-sh) \\ & \text{Symmetrical} & \lambda^2(sch+csh) & -\lambda ssh \\ & & & (sch-csh) \end{bmatrix}$$

where $s=\sin\lambda L$

$c=\cos\lambda L$

$ch=\cosh\lambda L$

$sh=\sinh\lambda L$

$$[J_e] = \frac{\gamma EA}{\sin\gamma L} \begin{bmatrix} \cos\gamma L & -1 \\ -1 & \cos\gamma L \end{bmatrix} \qquad \text{Eq.2.3.32}$$

§2.4 Assembly of the Overall Matrix

§2.4.1 Transformation to global coordinates

Having calculated the values of [J] for the individual elements into which the system is subdivided, the next step is to assemble these to form an overall matrix for the entire discretised system. This is done by ensuring that the equilibrium and compatibility conditions are satisfied at all nodes within the discretised system. The assemblege procedure, particularly its mechanisation by using a computer, is described fully in many textbooks.[19-24] However, for completeness the transformations to global coordinates is outlined. For ease of reference in this section only, the suffix g is used to denote the quantities referring to the global system.

Fig.2.4.1 shows an arbitrarily orientated element inclined at an angle ϕ to the global system. Axes x & y refer to the local coordinate system and X & Y refer to the global system. The transformation for nodal displacements is expressed as

$$\{\delta\} = [T]\,\{\delta_g\} \qquad 2.4.1$$

Writing these equations in full gives

$$\{\delta\} = \left[\begin{array}{ccc|ccc} \cos\phi & \sin\phi & 0 & & & \\ -\sin\phi & \cos\phi & 0 & & [0] & \\ 0 & 0 & 1 & & & \\ \hline & & & \cos\phi & \sin\phi & 0 \\ & [0] & & -\sin\phi & \cos\phi & 0 \\ & & & 0 & 0 & 1 \end{array}\right]\{\delta_g\} \qquad 2.4.2$$

The basic force-displacement relationship, $[J]\{\delta\} = \{P(t)\}$, for an element can be shown[21] to be transformed into

$$\{P_g(t)\} = [J_g]\,\{\delta_g\} \qquad 2.4.3$$

where the transformed dynamic stiffness matrix in global coordinates is given by

$$[J_g] = [T]^T\,[J]\,[T] \qquad 2.4.4$$

For any two rigidly connected elements, fig.2.4.2, the assemblege of the dynamic stiffness matrix is represented in the general form,

$$[J]\{\delta\} = \begin{bmatrix} (J_{aa})_i & (J_{ab})_i & 0 \\ & (J_{bb})_i + (J_{aa})_j & (J_{ab})_j \\ \text{Sym.} & & (J_{bb})_j \end{bmatrix}\begin{bmatrix} \delta_a \\ \delta_b \\ \delta_c \end{bmatrix} . \qquad 2.4.5$$

§2.4.2 The partitioning of the dynamic stiffness matrix

For beam structures, the overall matrix can be partitioned into two separate independent matrices which are associated with flexural and extensional vibrations. This separation is not applicable to frame structures since the vibration always incorporates both flexural and extensional displacements.

Consider two elements, referenced as i & j, and connected in two different ways as shown in fig.2.4.3 & 2.4.4. It can be seen in fig.2.4.3 that the element terms which refer to extensional displacements u_a, u_b & u_c can be extracted to form another dynamic stiffness matrix for extensional vibration. Obviously the dynamic stiffness matrix for flexural vibration is formed from the remaining element terms. This procedure cannot be performed with the orientation shown in fig.2.4.4 because the element terms for extensional displacements are coupled with those of flexural displacements. This may support the argument that axial effects should not be neglected in the analysis of frame structures.

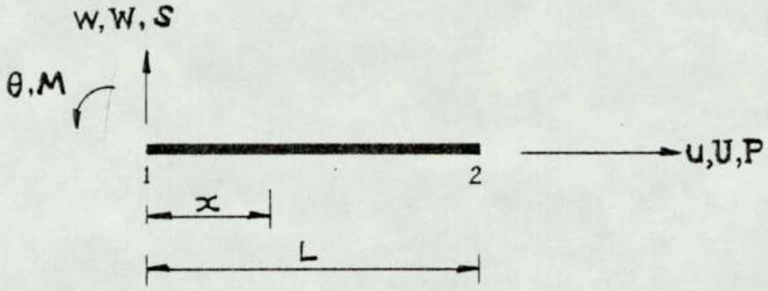

Fig.2.2.1 Sign convention for local axes

Fig.2.2.2 Degrees of freedom

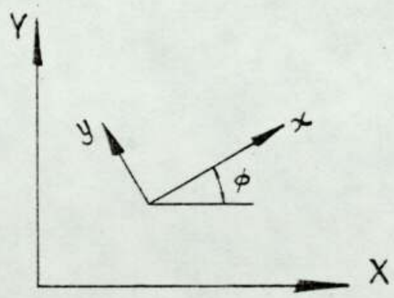

Fig.2.4.1
Coordinate system

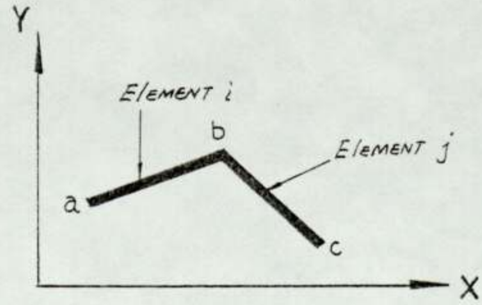

Fig.2.4.2
Assemblege of two elements

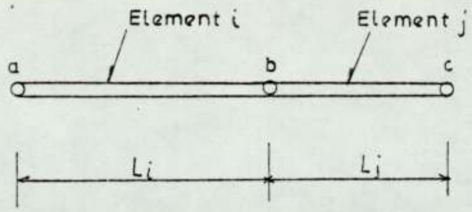

Fig.2.4.3
Overall matrix for
a continuous beam

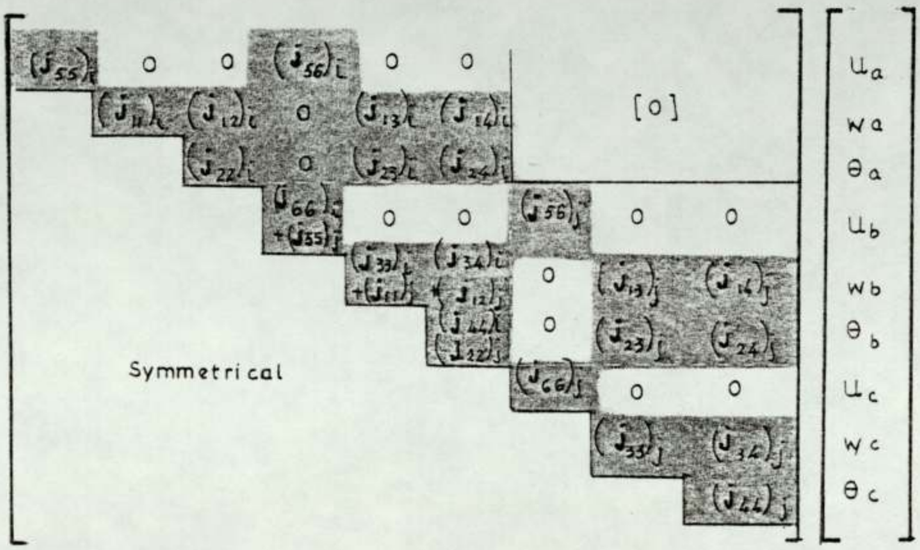

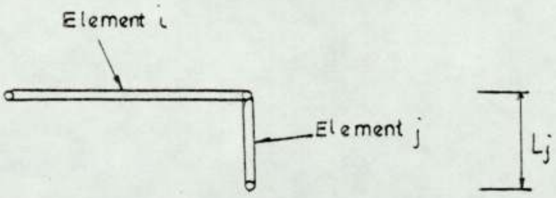

Fig.2.4.4
Overall matrix for
a cranked frame

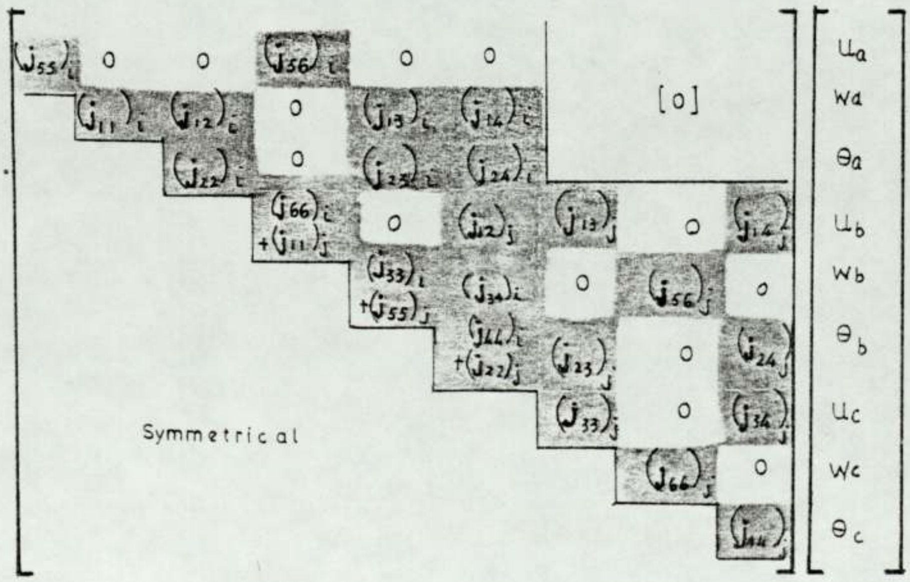

Chapter 3

Methods of solution

CHAPTER 3

METHODS OF SOLUTION

§3.1 Advances and Development

§3.1.1 A survey of solution methods

The study of free vibration is always linked with the solution of eigenvalue problems. The standard notation of the eigensystem is

$$[\bar{J}]\,\{\delta\} = \mu\,\{\delta\} \qquad 3.1.1$$

where $[\bar{J}]$ is a square matrix and μ is the eigenvalue associated with eigenvector $\{\delta\}$.

A large number of solution methods exist for obtaining natural frequencies and mode shapes, these being respectively the eigenvalues and eigenvectors of the eigenproblem, and recent publications on the general description of solution methods are those by Bathe & Wilson[32] and Jennings[33]. The methods may be broadly classified into

(a) those which employ the technique of matrix manipulation as the basis of the solution algorithm, and known as the Matrix Iteration Category and

(b) the Determinant Evaluation Category.

Within the first category, the basic iteration processes are forward and inverse iteration by which eigenvalues (frequencies) and eigenvectors (mode shapes) are obtained. This matrix iteration may be further modified by a matrix transformation into a form which can be more easily analysed. Many transformation techniques have been contributed by Jacobi, Givens, Householder, Wilkinson, Rutishauser, Francis, etc. With a large number of different solution technique available, it is obvious that no single algorithm always provides an efficient solution.

In the second category, it is noticed that the classical characteristic (determinantal) equation method is not suitable for computer implementation. However, with the facilities of the Sturm sequence and the inclusion of an iteration feature in the characteristic equation, the determinant evaluation method is shown to produce an efficient solution.[34] Furthermore, this method is also recommended in the solution of non-linear eigensystems[35,36] and large eigensystems.[37,38]

For reptitive structures,[39] due to the special feature of the repetition, the characteristic equation may be easily factorised into individual mathematical functions. Natural frequencies are then obtained accurately by the Newton-Raphson iterative method for these factorised functions. The derivation of this method is introduced later for continuous beams with exact displacement functions. The advantage of this special development is to achieve a systematic way of understanding the behaviour of natural frequencies.

The linear eigensystem, which is derived from the polynomial displacement function (eq.2.2.25), is frequency independent. On the other hand, the exact function , (eqs.2.3.7 & 2.3.8), is frequency dependent and hence a non-linear eigensystem results (eq.2.3.30). The linearity of the eigensystem is one of the crucial aspects that contributes to the choice of solution methods.

Basic considerations of linear eigensystems have been reported in many textbooks[47-54] of which a full documentation on properties is described by Jennings.[33] The nature of a linear eigensystem has also been discussed with the idea of bifurcation[55] which has been further extended to non-linear systems.[56-58] However, a well-established technique[34-36] for handling non-linear eigensystems which is widely recommended is used in this thesis.

§3.1.2 Choice of solution methods

Because of the large number of different solution techniques, it is not possible to assume one single algorithm which provides efficient solutions in every case. The size of eigensystems, the bandwidth, the number of required eigenvalues and eigenvectors or whether or not the system is linear are usually the factors which contribute to the decision of choosing a solution method. The methods in both categories are reported to be commendable. It is considered that the methods in the Matrix Iteration Category are efficient for linear systems, or even superior if all eigenvalues and eigenvectors are required, whereas the determinant method, with the Sturm sequence property, is an infallible method for non-linear eigensystem without any risk of modes being missed.

§3.2 Matrix Iteration Category

§3.2.1 Properties of element matrices

The equation for a standard eigenproblem has been shown in eq.3.1.1 where [J] is assumed to be given or readily evaluated. However, the consideration of [K] & [M] constitutes a generalised eigenproblem, thus

$$[K]\{\delta\} = \mu[M]\{\delta\} \qquad 3.2.1$$

The inverse manipulation of [M] gives

$$[M]^{-1}[K]\{\delta\} = \mu\{\delta\} \qquad 3.2.2$$

and the inverse manipulation of [K] gives

$$[K]^{-1}[M]\{\delta\} = \frac{1}{\mu}\{\delta\} \qquad 3.2.3$$

In vibration problems, [K] & [M] are positive definite matrices and symmetric in nature and both matrices have the same bandwidth. However, it should be pointed out that $[M]^{-1}[K]$ and $[K]^{-1}[M]$ are not necessarily symmetrical and a full matrix always results from these matrix multiplications. A full matrix utilises a large storage and requires a large number of solution operations. Realising that the properties of standard eigenproblems are more easily assessed, effective transformation procedures from the generalised eigenproblem into standard form are important.

The solution of a linear eigenproblem yields n eigenvalues, $(\lambda_1, \lambda_2, \ldots\ldots\ldots, \lambda_n)$, and corresponding eigenvectors, $(\{\delta_1\}, \{\delta_2\}, \ldots\ldots\ldots, \{\delta_n\})$, The back substitution of each eigenpair $(\lambda_i, \{\delta_i\})$ should satisfy the orthonormality relationship,[32] thus

$$\{\delta_i\}^T [M] \{\delta_i\} = 1 \qquad 3.2.4$$

[M] being a function of λ_i in non-linear eigensystems where $i = 1, 2, \ldots\ldots\ldots\ldots\ldots\ldots n$

The relationships of [M] and [K] - orthonormality,

$$\{\delta_i\}^T [M] \{\delta_j\} = \delta_{ij} \qquad 3.2.5$$

$$\{\delta_i\}^T [K] \{\delta_j\} = \delta_{ij} \qquad 3.2.6$$

where δ_{ij} = Kronecker delta symbol[60]

$$= \begin{bmatrix} 1 \\ 0 \end{bmatrix} \begin{matrix} \text{for } i = j \\ \text{for } i \neq j \end{matrix}$$

can be used as a check on the eigenvectors.

§3.2.2 Classical iterative method

As no explicit formula is available for the calculation of the roots of a characteristic equation, alternative methods of solution must be sought. The iteration operation is based on the generalised eigensystem as shown in eq.3.2.1. In vibration analysis, the iterative process is performed as follows.

The procedure is started with an initial assumed vector $\{x_1\}$. During the (n+1)th step of iteration, $\{\bar{x}_{n+1}\}$ is evaluated in this expression,

$$[K]\{\bar{x}_{n+1}\} = [M]\{x_n\} \qquad 3.2.7$$

An improved vector, $\{x_{n+1}\}$ is then obtained by substituting $\{\bar{x}_{n+1}\}$ into

$$\{x_{n+1}\} = \frac{\{\bar{x}_{n+1}\}}{\sqrt{\{\bar{x}_{n+1}\}^T[M]\{\bar{x}_{n+1}\}}} \qquad 3.2.8$$

The denominator, which is the norm of matrix and vector products, is a measure of convergence. It is a scalar quantity for achieving M-orthonormality as shown in eq.3.2.4.

The iteration is more effective if the eigenvalues are obtained during the process. The procedure is first to assume $\{y_1\} = [M]\{x_1\}$. During the (n+1)th step of iteration, $\{\bar{x}_{n+1}\}$ is evaluated from

$$[K]\{\bar{x}_{n+1}\} = \{y_n\} \qquad 3.2.9$$

This is then substituted into

$$\{\bar{y}_{n+1}\} = [M]\{\bar{x}_{n+1}\} \qquad 3.2.10$$

and an improved vector $\{y_{n+1}\}$ is obtained from

$$\{y_{n+1}\} = \frac{\{\bar{y}_{n+1}\}}{\sqrt{\{\bar{x}_{n+1}\}^T \{\bar{y}_{n+1}\}}} \qquad 3.2.11$$

It is noticed that the iteration is on $\{y_n\}$ rather than on $\{x_n\}$. The convergence is achieved on the value of $\{y_{n+1}\}$ which is evaluated in eq.3.2.11. During the iteration process, the eigenvalues can be obtained from the convergence of the Rayleigh quotient[31], Rq, which is given as

$$R_q = \frac{\{\bar{x}_{n+1}\}\{y_n\}}{\{\bar{x}_{n+1}\}^T \{\bar{y}_{n+1}\}} \qquad 3.2.12$$

The described iteration process is known as inverse iteration.[32] In vibration analysis, the preference of the inverse iteration over the direct iteration is that the former gives the smallest eigenvalue and corresponding eigenvector whereas the latter produces first the highest eigenvalue and corresponding eigenvector. Higher order eigenvalues may be obtained from the relationships of orthogonality which are shown in eqs.3.2.5 & 3.2.6.

§3.2.3 Transformation methods and large eigensystems

A transformation method transforms a matrix under investigation into another without any change in eigenvalues. The fundamental importance is that all the eigenvalues can be obtained directly from the transformed matrix. Transformation methods are particularly suitable for fully populated matrices, i.e. matrices with large bandwidths.

Recalling the generalised eigenproblem in eq.3.2.1, the decomposition of [M] may be expressed in the form of

$$[M] = [G][G]^T \qquad 3.2.13$$

where [G] is a non-singular matrix with zeros above the diagonal. Substituting for [M] into eq.3.2.1 gives,

$$[K]\{\delta\} = \mu [G][G]^T \{\delta\} \qquad 3.2.14$$

Multiplying and premultiplying gives

$$[G]^{-1}[K][G^T]^{-1} \cdot [G]^T\{\delta\} = \mu [G]^T \{\delta\} \qquad 3.2.15$$

where $[G^T]^{-1} = [G^{-1}]^T$

If $[\bar{K}] = [G]^{-1}[K][G^T]^{-1}$ 3.2.16

and $\{\bar{\delta}\} = [G]^T\{\delta\}$ 3.2.17

then $[\bar{K}]\{\bar{\delta}\} = \mu\{\bar{\delta}\}$ 3.2.18

where $[\bar{K}]$ is symmetrical.

Eq.3.2.18 is in the form of the standard eigenproblem. It is noticed that although [K] & [M] are banded, $[\overline{K}]$ is obtained as a full matrix which is inefficient for large order finite element analysis. For this reason, many solution algorithms for large eigensystems[60-64] have been developed, namely Jacobi, Givens, Householder, LR and QR, and most recently QZ.

Since [M] is always a positive definite matrix, it is not necessary to employ the classical LDL decomposition[32,33] method which is designed generally for non-symmetric matrices. Cholesky factorisation,[32,33] which is of the form of eq.3.2.13, is recommended as an effective decomposition method.

Jacobi's method[65] which may be regarded as the original transformation method is based on unitary transformation, i.e. the use of plane rotation. A special form of unitary matrix is an orthogonal matrix [P] which is a real matrix such that

$$[P]^T [P] = [P][P]^T = [I] \qquad 3.2.19$$

By definition, a matrix [B] is said to be related to [A] by by unitary transformation if

$$[B] = [P]^T [A][P] \qquad 3.2.20$$

The orthogonal matrix [P], analogous to rotation of axes in a plane, is typified as

$$[P] = \begin{bmatrix} 1 & \cdots & \cdots & & & \\ \vdots & 1 & \cdots & & & \\ \vdots & \vdots & \ddots & & & \\ \vdots & \vdots & & \cos\theta' & \sin\theta' & \\ \vdots & \vdots & & -\sin\theta' & \cos\theta' & \\ \vdots & \vdots & & & & \ddots \\ & & & & & 1 \end{bmatrix} \qquad 3.2.21$$

where θ' is the angle through which the axes rotate

In Jacobi's solution, the matrix [P] is selected in such a way that an off-diagonal element in [A] (eq.3.2.20) is zeroed. The iteration is hence centered on the selection of θ'. The plane rotation idea was also adopted by Givens (1954) to transform the matrix into a tridiagonal matrix. Givens' method is further extended to Householder's method which is more efficient for symmetric matrices. The consideration of computing time and storage space is investigated by Wilkinson (1960).[67]

A typical example of similarity transformation[68] is Rutishauser's LR method (1955). This involves the upper triangle of a matrix to produce another matrix with greater dominance, i.e. the diagonal terms become heavier with respect to the non-diagonal terms. The lower triangular matrix in the LR method is replaced by an orthogonal matrix in Francis's QR method (1961)[69]. It may be noted that the LR method has been gradually superseded by QR method and a very efficient procedure known as the Householder-QR-inverse iteration[62] has been compiled. An extension of the QR algorithm is the development of the QZ algorithm which accounts for singular matrices.[33]

A short survey of the variety of transformation methods has been briefly introduced. The descriptions and applications of all these methods are fully reported in textbooks[47-54] especially Bathe & Wilson[32] and Jennings.[33] Within the context of this thesis, as the investigation is concentrated on the vibrational behaviour of members rather than on the solution of huge complex structures, it is not intended to study the efficiency of large eigensystems with the various methods.

§3.3 Determinant Evaluation Category

§3.3.1 Explicit characteristic equation

The formulation of this equation is the fundamental method of solving an eigenproblem. The generalised eigenproblem in eq.1.2.1 may be expressed

$$[K - \omega^2 M]\{\delta\} = 0 \qquad 3.3.1$$

of which a non-trivial solution is possible if

$$\left| K - \omega^2 M \right| = 0 \qquad 3.3.2$$

This determinant is expanded in terms of eigenvalues to give a characteristic equation, the roots of which are the eigenvalues. For the polynomial displacement function, the characteristic equation is in the form of

$$(\alpha^4)^n + C_{n-1}(\alpha^4)^{n-1} + \ldots\ldots\ldots\ldots + C_1(\alpha^4) + C_0 = 0 \qquad 3.3.3$$

where α is the dimensionless frequency parameter and n is the number of degrees of freedom or the order of the matrix.

Examples of the explicit characteristic equation of a free cantilever beam, for both polynomial and exact functions are shown in eqs.3.3.4 & 3.3.5 respectively.

$$\alpha^8 - 1224\alpha^4 + 15120 = 0 \qquad 3.3.4$$

$$1 + \cos\alpha\cosh\alpha = 0 \qquad 3.3.5$$

It is noticed that the number of multiplications required to obtain the coefficients of a characteristic equation of a fully populated matrix is roughly proportional to n^4 . As the computional requirement is excessive and is sensitive to errors, the explicit characteristic equation method is not recommended for computer implementation.

§3.3.2 Non-linear eigensystems

The matrices for an exact solution are frequency dependent and form a non-linear eigensystem. As the methods which are presented for a linear eigensystem are inapplicable, the determinant method must be invoked. With the property of the Sturm sequence and the treatment of asymptotic poles, the determinant method has been proved efficient and reliable.

(a) Sturm sequence

The development and proof of Sturm's theorem[34] is not given here, but to illustrate its particular features for non-linear eigensystems, its application is presented. Originally designed for the solution of polynomial problems, the Sturm sequence has proved[35] to be applicable to non-linear eigensystems.

The Sturm sequence is defined as a sequence, $f_i(x)$, i= 1,2..... .... m, over an interval (a, b), such that

(i) $f_m(x)$ does not vanish in (a, b)

(ii) at any zero of $f_j(x)$, j= 2, 3 .... m - 1, the two adjacent functions are non-zero and have opposite sign.

In considering the solution of the real roots of f(x) = 0, the sequence may be obtained from the following expressions:-

$$
\begin{aligned}
f_1(x) &= f(x) \\
f_2(x) &= f'(x) \\
f_j(x) &= q_{j-1}(x)\, f_j(x) - f_{j-1}(x) \qquad j=2,3,\ldots\ldots,m-1 \\
f_{m-1}(x) &= q_{m-1}(x)\, f_m(x)
\end{aligned}
$$

where $q_{j-1}(x)$ is the quotient and

$f_{j+1}(x)$ is the negative of the remainder when

$f_{j-1}(x)$ is divided by $f_j(x)$.

3.3.6

The property of the Sturm sequence is further extended to Sturm's theorem which states that within an interval of (a, b), the difference between the number of changes in sign in the sequences

$$f_1(a), f_2(a), \ldots\ldots\ldots\ldots\ldots\ldots, f_m(a)$$

$$\& \quad f_1(b), f_2(b), \ldots\ldots\ldots\ldots\ldots\ldots, f_m(b)$$

is the number of roots of the function, $f(x)$.[54]

To facililate the understanding of utilisation, an example is given of the solution of the polynomial equation

$$f(x) = x^4 - 2.4x^3 + 1.03x^2 + 0.6x - 0.32 = 0 \qquad 3.3.7$$

The signs of the sequence of functions, f_1, f_2, ... f_m are shown in table 3.3.2a for values between $-\infty$ to $+\infty$. From the last row of table 3.2.2a, it is given that there is one root in (-1, 0), two roots in (0, 1) and one more root in (1, 2). By successive reduction of the intervals the roots may be obtained to any desired accuracy. As a check, the actual roots are -0.5, 0.5, 0.8 and 1.6.

Although the example here is polynomial in nature for simplicity, the Sturm sequence is not as efficient as the iterative methods in the treatment of this form of equation, but is extremely well suited to non-linear equations.

(b) Sign Count

The characteristic equation, from 3.3.2 is written as

$$|J| = 0 \qquad 3.3.8$$

The formulation is greatly enhanced by the Sturm sequence technique[34,35] for the case of symmetric matrices. It is well-known that the leading principal minors of [J] possess the Sturm sequence properties. The important feature is that the number of changes in sign of consecutive members of the sequence is a reliable instrument in identifying the order of the natural frequencies. Furthermore, as only the signs of the leading principal minors are of interest, full evaluation of the determinant is not required.

The number of negative characteristic values,[35] equal to the number of sign changes between consecutive leading principal minors of [J] in eq.3.3.8, was first named as the sign count, $s\langle J\rangle$ (the symbol $\langle\rangle$ denoting a bracketed expression), by Wittrick & Williams.[35] The process of undertaking a sign count involves no more additional time than the evaluation of a determinant. One way to effect a sign count algorithm is to reduce [J] into upper triangular form, $[J]^{\Delta}$, by a simple Gaussian elimination procedure (without row inter-change). The rth diagonal element of $[J]^{\Delta}$ is thus

$$[j_{rr}] = |J_r| \,/\, |J_{r-1}| \qquad 3.3.9$$

In vibration problems, it is extremely unlikely that one or more of the leading principal minors of $[J]^{\Delta}$ is zero. Even if it is, the iteration process can be continued with a sightly different trial value of frequency.

(c) Asymptotic pole algorithm

Recalling eqs.2.3.31 & 2.3.32, the denominators which are of particular interest are respectively

$$AP_f = 1 - \cos\alpha\cosh\alpha \qquad 3.3.10$$

$$AP_e = \sin\beta \qquad 3.3.11$$

which give infinity in $[J_f]$ & $[J_e]$ if

for flexural vibration,

$$1 - \cos\alpha\cosh\alpha = 0 \qquad 3.3.12$$

for extensional vibration,

$$\sin\beta = 0 \qquad 3.3.13$$

In fact, the roots of these two equations are solutions for a clamped-clamped element as shown in fig.3.3.2b. The roots are shown in table 3.3.2c. In many cases, when no element in a structure is constrained into a clamped-clamped boundary condition, these roots are in existence as asymptotic poles. The discontinuities (fig.3.3.2f) which so result will disturb the mechanism of the iteration process. In order to maintain a smooth iteration process, the above mentioned sign count algorithm is superimposed with the occurrence of these poles.

If a free vibration problem is defined by eq.3.3.1, $[K-\omega^2 M]\{\delta\}=0$, in which $\{\delta\}$ is the displacement vector, the asymptotic pole algorithm is designed to obtain the number of eigenvalues when the constraints are so applied to the structure as to cause $\{\delta\}$ to be zero. This zero displacement vector corresponds to the existence of asymptotic poles in the det.-frequency curve. The asymptotic pole algorithm is merged with the sign count to yield a general form of count algorithm, thus

$$S = \sum_{1}^{n}(S_f + S_e) + s\langle J\rangle \qquad 3.3.14$$

when n = total number of elements in a structure[34]

S_f and S_e are the counts obtained from the asymptotic pole algorithms for flexural and extensional vibration respectively. The rules of finding these values are given in table 3.3.2d. Typical determinant-frequency (D-F) curves are shown in fig. 3.3.2e and f.

(d) Summary of count algorithm

It should be stressed that the iteration process is also upset if a redundant algorithm is introduced, e.g. S_e should not be included if extensional displacement is not to be considered in a beam vibration. It is therefore necessary to reinforce the application of the count algorithm as in the following summary:-

(1) For linear eigensystems:-

$$S = s\langle J\rangle \qquad 3.3.15$$

(2) For non-linear eigensysyems:-

(i) Flexural vibration only

$$S = s\langle J\rangle + \sum_{1}^{n}(S_f) \qquad 3.3.16$$

(ii) Extensional vibration only

$$S = s\langle J\rangle + \sum_{1}^{n}(S_e) \qquad 3.3.17$$

(iii) Dual vibration

$$S = s\langle J\rangle + \sum_{1}^{n}(S_f + S_e) \qquad 3.3.18$$

§3.3.3 Convergence procedures

The count algorithm, the general form of which is given in eq.3.3.18, enables any eigenvalue to be iterated to any required accuracy. The procedure is designed to iterate between an upper bound, λ_u, and a lower bound, λ_l , which is firstly assumed to be zero. The two bounds are so defined that the difference in the total count between the two trial bounds is unity. This value of unity denotes that there should exist one eigenvalue between the two bounds. An improved trial value is obtained by bisection, thus

$$\lambda_q = (\lambda_l + \lambda_u)/2 \qquad 3.3.19$$

The procedure is iterated with another pair of bounds which may be (λ_l & λ_q), or (λ_q & λ_u) until the desired accuracy is achieved. The procedure for the iteration of a 3rd mode is illustrated in fig.3.3.3a. The convergence of iteration to the required eigenvalue is based on the idea of Rayleigh's theorem and a proof is given in Ref.35. Furthermore, if two specified bounds of frequencies are given, the number of eigenvalues within the range of order can be readily assessed by applying eq.3.3.18.

The iteration between upper and lower bounds for an eigenvalue of nth order may be continuous or asymptotic. The two cases are respectively shown in fig.3.3.3a & b with the indication of the total number of counts. The importance of the count algorithm is clearly demonstrated in the asymptotic case which exhibits a non-linear iteration. The difficulties in isolating an eigenvalue which is located near asymptotic poles can be imagined. This phenomenon frequently occurs in non-prismatic structural analyses and will be discussed with certain remedies in a later chapter.

§3.4 Further Analyses

The discussion in the former sections has concentrated on the determination of natural frequencies (eigenvalues). In this section certain techniques are discussed that can lead to improvements in the solution methods.

§3.4.1 Sub-structuring

A rather recently developed procedure in finite element assemblege is the sub-structuring technique.[59,72] It has been demonstrated conclusively that a saving of computer time and an unchanged small bandwidth are possible. The basic concept of assembling sub-structures is described as follows:-

Eq.3.3.1 is partitioned into

$$\begin{bmatrix} [J_{mm}] & [J_{ms}] \\ [J_{ms}]^T & [J_{ss}] \end{bmatrix} \begin{bmatrix} \{\delta_m\} \\ \{\delta_s\} \end{bmatrix} = 0 \qquad 3.4.1$$

where $\{\delta_m\}$ = displacement vector of (N-n) nodes

$\{\delta_s\}$ = displacement vector of n nodes

and suffices m & s denotes master and slave respectively.

The first equation from the matrix in eq.3.4.1 becomes

$$\{\delta_m\} = -[J_{mm}]^{-1}[J_{ms}]\{\delta_s\} \qquad 3.4.2$$

and the second equation becomes

$$\{\delta_s\} = -[J_{ms}^T]^{-1}[J_{ss}]\{\delta_m\} \qquad 3.4.3$$

Substituting for $\{\delta_m\}$ into eq.3.4.3 gives

$$[J_s]\{\delta_s\} = 0 \qquad 3.4.4$$

where $[J_s] = [J_{ss}] - [J_{ms}]^T [J_{mm}]^{-1} [J_{ms}]$

Eq.3.4.4 replaces eq.3.3.1 as an eigenproblem. $[J_s]$ is a symmetric matrix of order nxn which is smaller than NxN for $[J]$. However, if all the elements in $[J]$ are linear functions of λ, it is not necessarily true for $[J_s]$. It has been found that eq.3.5.4 behaves as a non-linear eigensystem which should be solved by the method as described in the last section.

§3.4.2 Mode shape

A program for the determinant method does not usually produce the eigenvectors corresponding to the associated eigenvalues. The reason is that the solution of the eigenvectors involves storing the whole band of $[J]$, increasing computation time and complicating the coding for programming. However, despite all these obstructions, there is no difficulty in amalgamating, into the determinant solution routine, a subroutine for evaluating eigenvectors and hence the mode shape.

Once an eigenvalue is obtained, the back substitution into the original frequency dependent matrix will produce a set of linear simultaneous equations, the solution of which[47-54] is straight forward and many library subroutines are available for this purpose. Alternatively, the eigenvectors can be effectively calculated by the technique of inverse iteration method which has been described in §3.2.2.

§3.4.3 D-f curve

This is a graphical output showing the value of determinants for different values of frequency. It is not intended to use the curves for finding the roots of eq.3.3.2, but to show a general view of the distribution of frquencies. Furthermore, an accurate plot of D-f curves can be used as an aid to explain the phenomenon of asymptotic poles, and other possible complexities of the behaviour of determinants which will be discussed later when dealing with non-prismatic structures.

An important aspect of D-f curves is the evaluation of determinants. Unfortunately, the absolute range of a variable in a digital computer (ICL 1904) is up to 10^{76} and so an overflow will be registered after 10 or even fewer multiplications. Two remedies are used successfully:-

(a) Before any matrix manipulation, each element of a matrix is divided by the value of Young's modulus, E, which is of the order 10^{10} KN/m² for concrete. If there is a risk of overflowing at 10^{-76}, EI instead of E is used as a common divisor.

(b) The numerical multiplication is executed in two operations, namely characteristic variable and power index (e.g., 3.76×10^{20}, 3.76 being the characteristic variable & 20 being the power index). The final product is stored as the combination of the characteristic variable multiplications and the addition of the power index. Theoretically, a real variable can be evaluated up to a limit of $10^{8388683}$. This is shown in table 3.4.3a and a flow chart for this algorithm is shown in 3.43b.

§3.5 A Special Development for Repetitive Structures

§3.5.1 Explicit characteristic equation

It has been mentioned that the handling of the explicit characteristic equation is excessive in computation time and sensitive to error, but the setting up of such equations is beneficial for non-linear eigenproblems. However more information can be obtained from an explicit characteristic equation than the finally obtained frequencies.

It can be seen in table 3.5.1a that the characteristic equations for simple beams are expressed in neat and general forms from which frequencies are effectively evaluated by the Newton-Raphson method. Similarly, simple expressions may be obtained for repetitive structures, for example, continuous beams formed by the repetition in simple beams. Furthermore, the equations for mode shapes are also given in simple forms which describe mode shapes of any order.

§3.5.2 Repetitive structures

As the order of a matrix becomes higher, the setting up of an explicit characteristic equation becomes increasingly time consuming. It is, however, not too complicated if a structure is repetitive in nature and the knowledge of sub-structuring[59,72] can always be an advantage. Multi-equal-span continuous beams with classical boundary conditions are typical examples which will be studied in detail. The investigation is presented in figs.3.5.2a to g inclusive.

(a) Matrix formulation (Figs.3.5.2a, b & c)

The presentation is easier if only flexural vibration is considered here and the procedure is extended to extensional vibration. As no vertical displacement at the nodes is experienced in continuous beams, the matrix formulation is much simplified with only rotational displacements. The elements which are associated with rotational displacements are J_{21}, J_{24} & J_{44} where for the exact function

$$A = J_{22} = J_{44} = (\sin\alpha\cosh\alpha - \cos\alpha\sinh\alpha)/AP_f \qquad 3.5.1$$

$$B = J_{24} \qquad = (-\sin\alpha + \sinh\alpha)/AP_f \qquad 3.5.2$$

and for the polynomial function,

$$A = J_{22} = J_{44} = 1680 - 4\alpha^4 \qquad 3.5.3$$

$$B = J_{24} \qquad = 840 - 3\alpha^4 \qquad 3.5.4$$

(b) Coefficient triangles (Figs.3.5.2d & e)

The expansion of the determinants of these matrices are explicit characteristic equations of which the coefficients exhibit a definite format. Coefficient triangles are prepared, which are similar to the Pascal's triangle in binomial expansions. For spans more than ten in number coefficients are formatted from the extension of coefficient triangles.

(c) Factorisation & solution (Fig.3.5.2f)

A rational approach to a solution is to factorise an explicit characteristic equation into as many simple expressions as possible. Each factorised expression will generate a set of roots which are infinite in number for the exact function. The solution of these roots are obtained with no difficulty by the Newton-Raphson method.

Due to the feature that spans are repetitive, a factorised expression may appear in some other multiples of spans. This implies that for spans of certain multiples, there should exist a definite frequency. It is shown that, from structure-system B in fig.3.5.2f, a natural frequency of =3.9266 occurs for m=1, 3, 5......., where m is the number of spans. This procedure may be extended to predict natural frequencies of a continuous beam of any number of spans.

(d) Determinant-frequency curve (D-f curve)

Each factorised expression possesses a different variation in D-f curves. A collection of these curves for some common factorised expressions in exact solutions is shown in table 3.5.2g. A common feature for all these curves is that the profile of each curve is repeated between asymptotic poles.

§3.5.3 Extensional vibration

As horizontal displacements are the only parameter in the displacement vectors, the procedure which is designed for flexural vibration is applicable to extensional vibration with slight modifications. This saves the unnecessary repetition of the procedure and emphasises the particular features of analogy which are outlined as follows.

(a) Elements in matrices

If rotational displacements are replaced by horizontal displacements, the corresponding elements of J_{55}, J_{56}, J_{66} are represented by
for the exact function,

$$A = J_{55} = J_{66} = \cos\beta / AP_e \qquad 3.5.5$$

$$B = J_{56} = -1/AP_e \qquad 3.5.6$$

where AP_e is defined in eq.3.3.11

for the polynomial function,

$$A = J_{55} = J_{66} = 6-2\beta^2 \qquad 3.5.7$$

$$B = J_{56} = -(6+\beta^2) \qquad 3.5.8$$

(b) Boundary conditions

The analogy between the boundary conditions at the extreme supports is shown in table 3.5.3a.

(c) The roots

Without performing the tedious procedures which are described formerly, it is possible to reduce the evaluation of natural frequencies, for the rth mode of n number of spans, into simple formulae, thus,

(i) for a system with one end inextensible and the other end extensible,

$$\beta = \pi(2r-1)/2n \qquad 3.5.9$$

(ii) for a system with both ends inextensible,

$$\beta = (r+\mathrm{INT}(\frac{r-1}{n-1}))\,\pi / n \qquad 3.5.10$$

It is noticed that the sequence of these roots exhibits a very strong proof of the exact displacement function. The natural frequencies of a continuous beam should be the same as the natural frequencies of a single span beam.

Table 3.3.2a An example on the Sturm sequence

x	$-\infty$	-1	0	1	2	∞
$f_1(x)$	+	+	-	-	+	+
$f_2(x)$	-	-	+	-	+	+
$f_3(x)$	+	+	+	+	+	+
$f_4(x)$	-	-	-	+	+	+
$f_5(x)$	+	+	+	+	+	+
No. of sign changes	4	4	3	1	0	0

where

$$f_1(x) = x^4 - 2.4x^3 + 1.03x^2 + 0.6x - 0.32 = 0$$

$$f_2(x) = x^3 - 1.8x^2 + 0.515x + 0.15$$

$$f_3(x) = x^2 - 1.3434x + 0.4071$$

$$f_4(x) = x - 0.6645$$

$$f_5(x) = 1$$

Table 3.3.2c
The roots of a clamped-clamped beam

i	$1-\cos\alpha\cosh\alpha=0$	$\sin\beta=0$
	α_i	β_i
1	4.73004	π
2	7.85320	2π
3	10.99561	3π
4	14.13717	4π
5	17.27876	5π
6	⋮	⋮
7		
8	$\frac{2i+1}{2}\pi$	$i\pi$
9	⋮	⋮

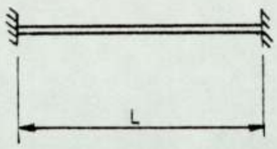

Fig.3.3.2b
A clamped-clamped beam

Table 3.3.2d Counts from the AP algorithms

<table>
<tr><th colspan="4">Value of S_f</th><th rowspan="2">Value of S_e</th></tr>
<tr><th colspan="2">AP_f / i_f</th><th>+ve (AP>0)</th><th>-ve (AP<0)</th></tr>
<tr><td rowspan="2">$i_f = INT(\alpha/\pi)$</td><td>odd</td><td>$S_f = i_f - 1$</td><td>$S_f = i_f$</td><td rowspan="2">$S_e = INT(\beta/\pi)$</td></tr>
<tr><td>even</td><td>$S_f = i_f$</td><td>$S_f = i_f - 1$</td></tr>
</table>

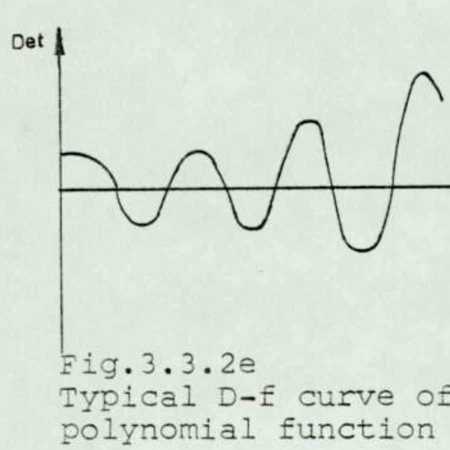

Fig.3.3.2e
Typical D-f curve of the polynomial function

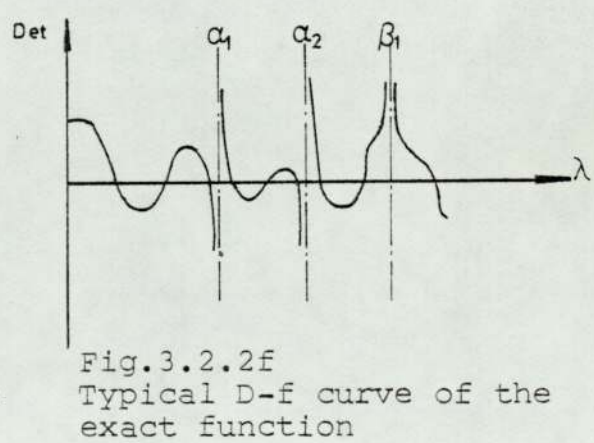

Fig.3.2.2f
Typical D-f curve of the exact function

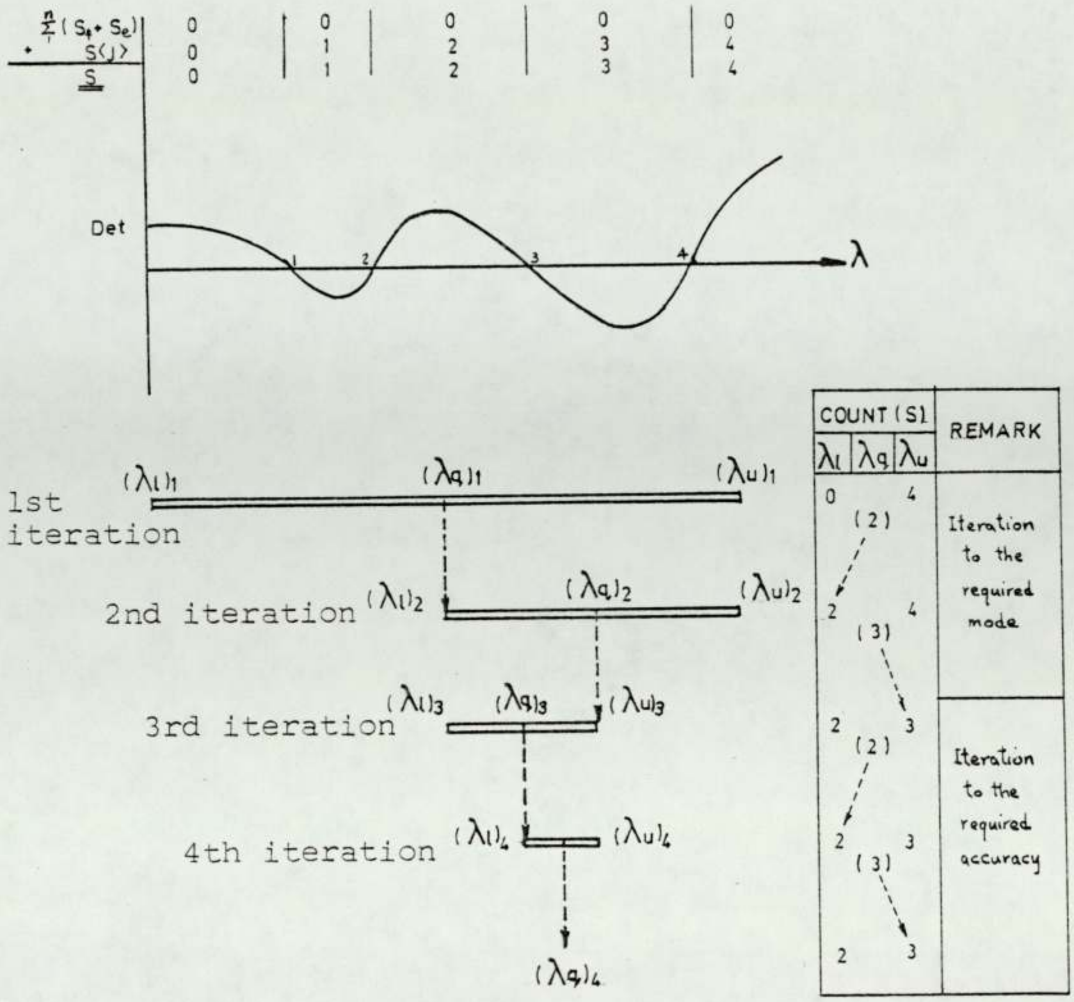

FIG. 3.3.3a ILLUSTRATED EXAMPLE OF THE ITERATION BY BISECTION

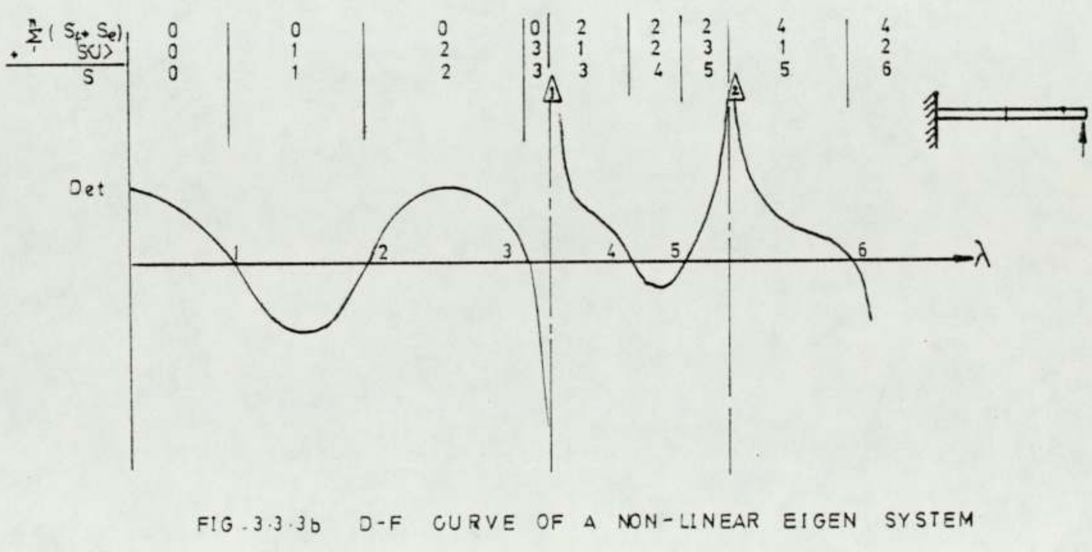

FIG. 3.3.3b D-F CURVE OF A NON-LINEAR EIGEN SYSTEM

Table 3.4.3a
Storage of high power multiplication

Multiplication of (2.36×10^{24}) (1.79×10^{31}) (5.84×10^{39})		
Numerical Multiplication	Characteristic variable	Power index
	$2.36 \times 1.79 \times 5.84$ $= 24.67$	$24 + 31 + 39$ $= 95$
	Product $= 2.467 \times 10^{96}$	
Limit	10^{76}	8388607
	Product $= 10^{8388683}$	

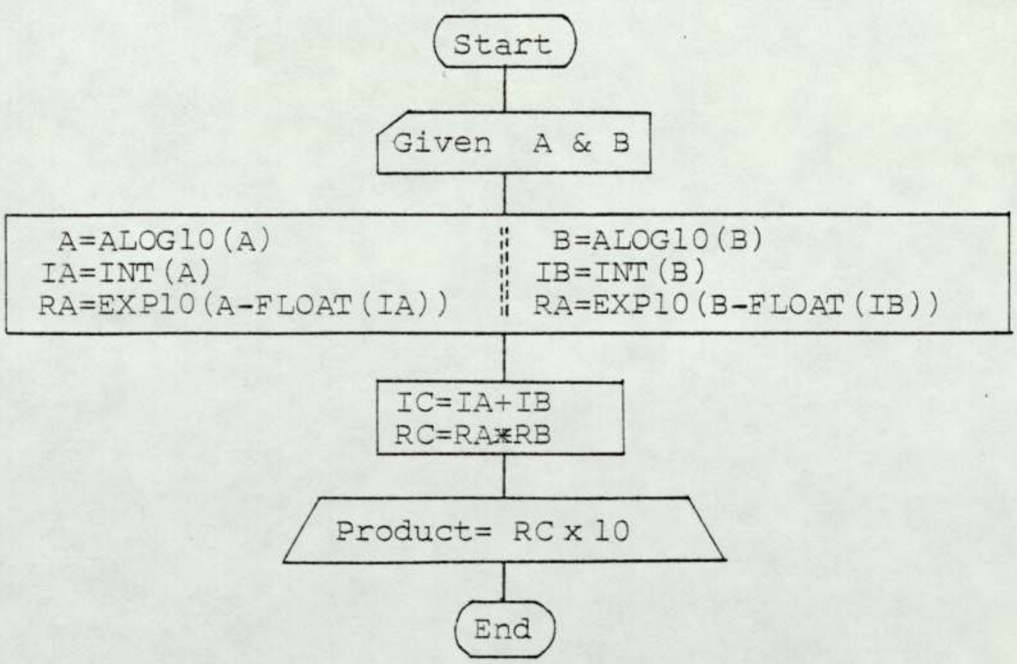

Fig.3.4.3b Flow chart for the multiplication of two values of large magnitude

Table 3.5.1 Flexural vibration of simple beams

Beam	Explicit Characteristic Equation	Displacement Equation, $W_{(x)}$	Remark
	$1+\cos\alpha\,\cosh\alpha = 0$	$(\sin\lambda x - \sinh\lambda x) - b_1(\cos\lambda x - \cosh\lambda x)$	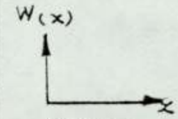 $0 < x < L$
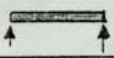	$\sin\alpha = 0$	$\sin\lambda x$	$b_1 = \frac{\sin\alpha + \sinh\alpha}{\cos\alpha + \cosh\alpha}$
	$\sin\alpha\cosh\alpha$ $\cos\alpha\sinh\alpha = 0$	$(\sin\lambda x - \sinh\lambda x) - b_2(\cos\lambda x - \cosh\lambda x)$	$b_2 = \frac{\sin\alpha - \sinh\alpha}{\cos\alpha - \cosh\alpha}$
	$1-\cos\alpha\,\cosh\alpha = 0$	$-(\sin\lambda x - \sinh\lambda x) + b_2(\cos\lambda x - \cosh\lambda x)$	

Table 3.5.3 Analogy between the boundary conditions

	Extensional Vibration	Flexural Vibration
a	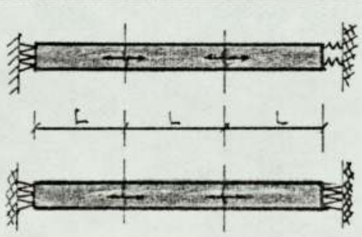	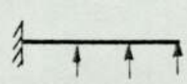
b		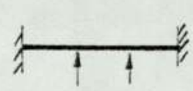

$$[K-\omega^2 M][\delta] = \begin{bmatrix} A & B & & & & & \\ B & 2A & B & & & [0] & \\ & B & 2A & \ddots & & & \\ & & \ddots & \ddots & \ddots & & \\ & [0] & & \ddots & 2A & B & \\ & & & & B & 2A & B \\ & & & & & B & A \end{bmatrix} \begin{bmatrix} \theta_1 \\ \theta_2 \\ \theta_3 \\ \vdots \\ \theta_{n-1} \\ \theta_n \\ \theta_{n+1} \end{bmatrix}$$

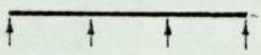

Fig.3.5.2a System A

$$[K-\omega^2 M][\delta] = \begin{bmatrix} 2A & B & & & & & \\ B & 2A & B & & & [0] & \\ & B & 2A & \ddots & & & \\ & & \ddots & \ddots & \ddots & & \\ & [0] & & \ddots & 2A & B & \\ & & & & B & 2A & B \\ & & & & & B & A \end{bmatrix} \begin{bmatrix} \theta_2 \\ \theta_3 \\ \theta_4 \\ \vdots \\ \theta_{n-1} \\ \theta_n \\ \theta_{n+1} \end{bmatrix}$$

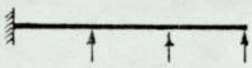

Fig.3.5.2b System B

$$[K-\omega^2 M][\delta] = \begin{bmatrix} 2A & B & & & & & \\ B & 2A & B & & & [0] & \\ & B & 2A & \ddots & & & \\ & & \ddots & \ddots & \ddots & & \\ & [0] & & \ddots & 2A & B & \\ & & & & B & 2A & B \\ & & & & & B & 2A \end{bmatrix} \begin{bmatrix} \theta_2 \\ \theta_3 \\ \theta_4 \\ \vdots \\ \theta_{n-1} \\ \theta_n \\ \theta_{n+1} \end{bmatrix}$$

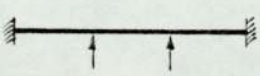

Fig.3.5.2c System C

Table 3.5.2d Flexural vibration of continuous beams

N.B. (i) Derivation of Coefficient Triangle, see Table 3.5.2 e (ii) Reference number of factorised function, see Table 3.5.2 f — System of continuous beams	Nº of Spans (n)	Index (i)	Multiplier	Coefficients A^i	$A^{i-2}B^2$ or B^2	$A^{i-4}B^4$ or B^4	$A^{i-6}B^6$ or B^6	$A^{i-8}B^8$ or B^8	$A^{i-10}B^{10}$ or B^{10}	Factorised Functions fn# 1	fn# 2	fn# 3	fn# 4	fn# 5	fn# 6	fn# 7	fn# 8	fn# 9	fn# 10	Explicit characteristic Equation (For triple Span)
(A) 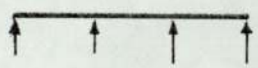	1	2		1	1					⊕										$(A^2-B^2)(4A^2-B^2)=0$
	2		A	2	2					⊕	⊕									
	3	4		4	5	1				⊕		⊕								
	4		A	8	12	4				⊕	⊕		⊕							
	5	6		16	28	13	1			⊕				⊕						
	6		A	32	64	38	6			⊕	⊕	⊕			⊕					
	7	8		64	144	104	25	1		⊕						⊕				
	8		A	128	320	272	88	8		⊕	⊕		⊕				⊕			
	9	.																		
	10																			
(B) 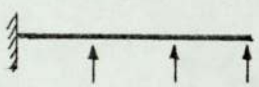	1	0	A	1							*									$A(4A^2-3B^2)=0$
	2	2		2	1								*							
	3	2	A	4	3						*				*					
	4	4		8	8	1											*			
	5	4	A	16	20	5					*								*	
	6	6		32	46	18	1						*							
	7	6	A	64	112	56	7				*									
	8	8		128	256	160	32	1												
	9										*				*					
	10												*							
(C) 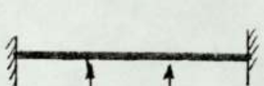	1	0		1						⊗										$AP_f(4A^2-B^2)=0$
	2	0	A	2						⊗	x									
	3	2		4	1					⊗		x								
	4	2	A	8	4					⊗	x		x							
	5	4		16	12	1				⊗				x						
	6	4	A	32	32	6				⊗	x	x			x					
	7	6		64	80	24	1			⊗						x				
	8	6	A	128	192	80	8			⊗	x		x				x			
	9																			
	10																			

Table 3.5.2e   Coefficient Triangles

No. of spans	Coefficient Triangles					
One spans	1 +1	1 +1 +0				
Two spans	2 +2	2 +2 +1				
Three spans	4 +4	5 +5 +2	1			
Four spans	8	12	4			
Five spans	16	28	13	1		
Six spans	32	64	38	6		
Seven spans	64	144	104	25	1	
7-span	${}_7T_1$	${}_7T_2$	${}_7T_3$	${}_7T_4$	1	
For n spans						
if n is odd	${}_nT_1$	${}_nT_2$	${}_nT_3$	......	1	
if n is even	${}_nT_1$	${}_nT_2$	${}_nT_3$	......	${}_nT_{\frac{n}{2}+1}$	
For (n+1) spans						
if n is odd	${}_nT_1$ ${}_nT_1$	${}_nT_2$ $+{}_nT_2$ $+{}_{(n-1)}T_1$	${}_nT_3$ $+{}_nT_3$ $+{}_{(n-1)}T_2$	....	1 +1 $+{}_{(n-1)}T_{\frac{n+1}{2}}$	
if n is even	${}_nT_1$ ${}_nT_1$	${}_nT_2$ $+{}_nT_2$ $+{}_{(n-1)}T_1$	${}_nT_3$ $+{}_nT_3$ $+{}_{(n-1)}T_2$	....	${}_nT_{\frac{n}{2}+1}$ ${}_nT_{\frac{n}{2}+1}$ ${}_{(n-1)}T_{\frac{n}{2}}$	1

Table 3.5.2f Roots of the factorised functions

Factorised Function		Occurnece of the functions			Roots
Ref. No.	Function	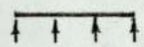	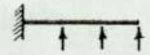	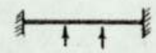	
$fn^{\#}1$	$A^2 - B^2$ (see foot-note)	m	/	m	$\pi, 2\pi, 3\pi, \ldots$ for $2ssh = 0$ $\alpha_1, \alpha_2, \alpha_3, \ldots.$ for $1-cch = 0$
$fn^{\#}2$	A	2m	2m-1	2m	3.9266, 7.0686, ...
$fn^{\#}3$	$4A^2 - B^2$	3m	/	3m	3.5564, 4.2975, 6.7076,....
$fn^{\#}4$	$2A^2 - B^2$	4m	2(2m-1)	4m	3.3932, 4.4633, 6.5454,....
$fn^{\#}5$	$16A^4 - 2A^2B^2 + B^4$	5m	/	5m	3.3090, 3.7004, 4.1529,,...
$fn^{\#}6$	$4A^2 - 3B^2$	6m	3(2m-1)	6m	3.2605, 4.6024, 6.4098,....
$fn^{\#}7$	$64A^6 - 80A^4B^2 + 24A^2B^4 - B^6$	7m	/	7m	3.2302, 3.4602, 3.7642,....
$fn^{\#}8$	$8A^4 - 8A^2B^2 + B^4$	8m	4(2m-1)	8m	3.2101, 3.6454, 4.2080,....
$fn^{\#}9$	$64A^6 - 86A^4B^2 + 36A^2B^4 - B^6$	9m	/	9m	3.1961, 3.3449, 3.8001,....
$fn^{\#}10$	$16A^4 - 16A^2B^2 + B^4$	10m	5(2m-1)	10m	3.1859, 3.4883, 4.3663,....

m =1, 2, 3, ...
(no. of spans)

N.B. $fn^{\#}1 = A^2 - B^2 = 2ssh$
or $= 1-cch$

Table 3.5.2g D-f curves for the factorised functions

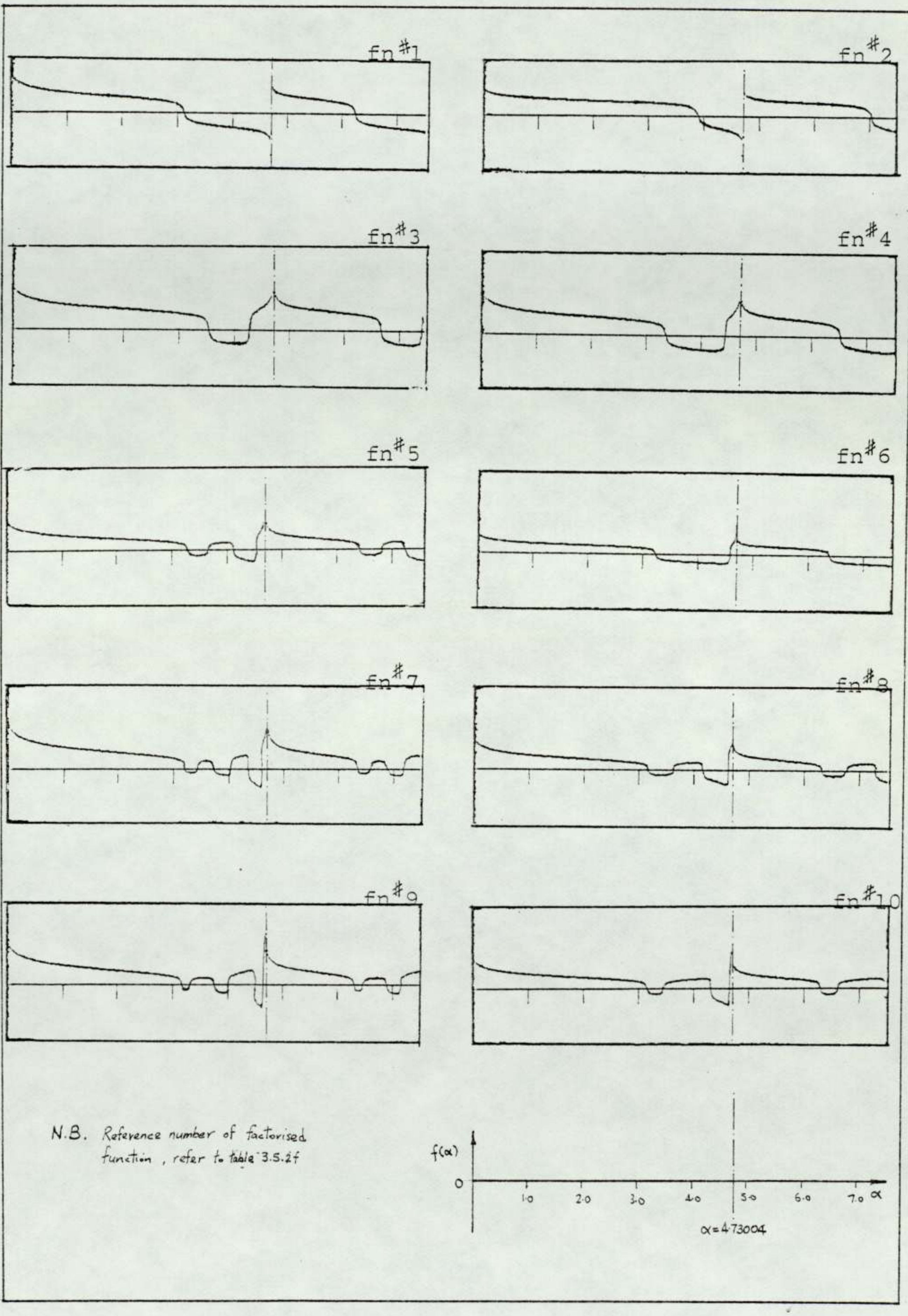

Chapter 4

Behaviour of prismatic plane structures

CHAPTER 4

BEHAVIOUR OF PRISMATIC PLANE STRUCTURES

§4.1 Introductory Notes

It is obvious that the displacement function which is obtained from the governing differential equation should give exact solutions. The purpose of demonstrating the convergence tests is to

(i) show that the assumed displacement functions are useable,

(ii) compare the efficiency of the different displacement functions in various discretisations.

The dynamic behaviour of structures is best appreciated by the studying of examples. The examples covered range from a simply supported beam to a multi-storey building. As far as this chapter is concerned, members of structures are of prismatic section and all results are obtained from the exact solution.

Comparison of natural frequency within the same type of structure by varying one of the design parameters is highly emphasised. (For example, in a multi-span continuous beam, different natural frequencies might be expected for different numbers of spans.) Graphical presentation is a simple way of demonstrating these comparisons. Throughout this chapter, frequencies are kept to the y-coordinates for the sake of consistency.

Wherever necessary, examples are illustrated with modal shapes. The symmetry of a structure is accompanied by a symmetry in modal displacement. Problems with symmetric and anti-symmetric modes are also investigated.

Results are generally given in terms of the following parameters:-

(a) Frequency characteristic equations

These characteristic equations describe the relationship between circular natural frequency, ω, and material and sectional properties, thus,

for flexural vibration,

$$\lambda^4 = \omega^2 \rho A/EI \qquad 4.1.1$$

$$\gamma^2 = \omega^2 \rho/E \qquad 4.1.2$$

(b) Natural frequency (f)

In general the unit for the natural frequency of a structure is denoted as cycles per second or hertz (HZ), i.e.,

$$f = \omega/2\pi \qquad 4.1.3$$

(c) Frequency parameters (λ & γ)

From eq.4.1.1 & 4.1.2 a relationship between λ & γ can be obtained. The frequency parameter describes the free vibration of a structure taking account of its material and sectional properties. The relationship between λ & γ is expressed in terms of the radius of gyration of a section, thus,

$$\gamma = \lambda^2 r_g \qquad 4.1.4$$

where $$r_g = \sqrt{I/A} \qquad 4.1.5$$

(d) <u>Dimensionless frequency parameters</u> (α & β)

The free vibration of a structure, especially a beam, is very often expressed in terms of dimensionless frequency parameters (which is abbreviated as DFP) for simplicity and generality. These are :-

for flexural vibration, $\alpha = \lambda L$ 4.1.6

for extensional vibration, $\beta = \gamma L$ 4.1.7

Substituting into eq.4.1.4, the relationship between the two DFPs may be written as

$$\alpha = \sqrt{(\beta \cdot L/r_g)} \qquad 4.1.8$$

Very often the extensional DFP (β) is required in flexural vibration. In this case eq.4.1.8 is therefore re-written as

$$\alpha_e = \sqrt{(\beta \cdot L/r_g)} \qquad 4.1.9$$

α_e being the flexural DFP in extensional vibration.

(e) <u>Sectional properties</u> (I & A)

The specification of second moment of area and cross sectional area can describe a section of any shape, e.g. rectangular section, I-section, etc. In many of the examples, when sectional shape is not explicitly mentioned, sections of any shape can be applicable. Sections of all members can be identical or in different configuration (§4.6).

(f) <u>Material properties</u> (E & ρ)

Unless otherwise stated, the material properties of concrete and steel were respectively specified as follows :-

Young's modulus,	25 &	200	KN/mm^2
Density,	2400 &	7500	Kg/m^3

§4.2 Convergence of Polynomial Function

Unless the exact displacement functions are used, the accuracy of the computed frequencies depends mainly on the number of split elements, and on the nature of the assumed displacement function.[75] The accuracy is increased by using more elements in the representation of the structure.

The polynomial expansions used in the assumed displacement function may be one of the causes that will affect the rate of convergence. The employed polynomial function is a complete[76] polynomial for an one-dimensional element. An improvement[77] to the polynomial function has been suggested.

The assumed function with consistent mass over-estimates the dynamic stiffness matrix, and so the convergence curves tail down to the exact solution. The curves tail up to a converged solution in the case of lumped mass representation.

Usual presentation of convergence is shown by a curve joining all the points of discrete values. In many of the following examples, if the rate of convergence cannot be shown distinctively, the points are joined with straight lines or the results are tabulated.

§4.2.1 Convergence in beam structures

Four standardised beam structures with classical boundaries are considered both for lumped mass and consistent mass representation. The convergence curves are shown in fig.4.2.1a. Comparatively slow convergence is experienced in lumped mass representation and extremely poor convergence is given in the free cantilever beam.

It is widely accepted that the accuracy of computed frequencies deteriorates with modes of higher order. Furthermore, it has also been found that the accuracy deteriorates with the higher magnitude of the dimensionless frequency parameters. It is observed, in fig.4.2.1b, that the convergence of the second mode in the free cantilever beam (λL=4.694) is better than that of the first mode in the encastre beam (λL=4.730). More examples on the comparison of convergence of higher modes are shown in fig.4.2.1c & d.

§4.2.2 Convergence in frame structures

For frame structures, it is shown in table 4.2.2a that the convergence using the lumped mass representation is not as rapid as that obtained from the consistent mass representation. Using the consistent mass representation in the polynomial function, an acceptable result ($\omega_{poly.}/\omega_{exact}$ =1.055) is obtained even when every member of the portal frame is taken as one element.

In the vibration of frames, the frequency parameters are relatively low in magnitude compared with those of the beams. The low value of parameters may be one of the reasons why a more rapid convergence is always obtained. More examples of the convergence of frames are shown in fig.4.2.2b & c.

§4.2.3 Justification on computing time

Besides the rate of convergence, another aspect of interest is to justify the polynomial function with respect to the computing time, CPU, based on the determinantal method. Similar comparison is also applicable to the other methods of solution.

It is noticed that the advantage of the diagonal feature in the lumped mass matrix is not utilised in the general algorithm of the determinantal method. As the difference in time of formulation, between lumped and consistent mass matrices is negligible, comparison is therefore concentrated on the polynomial function and exact function for members of consistent mass.

The characteristic equation for determinant method (eq.3.31) is described as

$$|J| = 0$$

$$\text{where} \quad [J] = [K] - \omega^2 [M] \qquad 4.2.1$$

The computing time consumed in the evaluation of a determinant may be divided into the following three aspects:-

(a) CPU_f — for the Formulation of [J] matrix.

The time for the assemblege into an overall matrix is also included. This depends on the total number of elements in a structure. The variation is approximately linear.

(b) CPU_m — for the matrix Manipulation.

The determinant is evaluated by the Gauss elimination method. It is obvious that the CPU_m is dependent on the matrix order N. The time taken is approximately proportional to N^3. It is identical for both displacement functions.

(c) CPU_s — for other Steering instruction

The initialisation of matrices, the organisation of variables, the count algorithm, etc. are included in CPU_s. It is comparatively significant if the matrix order is small.

Typical values of these CPUs are summarised in fig.4.2.3a, b, c & d. These are used as guidelines for the time comparison of displacement functions. Three types of simple structures are considered and they are shown in fig.4.2.3d.

§4.2.4 Conclusion on the choice of function

It has been shown that there is no advantage to be gained in using the lumped mass system. In the following chapters, the analysis is based on consistent mass distributed along the members of structures.

Rapid convergence, reliable results and stable iteration are given by the polynomial function. However, the price of good accuracy which should be obtained from more elements sometimes cannot be justified with computing time. As an exact solution can be obtained with a smaller amount of computing time, this is therefore recommended. The results of examples in the following sections are obtained from the exact displacement functions.

§4.3 Members Without Global Orientation

The basic requirement for this class of structure is the co-linearity of the centre lines of the members, the members being connected to each other in the same local orientation. The examples described are divided into standard principal beams and continuous beams with classical boundary conditions.

§4.3.1 Un-coupled matrix

The matrix in fig.4.3.1b is formulated for the continuous beam shown in fig.4.3.1a. The matrix clarifies the particular features of local coordinate formulation — the elements for both flexural and extensional vibrations are not coupled, and the technique of matrix partitioning can be so employed that two independent matrices are formed respectively for dual vibrations as shown in fig.4.3.1c & 4.3.1d.

The eigenvalues of the above two matrices are natural frequencies for flexural and extensional vibrations respectively. The amalgamation of these frequencies should be the same solution as that from the matrix in fig.4.3.1b. From the local coordinate matrix formulation, more features are then observed as follows:-

(a) Flexural vibration is distinguished clearly from extensional vibration, or vice versa.

(b) The solution of two partitioned matrices reduces computing time.

§4.3.2 The suppression of extensional vibration

The exact solutions for the standard principal beams can be seen in many texts, but generally no account is taken on the duality phenomenon of both flexural and extensional vibrations. As an example to point out the importance of duality, consider the third mode of a simple supported beam, i.e. $\alpha=3\pi$. If extensional vibration is taken into account, this is not always the third mode. The crucial factor is the choice of sectional properties, I and A or the radius of gyration r_g (eq.4.1.5). It is shown in table 4.3.3c that $\alpha=3\pi$ is the fourth mode. The third mode is in extensional vibration which is $\alpha_e=7.043$.

§4.3.3 Natural frequency in single span beams

The boundary conditions of beams and their corresponding modes are shown in table 4.3.3a, and for bars in table 4.3.3b. If both flexural and extensional vibrations are considered in beam structures, the natural frequencies are shown in table 4.3.3c. It is noticed that the suppression of the axial displacement would eliminate the extensional frequency results.

§4.3.4 Natural frequencies in continuous beams

A very detailed discussion of continuous beams has been mentioned in§3.5 for both flexural and extensional vibrations. Natural frequencies of typical continuous beams are tabulated in table 4.3.4. It is noticed that the first mode of a continuous beam may result from extensional vibration.

§4.3.5 Comment

Taking the advantages of local coordinate orientation, the formulated matrix can be partitioned into matrices for flexural and extensional vibrations. The corresponding eigenvalues can then be easily recognised as modes for either flexural or extensional displacements. The duality in vibration should be accounted for in the actual solution of a structure. There is also a reduction in computing time for partitioned matrices.

Generally, lower natural frequencies are expected for an increasing number of spans. If extensional vibration is neglected, the first mode for simply supported continuous beams is always $\lambda L=\pi$. The first mode of the other two types of continuous beams tends to $\lambda L=\pi$ if the number of spans increases to infinity, (fig.4.3.5).

§4.4 Frames with Global Orientation

§4.4.1 The re-orientation of the matrix

The frame shown in fig.4.4.1a is encastred at A & C, and the displacements at joint B are $[x_B\ y_B\ \theta_B]^T$. The dynamic stiffness matrices for members AB & BC in their local coordinates are respectively shown in fig.4.4.1c & d. In order to conform with the compatibility of overall matrix formulation for the whole structure, elements in $[j]_{BC}$ should be re-orientated as shown in fig.4.4.1e. The overall stiffness matrix is finalised in fig.4.4.1b.

A very important point which should be stressed is that the matrix cannot be partitioned as in the case of the continuous beams since the existence of pure flexural or extensional vibration does not occur. This interaction behaviour is investigated by considering various types of framework.

§4.4.2 Rectangular frame

The single storey portal is a commonly used structural frame. A detailed study would examine the many hidden features which would be the basis for further development. These features are discussed as follows:-

(a) Slenderness ratio (r_s)

The frequency characteristic equations of eq.4.1.1 can be expressed in terms of the radius of gyration (r_g) and the slenderness ratio (r_s), thus,

$$\omega = \sqrt{(E/\rho)}\ \lambda^2\ r_g \qquad 4.4.1$$

$$\& \quad \omega = \sqrt{(E/\rho)}\ \alpha^2/L \cdot 1/r_s \qquad 4.4.2$$

The natural frequencies of a structure are very much dependent on these two parameters. An example of this is shown in table 4.4.2a.

(b) Frame aspect ratio (r_f)

This is defined as a ratio of height to span of a frame, i.e. $r_f = H/L$. This ratio greatly affects the vibration of a frame both in terms of natural frequency and in DFP. An example showing the variation of natural frequency with frame aspect ratio is shown in fig.4.4.2b.

(c) Higher modes

For ease of explanation, the first mode of vibration is always considered. Similar behaviour should apply to modes of higher orders. When dealing with higher modes, more attention should be paid to the following points:-

(i) The evaluation of the function as it becomes higher in order.

(ii) the greater chance for the intrusion of asymptotic poles

(iii) the coincidence of modes

Generally, no problem arises in the solution of the first twenty modes. An example giving the outcome of higher modes is shown in fig.4.4.2c. Particular interest is drawn to the superposition of symmetric and anti-symmetric modes.

(d) Symmetry

If a frame exhibits geometrical symmetry, half structures may be simplified into symmetric and anti-symmetric components for vibration analysis (fig.4.4.2d). The results obtained from both half-structures are then arranged in ascending order to obtain the complete set of frequencies. The fundamental mode can result in either anti- or symmetric displacements. This phenomenon can be seen in fig.4.4.2c.

Theoretically, when the frame aspect ratio is 0.3119, the fundamental mode produces neither anti- nor symmetric displacements. It can be seen that the first two modes become almost coincident. Fig.4.4.2e demonstrates this coincidental phenomenon more precisely. Usually the coincidence appears more frequently in modes of higher order.

(e) Coincident mode

It is found that the displacements at the coincident mode are very unstable. The nature of the mode is very sensitive to a slight change in eigenvalues. Iteration of ill-conditioned matrices are expected in the vicinity of the coincidence, and the coincident mode can easily be undetected if the technique of the Sturm sequence is not employed in the analysis. It is even more difficult to obtain an associated set of eigenvectors used for plotting the modal shape. Some features on the coincident mode is shown in table 4.4.2f.

(f) Modal shape

Modal shape for a particular frequency is plotted with the information given by the associated set of eigenvectors. The methods in the matrix iteration category give the eigenvectors directly. As an example, the first two modes of a square frame are shown in fig.4.4.2g.

(g) Dimensional similitude

The variables in the frequency characteristic equations (eq.4.1.2) can be re-arranged in terms of dimensionless groups, thus

$$r_s \cdot \alpha^{-2} = \sqrt{(\rho/E)}\ \omega\ L \qquad 4.4.3$$

where r_s & α are the slenderness ratio & DFP respectively.

Design tables are prepared with the idea of similitude for structures in which the topological dimensions of all members are of the same scale. The variables for similarity are slenderness ratio and DFP. A typical design table for a square frame is shown in table 4.4.2h and an application is demonstrated in table 4.4.2i. Similar tables for other structures can be prepared in the same manner.

§4.4.3 Pitched frame

Pitched frames are more widely used than other structures. Developments of the simple pitched portals are the ' Mansard ' frame and the frame with bracing beam. Typical performances of these frames, with dimensions, are tabulated in table 4.4.3a, and fig.4.4.3b shows the variation in natural frequency with different frame aspect ratios.

§4.4.4 Experiment on frame of unequal leg

A steel strip was bent into a frame as shown in fig. 4.4.4a. Steel blocks which were welded to the end of the frame were clamped to a solid rigid foundation. Harmonic displacement excitation was applied at point E by means of an electrical excitor, and an accelerometer F was attached to the frame at various positions to measure the response. The frequencies at which the response reached its maximum were the natural frequencies of the various modes. These were then compared with computed results and results by Bishop & Johnson[10] (table 4.4.4b).

§4.5 Natural Frequency of Complex Structures

§4.5.1 Engineering decision on support fixity

In theoretical analyses the support conditions are usually either considered pinned or fixed, but in practice these conditions are never completely satisfied, the actual perfórmance of the supports being somewhere between a hinge and a fixity. The natural frequencies obtained from different support conditions are compared in fig.4.5.1a. The difference in the first mode is significant. The significance decreases for higher modes and also as the number of storeys increases.

The structures are built up as multiples of single-bay single-storey frames; the multiples of these frames in the horizontal direction producing multi-bay frames, and in the vertical direction multi-storey frames. The relationship between natural frequencies and the multiplicity is obviously non-linear. These features are discussed according to the following pattern of multiples:-

TRAIN (fig.4.5.1b)
- multiples in horizontal direction only

TOWER (fig.4.5.1c)
- multiples in vertical direction only

BLOCK (fig.4.5.1d)
- multiples in both direction

§4.5.2 TRAIN

The multi-bay frame is shown in fig.4.5.1b. The first six modes are obtained and are plotted against the number of bays in fig.4.5.2. The coincident modes usually occur when the mode order is greater than four. For higher mode orders only, the frequency decreases rapidly as the number of bays increases.

§4.5.3 TOWER

The multi-storey frame is shown in fig.4.5.1c and the first six modes are plotted against the number of storeys in fig.4.5.3. The coincident modes can occur as low as in the second mode. It is obvious that the frequency decreases rapidly as the number of storeys increases.

§4.5.4 BLOCK

In the example of BLOCK (fig.4.5.1d) the number of bays is equal to the number of storeys. Anti- and symmetric modes are considered separately at the plane of symmetry, and these modes are tabulated in table 4.5.4 . It is noticed that there exists no pattern in which the modes, resulting from anti- or symmetric deflected shapes, may be ordered.

§4.5.5 Discussion

It is obvious that a lower natural frequency would be expected from a taller structure, and the example of TOWER shows that lower natural frequencies result as the number of storeys increases. Similarly, from the example of TRAIN, the natural frequency is not increased if multiples of bays are attached to each other.

On the other hand, from the example of BLOCK, a 2-bay, 2-storey structure gives a higher natural frequency than that of a single bay, 2-storey structure. The fundamental modes of these three examples are summarised in table 4.5.5 .

§4.6 Variation in Geometric Configuration

§4.6.1 Types of discontinuity

Discontinuity in this context refers to members that have step changes in sectional properties. Such changes can result from an abrupt change in cross-sectional geometry or in beam material. While property discontinuities are shown schematically as geometrically discontinuous, they can be the result of the joining of sections of the same cross-sectional geometry, but of different material properties.

Geometrical discontinuities are considered in the following cases:-

(a) EI variable, ρA unchanged; $n_a = EI_1/EI_2$

(b) ρA variable, EI unchanged; $n_b = \rho A_1/\rho A_2$

(c) a special case such that $n_c = n_a = n_b$

(d) for rectangular section, depth varied but volume of material unchanged.

The first three cases of variation can be applied to all shapes of sections. The fourth case only applies to a rectangular section in which natural frequencies can be maximised in the optimisation process. The idea of optimisation will be discussed in §4.7.

Each case of variation exhibits certain features in terms of DFP and these features are summarised in table 4.6.1 . It can be noticed that geometrical discontinuities do not change the value of the frequency parameter for extensional vibration.

§4.6.2 Discontinuity for flexural vibration in beams

Single span beams with discontinuities at mid-spans are shown in table 4.6.2a. The four mentioned cases of discontinuity are studied accordingly and the resulting variations are compared with curves in figs.4.6.2b, c, d & e. Similar procedures can be extended to continuous beams and to different arrangements of discontinuity.

§4.6.3 Discontinuity for extensional vibration in bars

Three possible types of boundary conditions for extensional vibration are studied. Due to the simplicity in the mathematical expressions and similarities in boundary conditions, the resulting natural frequencies for the four mentioned discontinuity cases are explicitly summarised in table 4.6.3a. Furthermore, the following points are noted:-

(a) As the axial stiffness does not vary results for discontinuity case (a) will be constant.

(b) The other three discontinuity cases are dependent on ρA which is the only variable, and therefore they give identical solutions.

(c) Natural frequencies are independent of geometrical discontinuity in beams having similar end boundary conditions.

§4.6.4 Discontinuity at corners

If geometrical discontinuity is introduced at the corners of a frame (fig.4.6.4a), the interaction from flexural and extensional vibration can produce more interesting variations in natural frequency. The study of a rectangular frame with the four cases of discontinuity are shown in figs.4.6.4b, c, d & e. The profiles of curves are different from those of the beams. In fig.4.6.4e, distinct peak values are obtained for the optimisation procedure.

§4.6.5 Lumped mass simplification

By this simplification a portal structure may be solved as a single degree of freedom system by manual analysis, and an estimation of the magnitude of the fundamental mode obtained quite rapidly. In applying the method to a rectangular frame the following assumptions are made:-

(i) lumped mass

(ii) exclusion of axial deformation

(iii) expected mode shape prescribed

Warburton[78] gives an example of a square frame in which sway movement is an assumed modal shape. The above three assumptions are employed and the example of a square frame is extended to any rectangular frame of various frame aspect ratio.

If the frame shown in fig.4.6.4a is reduced to a one degree of freedom system with the above three assumptions, it gives

$$\lambda L = \sqrt[4]{\frac{24}{(n_c + r_f)\, r_f^{\,3}}} \qquad 4.6.1$$

The reliability of the lumped mass simplification in a frame can be observed from the following two comparisons:-

(a) Estimated and computed results are tabulated in table 4.6.5a with different values of n_c. A significant difference is noticeable when n_c is less than 1.0, $n_c = 1.0$ being a rectangular section.

(b) For a frame of rectangular section, estimated and computed results are tabulated in table 4.6.5b with different frame aspect ratio.

§4.7 Optimised Natural Frequency

§4.7.1 Engineering decision

One of the first design decisions is the geometry of the structure, and the sectional properties of the members. In a static analysis, the design criteria would vary from stress to deflection limitation, but as far as free vibration is concerned, the most important criterion is the natural frequency. The optimised sectional properties should give the highest frequency.

If the topology of the structure and volume of material are kept constant, different natural frequencies would be expected for different volumes of material allocated to each member, and there should exist one highest natural frequency for a certain ratio of allocation.

It is obvious that the beam of fig.4.7.1a would give a higher natural frequency than that of fig.4.7.1b. It is not so obvious to make a decision on the ratio of the section depths (n_d). (The highest natural frequency is later found to occur when the depth ratio between the two sections is 0.389)

§4.7.2 The rigidity of commonly used sections

The variation of radius of gyration produces different values of natural frequency. If I is kept constant, ω will decrease with the increase of A (fig.4.7.2a). The two extreme values of radius of gyration are zero and infinity, but the commonly used sections never tend to either extreme. Table 4.7.2b is a summary of different types of sections and the manufacturer's products are well within $\pm$ 5% of these listed radii of gyration. These sections are marked accordingly on fig.4.7.2a to give a comparison.

§4.7.3 Continuous beams

The simplest demonstration of optimisation is described with beams. Both flexural and extensional vibrations are separately considered, and the optimised natural frequency is compared with its equivalent uniform section for the optimised percentage. The layout of the examples is illustrated in §4.6.2 & §4.6.3, from which the information in table 4.7.3 is extracted.

§4.7.4 Frames

The frame considered in §4.6.4 supplies the information for optimisation. The optimised values are tabulated in table 4.7.4 .

§4.7.5 Bridge

The principle of optimisation can be extended to other structures such as bridges which are composed of continuous beams and columns. Consider the bridge whose topology is shown in fig.4.7.5a. By altering the section depths to those shown in fig.4.7.5b the natural frequency is increased by 27%. Table 4.7.5c shows the progression to the optimised state.

The rapid convergence to the highest natural frequency suggests that two iterations are adequate. Further improvement will involve the curtailment of beams into stepped beams, or with greater sophistication, the introduction of tapered sections. These will be investigated later.

§4.7.6 Comment on optimisation

Hollow sections which reduce the weight but still maintain the rigidity of the section are favoured in vibration. As can be seen in table 4.7.2b, a steel box section can have a natural frequency 2.7 times higher than that of a concrete rectangular section.

The natural frequency can also be increased by a logical choice of sectional dimensions. In some cases the optimum design is a structure with members of identical section; a step in a span may result in a tremendous decrease in natural frequency. In some particular cases, natural frequency is independent of the change in sections, especially in extensional vibration. In many cases, an intelligent choice of section can increase the natural frequency by as much as 66% as is shown for a stepped cantilever beam.

A stepped cantilever beam with thicker section at the fixed end and a thinner section at the free end is a primary generating idea in having a tapered section which would increase the natural frequency and eliminate an awkward step in mid-span.

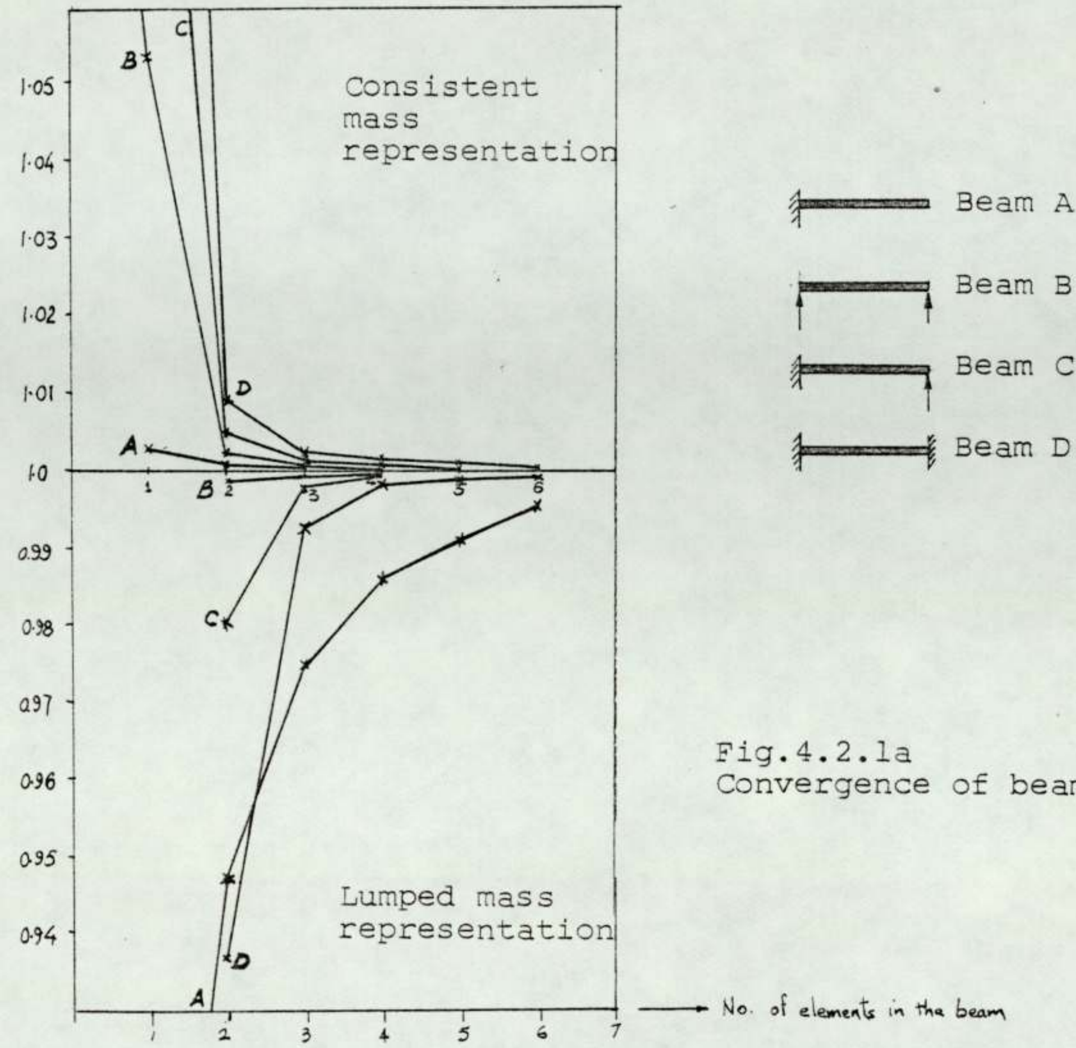

Fig.4.2.1a
Convergence of beams

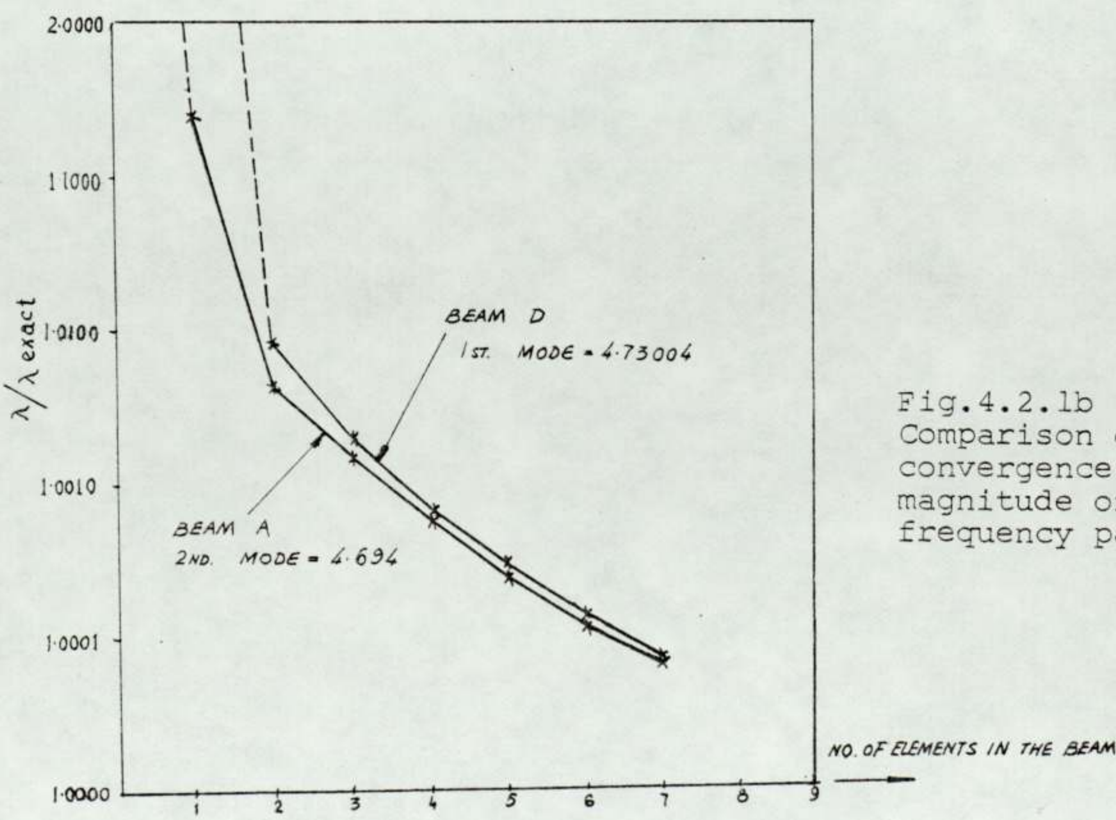

Fig.4.2.1b
Comparison of
convergence on the
magnitude of the
frequency parameters

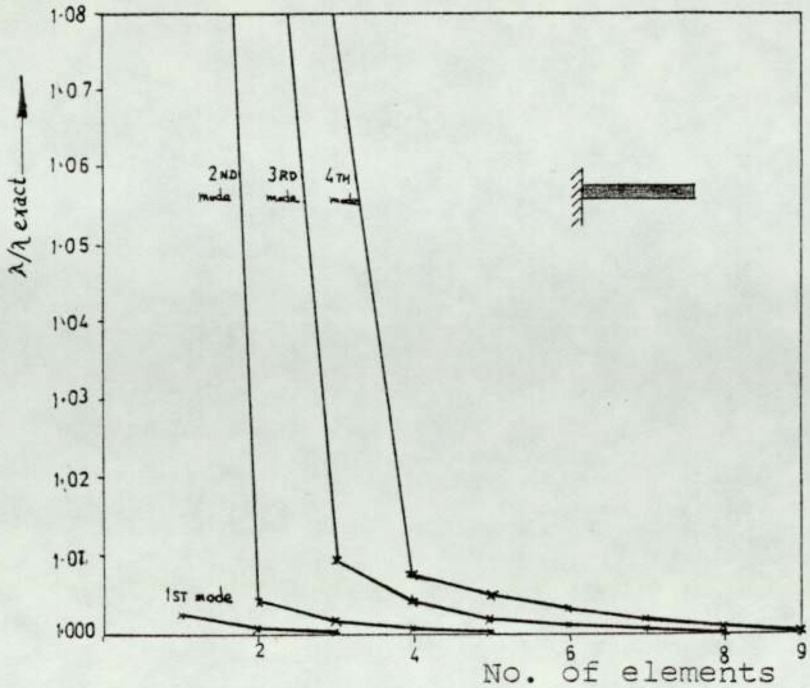

Fig.4.2.1d
Convergence of higher modes in
a free cantilever beam

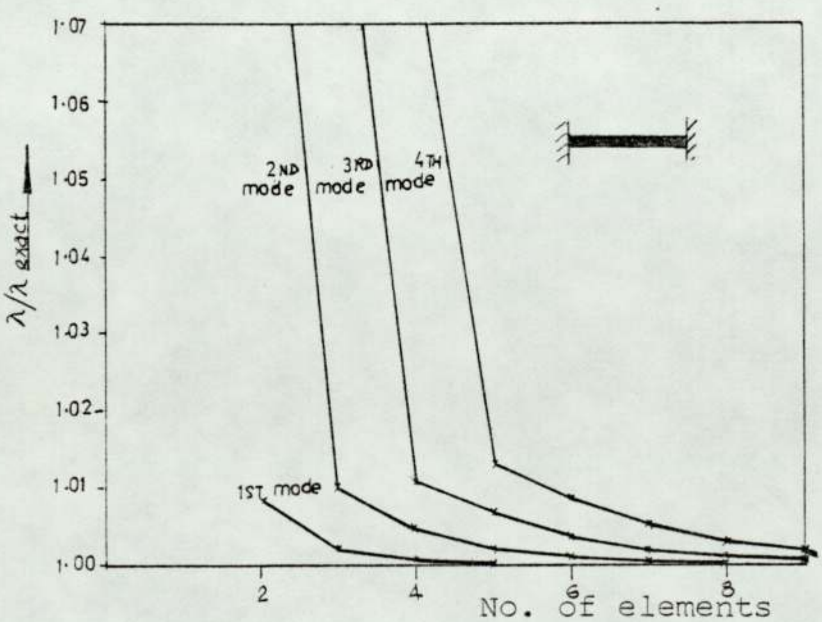

Fig.4.2.1d
Convergence of higher modes in an encastre beam

Table 4.2.2a Convergence of lumped & consistent mass representation

No. of elements in each member	ω / ω_{exact} LUMPED	ω / ω_{exact} CONSISTENT	
1	2.111	1.055	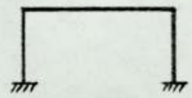
2	0.921	1.012	γ_f = 0.3
3	0.989	1.002	γ_s = 50
4	0.997	1.000	Exact solution = 18.26 Hz
5	0.999	1.000	

Table 4.2.2b Convergence of Frame

No. of elements in each member	$\omega_{polynomial} / \omega_{exact}$				
	γ_f = 0.4	γ_f = 0.5	γ_f = 0.6	γ_f = 0.7	
1	1.0028	1.0017	1.0014	1.0012	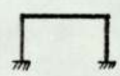
2	1.0008	1.0004	1.0002	1.0002	
3	1.0003	1.0001	1.0001	1.0000	γ_f = H/L
4	1.0000	1.0000	1.0000	1.0000	γ_s = 50
Exact solution (Hz)	12.92	9.41	7.20	5.72	

Table 4.2.2c Convergence of multi-bay frames

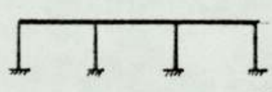

Natural frequency from Polynomial function (Hz)		No. of Bays 1	2	3	4	5	6
No. of elements in each member	1	10.625	9.748	9.464	9.308	9.212	9.146
	2	10.617	9.742	9.460	9.303	9.208	9.143
	3	10.612	9.735	9.454	9.299	9.203	9.138
Exact solution		10.609	9.733	9.452	9.296	9.201	9.136

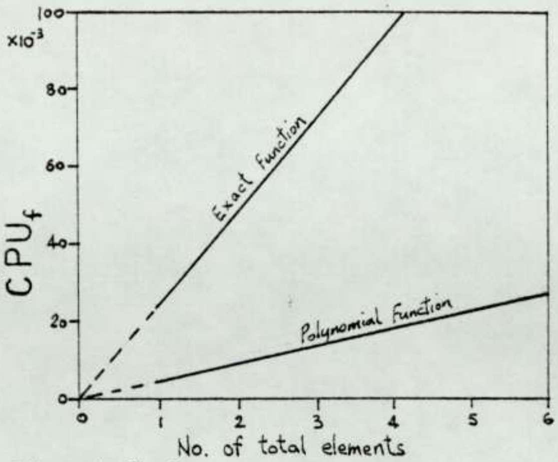

Fig.4.2.3a
CPU for matrix formulation

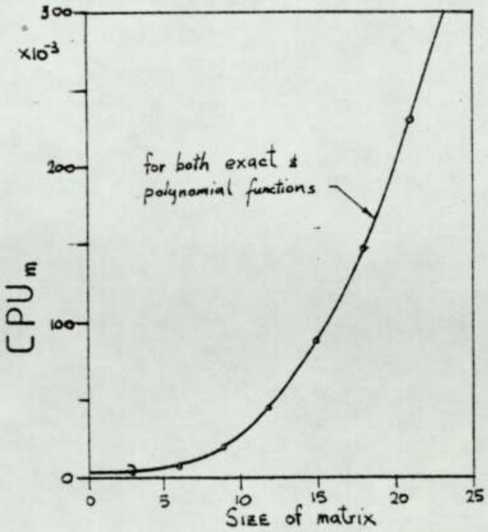

Fig.4.2.3b
CPU for matrix manipulation

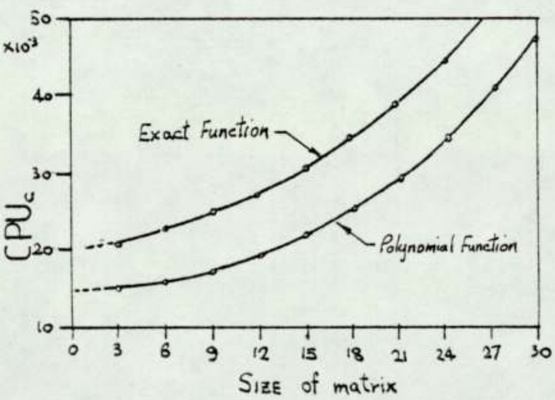

Fig.4.2.3c
CPU for steering instruction

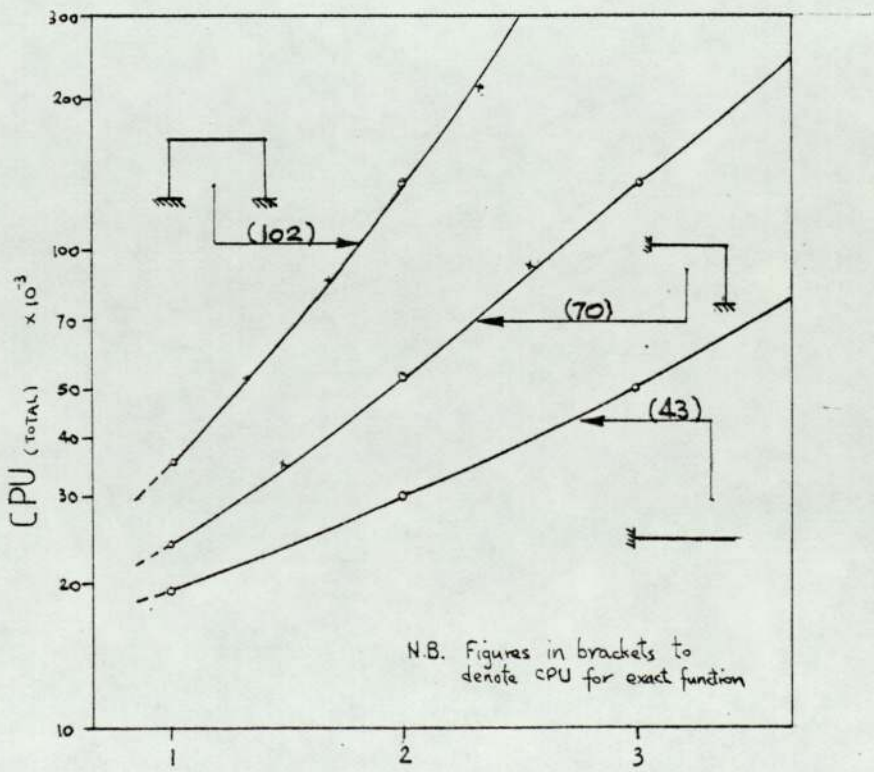

Fig.4.2.3d
CPU in typical example structures for polynomial function

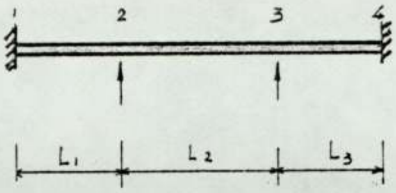

Fig.4.3.1a
A continuous beam

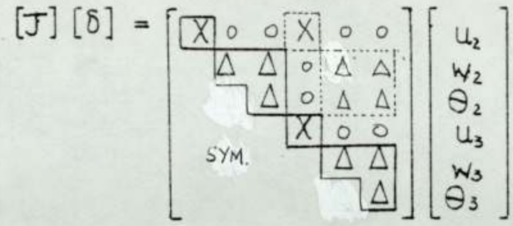

O – ZERO ELEMENT
X – ELEMENTS FOR EXTENSIONAL VIBRATION
Δ – ELEMENTS FOR FLEXURAL VIBRATION

Fig.4.3.1b
Matrix formulation for dual vibration

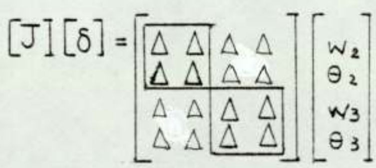

Fig.4.3.1c
Matrix formulation for flexural vibration

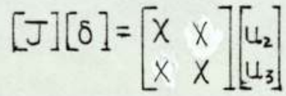

Fig.4.3.1d
Matrix formulation for extensional vibration

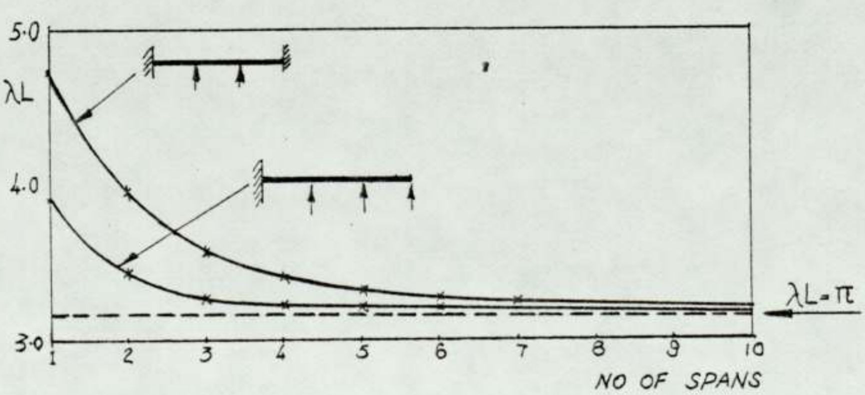

Fig.4.3.5c Fundamental mode of continuous beams

Table 4.3.3a Natural frequency of beams in flexural vibration

Beam Ref.	Boundary Conditions	Order of Mode ($\alpha = \lambda L$) 1st	2nd	3rd	4th	nth
BM1		1.875	4.694	7.855	10.996	$(2n-1)\pi/2$
BM2		π	2π	3π	4π	$n\pi$
BM3		3.927	7.067	10.210	13.352	$(4n+1)\pi/4$
BM4		4.730	7.853	10.996	14.137	$(2n+1)\pi/2$

Table 4.3.3b Natural frequency of Bars in extensional vibration

Bar Ref.	Boundary Conditions	$\beta =$ L for nth mode	Remark
BR1		$(n-1)\pi$	
BR2		$(2n-1)\pi/2$	$\alpha=\sqrt{\beta r_s}$
BR3		$(2n-1)\pi$	

Table 4.3.3c Natural frequency of Beam structures

Beam & Bar Ref.	Beam Structures	Order of Mode (λ L) $(r_s)^2=1000$ 1st	2nd	3rd	4th	5th	6th
BM1+BR2		1.875	4.694	(7.048)	7.855	10.996	(12.207)
BM2+BR2		π	2π	(7.048)	3π	(12.207)	4π
BM3+BR2		3.927	(7.048)	7.069	10.210	(12.207)	13.352
BM4+BR3		4.730	7.853	(9.967)	10.996	14.137	(17.264)

N.B. Figures in brackets for extensional mode.

Table 4.3.4a Dimensionless Frequency Parameter of Continuous beams

System of continuous beams	no. of spans	Mode order 1st	2nd	3rd	4th	5th	6th	7th	8th	9th	10th
System A	1	π	2π	(9.33)	3π	4π	5π	(16.16)	6π	(20.86)	7π
	2	π	3.93	2π	(6.60)	7.07	3π	10.21	(11.43)	4π	13.35
	3	π	3.56	4.30	(5.39)	2π	6.71	7.43	(9.33)	3π	9.85
	4	π	3.39	3.93	4.46	(4.66)	2π	6.54	7.07	7.59	(8.08)
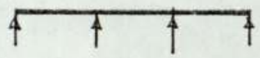	5	π	3.31	3.70	4.15	(4.17)	4.55	2π	6.46	6.85	(7.23)
	6	π	3.26	3.56	(3.81)	3.93	4.30	4.60	2π	6.41	(6.60)
	7	π	3.23	3.46	(3.53)	3.76	4.09	4.40	4.63	(6.11)	2π
	8	π	3.21	(3.30)	3.39	3.64	3.93	4.21	4.46	4.66	(5.71)
	9	(3.11)	π	3.20	3.34	3.56	3.80	4.05	4.30	4.51	4.67
	10	(2.95)	π	3.19	3.31	3.49	3.70	3.93	4.15	4.37	4.55
System B	1	3.93	7.07	(9.33)	10.21	13.35	(16.16)	16.49	19.64	(20.86)	22.78
	2	3.39	4.46	6.54	(6.60)	7.59	9.69	10.73	(11.43)	12.83	13.88
	3	3.26	3.93	4.60	(5.39)	6.41	7.07	7.73	(9.33)	9.55	10.21
	4	3.21	3.64	4.21	4.66	(4.67)	6.36	6.80	7.34	7.78	8.08
	5	3.19	3.49	3.93	(4.17)	4.37	4.68	6.33	6.64	7.07	7.23
	6	3.17	3.39	3.74	(3.81)	4.12	4.46	4.70	6.32	6.54	6.60
	7	3.16	3.33	(3.53)	3.61	3.93	4.25	4.53	4.71	(6.11)	6.31
	8	3.16	3.29	(3.30)	3.51	3.78	4.07	4.34	4.57	4.71	5.71
	9	(3.11)	3.16	3.26	3.44	3.68	3.93	4.18	4.41	4.60	4.72
	10	(2.95)	3.15	3.24	3.39	3.59	3.81	4.04	4.26	4.46	4.62
System C	1	α_1	α_2	α_3	α_4	(13.20)	α_5	α_6	(22.86)	α_7	α_8
	2	3.93	α_1	7.07	α_2	(9.33)	10.21	α_3	13.20	13.35	α_4
	3	3.56	4.30	α_1	6.71	7.43	(7.62)	α_2	9.85	10.57	(10.77)
	4	3.39	3.93	4.46	α_1	6.54	(6.60)	7.07	7.59	α_2	(9.33)
	5	3.31	3.70	4.15	4.55	α_1	(5.90)	6.46	6.85	7.29	7.68
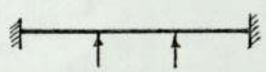	6	3.26	3.56	3.93	4.30	4.60	α_1	(5.39)	6.41	6.71	7.07
	7	3.23	3.46	3.76	4.09	4.40	4.63	α_1	(4.99)	6.38	6.61
	8	3.21	3.39	3.64	3.93	4.21	4.46	4.66	(4.66)	α_1	6.36
	9	3.20	3.34	3.56	3.80	4.05	4.30	(4.40)	4.51	4.67	α_1
	10	3.19	3.31	3.49	3.70	3.93	4.15	4.17	4.37	4.55	4.68

N.B.
Figures in brackets for extensional mode

$\alpha_1 = 4.73004$
$\alpha_2 = 7.85320$
$\alpha_3 = 10.9956$
$\alpha_4 = 14.1372$
⋮

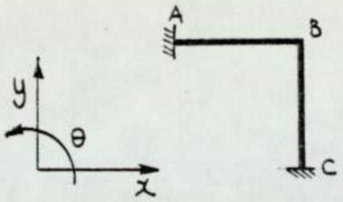

Fig.4.4.1a A cranked frame

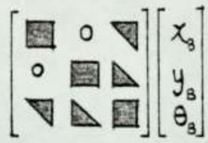

Fig.4.4.1b Overall matrix

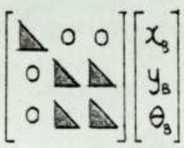

Fig.4.4.1c
Matrix of member AB

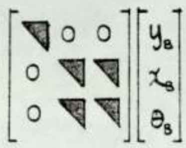

Fig.4.4.1d
Matrix of member BC

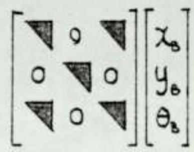

Fig.4.4.1e
Re-orientated matrix of member BC

Table 4.4.2a
Natural frequency of different slendernes ratio

r_s	Frequency		Structure
	α	HZ	
250	1.2095	0.30	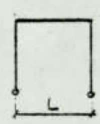
200	1.2095	0.38	
150	1.2094	0.50	
100	1.2093	0.75	
50	1.2087	1.50	
20	1.2042	2.72	$r_f = 1.0$
10	1.1887	7.26	

N.B. $r_s = \sqrt{(AL/I)}$

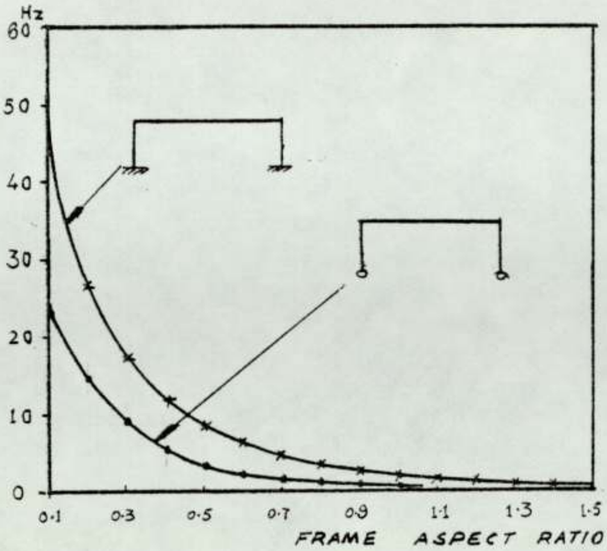

Fig.4.4.2b The first anti-symmetric mode of different frame aspect ratios

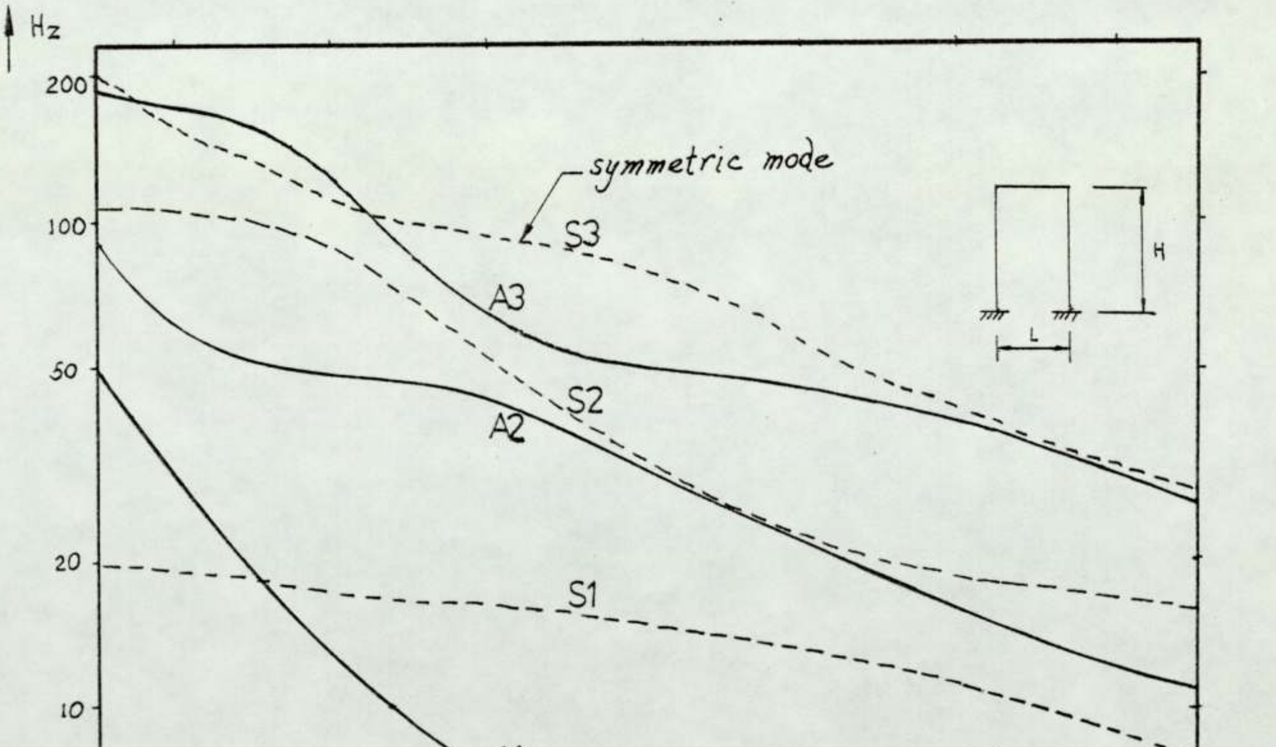

Fig.4.4.2c Symmetric and anti-symmetric modes of different frame aspect ratios

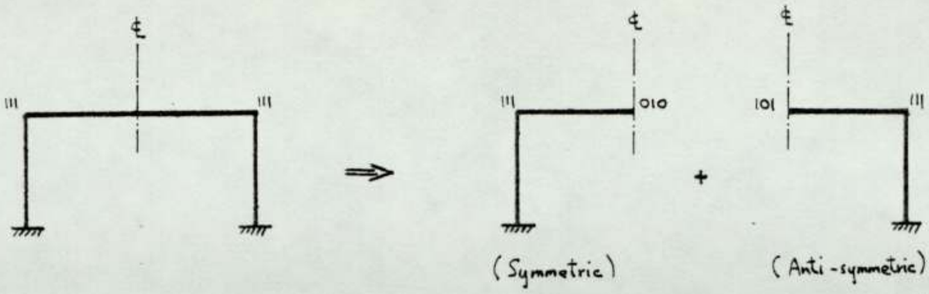

(INTEGER REPRESENTATION as shown in fig 9.3.1a)

Fig.4.4.2d The symmetry of a frame

Table 4.4.2e
Natural frequencies of symmetric & anti-symmetric modes

r_f	1st Mode	2nd Mode
0.3105	(18.172)	18.268
0.3110	(18.168)	18.229
0.3110	(18.163)	18.190
0.3116	(18.162)	18.182
0.3117	(18.162)	18.174
0.3118	(18.161)	18.167
0.3119	18.160	18.160
0.3120	18.151	(18.159)
0.3140	17.997	(18.143)
0.3150	17.921	(18.134)
0.3160	17.845	(18.126)
0.3180	17.695	(18.110)

← coincident mode

N.B. figures in brackets for extensional modes

Table 4.4.2f Features of the coincident mode

Dimensions	Frequency	Modal shape
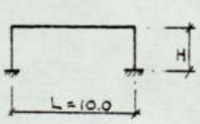 $r_f = 0.3119$ $r_s = 50$	$\alpha=4.2043$ $f=18.160$ The coincidence of the 1st & 2nd mode	

Fig.4.4.2g Modal shapes of a square frame

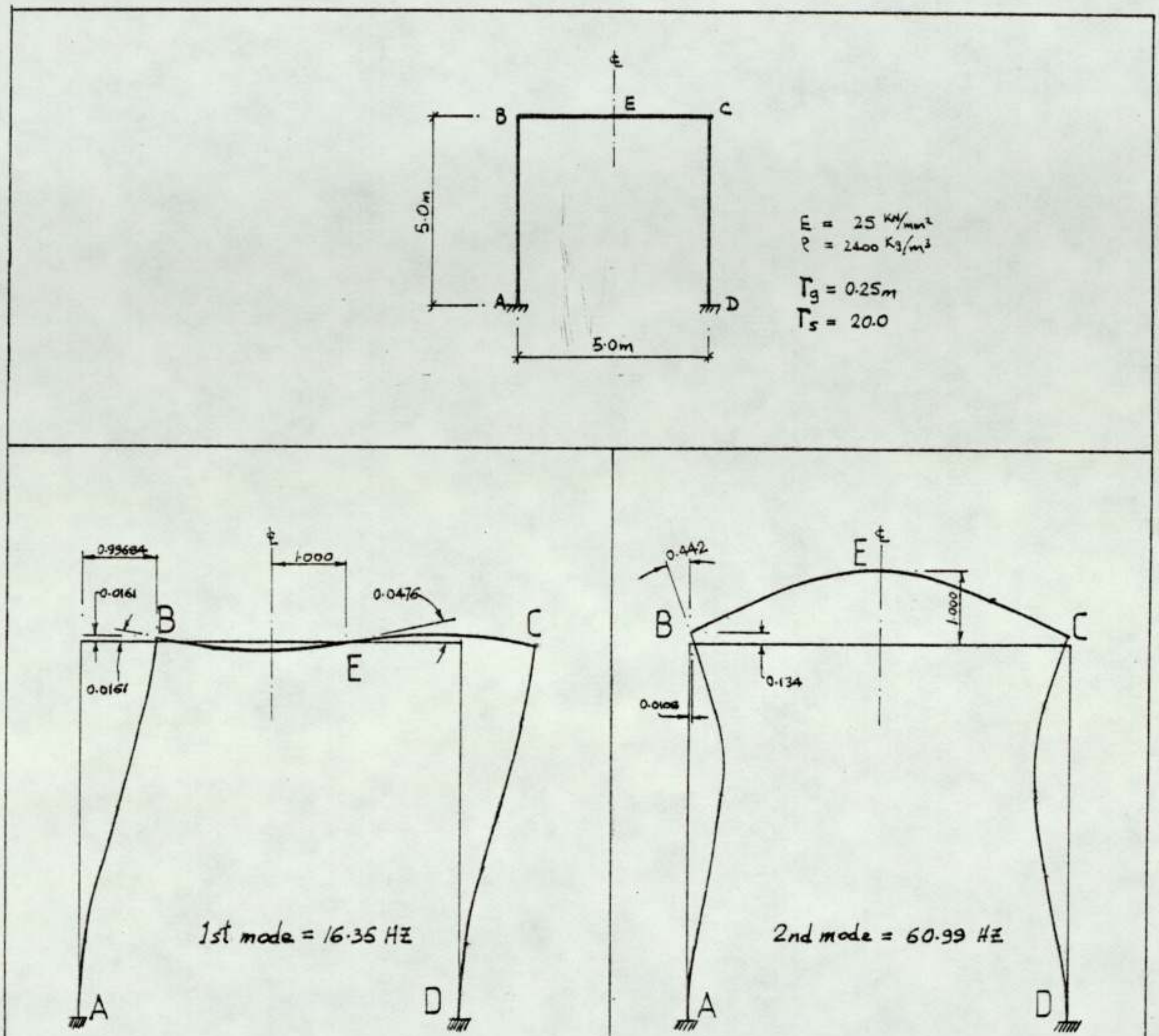

If the slope displacement at joint B to be normalised,

	1st mode	2nd mode
X_B	8.7392	0.0240
Y_B	0.1409	0.3024
θ_B	-1.0000	1.0000
X_E	8.7669	0.0000
Y_E	0.0000	2.2619
θ_E	0.4170	0.0000

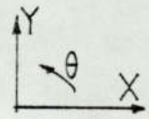

Table 4.42h DFP for a square frame

Mode order	Slenderness ratio (r_s)						
	10	20	50	100	150	200	250
1	1.766	1.784	1.789	1.790	1.790	1.790	1.790
2	(3.038)	(3.446)	(3.541)	(3.552)	(3.555)	(3.556)	(3.556)
3	3.675	(4.422)	4.539	4.541	4.542	4.542	4.542
4	(3.849)	4.525	(4.687)	(4.720)	(4.725)	(4.727)	(4.728)
5	4.474	5.058	6.559	6.693	6.710	6.716	6.719
6	(4.631)	(5.660)	(7.355)	(7.413)	(7.422)	(7.426)	(7.427)
7	(5.474)	(6.670)	7.759	7.956	7.977	7.984	7.987
8	6.116	6.914	(8.277)	(9.716)	(9.805)	(9.826)	(9.835)

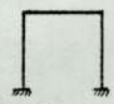

$r_f = 1.0$

N.B. Figures in brackets for symmetric mode.

Table 4.4.2i Application of table 4.4.2h

Structure	Geometrical Dimension			r_s	Frequency		
	I	A	L		mode order	α from table	$f = \alpha^2 \sqrt{\frac{E}{\rho}} \frac{r_s}{2\pi L^2}$
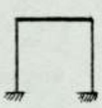	1.61	3.0	11.0	225	1st 8th	1.790 9.830	1.03 HZ 31.07 HZ
$r_f = 1.0$ $\sqrt{\frac{E}{\rho}} = 5000$	0.267	0.25	4.0	15	1st 8th	1.775 6.525	41.78 HZ 564.68 HZ

Table 4.4.3a Typical examples of pitched portals

Type		pinned	fixed	Mansard	With bracing beam
Frames with Dimension		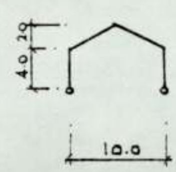	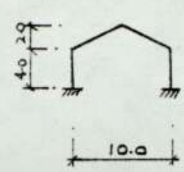	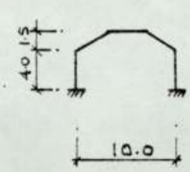	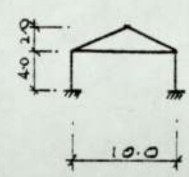
Frequency	α	2.275	3.378	3.323	3.154
	HZ	5.32	11.72	11.35	10.22
Remark		$r_g = 0.20$	$\sqrt{\frac{E}{\rho}} = 3227$	$f = \alpha^2 \sqrt{\frac{E}{\rho}}\, r_g/2\pi L^2$	

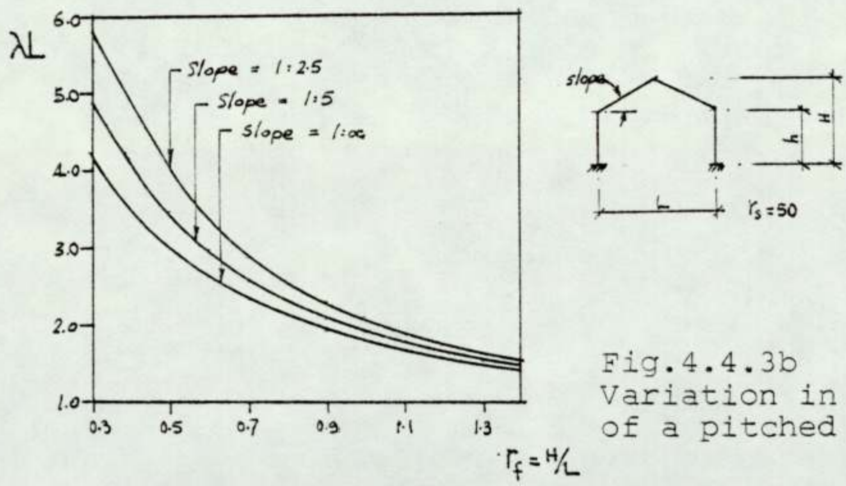

Fig.4.4.3b
Variation in frame aspect ratio of a pitched portal

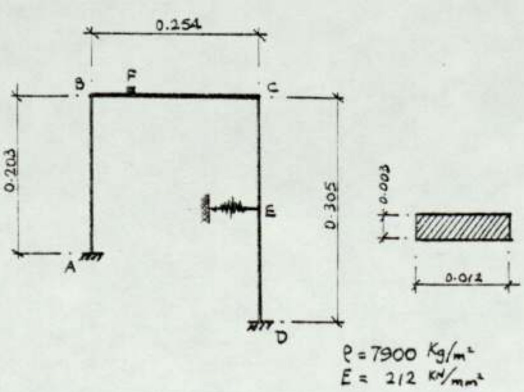

Fig.4.4.4a
An unequal leg frame

Table 4.4.4b
Frequencies of an unequal leg frame

Mode order	From Bishop & Johnson	Results		
		Experimental (HZ)	Computed (HZ)	% difference
1	42.5	42.3	40.57	4.3
2	147	141.2	139.39	1.3
3	215	197.8	201.42	1.8
4	377	355.7	358.42	0.8
5	475	455.6	448.43	1.6

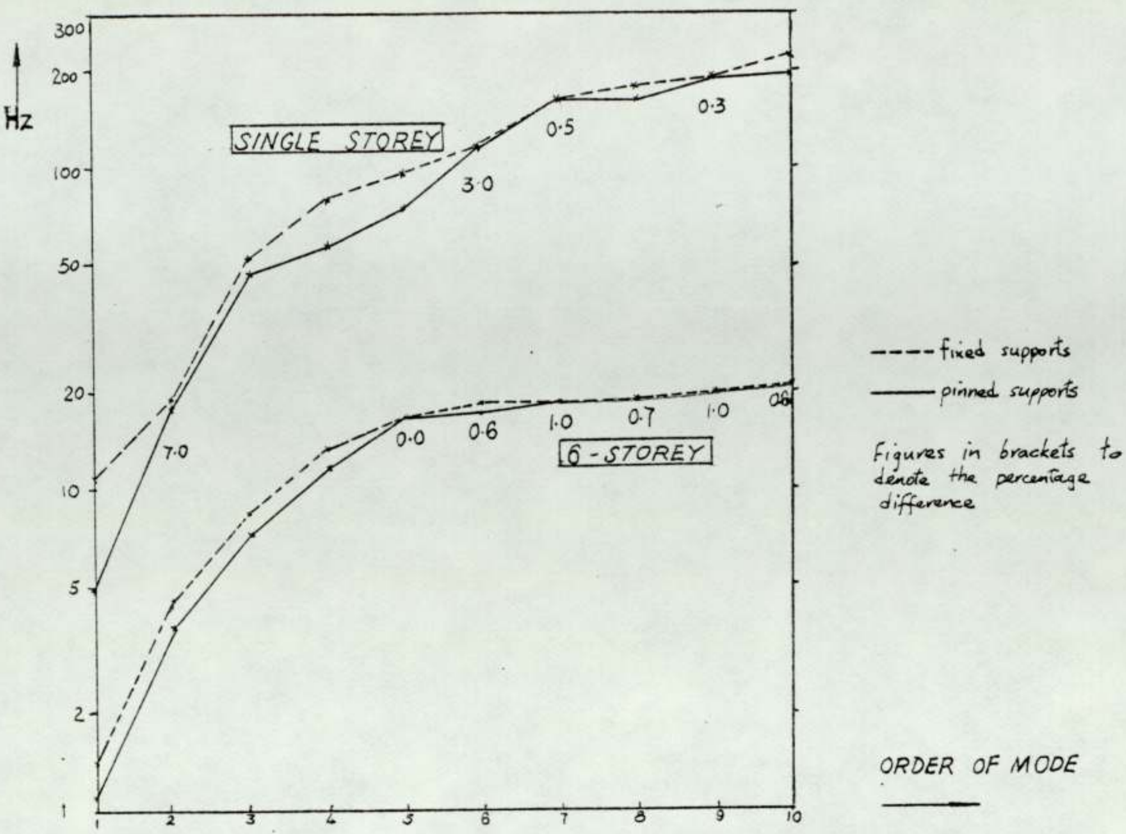

Fig.4.5.1a Comparison of support fixity

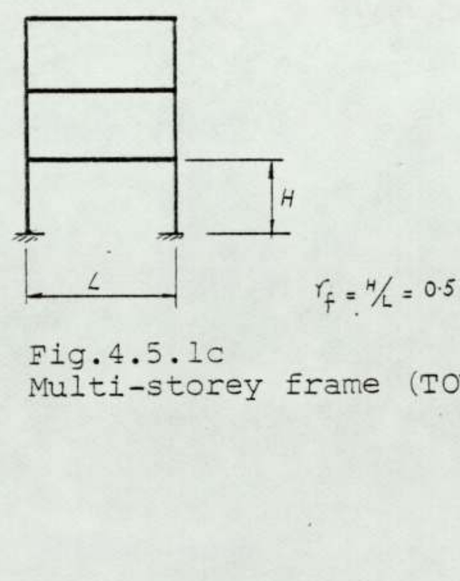

Fig.4.5.1c
Multi-storey frame (TOWER)

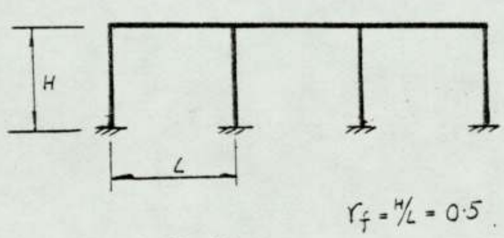

Fig.4.5.1b
Multi-bay frame (TRAIN)

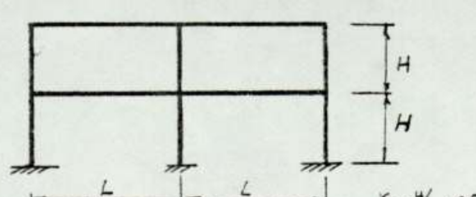

Fig.4.5.1d
Multi-bay multi-storey frame (BLOCK)

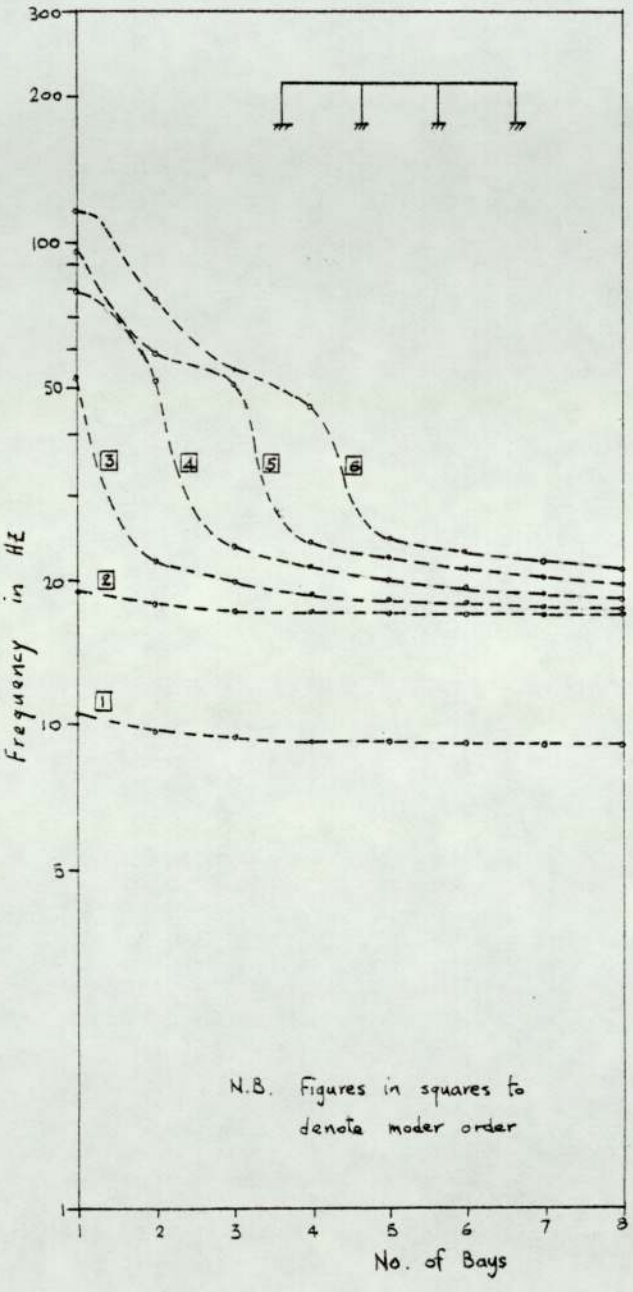

Fig.4.5.2
Natural frequency of TRAIN

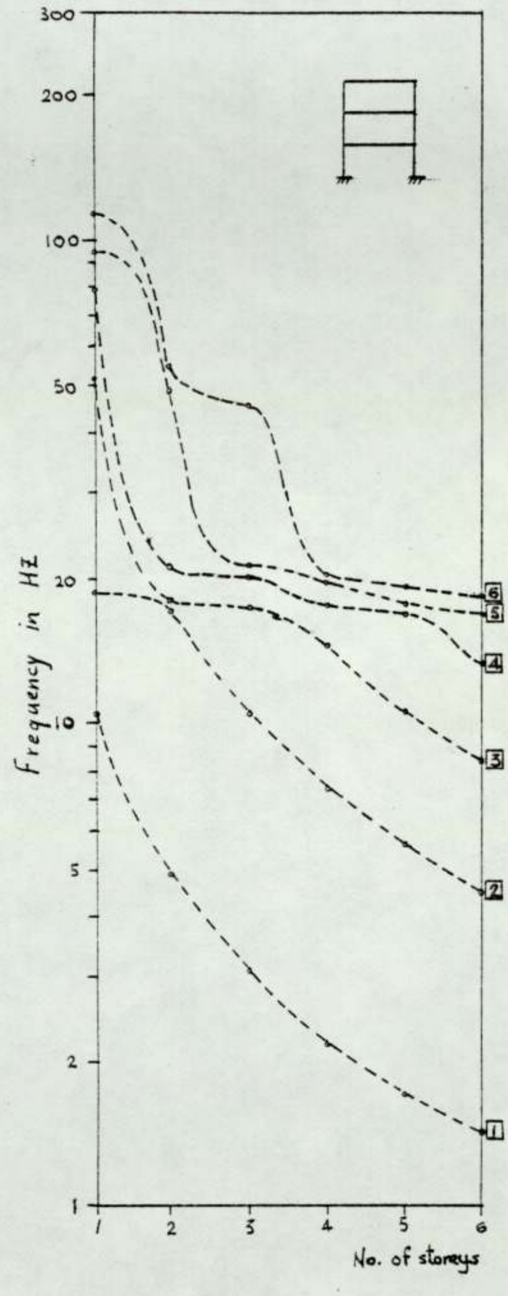

Fig.4.5.3
Natural frequency of TOWER

Table 4.5.4 Natural Frequency of BLOCK

Mode Order	No. of storeys 1	2	3	4	5	6
1	10.61	7.82	4.97	3.64	2.88	2.38
2	(18.90)	25.97	16.51	11.79	9.14	7.46
3	52.39	28.79	(27.29)	21.70	16.58	13.33
4	(79.10)	33.98	29.80	26.88	24.99	20.07
5	96.08	(35.11)	(31.67)	(29.37)	(26.69)	26.53
6	(115.43)	(38.21)	31.69	30.26	28.36	(26.94)
7	161.47	81.46	(34.07)	31.82	(29.40)	27.19
8	(176.41)	(86.91)	34.75	(32.50)	(30.12)	27.35
9	(189.03)	92.47	(35.91)	32.67	(30.27)	(27.69)
10	220.86	(93.07)	36.11	32.78	30.35	(28.02)

frequencies in brackets for symmetric modes

Table 4.5.5 Fundamental modes in complex structures

BLOCK

TOWER

No. of Storeys	No. of Bays 1	2	3	4	5	6
6	1.408					2.38
5	1.723				2.88	
4	2.210			3.64		
3	3.062		4.97			
2	4.880	7.82				
1	10.61	9.733	9.452	9.296	9.201	9.136

TRAIN

N.B. Frequencies in HZ

Table 4.6.1 Cases of discontinuity

Case	a	b	c	d
Ratio	$n_a = \frac{EI_1}{EI_2}$	$n_b = \frac{\rho A_1}{\rho A_2}$	$n_c = \frac{EI_1}{EI_2} = \frac{\rho A_1}{\rho A_2}$	$n_d = \frac{d_1}{d_2}$
Flexural Vibration	$n_a \lambda_1^4 = \lambda_2^4$	$\lambda_1^4 = n_b \lambda_2^4$	$\lambda_1 = \lambda_2$	$n_d \lambda_1^2 = \lambda_2^2$
Extensional Vibration	$\gamma_1 = \gamma_2$	$\gamma_1 = \gamma_2$	$\gamma_1 = \gamma_2$	$\gamma_1 = \gamma_2$

Table 4.6.2a Discontinuity in mid span of beams

Beam	A	B	C	D
Boundary Condition	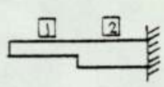	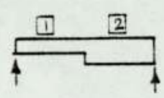	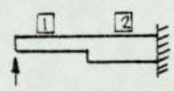	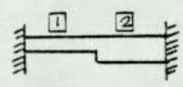

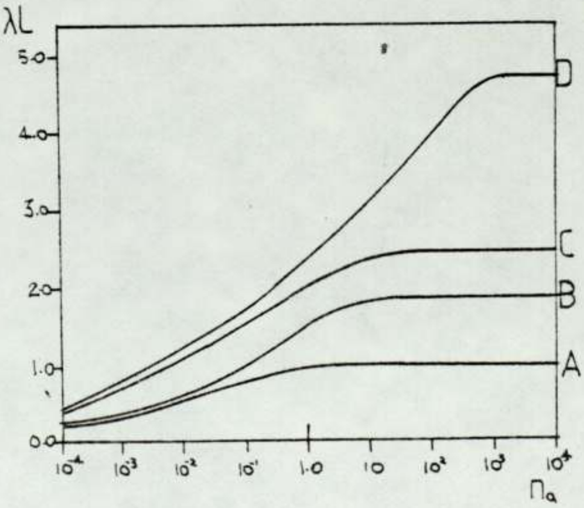

Fig.4.6.2b
Variation in n_a

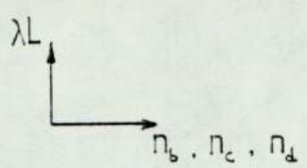

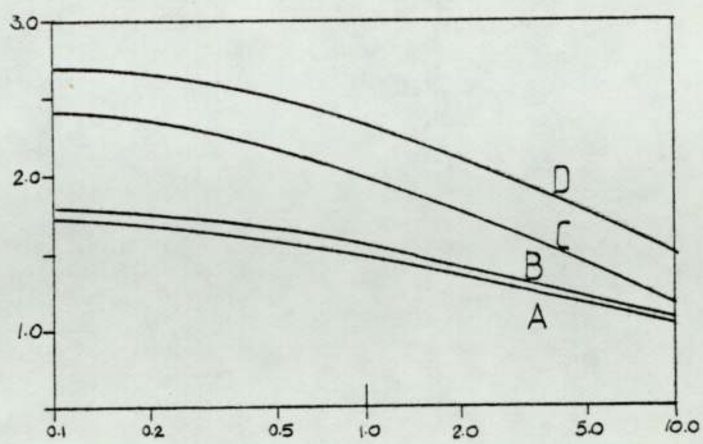

Fig.4.6.2c
Variation in n_b

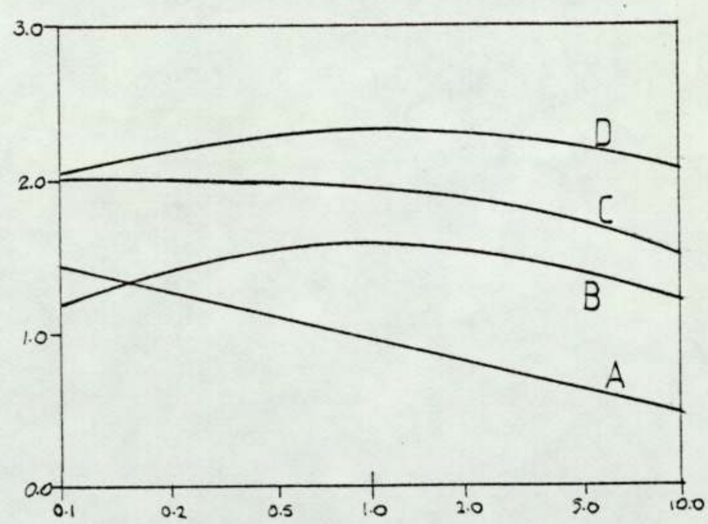

Fig.4.6.2d
Variation in n_c

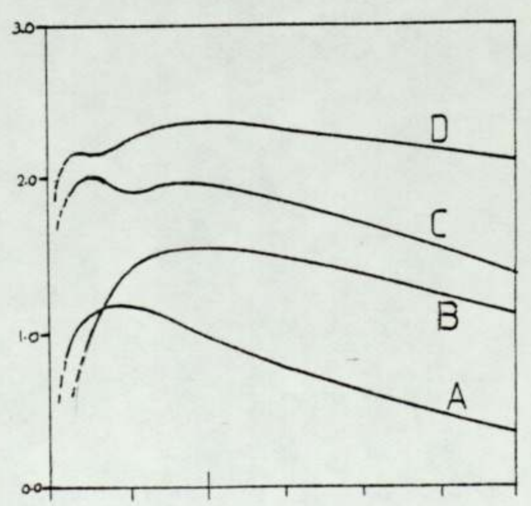

Fig.4.6.2e
Variation in n_d

Table 4.6.3a Discontinuity for extensional vibration

BAR		case of discontinuity a	b	c	d
A	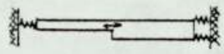	$\gamma L = 0.0$ for all			
B	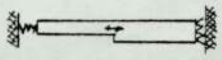	Constant $\gamma L = \pi/4$	Variation, fig.4.6.3b		
C	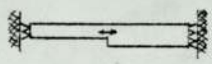	constant, $\gamma L = \pi/2$			

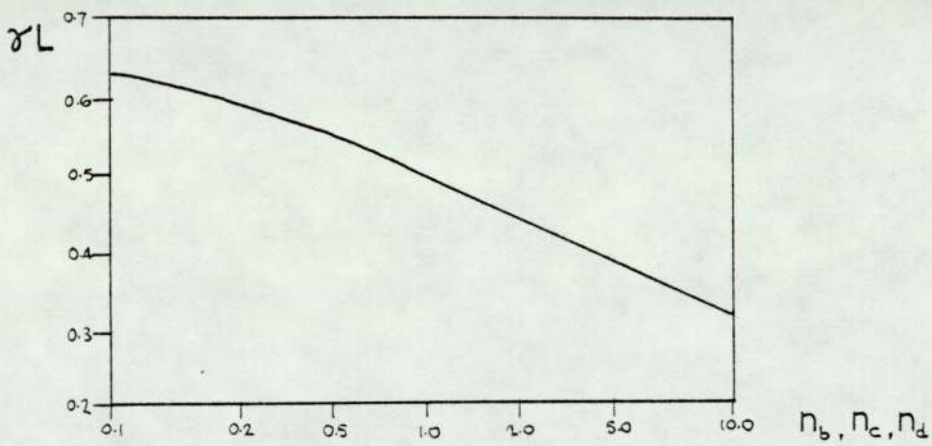

Fig.4.6.3b Discontinuity in Bar-B

Table 4.6.5a
Variation in n_c

$n_c = EI_1/EI_2 = \rho A_1/\rho A_2$	DFP (λL) $\lambda L = \sqrt{\frac{24}{n_c+1}}$	computer result	% error
0.5	2.0000	1.8881	5.9
1.0	1.8612	1.7891	4.0
2.0	1.6818	1.6400	2.5
5.0	1.4142	1.3597	1.3
10.0	1.2154	1.2052	0.8

Table 4.6.5b
Variation in r_f

r_f	$\lambda L = \sqrt[4]{\frac{24}{(r_f+1)r_f^3}}$	computer result	% error
0.3	5.1130	4.2158	21.2
0.4	4.0455	3.5465	14.0
0.5	3.3636	3.0257	11.1
0.6	2.8868	2.6475	9.0
0.7	2.5329	2.3588	7.2
0.8	2.2590	2.1302	6.0
0.9	2.0402	1.9440	4.9
1.0	1.8612	1.7891	4.0
1.1	1.7118	1.6580	3.1
1.2	1.5851	1.5455	2.5

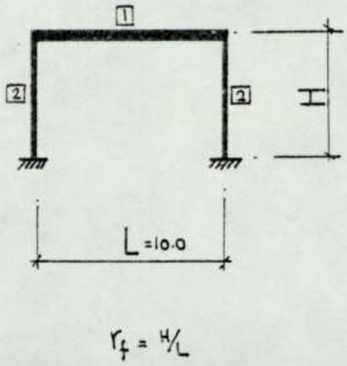

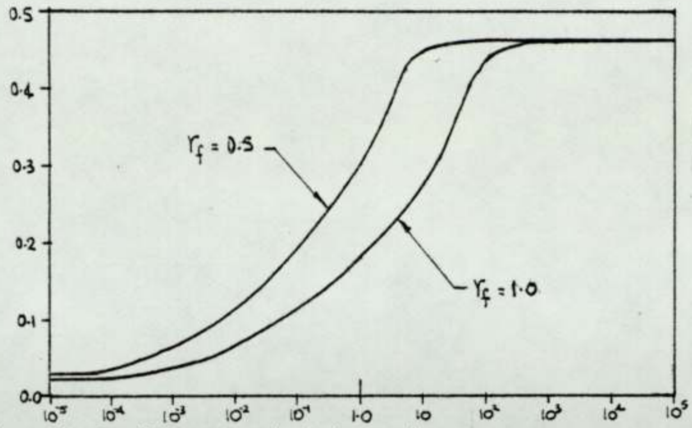

Fig.4.6.4a
Discontinuity at corners of a frame

Fig.4.6.4b Variation in n_a

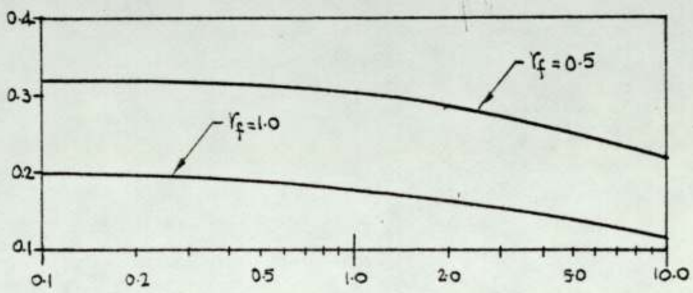

Fig.4.6.4c
Variation in n_b

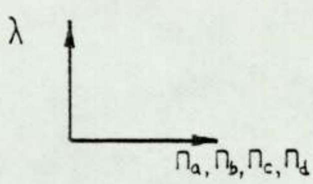

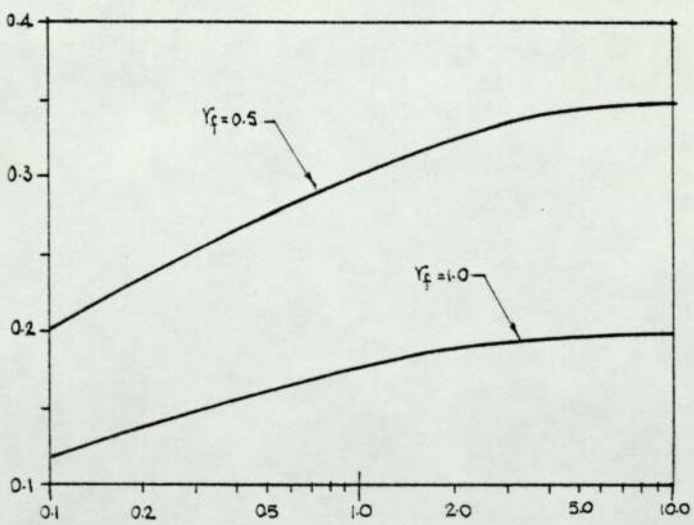

Fig.4.6.4d
Variation in n_c

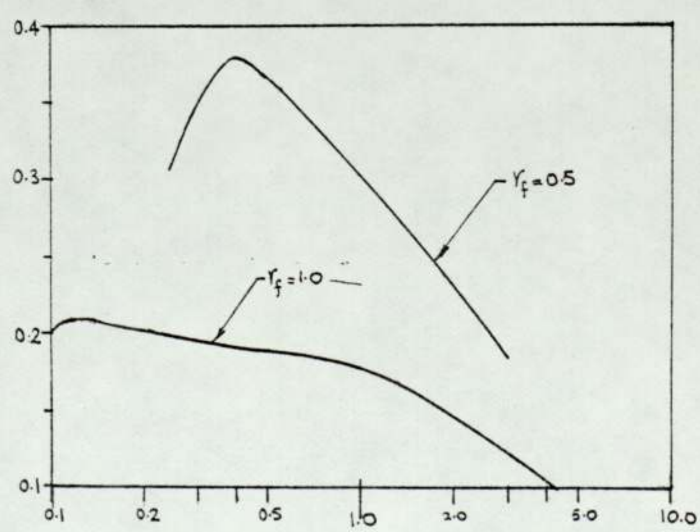

Fig.4.6.4e
Variation in n_d

Fig.4.7.1a
Stepped Cantilever Beam with shallow end being free

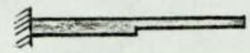

Fig.4.7.1b
Stepped Cantilever Beam with deep end being free

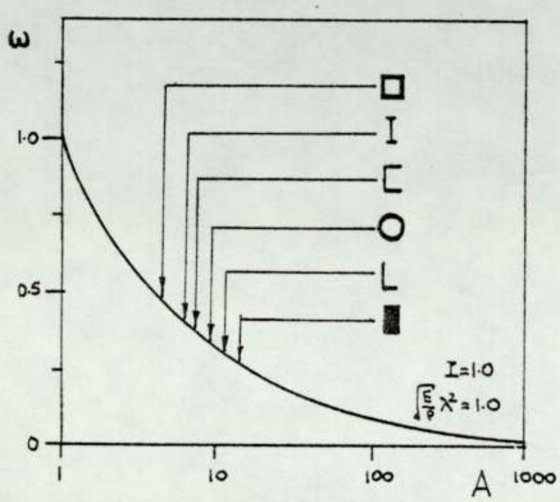

Fig.4.7.2a
Cross-sectional area in commonly used section

Table 4.7.2b
r_g of commonly used sections

Section	Shape	r_g/D
Box	□	0.47
Universal	I	0.40
Channel	[	0.38
Hollow	O	0.34
Angle	L	0.30
Rectangular	■	0.29

D = extensional dimension about an axis of vibration

Table 4.7.3 Optimisation in beams

Type of Vibration	Beam / Bar	Optimised section d_1/d_2	Optimised section λL	Uniform Section λL	Optimised percentage
Flexural	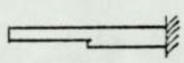	0.389	2.4138	1.8752	66%
	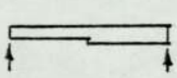	1.0	no optimisation		
	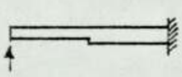	0.220	4.0118	3.9266	4%
	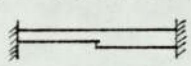	1.0	no optimisation		
Extensional	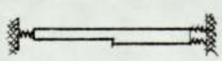	constant	not applicable		
	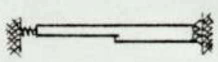	0.0	10.432	7.3766	200%
	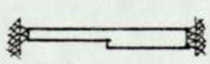	constant	not applicable		

Table 4.7.4 Optimisation in frame

Notation	r_f	Optimised structure		Frequency of Equivalent Uniform section	Optimised %
		Structure (to scale)	Frequency		
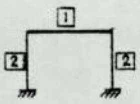	0.5	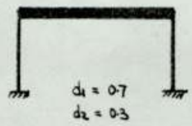	α=3.8216 f=9.34HZ	α=3.0269 f=6.79HZ	38%
b=0.3 L=10.0 (dimensions in m)	1.0	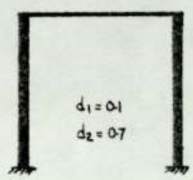	α=2.0873 f=3.23HZ	α=1.7896 f=2.36HZ	36%

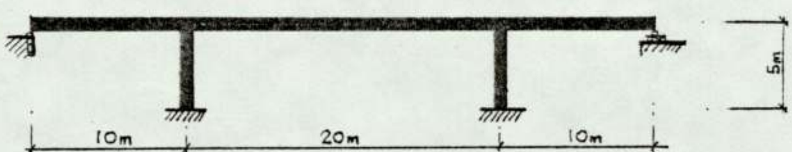

Fig.4.7.5a
Bridge with members of identical rectangular section

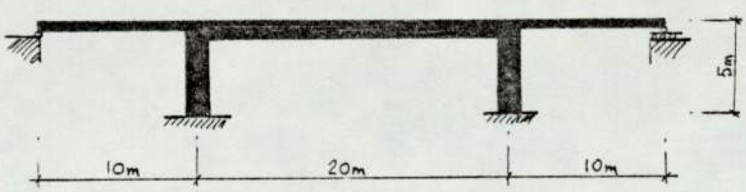

Member	d
End span	0.50 m
Middle span	1.25 m
Column	1.50 m

Fig.4.7.5b
Bridge of optimised section

Table 4.7.5c Optimisation in a bridge

Trial Nº.	Section (depth)			Natural Freq.		Remark
	End span	Mid span	Column	Hz	Mode shape	
First Trial	0.2	1.8	1.0	4.566	S	
	0.4	1.6	1.0	8.106	A	*
	0.6	1.4	1.0	7.755	A	
	0.2	1.55	1.5	4.568	A	
	0.4	1.35	1.5	8.988	A	⊛
	0.6	1.15	1.5	8.504	S	
	0.2	1.30	2.0	4.569	A	
	0.4	1.10	2.0	8.611	S	*
	0.6	0.90	2.0	7.221	S	
Second Trial	0.4	1.5	1.2	8.749	S	
	0.5	1.4	1.2	8.766	S	*
	0.6	1.3	1.2	8.498	S	
	0.4	1.35	1.5	8.988	A	
	0.5	1.25	1.5	8.991	S	⊛
	0.6	1.15	1.5	8.504	S	
	0.3	1.3	1.8	6.833	A	
	0.4	1.2	1.8	8.988	S	*
	0.5	1.1	1.8	8.505	S	

A for anti-symmetric mode

S for symmetric mode

* for the optimised value

⊛ for the final optimised value

Chapter 5

Formulation of matrices for tapered beams

CHAPTER 5

FORMULATION OF MATRICES FOR TAPERED BEAMS

§5.1 Introduction

Some of the earliest work carried out into the behaviour of tapered beams is that by Cranch & Adler[7] where the transverse natural frequencies of certain beams tapered to a point are investigated analytically. This work was extended by Jones[80] to include a wider range of boundary conditions.

The finite element approach to tapered beams has been considered by a number of authors.[81,83,84,88] The basic cubic approximation of the transverse displacement profile was investigated by Lindberg[81] where the behaviour of a pointed wedged cantilever was studied. This form of beam has been further investigated by Thomas & Dokumaci[83] using quintic displacement functions, and results were compared with those by Lindberg[81] and also with exact analytical results given by Sanger.[82] Other work on higher order functions has been carried out by To[88] who also investigated by the behaviour of a tapered cantilever.

Of other investigations carried out on tapered members it may be of interest to note that Eastep[86] and Irie et. al.[89] have studied the problem using perturbation approaches, and that large amplitudinal vibrations have also been considered.[85,87]

In this chapter two forms of displacement function for tapered members are examined, and also, in addition to flexural displacement, axial deformation is included. Firstly the basic cubic representation for flexural displacement, together with the corresponding linear representation of axial deformation, is considered, and this is compared with formulations ulitising the hyperbolic-trigonometrical forms of displacement function described previously.

§5.1.1 Extension to the solution of tapered sections

The most common method of dealing with non-prismatic sections is to idealise the member into a number of prismatic portions as shown in fig.5.1.1a. The accuracy of the solution increases as the number of divisions becomes larger. The method will in most cases lead to a satisfactory analysis. However, it leads to the solution of a large order matrix which is uneconomic in computing time and to a large amount of data preparation which also requires extensive storage.

In order to obtain an analysis in the same manner as that of prismatic members, the dynamic stiffness matrix of a non-prismatic member should be formulated. The formulations are presented with the following two assumed displacement functions:-

(a) Polynomial function

$$W = a_1 + a_2 x + a_3 x^2 + a_4 x^3 \qquad 5.1.1a$$

$$U = a_5 + a_6 x \qquad 5.1.1b$$

(b) Quasi-exact function

$$W = a_1 \sin\lambda x + a_2 \cos\lambda x + a_3 \sinh\lambda x + a_4 \cosh\lambda x \qquad 5.1.2a$$

$$U = a_5 \sin\gamma x + a_6 \cos\gamma x \qquad 5.1.2b$$

from which exact solutions were obtained for uniform members.

The exact solution of non-prismatic members, which involves the utilisation of Bessel functions, is also developed. However, the exact solution does not appear to be justified due to the large amount of computational work. The accumulated rounding errors during the extensive computation may also decrease the accuracy of the exact solution. The exact solution may be suitable for simple structures such as beams with classical boundary conditions.

A considerable amount of computation is encountered in the determination of the dynamic stiffness matrix with the quasi-exact function. The accumulation of rounding errors which results from the large amount of computation is significant, and the evaluations near the asymptotic poles are extremely unsteady. Certain remedial measures are suggested so that smooth iterations are maintained.

The convergence of natural frequencies of non-prismatic structures is studied for the stepped uniform section idealisation and for the two assumed displacement functions. The behaviour of tapered sections is presented with different degrees of, and different forms of, taper. The investigation is further extended to non-prismatic structures such as haunched beams, portal frames and bridges. The study is also supplemented with experimental evidence,

§5.1.2 Special features of tapered sections

Because of aesthetic appearance and a more economical use of material, the use of non-prismatic sections in structures is often implemented. For generality, the formulation of the dynamic stiffness matrix is based on a doubly tapered beam. The same procedure can be applied to other forms of non-uniformity. For ease of reference the different forms of non-uniformity in straight members are defined. These are:-

(i)	Prismatic member	(fig.5.1.2a)	- uniform
(ii)	Devetailed member	(fig.5.1.2b)	- tapered in breadth
(iii)	Wedged member	(fig.5.1.2c)	- tapered in depth
(iv)	Doubly tapered member	(fig.5.1.2d)	- tapered both in breadth and depth.

It is obvious that more parameters are involved in the definition of tapered than in prismatic members. In order to clarify the possible ambiguity in notation, and to facilitate the explanation in the matrix formulations, certain specifications are noted here.

(a) The degree of taper

This is commonly designated by the depth and breadth ratios. In connection with fig.5.1.2b & c respectively,

Breadth ratio, $n = b_1 / b_2$ 5.1.3a

Depth ratio, $m = d_1 / d_2$ 5.1.3b

(b) Equivalent uniform section

It is more convenient if the breadths and depths are referred to an equivalent uniform section. With the aid of fig.5.1.2e, the equivalent uniform section is defined as

(i) for the ith local member

$$(b_o)_i = \frac{(b_1)_i + (b_2)_i}{2} \qquad 5.1.4a$$

$$(d_o)_i = \frac{(d_1)_i + (d_2)_i}{2} \qquad 5.1.4b$$

(ii) for the whole system

$$b_o = \sum_{i=1}^{n} (b_o)_i \Big/ \sum_{i=1}^{n} L_i \qquad 5.1.5a$$

$$d_o = \sum_{i=1}^{n} (d_o)_i \Big/ \sum_{i=1}^{n} L_i \qquad 5.1.5b$$

where i = 1, 2, 3, ... n, the total number of members.

The transformation of the sectional properties of every element into the equivalent uniform section enhances the systematic formation of the matrix. It is shown in fig.5.1.2f that the sectional properties at the jth joint are related to the equivalent uniform section by

$$p_j = \frac{d_j}{d_o} \qquad 5.1.6a$$

$$q_j = \frac{b_j}{b_o} \qquad 5.1.6b$$

(c) The transformation in the frequency parameter

The frequency parameter of a structure, for flexural vibration in the general form, is denoted by

$$\lambda^4 = \frac{\rho A}{EI} \omega^2 \tag{5.1.7}$$

For an equivalent uniform section, it is

$$\lambda_o^4 = \frac{\rho A_o}{EI_o} \omega^2 \tag{5.1.8}$$

and at the jth joint, it is

$$\lambda_j^4 = \frac{\rho A_j}{EI_j} \omega^2 \tag{5.1.9}$$

For a homogenous rectangular section, the relationship of λ_o & λ_j is given by

$$\lambda_j = \frac{\lambda_o}{\sqrt{p_j}} \tag{5.1.10}$$

For extensional vibration, the frequency parameter, γ, in

$$\gamma^2 = \frac{\rho}{E} \omega^2 \tag{5.1.11}$$

is not a function of geometrical properties, and hence the relationship is constant, thus

$$\gamma_j = \gamma_o \tag{5.1.12}$$

(d) The function of linearly varying section

Considering the ith element of a structure as shown in fig.5.1.2g, the sectional properties at a section distance x from node 1 are expressed in terms of linearly varying section functions which are defined as

$$m(x) = 1 + \frac{m-1}{L} x \qquad 5.1.13$$

$$n(x) = 1 + \frac{n-1}{L} x \qquad 5.1.14$$

and the sectional properties are therefore

$$d_x = d_1 \cdot m(x) \qquad 5.1.15a$$

$$b_x = b_1 \cdot n(x) \qquad 5.1.15b$$

$$A_x = A_1 \cdot m(x)\, n(x) \qquad 5.1.15c$$

$$I_x = I_1 \cdot m^3(x)\, n(x) \qquad 5.1.15d$$

These physical parameters are related to the equivalent uniform section, thus

$$d_x = p\, d_o\, m(x) \qquad 5.1.16a$$

$$b_x = q\, b_o\, n(x) \qquad 5.1.16b$$

$$A_x = pq\, A_o\, m(x)\, n(x) \qquad 5.1.16c$$

$$I_x = p^3 q\, I_o\, m^3(x)\, n(x) \qquad 5.1.16d$$

§5.1.3 Simplified forms for matrix formulation

As mentioned in §5.1.2d, for non-prismatic sections, the sectional properties are expressed as functions of the length of the member, i.e. m(x) and n(x). It follows that the flexural rigidity (EI), the extensional rigidity (EA) and mass per unit length (ρA) in eqs.1.3.8, 1.3.9 & 1.3.15 respectively are also functions of x. These equations are therefore re-written respectively as:-

$$[K_f] = [C^{-1}]^T \cdot \int_0^L EI_x [A]^T[A] \, dx \cdot [C]^{-1} \qquad 5.1.17$$

$$[K_e] = [C^{-1}]^T \cdot \int_0^L EA_x [A]^T[A] \, dx \cdot [C]^{-1} \qquad 5.1.18$$

$$[M] = [C^{-1}]^T \cdot \int_0^L \rho A_x [N]^T[N] \, dx \cdot [C]^{-1} \qquad 5.1.19$$

For ease of reference, the matrix which results from the integration of the product of the matrices and linearly varying section functions is denoted by [X], i.e. [X] is always sandwiched between the constraint matrices $[C^{-1}]^T$ & $[C]^{-1}$ so that the form $[C^{-1}]^T[X][C]^{-1}$ is obtained. It is noticed that the constraint matrices are common to those of the prismatic sections, and the main task is to evaluate [X]. In order to facilitate the formulation of the property stiffness matrices for different types of taper, the above three equations are interpretated into simplified general forms.

Referring to eq.5.1.16 & fig.5.1.2g, the substitution of the linearly varying section functions into eqs.1.3.8 & 1.3.9 gives :-

for flexural vibration,

$$[K_f] = p^3 q\, EI_o \cdot [C^{-1}]^T \cdot \int_0^L [A]^T [A] m^3(x) n(x) dx \cdot [C]^{-1} \qquad 5.1.20$$

for extensional vibration,

$$[K_e] = pq\, EA_o \cdot [C^{-1}]^T \cdot \int_0^L [A]^T [A] m(x)\, n(x) dx \cdot [C]^{-1} \qquad 5.1.21$$

Similarly, into eq.1.3.15, it gives :-

$$[M] = pq\, \rho A_o \cdot [C^{-1}]^T \cdot \int_0^L [N]^T [N] m(x) n(x) dx \cdot [C]^{-1} \qquad 5.1.22$$

As described in §2.3.4, considering $[J]=[K]-\omega^2[M]$, the dynamic stiffness matrix is given as

for flexural vibration,

$$[J_f] \qquad 5.1.23$$
$$= pq\, EI_o \lambda_o^4 \cdot [C^{-1}]^T \cdot \int_0^L \left(\frac{p^2}{\lambda_o^4} [A]^T [A] m^2(x) - [N]^T [N] \right) m(x) n(x)\, dx \cdot [C]^{-1}$$

for extensional vibration,

$$[J_e] \qquad 5.1.24$$
$$= pq\, EA_o \gamma_o^2 \cdot [C^{-1}]^T \cdot \int_0^L \left(\frac{1}{\gamma_o^2} [A]^T [A] - [N]^T [N] \right) m(x) n(x)\, dx \cdot [C]^{-1}$$

§5.2 Polynomial Displacement Function

The derivation of $[C]^{-1}$, $[A]$, & $[N]$, which are identical to those of prismatic members, are shown in eqs.2.2.7, 2.2.10 and 2.2.22 & 2.2.23 respectively. (Since the resulting eigen-system is linear, matrix iteration methods as described in §3.3 could be used.) It is therefore necessary to formulate the matrices $[K]$ & $[M]$ for the solution of eq.3.2.1 which is re-written here as

$$[K][\delta] = \omega^2[M][\delta] \qquad 5.2.1$$

The matrices $[K]$ & $[M]$ are then substituted into $[J] = [K] - \omega^2[M]$ to give $[J]$ which was solved by the determinantal method with the facility of the count algorithm. The formulation is started with a doubly-tapered member. The property stiffness matrices are then reduced to a wedged member and to a dovetailed member, and further to a prismatic member, the matrices for which are given in §2.3. Again, for a wedged member and a dovetailed member, the same property stiffness matrix is formulated if the derivation is started from the integration of the matrices.

§5.2.1 Static stiffness matrix

(a) Doubly tapered member

With reference to eqs.5.1.20 & 5.1.21, $[X]$ is written as;-

for flexural vibration

$$[X_f] = \int_0^L [A]^T [A] m^3(x)\, n(x) dx \qquad 5.2.2$$

and for extensional vibration

$$[X_e] = \int_0^L [A]^T [A] m(x) n(x) dx \qquad 5.2.3$$

The mathematical operations in these two equations gives $[X_k]$ in a rational form as

$$[X_k] = \begin{bmatrix} 0 & 0 & 0 & 0 & & \\ & 0 & 0 & 0 & [0] & \\ & & X_{33} & X_{34} & & \\ & & & X_{44} & & \\ & \text{Sym.} & & & 0 & 0 \\ & & & & & X_{66} \end{bmatrix}$$

where
$$X_{33} = 4L \left(1 + \frac{3r+s}{2} + \frac{3r(r+s)}{3} + \frac{r^2(r+s)}{4} + \frac{r^3 s}{5} \right)$$
$$X_{34} = 12L^2 \left(\tfrac{1}{2} + \frac{3r+s}{3} + \frac{3r(r+s)}{4} + \frac{r^2(r+s)}{5} + \frac{r^3 s}{6} \right)$$
$$X_{44} = 36L^3 \left(\tfrac{1}{3} + \frac{3r+s}{4} + \frac{3r(r+s)}{5} + \frac{r^2(r+s)}{6} + \frac{r^3 s}{7} \right)$$
$$X_{66} = L \left(1 + \frac{r+s}{2} + \frac{rs}{3} \right)$$

and where $r = m-1$
$\& \; s = n-1$ 5.2.4

Substituting $[X_k]$ into eqs.5.1.20 & 5.1.21, and performing the triple multiplication gives the static stiffness matrix as shown in eq.5.2.5

Eq.5.2.5 on P.138

(b) Wedged member

For a member of constant width, the breadth ratio is unity in the doubly-tapered matrix formulation. Substituting **n**=1 into eq.5.2.5 gives the static stiffness matrix for a wedged member.

(c) Dovetailed member

Similarly for a dovetailed member, substituting m=1 into eq.5.2.5 gives the static stiffness matrix.

(d) Prismatic member

The substitution of m=1 & n=1 into 5.2.5 gives the same stiffness matrix as shown in eq.2.2.17

Eq.5.2.5 Static Stiffness Matrix of Polynomial Function

$$[K] = \left[\begin{array}{c|c} K_f & 0 \\ \hline 0 & K_e \end{array}\right] = \left[\begin{array}{cccc|cc} K_{11} & K_{12} & K_{13} & K_{14} & & \\ & K_{22} & K_{23} & K_{24} & & [0] \\ \text{sym.} & & K_{33} & K_{34} & & \\ & & & K_{44} & & \\ \hline & & [0] & & K_{55} & K_{56} \\ & & & & & K_{66} \end{array}\right]$$

where

$K_{11} = Za\ (\ 132mn + 15m + 45mn + 18m + 18mn + 45m + 15n + 132\ )$

$K_{12} = Za\ (\ 38mn + 4m + 12mn + 9m + 9mn + 33m + 11n + 94\ )\ L$

$K_{13} = -K_{11}$

$K_{14} = Za\ (\ 94mn + 11m + 33mn + 9m + 9mn + 12m + 4n + 38\ )\ L$

$K_{22} = Za\ (\ 12mn + 2m + 6mn + 8m + 8mn + 27m + 9n + 68\ )\ L^2$

$K_{23} = -K_{12}$

$K_{24} = Za\ (\ 26mn + 2m + 6mn + m + mn + 6m + 2n + 26\ )\ L^2$

$K_{33} = K_{11}$

$K_{34} = -K_{14}$

$K_{44} = Za\ (\ 68mn + 9m + 27mn + 8m + 8mn + 6m + 2n + 12\ )\ L^2$

$K_{55} = pqEA/6L\ (\ 2mn + m + n + 2\ )$

$K_{56} = -K_{55}$

$K_{66} = K_{55}$

and where $Za = p^3 q EI / 35L^3$

§5.2.2 Mass Matrix

(a) Doubly tapered member

With reference to eq.5.1.22, [X] is written as

$$[X_M] = \int_0^L [N]^T [N] m(x) n(x)\, dx \qquad 5.2.6$$

The mathematical operation gives [X] in a rational form as shown in eq.5.2.7. Substituting [X] into eq.5.1.22 and performing the triple multiplication give the mass matrix as shown in eq.5.2.8.

Eq.5.2.7 on P.140

Eq.5.2.8 on P.141

(b) Wedge member

For a wedged member, substituting n=1 into eq.5.2.8 gives the mass matrix.

(c) Dovetailed member

For a dovetailed member, substituting m=1 into eq.5.2.8 gives the mass matrix.

(d) Prismatic member

The substitution of m=1 & n=1 into eq.5.2.8 gives the same mass matrix as shown in eq.2.2.24.

§5.2.3 Dynamic stiffness matrix

The expressions for the static stiffness matrix (eq. 5.2.5) and the mass matrix (eq .5.2.6) are substituted into $[J]=[K]-\omega^2[M]$ to give the dynamic stiffness matrices. These are in the simplest form that are available and the coding for the computer programming is straight forward.

Eq.5.2.7 Matrix [X] of Polynominal Function

$$[X] = \left[\begin{array}{cccc|cc} X_{11} & X_{12} & X_{13} & X_{14} & & \\ & X_{22} & X_{23} & X_{24} & [0] & \\ & \text{sym.} & X_{33} & X_{34} & & \\ & & & X_{44} & & \\ \hline & [0] & & & X_{55} & X_{56} \\ & & & & & X_{66} \end{array}\right]$$

Where

$X_{11} = L \;(1 + (r+s)/2 + rs/3)$

$X_{12} = L^2 \;(1/2 + (r+s)/3 + rs/4)$

$X_{13} = L^3 \;(1/3 + (r+s)/4 + rs/5)$

$X_{14} = L^4 \;(1/4 + (r+s)/5 + rs/6)$

$X_{22} = X_{13}$

$X_{23} = X_{14}$

$X_{24} = L^5 \;(1/5 + (r+s)/6 + rs/7)$

$X_{33} = X_{24}$

$X_{34} = L^6 \;(1/6 + (r+s)/7 + rs/8)$

$X_{44} = L^7 \;(1/7 + (r+s)/8 + rs/9)$

$X_{55} = X_{11}$

$X_{56} = X_{12}$

$X_{66} = X_{22}$

‡ Where

$r = m-1$

$s = n-1$

Eq.5.2.8 Mass Matrix for Polynominal Function

$$[M] = \left[\begin{array}{cccc|cc} M_{11} & M_{12} & M_{13} & M_{14} & & \\ & M_{22} & M_{23} & M_{24} & [0] & \\ \text{sym.} & & M_{33} & M_{34} & & \\ & & & M_{44} & & \\ \hline & & [0] & & M_{55} & M_{56} \\ & & & & & M_{66} \end{array}\right]$$

Where

$$M_{11} = Z_b\ (76mn + 140m + 140n + 580)$$

$$M_{12} = Z_b\ (17mn + 25m + 25n + 65)\ L$$

$$M_{13} = Z_b\ (92mn + 140m + 140n + 92)$$

$$M_{14} = -Z_b\ (19mn + 17m + 17n + 25)\ L$$

$$M_{22} = Z_b\ (4mn + 5m + 5n + 10)\ L^2$$

$$M_{23} = Z_b\ (25mn + 17m + 17n + 19)\ L$$

$$M_{24} = -Z_b\ (5mn + 4m + 4n + 5)\ L^2$$

$$M_{33} = Z_b\ (580mn + 140m + 140n + 76)$$

$$M_{34} = -Z_b\ (65mn + 25m + 25n + 17)\ L$$

$$M_{44} = Z_b\ (10mn + 5m + 5n + 4)\ L^2$$

$$M_{55} = \rho AL/60\ (2mn + 3n + 3n + 12)$$

$$M_{56} = \rho AL/60\ (3mn + 2m + 2n + 3)$$

$$M_{66} = \rho AL/60\ (12mn + 3m + 3n + 2)$$

and where $Z_b = pq\rho AL/2520$

§5.3 Quasi-exact Displacement Function

In using this function, a non-linear eigensystem results, and as has been mentioned in §2.3.4, the expressions in the dynamic stiffness matrix are simpler than those in the static stiffness matrix and mass matrix. Hence it is not intended to formulate the complicated [K] and [M]. Also, since the proposed direct formulation procedure is able to avoid the unnecessary complicated mathematical operations, the formulation of the dynamic stiffness matrix is therefore carried out by directly employing eq.5.1.23 & 5.1.24.

The integration of the matrices may be carried out by numerical integration, but to minimize the risk of rounding errors and to save computing time, analytical integration was carried out. The triple multiplication, $[C^{-1}]^T[X][C]^{-1}$, is then programmed for numerical multiplication.

§5.3.1 The product of poly-circular-hyperbolic functions

The mathematical procedure is simpler if the trigonometrical and hyperbolic functions are referred to node 1 of an element (fig.5.1.2f). For this reason, eqs.5.1.23 & 5.1.24 are rewritten as

for flexural vibration

$$[J_f] = pq\,EI_o\,\lambda_o^4\,[C^{-1}]^T[X_f][C]^{-1} \qquad 5.3.1$$

where $$[X_f] = \int_0^L [Y_f]\,dx \qquad 5.3.2$$

where $$[Y_f] = \left(\frac{[A]^T[A]}{\lambda_1^4}\,m^2(x) - [N]^T[N]\right)m(x)\,n(x) \qquad 5.3.3$$

and for extensional vibration,

$$[J_e] = pq\ EA_0\gamma_0^2\,[C^{-1}]^T\ [X_e]\ [C]^{-1} \qquad 5.3.4$$

$$\text{where}\quad [X_e] = \int_0^L [Y_e]\,dx \qquad 5.3.5$$

$$\text{\& where}\quad [Y_e] = \left(\frac{[A]^T[A]}{\gamma_1^2} - [N]^T[N] \right) m(x)n(x) \qquad 5.3.6$$

Matrices [A] & [N] are given in eqs.2.3.20 and 2.3.25&26 respectively. Substituting for [A] & [N] into eq.5.3.3 gives, for flexural vibration,

$$[Y_f] = \left[\begin{array}{cccc} u(x)\cdot s^2(x) & u(x)\cdot s(x)\cdot c(x) & v(x)\cdot s(x)\cdot sh(x) & v(x)\cdot s(x)\cdot ch(x \\ & u(x)\cdot c^2(x) & v(x)\cdot c(x)\cdot sh(x) & v(x)\cdot c(x)\cdot ch(x \\ & & u(x)\cdot sh^2(x) & u(x)\cdot sh(x)\cdot ch(x \\ \text{Sym.} & & & u(x)\cdot ch^2(x) \end{array}\right.$$

where
$$u(x) = (\ m^2(x)-1\ )m(x)n(x)$$
$$= \tfrac{1}{L^4}\{2rL^3x + r(3r+2s)L^2x^2 + r^2(r+3s)Lx^3 + r^3sx^4\}$$

$$v(x) = (-m^2(x)-1\ )m(x)n(x)$$
$$= \tfrac{1}{L^4}\{-2L^4 - 2(2r+s)L^3x - r(3r+4s)L^2x^2 + r^2(r+3s)Lx^3 + r^3sx^4\}$$

$$r=m-1 \quad \& \quad s=n-1$$

and where
$$\begin{aligned} s(x) &= \sin\lambda_1 x \\ c(x) &= \cos\lambda_1 x \\ sh(x) &= \sinh\lambda_1 x \\ ch(x) &= \cosh\lambda_1 x \end{aligned} \qquad 5.3.7$$

and into eq.5.3.6 gives, for extensional vibration,

$$[Y_e] = \begin{bmatrix} t(x)(\cos^2\gamma_1 x-\sin^2\gamma_1 x) & -t(x)2\sin\gamma_1 x\ \cos\gamma_1 x \\ \text{symmetrical} & t(x)(\sin^2\gamma_1 x-\cos^2\gamma_1 x) \end{bmatrix}$$

where
$$t(x) = \frac{1}{L^2}\left(L^2+(r+s)Lx+rsx^2 \right) \qquad 5.3.8$$

§5.3.2 The definite integral

It is noticed that the integration of every element term follows the general form

$$\sum_{n=1}^{n} \left\{ g_n \int_0^L h(x)\, x^n \, dx \right\} \qquad 5.3.9$$

where n=1,2,3,.....

h(x) being the product of trigonometrical and/or hyperbolic functions

& g_n being the coefficients

The definite integral of $\int_0^L h(x)x^n\,dx$ is given in Appendix A. The application of these integrals to the evaluation of each element term in $[X_f]$ of eq.5.3.2 and $[X_e]$ of eq.5.3.5 is shown by an example. To evaluate the element term, X_{11}, for a wedged member,

$$\begin{aligned} X_{11} &= \frac{1}{L^4}\int_0^L (\sin^2\lambda x)(2rL^3x + 3r^2L^2x^2 + r^3Lx^3)\,dx \qquad 5.3.10 \\ &= \frac{2r}{L}\int_0^L x\sin^2\lambda x\,dx + \frac{3r^2}{L^2}\int_0^L x^2\sin^2\lambda x\,dx + \frac{r^3}{L^3}\int_0^L x^3\sin^2\lambda_1 x\,dx \\ &= \frac{rL}{2\alpha_1^2}(\alpha_1^2 - 2\alpha_1 sc + s^2) \\ &\quad + \frac{r^2L}{4\alpha_1^3}(2\alpha_1^3 + 6\alpha_1^2 sc + 6\alpha_1 s^2 - 3\alpha_1 + 3sc) \\ &\quad + \frac{r^3L}{16\alpha_1^4}(2\alpha_1^4 - 8\alpha_1^3 sc + 12\alpha_1^2 s - 6\alpha_1 + 12\alpha_1 sc - 6s^2) \\ &= \frac{rL}{16\alpha_1^4}\Big\{ 2\alpha_1^4(r+2)^2 - 8\alpha_1^3 sc(r+1)(r+2) + 4\alpha_1^2 s^2(3r^2+6r+2) \\ &\qquad - 6\alpha_1^2 r(r+2) + 12\alpha_1 sc\cdot r(r+1) - 6s^2r^2 \Big\} \end{aligned}$$

The procedure for the evaluation of other element terms is similar. A complete set of elements for the matrix $[X_f]$ is given in Appendix B .

§ 5.3.3 Dynamic stiffness matrix

Due to the complexity of the integrations, explicit triple multiplication for flexural vibration becomes unwieldy and hence the multiplication of $[C^{-1}]^T[X][C]^{-1}$ was programmed for computer implementation.

Although the evaluation of the dynamic stiffness matrix for extensional vibration may be processed as described above, in this case an explicit approach is feasible. Undertaking the integration in eq.5.3.5, $[X_e]$ is given as

$$X_{55} = \frac{L}{2\beta}\left\{(mn-1)\beta^2 - 2mn\beta^2 s^2 - (2mn-m-n)\beta sc + (m-1)(n-1)s^2\right\}$$

$$X_{56} = \frac{L}{2\beta}\left\{2mn\beta^2 sc - (2mn-m-n)\beta s^2 + (m-1)(n-1)(\beta - sc)\right\}$$

$$X_{66} = -X_{55} \tag{5.3.11}$$

where $\beta=\gamma_1 L$, $s=\sin\gamma_1 L$, $c=\cos\gamma_1 L$

The triple multiplication gives the dynamic stiffness matrix, the elements of which are

$$\begin{aligned} J_{55} &= Z_c\left\{2\beta^2 sc + (m+n-2)\beta s^2 + (m-1)(n-1)(\beta - sc)\right\} \\ J_{56} &= -Z_c\left\{(mn+1)\beta^2 s + (m-1)(n-1)(\beta - sc)\right\} \\ J_{66} &= Z_c\left\{2mn\beta^2 sc - (2mn-m-n)\beta s^2 + (m-1)(n-1)(\beta c - s)\right\} \end{aligned} \tag{5.3.12}$$

where $\beta=\gamma_1 L$

$s=\sin\gamma_1 L$

$c=\cos\gamma_1 L$

$Z_c = pq\,\frac{EA}{L}\,\frac{1}{2\beta s^2}$

§5.4 Exact Solution with Bessel Functions

§5.4.1 The general solution of the governing differential Equation

(a) Flexural vibration

The equation of motion in its general form is shown in eq.1.2.2. For non-prismatic beams, also assuming oscillatory motion $w = W\sin(\omega t + \phi')$, the differential equation is written as

$$\frac{d}{dx}\left[EI_x\frac{d^2W}{dx^2}\right] - \omega^2\rho A_x W = 0 \qquad 5.4.1$$

or on expanding

$$I_x\frac{d^4W}{dx^4} + 2\frac{dI_x}{dx}\frac{d^3W}{dx^3} + \frac{d^2I_x}{dx^2}\frac{d^2W}{dx^2} - \omega^2\frac{\rho}{E}A_xW = 0 \qquad 5.4.2$$

I_x and A_x of a wedgedsection, which are indicated in fig.5.1.2f, are expressed as a function X such that,

$$I_x = I_1X^3 \qquad 5.4.3$$

$$A_x = A_1X \qquad 5.4.4$$

$$\text{where} \quad X = m(x) = 1+\frac{m-1}{L}x \qquad 5.4.5$$

The variable x in eq.5.4.2 is replaced by X , thus giving

$$X^2\frac{d^4W}{dX^4} + 6X\frac{d^3W}{dX^3} + 6\frac{d^2W}{dX^2} - \frac{\alpha_1^4}{r^4}W = 0 \qquad 5.4.6$$

where $\alpha_1^4 = \lambda_1^4L^4 = \frac{\rho A_1}{EI_1}L^4\omega^2$, and $r=m-1$

It is intended to transform eq.5.4.6 into a standard form from which the general solution can be expressed in Bessel functions. The transformation is commenced with the introduction of two variables, ψ & φ , where

$$\psi = W\varphi \qquad 5.4.7$$

$$\& \quad \varphi = \frac{2\alpha_1}{r} X^{\frac{1}{2}} \qquad 5.4.8$$

The derivatives of ψ , φ , W & X are given in Appendix C. The substitution of these derivatives into eq.5.4.6 gives

$$\varphi^4 \frac{d^4\psi}{d\varphi^4} + 2\varphi^3 \frac{d^3\psi}{d\varphi^3} - 3\varphi^2 \frac{d^2\psi}{d\varphi^2} + 3\varphi \frac{d\psi}{d\varphi} - 3\psi - \varphi^4\psi = 0 \qquad 5.4.9$$

This equation can be factorised into

$$\left[\varphi^2 \frac{d^2}{d\varphi^2} + \varphi \frac{d}{d\varphi} + (\varphi^2 - 1)\right]\left[\varphi^2 \frac{d^2}{d\varphi^2} + \varphi \frac{d}{d\varphi} - (\varphi^2 + 1)\right]\psi = 0 \qquad 5.4.10$$

and is satisfied if either

$$\varphi^2 \frac{d^2\psi}{d\varphi^2} + \varphi \frac{d\psi}{d\varphi} + (\varphi^2 - 1)\psi = 0 \qquad 5.4.11$$

or

$$\varphi^2 \frac{d^2\psi}{d\varphi^2} + \varphi \frac{d\psi}{d\varphi} - (\varphi^2 + 1)\psi = 0 \qquad 5.4.12$$

Eqs.5.4.11 & 5.4.12 are Bessel's equations of the first order whose solutions may be expressed in terms of cylindrical functions. The general solution of eq.5.4.9 is therefore

$$\psi = a_1 J_1(\varphi) + a_2 N_1(\varphi) + a_3 I_1(\varphi) + a_4 K_1(\varphi) \qquad 5.4.13$$

where J_1, N_1, I_1, K_1, are the cylindrical functions of the first order. Substituting eq.5.4.7 gives the displacement function as

$$W = \frac{1}{\varphi}\left\{ a_1 J_1(\varphi) + a_2 N_1(\varphi) + a_3 I_1(\varphi) + a_4 K_1(\varphi) \right\} \qquad 5.4.14$$

It may be noted that the same equation results from the theory of circular tanks of variable wall thickness[4].

(b) Extensional vibration

Assuming oscillatory motion, the differential equation in eq.1.2.3 is written as

$$\frac{d}{dx}\left(EA_x \frac{dU}{dx} \right) + \omega^2 \rho A_x U = 0 \qquad 5.4.15$$

or on expanding

$$A_x \frac{d^2U}{dx^2} + \frac{dA_x}{dx}\frac{dU}{dx} + \omega^2 \frac{\rho}{E} A_x U = 0 \qquad 5.4.16$$

Substituting for eqs.5.4.4 & 5.4.5, the variable x is replaced by X, thus giving,

$$X \frac{d^2U}{dX^2} + \frac{dU}{dX} + \frac{\beta_1^2}{r^2} X U = 0 \qquad 5.4.17$$

where $\beta_1^2 = \frac{\rho}{E}\omega^2 L^2$

Introducing two variables,

$$\bar{\Psi} = U\bar{\Phi} \qquad 5.4.18$$

$$\& \quad \bar{\Phi} = \frac{\beta_1}{r} X \qquad 5.4.19$$

the differential equation is written as

$$\bar{\Phi}^2 \frac{d^2\bar{\Psi}}{d\bar{\Phi}^2} + \varphi \frac{d\bar{\Psi}}{d\bar{\Phi}} + (\bar{\Phi}^2 - 1)\bar{\Psi} = 0 \qquad 5.4.20$$

of which the general solution is given as

$$\bar{\Psi} = a_5 J_1(\bar{\Phi}) + a_6 N_1(\bar{\Phi}) \qquad 5.4.21$$

Substituting eq.5.4.18 gives the displacement function as

$$U = \frac{1}{\bar{\Phi}} \left\{ a_5 J_1(\bar{\Phi}) + a_6 N_1(\bar{\Phi}) \right\} \qquad 5.4.22$$

§5.4.2 The properties of Bessel functions

The expressions for the Bessel functions of zero order are given as

(a) the first kind,

$$J_0(\varphi) = 1 - \frac{\varphi^2}{2^2} + \frac{\varphi}{2^2 \cdot 4^2} - \frac{\varphi}{2^2 \cdot 4^2 \cdot 6^2} + \cdots\cdots \qquad 5.4.23$$

$$I_0(\varphi) = 1 + \frac{\varphi^2}{2^2} + \frac{\varphi^4}{2^2 \cdot 4^2} + \frac{\varphi^6}{2^2 \cdot 4^2 \cdot 6^2} + \cdots\cdots$$

(b) the second kind,

$$N_0(\varphi) = J_0(\varphi)\,\frac{2}{\pi}\left(\ln\frac{\varphi}{2}+\nu\right) + \frac{2}{\pi}\left\{\frac{\varphi^2}{2^2} - \frac{\varphi^4}{2^2 \cdot 4^2}\left(1+\tfrac{1}{2}\right) + \frac{\varphi^6}{2^2 \cdot 4^2 \cdot 6^2}\left(1+\tfrac{1}{2}+\tfrac{1}{3}\right) + \cdots\cdots\right\}$$

$$K_0(\varphi) = -I_0(\varphi)\left(\ln\frac{\varphi}{2}+\nu\right) + \frac{\varphi^2}{2^2} + \frac{\varphi^4}{2^2 \cdot 4^2}\left(1+\tfrac{1}{2}\right) + \frac{\varphi^6}{2^2 \cdot 4^2 \cdot 6^2}\left(1+\tfrac{1}{2}+\tfrac{1}{3}\right) + \cdots\cdots$$

ν being Euler's constant = 0.5772156....

Also the Bessel functions of the first order may be expressed in items of those of zero order thus

$$J_1(\varphi) = -J_0'(\varphi) \qquad 5.4.24$$

$$I_1(\varphi) = I_0'(\varphi)$$

$$N_1(\varphi) = -N_0'(\varphi)$$

$$K_1(\varphi) = -K_0'(\varphi)$$

The Bessel functions of the first kind are then readily obtained as

$$J_1(\varphi) = \frac{\varphi}{2^2} - \frac{\varphi^3}{2^2 \cdot 4^2} - \frac{\varphi^5}{2^2 \cdot 4^2 \cdot 6^2} - \frac{\varphi^7}{2^2 \cdot 4^2 \cdot 6^2 \cdot 8^2} - \cdots\cdots \qquad 5.4.25$$

$$I_1(\varphi) = \frac{\varphi}{2} + \frac{\varphi^3}{2^2 \cdot 4^2} + \frac{\varphi^5}{2^2 \cdot 4^2 \cdot 6^2} + \frac{\varphi^7}{2^2 \cdot 4^2 \cdot 6^2 \cdot 8^2} + \cdots\cdots$$

For Bessel functions of higher orders, it is necessary to assume the knowledge of the recurrence formulae which are given in most mathematical texts dealing with Bessel functions.

In the following sections, only examples of flexural vibration are considered. Problems involving extensional vibration may be treated in a similar manner.

§5.4.3 The formulation of the dynamic stiffness matrix

The first derivatives of eq.5.4.14 with respect to x gives the slope as

$$-\frac{2\alpha_1^2}{(m-1)L\varphi}\left(a_1 J_2(\varphi) + a_2 N_2(\varphi) - a_3 I_2(\varphi) + a_4 K_2(\varphi) \right) \qquad 5.4.26$$

which is differentiated again to give the curvature as

$$\frac{4\alpha_1^4}{(m-1)^2 L^2 \varphi^3}\left(a_1 J_3(\varphi) + a_2 N_3(\varphi) + a_3 I_3(\varphi) + a_4 K_3(\varphi) \right) \qquad 5.4.27$$

Considering the strain-displacement relationship, substituting eq.5.4.27 into eq.1.3.4 gives

$$[A] = \frac{4\alpha_1^4}{(m-1)L\varphi^3}\left[J_3(\varphi) \quad N_3(\varphi) \quad I_3(\varphi) \quad K_3(\varphi) \right] \qquad 5.4.28$$

and the displacement function in eq.5.4.14 gives

$$[N] = \frac{1}{\varphi}\left[J_1(\varphi) \quad N_1(\varphi) \quad I_1(\varphi) \quad K_1(\varphi) \right] \qquad 5.4.29$$

Substituting the end conditions, x=0 for node 1 and x=L for node 2, into eq.5.4.14 & 5.4.26 gives

$$\begin{bmatrix} W_1 \\ \theta_1 \\ W_2 \\ \theta_2 \end{bmatrix} = \begin{bmatrix} \frac{J_1(\varphi_1)}{\varphi_1} & \frac{N_1(\varphi_1)}{\varphi_1} & \frac{I_1(\varphi_1)}{\varphi_1} & \frac{K_1(\varphi_1)}{\varphi_1} \\ \frac{J_2(\varphi_1)}{Z_1} & \frac{N_2(\varphi_1)}{Z_1} & -\frac{I_2(\varphi_1)}{Z_1} & \frac{K_2(\varphi_1)}{Z_1} \\ \frac{J_1(\varphi_2)}{\varphi_2} & \frac{N_1(\varphi_2)}{\varphi_2} & \frac{I_1(\varphi_2)}{\varphi_2} & \frac{K_1(\varphi_2)}{\varphi_2} \\ \frac{J_2(\varphi_2)}{Z_2} & \frac{N_2(\varphi_2)}{Z_2} & -\frac{I_2(\varphi_2)}{Z_2} & \frac{K_2(\varphi_2)}{Z_2} \end{bmatrix} \begin{bmatrix} a_1 \\ a_2 \\ a_3 \\ a_4 \end{bmatrix} \qquad 5.4.30$$

where $\varphi_1 = \dfrac{2\alpha_1}{(m-1)}$, $\varphi_2 = \dfrac{2m\alpha_1}{(m-1)}$

$$Z_1 = \frac{(m-1)L\varphi_1^2}{2\alpha_1^2}, \quad Z_2 = \frac{(m-1)L\varphi_2^2}{2\alpha_1^2}$$

of which the inverse gives $[C]^{-1}$. The dynamic stiffness matrix is obtained if $[C]^{-1}$, $[A]$ & $[N]$ are substituted into eq.5.1.23 .

The mathematical operations required to form the inverse matrix, $[C]^{-1}$, and hence the multiplications of $[A]^T[A]$ and $[N]^T[N]$ are formidable. Furthermore, it is not practical to attempt to carry out the integration and triple multiplication because of the huge amount of work thus generated. Even if a computer program is designed for all these tedious operations, the success in giving a correct result may be suspect due to the rounding errors which could be accummulated during the executions.

§5.4.4 The application to simple beams

Although it is considered not practical to program for the exact solution, the Bessel function solution may be applied to simple beams. By substituting the boundary conditions into eqs.5.4.14, 5.4.26 & 5.4.27 , the coefficients a_1, a_2, a_3, a_4, and the natural frequencies can be computed. The application is demonstrated in the solution of a propped cantilever as shown in fig.5.4.4. The boundary conditions are,

At $x=0$, $W=0$ & $\dfrac{d^2W}{dx^2}=0$

At $x=L$, $W=0$ & $\dfrac{dW}{dx}=0$

Using these boundary conditions, eqs.5.4.14, 5.4.26 & 5.4.27, gives the following equations

$$a_1J_1(\varphi) + a_2N_1(\varphi) + a_3I_1(\varphi) + a_4K_1(\varphi) = 0 \qquad 5.4.31a$$

$$a_1J_3(\varphi) + a_2N_3(\varphi) + a_3I_3(\varphi) + a_4K_3(\varphi) = 0 \qquad 5.4.31b$$

$$a_1J_1(\varphi) + a_2N_1(\varphi) + a_3I_1(\varphi) + a_4K_1(\varphi) = 0 \qquad 5.4.31c$$

$$a_1J_2(\varphi) + a_2N_2(\varphi) - a_3I_2(\varphi) + a_4K_2(\varphi) = 0 \qquad 5.4.31d$$

The natural frequencies are then obtained from the determinantal equation,

$$\begin{vmatrix} J_1(\varphi) & N_1(\varphi) & I_1(\varphi) & K_1(\varphi) \\ J_3(\varphi) & N_3(\varphi) & I_3(\varphi) & K_3(\varphi) \\ J_1(\varphi) & N_1(\varphi) & I_1(\varphi) & K_1(\varphi) \\ J_2(\varphi) & N_2(\varphi) & -I_2(\varphi) & K_2(\varphi) \end{vmatrix} = 0 \qquad 5.4.32$$

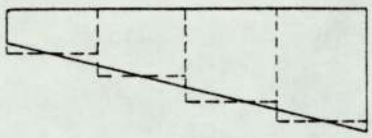

Fig.5.1.1a Stepwise uniform section idealisation

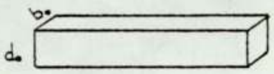

Fig.5.1.2a
Prismatic member

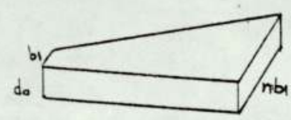

Fig.5.1.2b
Dovetailed member

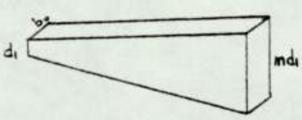

Fig.5.1.2c
Wedged member

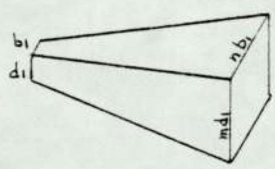

Fig.5.1.2d
Doubly tapered member

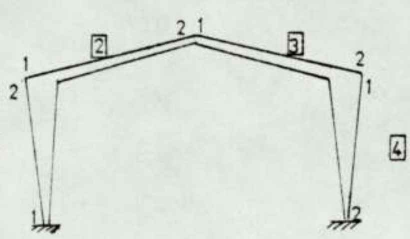

Fig.5.1.2e Equivalent uniform section

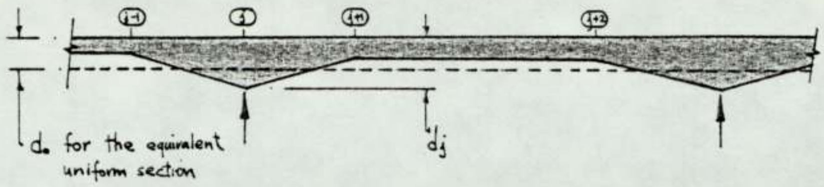

Fig.5.1.2f
Transformation of the jth joint

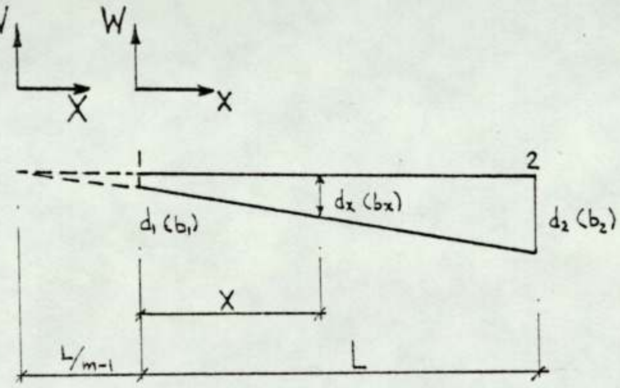

Fig.5.1.2g
Linearly varying secton of the ith element

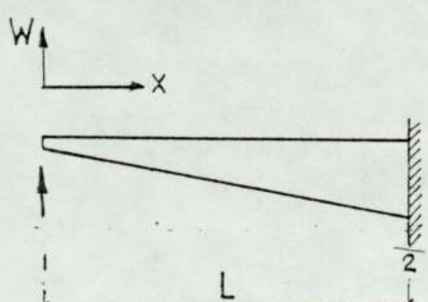

Fig.5.4.4
A propped cantilever beam

Chapter 6

The difficulties in solution routines & interpretation

CHAPTER 6

THE DIFFICULTIES IN SOLUTION ROUTINES & INTERPRETATION

In the matrix formulation using the polynomial functions, the expressions for tapered sections are more complicated than those for prismatic sections. However, although more arithmetic executions are required to evaluate each expression, the numerical operations are well within the capability of a computer. No difficulties nor suspectability of the solution routines, which are discussed in Chapter 3, is reported. The solution routines from the matrix iteration methods and the determinantal methods are capable of giving successful results.

The complexities of the trigonometrical and hyperbolic functions are increased in the matrices produced from the quasi-exact functions. The risk of incorrect evaluation becomes higher as the dimensionless frequency parameter (λL) increases in magnitude. The evaluation is even more misleading if the dimensionless frequency parameter approaches the asymptotic poles. In this chapter the difficulties in the solution routines for the quasi-exact function are discussed. For ease of documentation, the two terms which are repeatedly used in this chapter are abbreviated as CA and AP respectively for count algorithm and asymptotic pole.

§6.1 The Limitation in Numerical Evaluation

§6.1.1 The rounding error

Inherent in computer technology is the fact that a computer operates using only a certain number of significant figures. In the ICL 1904s system, every execution accommodates 11 significant figures for single precision implementation. The greater the number of numerical executions, the higher the risk that the rounding errors become prominent. An example on rounding errors may be shown by obtaining the difference of two numbers of similar magnitude, such as

$$\text{Difference} = 7.81542341176 \times 10^{32} - 7.81542341174 \times 10^{32} \tag{6.1.1}$$

Instead of carrying $2\text{x}10^{21}$, the computer may take the difference as zero for the next execution.

For tapered members, as it is not possible to construct every element term of the dynamic stiffness matrix as elegently as those of prismatic members, the matrix is formulated by the summation of the triple multiplications. The arithmetic execution is so heavy that deviated evaluations are unavoidable. The occurrence of rounding errors is further emphasised in the following example.

A free cantilever beam which is wedged in section (fig.6.1.1a) is described by a depth ratio m. A depth ratio of unity should re-define the beam as a prismatic beam (fig.6.1.1b). Similarly, the substitution of m=1 into the dynamic stiffness matrix formulation of a wedged section (§5.3 & subroutine JWEDGE) should give the same result as that of a prismatic section (fig.2.3.30 & subroutine JPRISM). The two sets of evaluations are plotted in the D-f curves (fig.6.1.1c & d), where the discrepancy can be easily visualised.

In fig.6.1.1c, as the evaluations are performed with simple expressions, the profile of the D-f curves are well-defined and so are the eigenvalues which clearly intersect the abscissa. The same profile can not be achieved in fig.6.1.1d. The portions of curves which are drawn in dotted lines signify the uncertainties. These uncertainties always appear near the APs. For a wedged section of greater taper, the uncertainties in the D-f curve (fig.6.3.1c) may span across the abscissa to another AP.

§6.1.2 The singularity

It has been shown that the uncertainties occur near the APs. This is mainly due to the evaluation of

$$1/(1-\cos\lambda L\cosh\lambda L) \qquad 6.1.2$$

in the $[C]^{-1}$ & $[C^{-1}]^{T}$ matrices of eq.2.3.14. This expression may also need to be evaluated in the integration matrix, [X], in eq.5.3.9. The evaluation of expression (6.1.2) is extremely sensitive when λL is near the APs.

In the determinantal method, a change of sign may signify a possibility of the existence of a root. The inaccurate evaluation of expression (6.1.2) gives misleading information. In fig.6.1.1d, attention is drawn to asymptotic poles of the 2nd, 4th & 6th order. The values of these poles are respectively

$$\begin{aligned}\alpha_2 &= 7.85321\\ \alpha_3 &= 10.99561\\ \alpha_4 &= 14.13717\end{aligned} \qquad 6.1.3$$

which are roots of eq.2.3.10, i.e.,

$$AP_f = 1 - \cos\lambda L\cosh\lambda L = 0 \qquad 6.1.4$$

It is increasingly clear that the evaluations near the APs are unreliable. The regions in the vicinity of these poles are identified as prohibited ranges[73] (fig.6.2.1a). The ranges may vary from negligible, e.g. the first pole in fig.6.1.1c; to a full span from pole to pole. (fig.6.3.1c)

§6.2 Difficulties Arising in the Solution Routines

§6.2.1 The inconsistent evaluation in the prohibited range

It can be seen, in fig.6.1.1c, that the fourth mode is situated very close to the second AP. Due to the rounding errors that accumulate from the complicated formulation incurred using the quasi-exact function, the fourth mode cannot be well-defined as can be seen in fig.6.1.1d. The same curves are magnified in fig.6.2.1a showing the prohibited range, and their determinantal values are tabulated in table 6.2.1b.

With subroutine JPRISM, the curve intersects the abscissa at $\lambda L=7.85476$. This intersection, one of the roots, is confirmed by the CA as the fourth mode. Situated not far before the root is an AP, $\lambda L=7.85321$, where singularity is present. The determinants are evaluated for every interval of 0.0001 in λL and the evaluations are very steady. If 0.0001 is taken as the prohibited range, the root of $\lambda L=7.85476$ is well beyond it. It may therefore be concluded that a steady iteration is always obtained in prismatic sections using the exact function.

Due to the unsteady evaluation with the quasi-exact function in the subroutine JWEDGE, the prohibited range, in fig.6.1.1d, is required to be widened. The range is increased in both directions until steady evaluations are maintained. The prohibited range is now bounded by ($\lambda L=7.8519$) and ($\lambda L=7.8554$) for the second AP. The expected root which lies within the prohibited range cannot now be well-defined.

§6.2.2 The misleading count algorithm

In a normal CA, if the sign count increases by one, it signifies the existence of a root with a well-defined values — a definite root. If the asymptotic algorithm increases by S_n, (S_n being obtained from eq.3.3.14), and the sign count decreases by S_n leaving the CA unchanged, there should exist an AP. The unchanged CA argues that the point of singularity is not a root even though the determinants change sign about the AP. The AP may therefore be termed a biased root. A normal CA which quantifies either definite roots or biased roots is operated with subroutine JPRISM.

If the use of the subroutine JPRISM is replaced by JWEDGE, it can be seen in fig.6.1.1d that the normality of the CA is maintained up to the third mode. The CA in the prohibited range of the second AP is very misleading. As can be seen in table 6.2.1b, the following abnormal counts are noted:-

(a)(i) DUPLICATED mode — the third mode has already been clearly defined as $\lambda L=7.37658$ which is an extensional mode, If the CA at $\lambda L=7.8520$ (which is 1+3=4) is accepted as a normal count, the CA at $\lambda L=7.8525$ (which is 1+2=3) will indicate the existence of another third mode. It can also be noticed that the CA of (1+2=3) and (1+3=4) are repeated within the prohibited range.

(ii) DEVIATED mode — the misleading CA indicated that any of the many intersections within the prohibited range can be taken as the fourth mode. The result obtained from the iteration process with subroutine JWEDGE is not always the same value as that obtained from subroutine JPRISM.

(b)(i) ASYMPTOTIC mode — it can be seen in fig.6.3.1c that the roots coincide with the APs. There is no indication that a definite root is able to be isolated from the APs even though the determinants are evaluated with very small intervals. The values of the determinants are tabulated in table 6.2.2a .

(ii) MISSING mode — in fig.6.3.1c, the profile of the curve is expected to intersect the abscissa to give the second mode. However, due to the rounding errors, the curve bends down and tends to the negative asymptote. The CA before and after the first AP, (0+1=1) & (1+1=2) respectively, shows that there should be a mode of second order before it. Nevertheless, the change of curvature at the proximity of the intersection omits this root.

§6.2.3 <u>The interruption in the iteration process</u>

A smooth iteration is maintained provided that the CA gives a normal count. As the iteration is recurrent in nature, the process can be continued even with a misleading CA. It is obvious that a misleading CA is liable to give an inaccurate root. Once a root is evaluated with a misleading CA, the reliability of the following roots is highly suspect. It is also necessary to identify the definite roots from all the other roots.

There is a possibility that the iteration falls within the prohibited range. The evaluation is so sensitive that an overflow would be registered during the execution. The iteration process may either be terminated unexpectedly, or be continued with a risk of transmitting false information.

§6.3 The Remedial Measures

§6.3.1 The avoidance of the first asymptotic poles

The misleading CA always occurs within the prohibited range. If the first asymptotic pole can be transplanted sufficiently behind the required number of roots, the iteration is free from the danger of evaluating singularity. The roots which result before the first AP are therefore definite and accurate, and hence it is ideal if as many roots as possible occur before the first AP. The manner in which this is achieved, i.e. how the value of the position of the first AP is increased, is described below.

The solution of eq.2.3.10 gives the first root as α_1=4.73004. If the member in fig.6.1.1a is split into n elements as shown in fig.6.3.1a, the position of the first AP of the first element may be calculated as

$$(\alpha_1)^1 = \sqrt{\frac{d_1}{d_0}}\,\frac{L}{L_1}\,\alpha_1 \qquad 6.3.1$$

and for the ith element,

$$(\alpha_1)^i = \sqrt{\frac{d_i}{d_0}}\,\frac{L}{L_1}\,\alpha_1 \qquad 6.3.2$$

In order to obtain all the required roots with definite values, it must be ensured that the smallest of $(\alpha_1)^i$ is larger than the roots. The ideal is for all the APs of the elements, i.e. $(\alpha_1)^1$, $(\alpha_1)^2$,....... $(\alpha_1)^i$........ $(\alpha_1)^n$, to be very close to each other. This will maximize the position of the first AP. For elements split into equal lengths, the APs are tabulated in table 6.3.1b.

It is noticed that the avoidance of the first AP is effectively achieved by splitting a member into more elements. This is in parallel to the rate of convergence to the exact solution. The D-f curves for the wedged cantilever beam in fig.6.3.1a are shown in fig.6.3.1c for different number of elements. It can be seen that more roots are well-defined and that these roots are converging as the number of elements increases.

§6.3.2 <u>The by-passing of prohibited range</u>

It has been shown that the evaluation in the prohibited range is unreliable. In order to maintain a smooth iteration for as many roots as required without having the iteration process interrupted, the evaluations are kept away from the prohibited ranges. For the particular cases within the prohibited range, certain assumptions are made with the support of the CA. The following two suggestions are interpreted as a result of the abnormal CAs described in §6.2.2.

(a) <u>APPOINTED mode</u>

As there is only one real root for a particular mode, it is not possible to accept all the intersections of the same CA as the modes; and a sensible decision is necessary. In fig.6.3.1c, if $\lambda L=8.8301$ is taken as the second mode, it would be illogical to have the third mode well defined as $\lambda L=8.3779$. Such illogicality is rectified by taking the itersection at the smallest value as an approximate root. This is to maintain the validity of $\omega_r < \omega_{r+1}$. Also, a smaller value of λL always avoids interference by the first AP.

(b) ASYMPTOTIC mode

It is very common that the profile of a curve tends to the asymptote and the CA after the AP shows that a mode should exist. It is therefore considered that the AP be taken as an approximate root since no definite value of the root is obtained, not even by reducing the iteration interval.

It must be noted that these two suggestions only give approximations. An approximate root would preferably be accompanied by an associated message commenting on the abnormality. Wherever necessary, it is helpful if the CAs for the suspected range are fully listed. The profile of the D-f curves is also a means of envisaging the difficulties arising. It is also recommended that the APs are predicted independently so as to guide the CAs.

§6.3.3 The appraisal of the count algorithm

The importance and function of the CA has been shown to be of great interest. Originally derived from the Sturm sequence to locate the roots of a polynomial function, the CA enables the solution of non-linear eigensystems with the introduction of the asymptotic pole algorithm to be carried out. It has been mentioned in Chapter 3 that for prismatic structures, an infallible solution is guaranteed.

The application to the nonlinear eigensystems has been extended from prismatic structures to non-prismatic structures. Due to the complicated expressions in the matrix formulations, difficulties arise with the standard solution routines. It is with the aid of the CA that these difficulties are overcome. The most prominent feature of the CA is its ability to facilitate the remedial procedures.

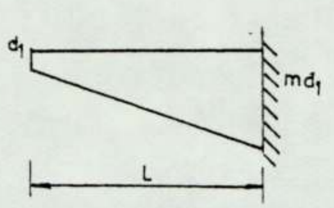

$$d_o = \frac{m+1}{2} d_1$$

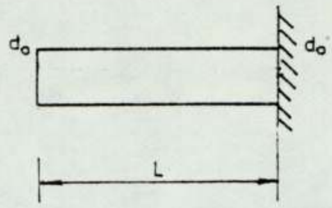

FIG. 6·1·1a WEDGED MEMBER

FIG. 6·1·1b PRISMATIC MEMBER

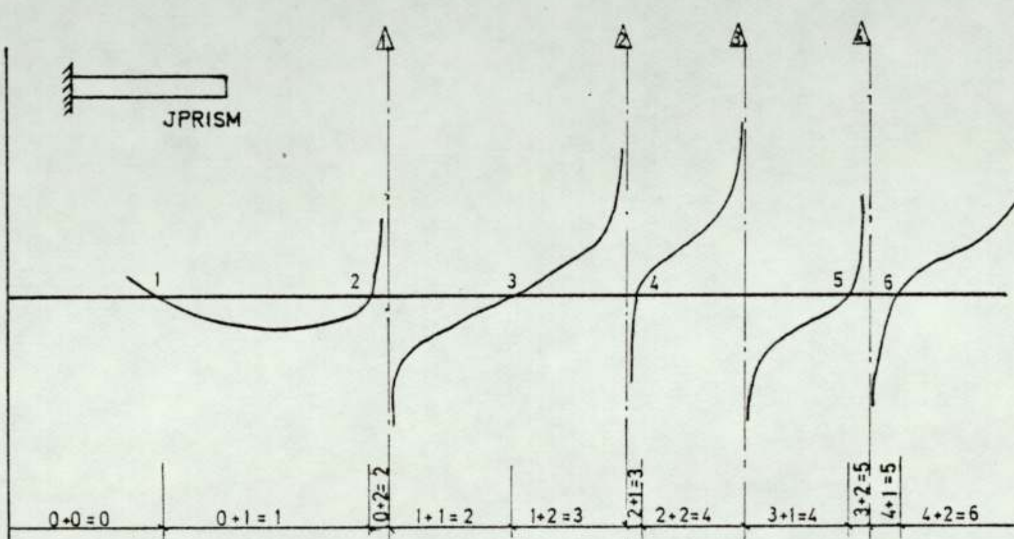

FIG. 6·1·1c D–F CURVE FROM SUBROUTINE JPRISM

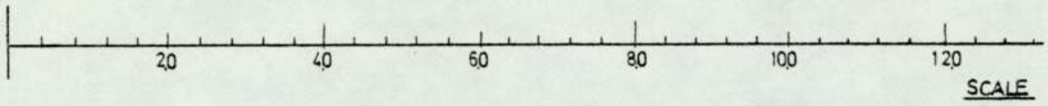

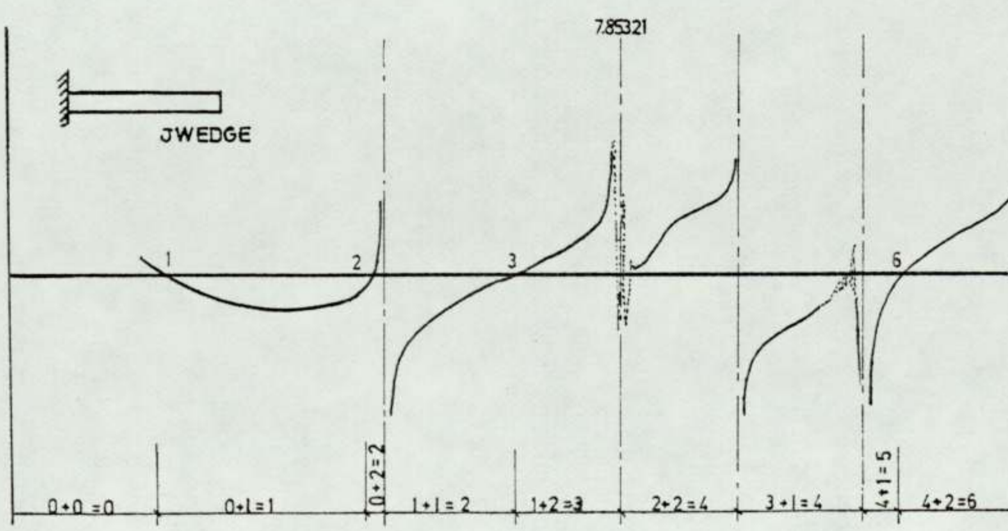

FIG. 6·1·1·d D–F CURVE FROM SUBROUTINE JWEDGE

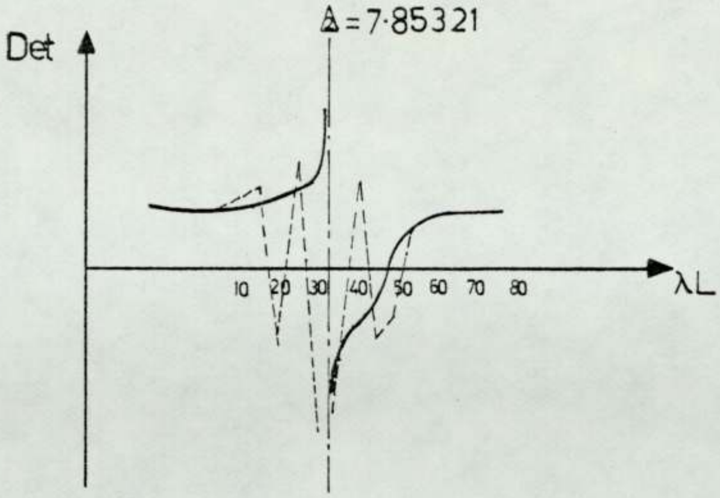

Fig 6.2.1a D-F CURVE AT THE PROHIBITED RANGE

Table 6.2.1b Prohibited range of the 2nd AP

	Subroutine JPRISM		Subroutine JWEDGE	
	Determinant	count Algorithm	Determinant	count Algorithm
7.8510	7.15E25	1+2=3	9.02E25	1+2=3
7.8515	8.03E25	1+2=3	1.07E26	1+2=3
7.8520	9.64E25	1+2=3	-1.24E26	1+3=4
7.8525	1.35E26	1+2=3	8.00E26	1+2=3
7.8530	3.63E26	1+2=3	-1.25E28	1+3=4
7.8535	-1.80E26	2+1=3	-5.29E27	2+1=3
7.8540	-4.03E25	2+1=3	3.72E26	2+2=4
7.8545	-8.43E24	2+1=3	-8.45E25	2+1=3
7.8550	5.74E24	2+2=4	-3.45E25	2+1=3
7.8555	1.38E25	2+2=4	2.04E25	2+2=4

Table 6.2.2a Prohibited range of the 1st AP

	Determinant	count Algorithm
2.9911	2.34483E30	0+0=0
2.9912	-5.47994E30	0+1=1
2.9913	8.88815E29	0+0=0
2.9914	2.26730E32	0+0=0
2.9915	2.91564E31	0+0=0
2.9916	-6.14823E33	1+1=2
2.9917	-1.24082E31	1+1=2
2.9918	-5.59675E30	1+1=2
2.9919	4.23714E29	1+0=0
2.9920	3.09534E30	1+0=1

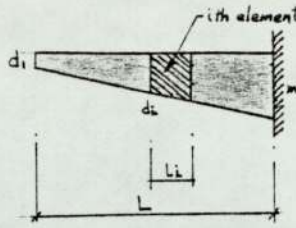

Fig.6.3.1a
A free cantilever beam showing the ith element

Fig.6.3.1b
Asymptotic poles of the elements

No. of elements in the member	Depth of the element	Calculation (from eq. 6.3.2)	Asymptotic Pole
1	$d_1 = 0.4$	Multiplier $Q_m = \sqrt{\frac{0.4}{1.0}} \cdot \frac{10}{10}$; $Q_m \times 4.73004 =$	2.99154
	"	$Q_m \times 7.85320 =$	4.96680
	"	$Q_m \times 10.9956 =$	6.95423
	"	$Q_m \times 14.1372 =$	8.94115
2	$d_1 = 0.4$	$\sqrt{0.4/1.0} \cdot \frac{10}{5} \times 4.73004 =$	5.98308
	"	$\sqrt{0.4/1.0} \cdot \frac{10}{5} \times 7.85320 =$	9.93360
	$d_2 = 1.0$	$\sqrt{1.0/1.0} \cdot \frac{10}{5} \times 4.73004 =$	9.46008
3	$d_1 = 0.4$	$\sqrt{0.4/1.0} \cdot \frac{10}{10/3} \times 4.73004 =$	8.97460
4	$d_1 = 0.4$	$\sqrt{0.4/1.0} \cdot \frac{10}{10/4} \times 4.73004 =$	11.96616

Fig.6.3.1c D-f curves for different number of elements

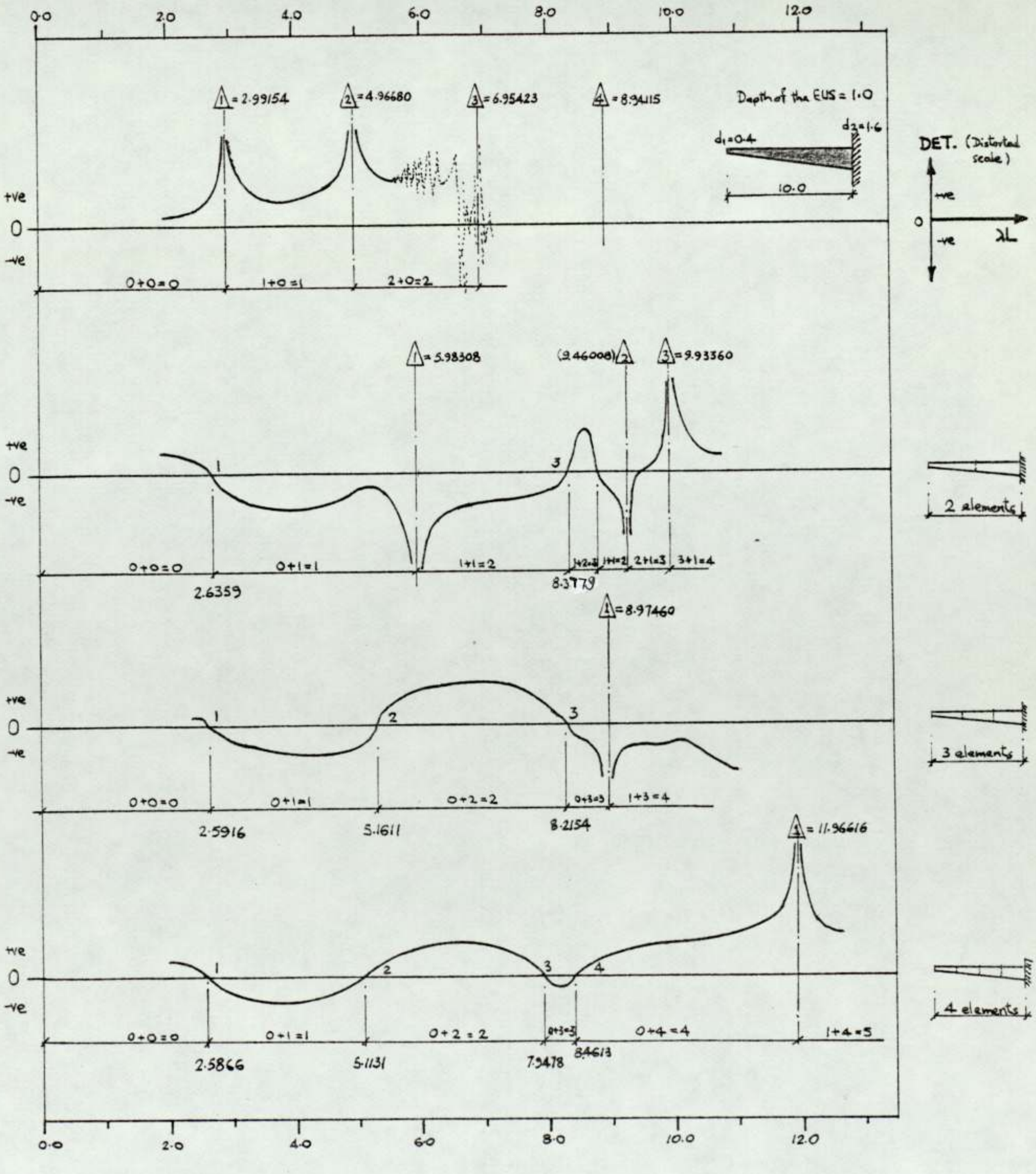

Chapter 7

Behaviour of Non-prismatic plane structures

CHAPTER 7

BEHAVIOUR OF NON-PRISMATIC PLANE STRUCTURES

§7.1 Convergence

Convergence tests are studied for the following three assumptions (assumed displacement functions and discretisation)

(i) The exact function in the stepwise idealisation.

(ii) The quasi-exact function in the tapered discretisation.

(iii) The polynomial function in the tapered discretisation.

To facilitate the presentation of the convergence curves, specified notations are allocated and are summarised in table 7.1.

§7.1.1 Beam structures

(a) Fundamental modes of simple beam structures (fig.7.1.1a)

The boundary conditions of the four structures examined are:- Beams in flexural vibration,

(i) Beam A —— free cantilever

(ii) Beam B —— both ends encastré.

Bars in extensional vibration,

(iii) Bar C —— extensible at the shadow end and inextensible at the deep end.

(iv) Bar D —— both ends inextensible.

For comparison purposes, the sectional properties of these members are identical. The members are wedged in section with a depth ratio of 4.0. The convergence curves are shown in fig.7.1.1a.

Every set of curves converges to a value which is considered to be the exact solution. Obviously the rate of convergence from the stepwise idealisation is inferior to that from the tapered discretisation. In case (iv), as the matrix formulation for the stepwise idealisation is in the same format as that for the tapered discretisation, the two convergence curves are therefore identical.

Although the examples are considered with members of wedged section, similar rates of convergence can be obtained for dove-tailed sections and doubly tapered sections.

(b) <u>Higher modes</u> (fig.7.1.1b)

It is noticed that if extensional vibration is not suppressed in a beam, the result of case (iii) is the fourth mode in a free cantilever beam, and the result of case (iv) is the third mode in an encastré beam. For a free cantilever beam, the convergence of the second and the third modes are shown in fig.7.1.1b.

(c) <u>Haunch beam</u> (fig.7.1.1c)

The haunch beam shown in fig.7.1.1c is composed of two tapered members and one prismatic member. By using the quasi-exact function (exact in prismatic member), no subdivision is necessary in the prismatic member; subdivisions are applied to the two tapered members only. On the other hand, by using the polynomial function, subdivisions are applied to every member.

In order to obtain a conformable comparison on the rate of convergence, the convergence curves are plotted against the member of degrees of freedom, i.e. the size of the matrix to be solved.

It is observed that the curves tail to a converged value. Again the curve obtained from the stepwise idealisation is not as rapid as that from the tapered discretisation, and the curve obtained from the quasi-exact function exhibits a higher performance than that from the polynomial function.

§7.1.2 Frame structures

(a) Pitched portal frame

A model pitched portal frame, which has been statically analysed by Just,[79] is investigated here dynamically. (§7.4). In order to facilitate the presentation of the information, the physical properties of the pitched frame are preferably shown in §7.4 (fig.7.4.1). However, the rate of convergence for the pitched frame is shown in table 7.1.2a.

It is found that the converged value for the fundamental mode of the pitched frame is 41.53 HZ. A rapid convergence is obtained from the tapered discretisation. For coarser subdivision, the quasi-exact function gives a closer approximation. If no subdivision is applied to the frame, the approximated natural frequency is over estimated by about 22%. The over-estimation is reduced to 8% by subdividing each member into 2 elements, and to 3% from a 3 element subdivision.

(b) Mansard frame

A Mansard frame is shown in table 7.1.2b. Although the rate of convergence is tabulated with the number of elements in each member, it is understood that no subdivision is required in the prismatic member when using the quasi-exact function. Again, the stepwise idealisation produces the poorest convergence.

(c) Motorway bridge

The dimensions of a motorway bridge and the rate of convergence are shown in table 7.1.2c. A poor convergence using the stepwise idealisation is obtained as expected. In the tapered discretisation, the rate of convergence of the polynomial function is nearly identical to that in the quasi-exact function.

§7.1.3 Discussion on the choice of function

The most obvious observation from the convergence tests is that the stepwise idealisation converges relatively very slowly and is hence an uneconomical form of representation. Consequently, it follows that the tapered discretisation is a better form for reliable and rapid convergence. In tapered discretisation, the decision on the choice between the quasi-exact function and the polynomial function is not so obvious.

If a structure consists of prismatic members, it is preferable to use the quasi-exact function as no subdivision in a prismatic member can increase the convergence rate, and hence decrease the computing time. Furthermore, from the experience of analysing many examples of other structures, the quasi-exact function almost always gives a better approximation for fewer subdivisions in a tapered member.

For a large number of subdivisions in a member, the natural frequency from the polynomial function is nearly identical to that from the quasi-exact function. If it is necessary to justify the convergence with respect to the computing time, the polynomial function is preferred to the quasi-exact function. The time consumed in the matrix formulation in the latter is more than five times that in the former. This comparison is shown in table 7.1.3a for a particular example. Also the solution routines with the polynomial functions avoid the difficulties (as mentioned in Chapter 6) which arise with the quasi-exact function.

§7.2 Variation in Parameters

§7.2.1 Depth ratio in wedged members

Beams and bars with classical boundary conditions are considered. The fundamental modes (in DFP) of these examples are plotted with the variations in depth ratio as shown in fig. 7.2.1. In a free cantilever beam, an increase of frequency results from the increase in taper (the shallow end being free). An optimised frequency is obtained in a propped cantilever (the shallow end being propped) at a depth ratio of about 3.0. It is seen that a tapered member as an encastré beam or a simply supported beam gives a lower value of frequency.

§7.2.2 Depth ratio of higher modes

Natural frequencies of higher modes are plotted in fig. 7.2.2 against the depth ratio for a wedged cantilever beam. If axial deformation is taken into consideration, the existence of an extensional mode is very much dependent on the depth ratio. In a prismatic member, the third mode is in extensional vibration. The axial mode becomes the fourth if the depth ratio is greater than about 2.2. It is noticed that an optimised frequency is obtained at a depth ratio of about 2.0 for the third mode of the wedged cantilever beem (extensional vibration being suppressed).

§7.2.3 Different types of taper

A free cantilever beam (the shallow end being free) is considered in dovetailed section, wedged section, and doubly tapered section (the depth and breadth ratios being identical). The comparison of the natural frequency resulting from different depth or breadth ratios is shown in fig.7.2.3.

§7.2.4 Haunch ratio in haunch beams

Fig.7.2.4 shows the natural frequency (DFP) of haunch beams with the variation of haunch ratio for different depth ratios. For commonly used haunch beams, the optimised frequency is obtained if the haunch length is about $\frac{1}{4}$ to $\frac{1}{3}$ of the length of the beam.

§7.2.5 Optimisation of a bridge

The example given in §4.7.5 of a prismatic bridge is further investigated here by introducing tapered sections. Different natural frequencies are expected if the bridge is modified by using one or more of the following sections:-
(fig.7.2.5a shows a bridge with all of the following)

(i) End span - a depth ratio of 3.0 with the shallow end being propped.

(ii) Column - a depth ratio of 2.0 with the shallow end being connected to the foundation.

(iii) Mid-Span - a haunch beam with haunch and depth ratios of 0.25 and 2.0 respectively.

Table 7.2.5b shows the natural frequencies with different combinations of the above tapered sections. The fundamental mode of the bridge with all sections tapered (fig.7.2.5a) is 8.78HZ which is smaller than that of the prismatic bridge of equivalent uniform section (i.e. 8.99HZ obtained in §4.7.5). This is the result obtained from the assumption that the bridge supports are perfectly fixed. When the bridge supports are perfectly pinned, the natural frequency is increased by 13% .

§7.3 Modal Shape

The profile of the modal shape of a structure is more accurately assessed if more nodal displacements are available. It has been stated in §7.1.3 that as the number of subdivisions in a structure becomes greater the rate of convergence obtained from the polynomial function is the same as that from the quasi-exact function. Also the suitability of the polynomial function is indicated because of the smaller amount of computing time consumed. Furthermore, the linear eigensystem which results from the polynomial function is preferably solved with the matrix iteration methods. In the matrix iteration methods, eigenvectors (with the associated eigenvalues) are given directly in the same iteration process.

§7.3.1 A free cantilever beam

A free cantilever beam (the shallow end being free) is considered with the following four sections:-

(a) Beam A - Prismatic section

(b) Beam B - Dovetailed section, $n=4.0$

(c) Beam C - Wedged section, $m=4.0$

(d) Beam D - Doubly tapered section, $m=n=4.0$

The mode shapes of the first four modes (in pure flexural vibration) are shown in fig.7.3.1. The slope at the free end for every beam is normalised for comparison. The magnitudes of the relative peak values decrease if the flexural rigidity is increased. It is noted that the four sections mentioned above are in an ascending order of flexural rigidity.

§7.3.2 Pitched portal

The modal shapes of the first eight modes of the pitched portal frame are shown in fig.7.3.2. The physical properties of this frame are shown in fig.7.4.1. Comparison is made by superimposing the modal shapes which are obtained from a frame of equivalent uniform section. As the frame is symmetrical in geometry, either symmetric or anti-symmetric modes result.

§7.4 A Detailed Investigation of the Pitched Portal

§7.4.1 Physical properties of the frame

The frame, which had undergone static tests,[79] is a mild steel pitched portal frame. The dimensions are shown in fig. 7.4.1. The modulus of elasticity and the density are given as 223 KN/mm^2 and 7689 Kg/m^3 respectively.

If the results obtained from this frame are to be compared with those from a frame of prismatic section, the depth and the breadth of the equivalent uniform section must be taken as 7.5mm and 44.55mm respectively.

§7.4.2 Vibrational analysis of the frame

The natural frequencies of the first eight modes from the pitched frame are compared in table 7.4.2 with those from the frame of equivalent uniform section. A decrease in the natural frequency (33% in the fundamental mode) is expected if the supports are perfectly fixed. The natural frequencies for the frame with pinned supports are also shown in table 7.4.2, and an increase of 16% in the fundamental mode is noted. Also shown in fig.7.3.2 are the modal shapes of the first eight modes of both the pitched frame and those of the frame of equivalent uniform section.

§7.4.3 Experiment on the frame

The apparatus for the experiment is illustrated in Plate 1. The frequency of the test frame is the frequency of the vibrator which is driven by an oscillator power amplifier, and the frequency is obtained from the frequency counter. The signal for the source of excitation to which the stationary accelerometer is closely placed is indicated in the serviscope. A resonance is obtained by when a maximum amplitude of the response curve in the serviscope is observed. The natural frequencies obtained from the experiment are compared with the computed results in table 7.4.3 .

The moving accelerometer is to measure the response at any point along the frame. The deflected shape of the frame is obtained by relating the amplitude of the response curve from the moving accelerometer to that from the stationary accelerometer. It is found that the experimental deflected shapes at resonance are very similar to the modal shapes as shown in fig.7.3.2 .

Table 7.1 Notation on curves

Function	Exact function Stepwise Idealisation	Quasi-exact function	Polynomial function
		Tapered discretisation	
Notation	(E-S)	(Q-T)	(P-T)

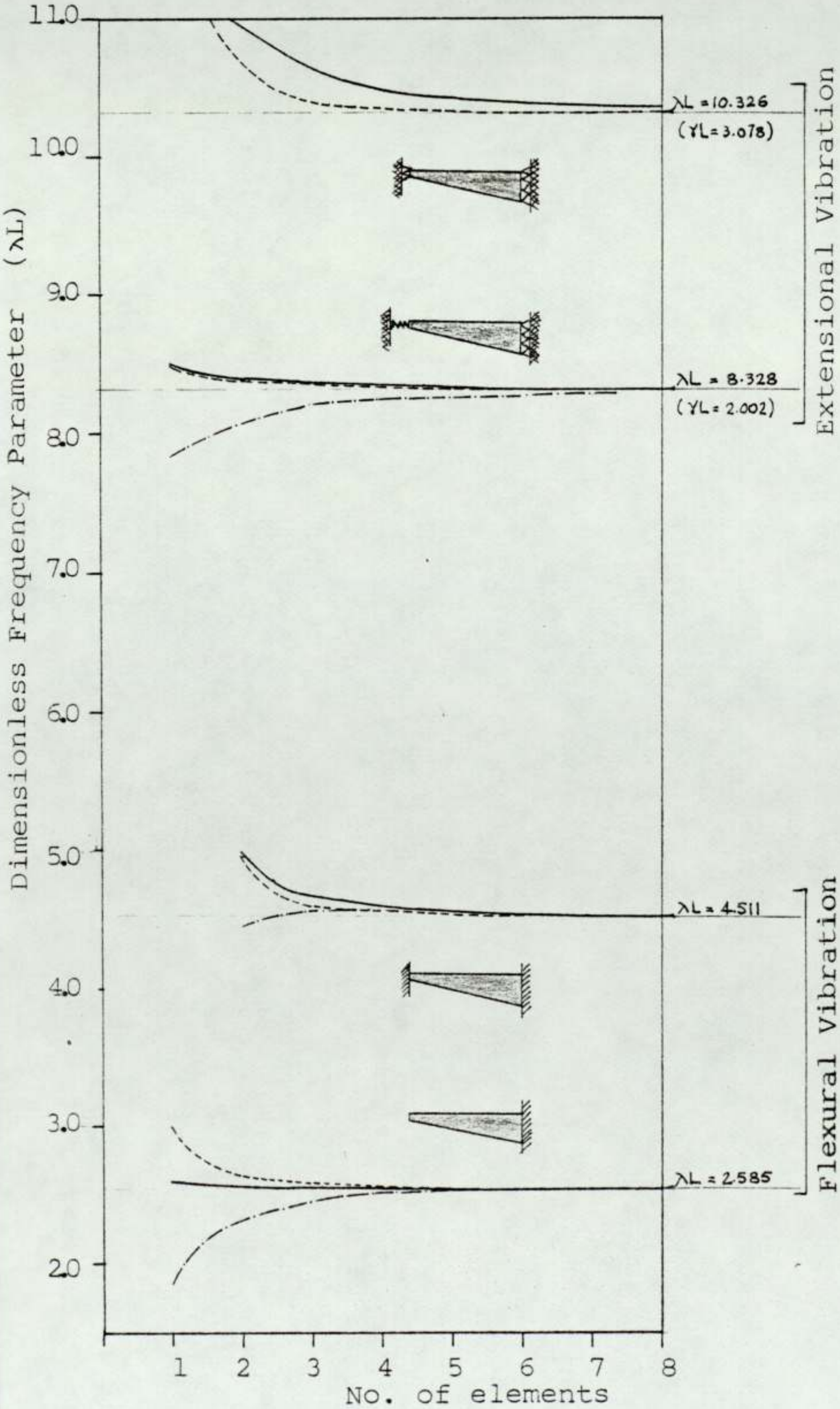

Fig.7.1.1a

Convergence of Fundamental mode of a wedged beam (m=4.0)

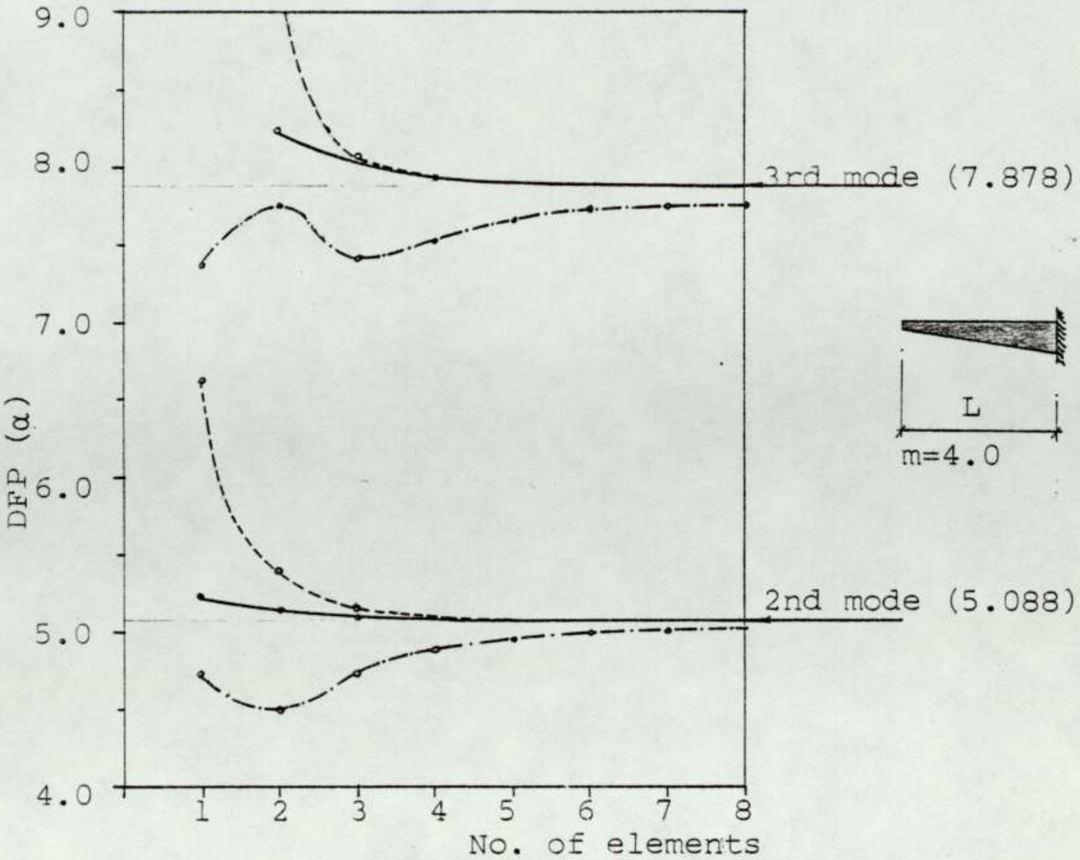

Fig.7.1.1b Convergence of higher modes

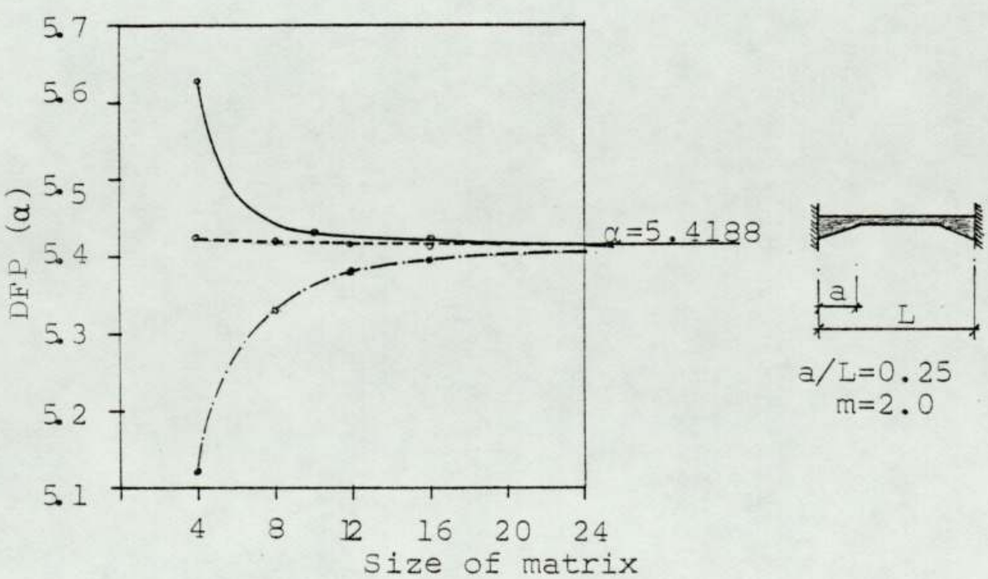

Fig.7.1.1c Convergence of a haunch beam

Table 7.1.2a Convergence of a pitched frame

No. of elements in each member	Stepwise idealisation	Tapered Discretisation	
	Exact function	Quasi-exact function	Polynomial function
1	54.95	50.62	53.84
2	46.77	45.02	45.09
3	44.57	42.83	42.85
4	43.55	42.11	42.11
5	42.96	41.82	41.82
6	42.59	41.68	41.68

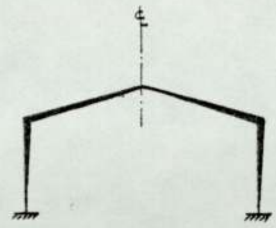

Exact solution = 41.53 HZ
(for dimensions, see fig. 7A.1)

Table 7.1.2b Convergence of a Mansard frame

No. of elements in each member	Stepwise Idealisation	Tapered Discretisation	
	Exact function	Quasi-exact function	Polynomial function
1	10.61	8.53	8.64
2	8.64	7.87	7.87
3	8.18	7.78	7.78
4	8.00	7.56	7.76
5	7.91	7.75	7.75

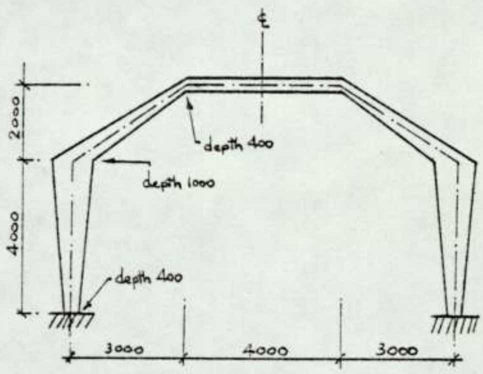

Table 7.1.2c Convergence of a bridge

No. of elements in each member	Stepwise Idealisation	Tapered Discretisation	
	Exact function	Quasi-exact function	Polynomial function
1	7.49	6.73	6.72
2	6.68	6.31	6.31
3	6.46	6.26	6.26
4	6.37	6.25	6.25
5	6.33	6.25	6.25
6	6.31	6.25	6.25

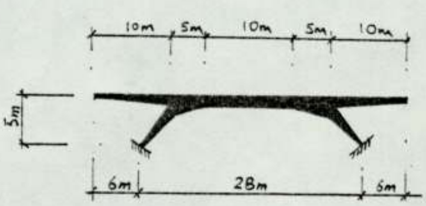

N.B. Frequency in HZ, & dimensions in mm.

Table 7.1.3 CPU for polynomial & Quasi-exact functions

Section	CPU $(\times 10^{-3})$ Polynomial function	Quasi-exact function
Prismatic member	4	22
Dovetailed member	4	23
Wedged member	6	44
Doubly tapered member	6	48

Fig.7.2.1

Fundamental mode with different depth ratio (wedged section)

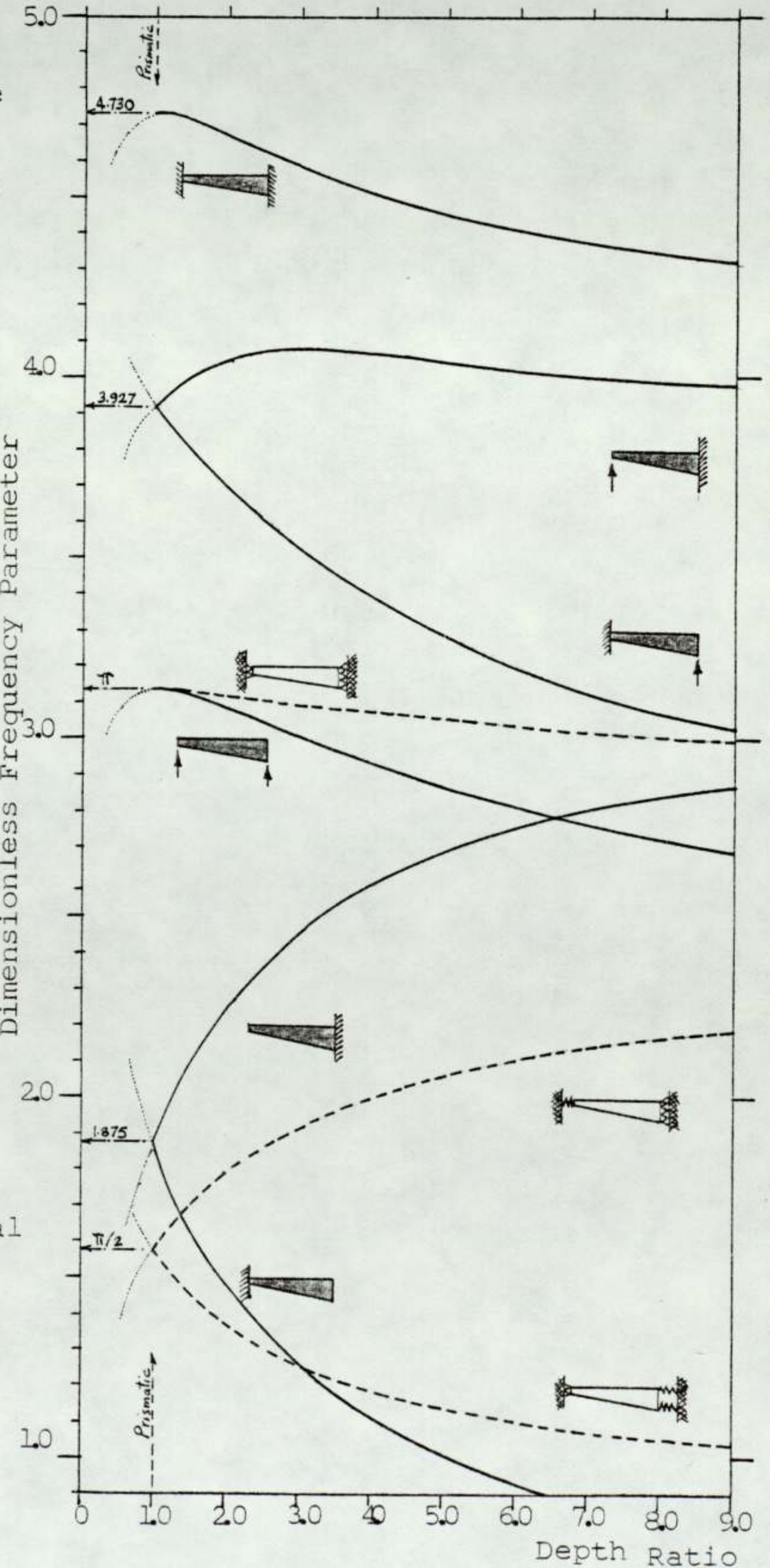

for flexural vibration, (DFP in λL)

for extensional vibration (DFP in γL)

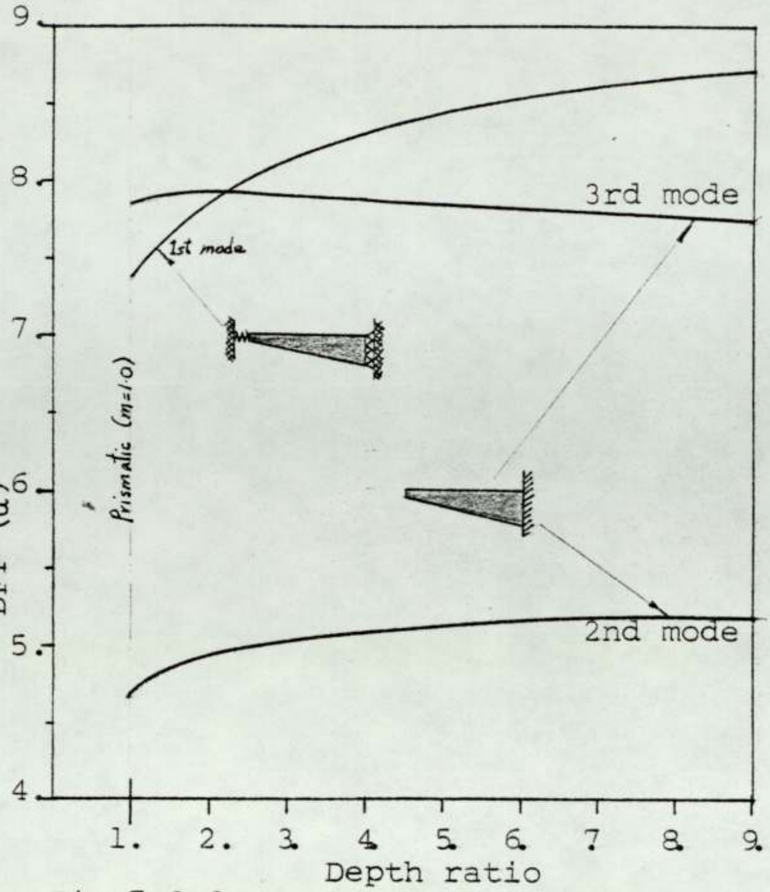

Fig.7.2.2
Higher modes with different depth ratio

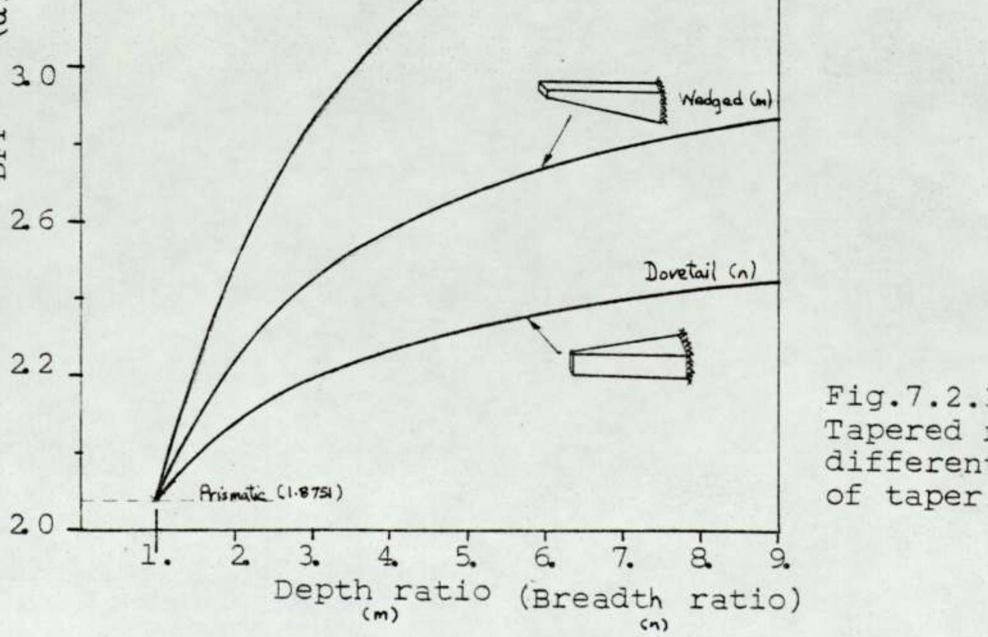

Fig.7.2.3
Tapered ratio in different types of taper

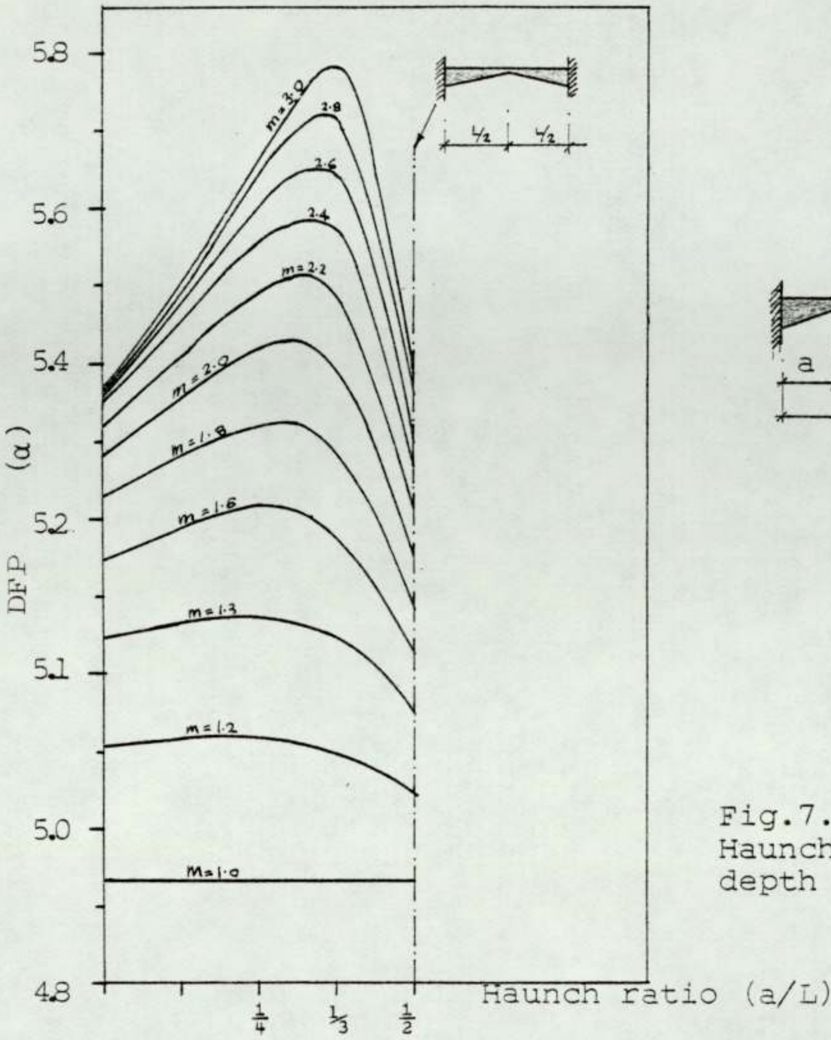

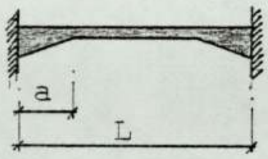

Fig.7.2.4
Haunch ratio and
depth ratio

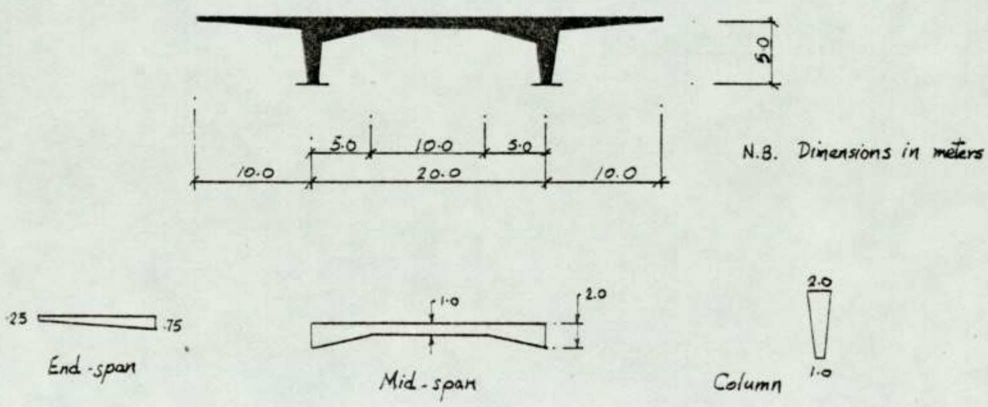

Fig.7.2.5a Dimensions of a bridge with all members
in tapered section

Table 7.2.5b Fundamental mode of bridges

Bridge structures	Fixed supports	Pinned supports
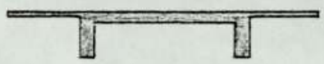	8.99 HZ	(4.45 HZ)
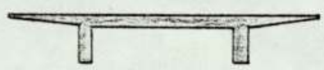	8.97 HZ	(4.48 HZ)
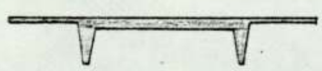	(8.68 HZ)	(4.57 HZ)
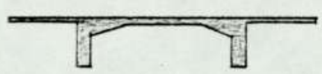	10.25 HZ	(4.85 HZ)
	10.19 HZ	(4.87 HZ)
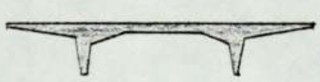	(8.78 HZ)	(5.02 HZ)

N.B. Figures in brackets
for symmetric modes

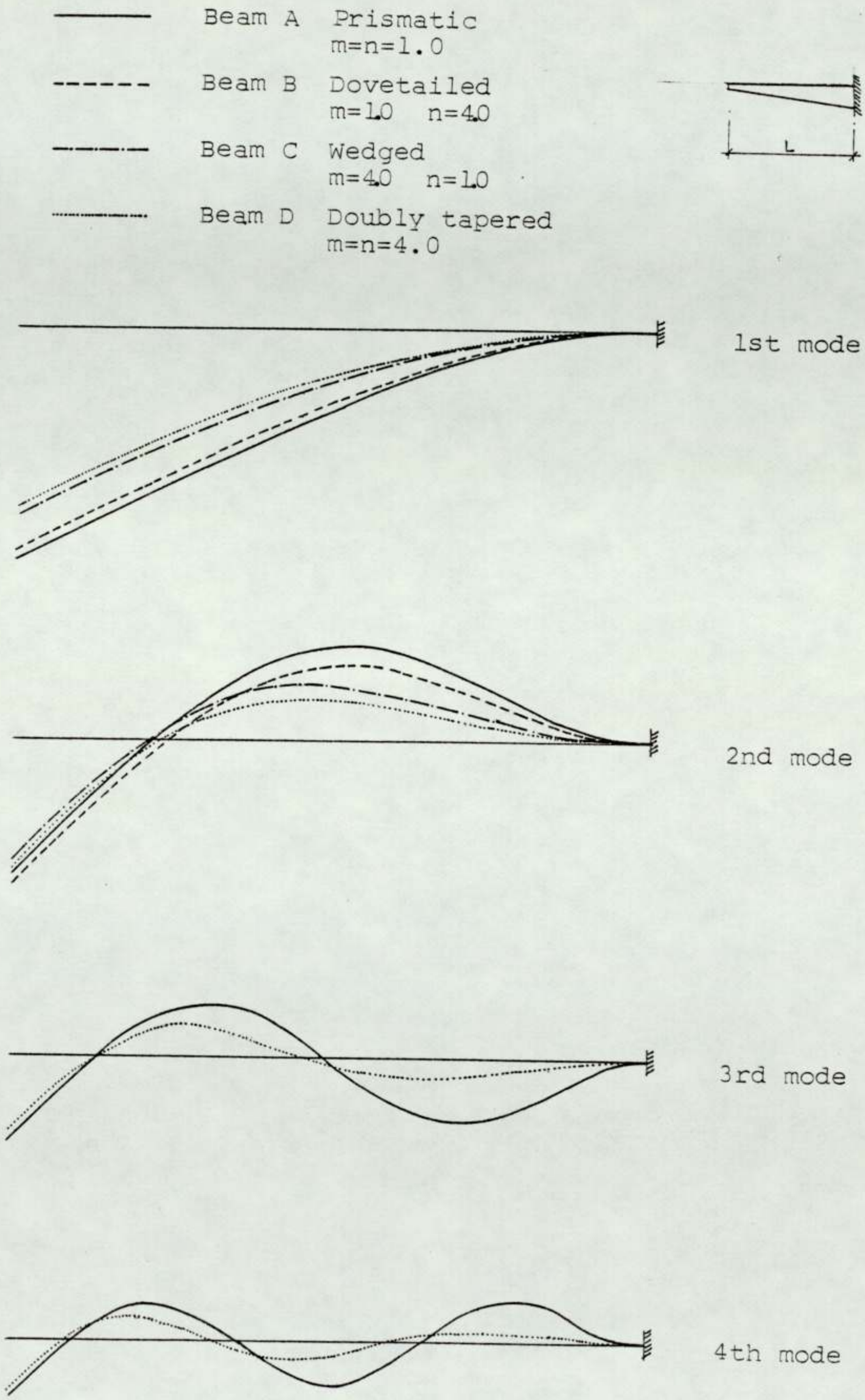

Fig.7.3.1 Modal shapes of a free cantilever beam

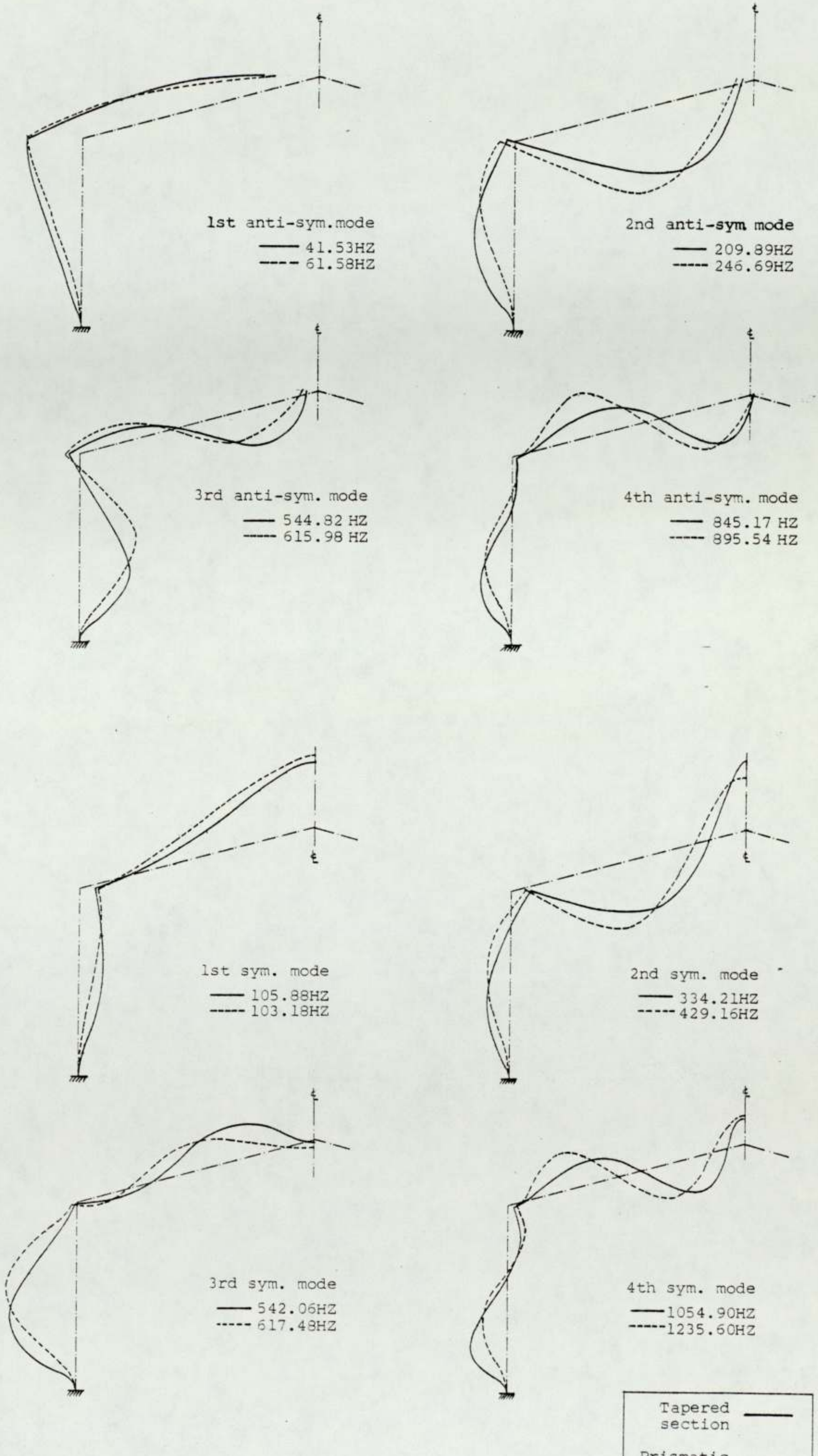

Fig.7.3.2 Modal shapes of a pitched portal frame

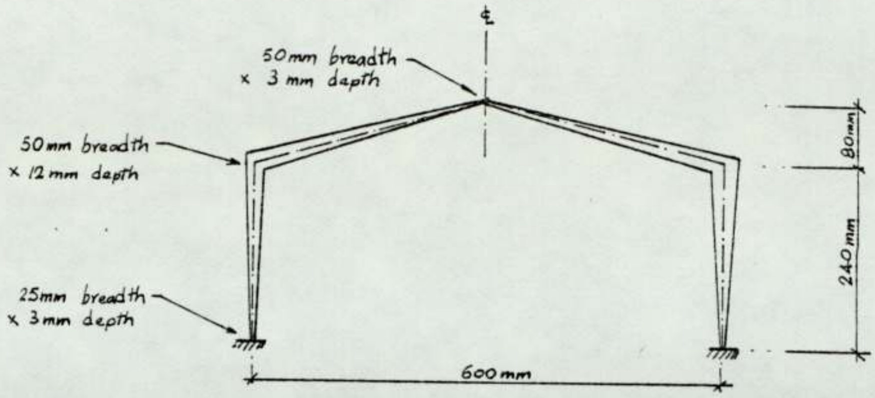

Fig.7.4.1 Dimension of a model pitched frame

Table 7.4.2 Comparison of natural frequencies (HZ)

Mode	Fixed supports		Pinned supports	
	Tapered section	Prismatic section	Tapered section	Prismatic section
1	41.53	61.58	32.04	27.74
2	(105.88)	(103.18)	(91.42)	(87.54)
3	209.89	246.69	192.82	223.99
4	(334.21)	(429.16)	(324.95)	(379.22)
5	(542.06)	615.98	(480.93)	462.58
6	544.82	(617.48)	485.22	(485.59)
7	845.17	895.54	813.70	855.93
8	(1054.90)	(1235.60)	(1012.23)	(1156.62)

Table 7.4.3 Computed & experimental results of pitched frame

Mode	Nautral frequency (HZ)		% error
	Computed	Experimental	
1	41.53	41	1
2	(105.89)	106	0
3	209.89	199	5
4	(334.21)	318	5
5	(542.06)	506	7
6	544.82	543	0
7	845.17	802	5
8	(1054.90)	1020	3

N.B. Figures in brackets to indicate symmetric modes.

Chapter 8

Dynamic Response

CHAPTER 8

DYNAMIC RESPONSE

§8.1 Survey of Methods

§8.1.1 Introduction

The time variation of the force vector $\{P(t)\}$ in eq.2.1.4 may be harmonic, transient or random. For forces of harmonic motion, the steady-state response of the structure can be found by the frequency response method or the normal mode method. The application of these two methods are discussed in the next section.

The numerical integration method can also be applied to the solution of problems involving harmonic exciting forces although this method becomes economical computationally in the analysis of non-harmonic response. The basic assumptions of this method are made about the variation of the displacements or accelerations during small time intervals. With such assumptions the set of n second order differential equations (eq.2.4.1) is replaced, in general, by n simultaneous equations. Different approaches and assumptions to this method are reported[31,96].

It is the intention of this chapter to examine the behaviour of the dynamic stiffness matrix for tapered section (as derived in Chapter 5) in the dynamic response analysis, and results obtained from the tapered section are compared with those from the prismatic section. Although the exciting forces are assumed to be harmonic in nature, similar comparisons may be obtained for exciting forces of different natures which may involve using the numerical integration method. However, for harmonic forces the frequency response method and the normal mode method are discussed here with particular attention to the tapered discretisation.

§8.1.2 The frequency response method

For an undamped system, the equation of motion (eq.2.1.4) is rewritten as

$$[K]\{x\} + [M]\{\ddot{x}\} = \{P(t)\} \qquad 8.1.1$$

The harmonic excitation, $\{P(t)\}$, is given in the form

$$\{P(t)\} = \{F\}\sin\Omega t \qquad 8.1.2$$

where $\{F\}$ is a vector of the driving force amplitude and Ω is the forcing frequency. If the system is also considered to be in steady-state vibration, the response vector may be assumed to be given by

$$\{x\} = \{d\}\sin\Omega t \qquad 8.1.3$$

where $\{d\}$ is an unknown vector of the response amplitude. Substituting for $\{P(t)\}$ & $\{x\}$ into eq.8.1.1 gives

$$[K-\Omega^2 M]\{d\} = \{F\} \qquad 8.1.4$$

If Ω is not a natural frequency, the square matrix $[K-\Omega^2 M]$ is non-singular and may be inverted to yield

$$\{d\} = [K-\Omega^2 M]^{-1}\{F\} \qquad 8.1.5$$

The response amplitude is thus expressed in terms of the driving force amplitude.

8.1.3 The normal mode method

Consider any arbitrary vector $\{y\}$,

$$\{y\} = \sum_{r=1}^{n} \{\delta_r\} a_r \qquad 8.1.6$$

where $\{\delta_r\}$ is the rth eigenvector of the general eigensystem, $[K]\{\delta\} = \omega^2[M]\{\delta\}$ (in eq.3.2.1) and a_r is a scalar mode multiplier. Premultiplying both sides of this equation by $\{\delta_s\}^T[M]$ gives

$$\{\delta_s\}^T[M]\{y\} = \sum_{r=1}^{n}\{\delta_s\}^T[M]\{\delta_r\} a_r \qquad 8.1.7$$

Because of the orthogonality relation of eq.3.2.5, all the terms on the right hand side vanish except the one for which r=s, thus

$$\{\delta_s\}^T[M]\{y\} = \{\delta_r\}^T[M]\{\delta_r\} a_r \qquad 8.1.8$$

Substituting the value of the scalar mode multiplier so obtained into eq.8.1.6 gives

$$\{y\} = \sum_{r=1}^{n} \frac{\{\delta_r\}\{\delta_r\}^T[M]}{\{\delta_r\}^T[M]\{\delta_r\}} \{y\} \qquad 8.1.9$$

It is noticed that the summation of the matrix manipulation gives the identity,

$$\sum_{r=1}^{n} \frac{\{\delta_r\}\;\{\delta_r\}^T[M]}{\{\delta_r\}^T[M]\;\{\delta_r\}} = [I] \qquad 8.1.10$$

and it follows that $\{y\}$ is completely arbitrary and independent. If the arbitrary vector is replaced by the driving force amplitude vector $\{F\}$, this may be expressed as

$$\{F\} = \sum_{r=1}^{n} \frac{\{\delta_r\}\{\delta_r\}^T[M]}{\{\delta_r\}^T[M]\{\delta_r\}}\{F\} \qquad 8.1.11$$

Also let the response amplitude vector $\{d\}$ be represented by

$$\{d\} = \sum_{r=1}^{n} \{\delta_r\} b_r \qquad 8.1.12$$

where b_r is an unknown coefficient. The natural frequency at the rth mode (from the general eigensystem) is given as

$$\omega_r^2 = [M]^{-1}[K] \qquad 8.1.13$$

Substituting for eqs.8.1.13 & 8.1.12 into eq.8.1.4 gives

$$\sum_{r=1}^{n} (\omega_r^2 - \Omega^2)[M]\{\delta_r\} b_r = \{F\} \qquad 8.1.14$$

Premultiplying both sides of the equation by $\{\delta_r\}^T$, and again using the orthogonality relationship, the unknown coefficient is obtained as

$$b_r = \frac{1}{\omega_r^2 - \Omega^2} \frac{\{\delta_r\}^T\{F\}}{\{\delta_r\}^T[M]\{\delta_r\}} \qquad 8.1.15$$

Substituting for b_r into eq.8.1.12, the effect of frequency on the response is clearly indicated as

$$\{d\} = \sum_{r=1}^{n} \frac{1}{\omega_r^2 - \Omega^2} \frac{\{\delta_r\}\{\delta_r\}^T}{\{\delta_r\}^T[M]\{\delta_r\}} \{F\} \qquad 8.1.16$$

§8.2 Analytical Study of Prismatic Beam

The beam considered is shown in fig.8.2 . To simplify the presentation, extensional displacement is suppressed. Flexural displacements (W_1, θ_1) are excited by harmonic forces denoted as $F\sin\Omega t$ and $M\sin\Omega t$. In the vibration of a beam, the frequency is better referred to the dimensionless frequency parameter, λL. The frequencies at resonance for the beam shown in fig.8.2 are λL=1.8751, 4.6941, 7.8548, etc.

§8.2.1 The frequency response method

(a) Polynomial function

Substituting the boundary conditions into the equations for the formulation of the dynamic stiffness matrix (eq.2.2.25) gives

$$\frac{EI}{420L^3}\begin{bmatrix} (5040-156\alpha^4) & (2520-22\alpha^4)L \\ \text{sym.} & (1680-4\alpha^4)L^2 \end{bmatrix}\begin{bmatrix} W_1 \\ \theta_1 \end{bmatrix} = \begin{bmatrix} F \\ M \end{bmatrix} \qquad 8.2.1$$

Manipulating the inverse of the dynamic stiffness matrix and substituting into eq.8.1.5, the response amplitude vector is found to be

$$\begin{bmatrix} W_1 \\ \theta_1 \end{bmatrix} = Q\begin{bmatrix} (1680-4\alpha^4)L^2 & -(2520-22\alpha^4)L \\ \text{sym.} & (5040-156\alpha^4) \end{bmatrix}\begin{bmatrix} F \\ M \end{bmatrix} \qquad 8.2.2$$

where $Q = \dfrac{3L}{EI(\alpha^8 - 1224\alpha^4 + 15120)}$

If $\alpha=0.0$, the static displacement of the beam is given, thus

$$\begin{bmatrix} W_1 \\ \theta_1 \end{bmatrix} = \begin{bmatrix} L^3/3EI & -L^2/2EI \\ \text{Sym.} & L/EI \end{bmatrix} \begin{bmatrix} F \\ M \end{bmatrix} \qquad 8.2.3$$

If $\alpha=1.8796$, which is the frequency at resonance from the assumed polynomial function, the value of Q in eq.8.2.2 becomes zero and hence every element term becomes infinite. However, for $\alpha=1.8751$, which is the exact frequency at resonance, the response amplitude vector becomes

$$\begin{bmatrix} W_1 \\ \theta_1 \end{bmatrix} \quad \frac{1}{EI} \begin{bmatrix} 34.62L^3 & -47.73L^2 \\ \text{sym.} & 66.06L \end{bmatrix} \begin{bmatrix} F \\ M \end{bmatrix} \qquad 8.2.4$$

(b) <u>Exact function</u>

Substituing the boundary conditions into eq.2.3.31 gives

$$\frac{EI}{L^3}\,\frac{\alpha}{1-cch} \begin{bmatrix} (sch+csh)\alpha^2 & (ssh)\alpha L \\ \text{Sym.} & (sch-csh)L^2 \end{bmatrix} \begin{bmatrix} W_1 \\ \theta_1 \end{bmatrix} = \begin{bmatrix} F \\ M \end{bmatrix} \qquad 8.2.5$$

Manipulating the inverse of the dynamic stiffness matrix and substituting into eq.8.1.5, the response amplitude vector is found to be

$$\begin{bmatrix} W_1 \\ \theta_1 \end{bmatrix} = \frac{L}{EI(1+cch)\alpha^3} \begin{bmatrix} (sch-csh)L^2 & -(ssh)\alpha L \\ \text{sym.} & (sch+csh)\alpha^2 \end{bmatrix} \begin{bmatrix} F \\ M \end{bmatrix} \qquad 8.2.6$$

To obtain the element terms as rational values, the evaluation is achieved by using the series expansions of the trigonometrical and hyperbolic functions (Appendix D)

§8.2.2 The normal mode method

The free vibration of the beam is the solution of the eigenproblem which is obtained by equating the driving force amplitude vector $\{F\}$ in eq.8.1.4 to zero. From the polynomial function, the eigenvalues are respectively $\alpha_r = 1.8796$ & 5.8997 for r=1 & 2. By normalising the slope displacement, the modal shapes are described by

$$\{\delta_r\} = \begin{bmatrix} W_r \\ 1 \end{bmatrix} \quad 8.2.7$$

$$\text{where} \quad W_r = -\frac{2520-22\alpha_r^4}{5040-156\alpha_r^4}L \quad 8.2.8$$

From eq.2.2.24 the mass matrix of the beam is written as

$$[M] = \rho AL/420 \begin{bmatrix} 156 & 22L \\ \text{Sym.} & 4L^2 \end{bmatrix} \quad 8.2.9$$

and hence the denominator of eq.8.1.16 is

$$\{\delta_r\}^T[M]\{\delta_r\} = \rho AL^3 Q_r \quad 8.2.10$$

$$\text{where} \quad Q_r = \frac{\alpha_r^8 - 840\alpha_r^4 + 98960}{3(11\alpha_r^4 - 1260)^2} \quad 8.2.11$$

Substituting $\{\delta_r\}$ into the numerator of eq.8.1.16 gives

$$\{\delta_r\}\{\delta_r\}^T\{F\} = \begin{bmatrix} W_r^2 & W_r \\ W_r & 1 \end{bmatrix}\begin{bmatrix} F \\ M \end{bmatrix} \quad 8.2.12$$

Substituting for eqs.8.2.10 & 8.2.12 into eq.8.1.16, the response amplitude vector at the free end of the beam is expressed as

$$\begin{bmatrix} W_1 \\ \theta_1 \end{bmatrix} = \frac{L}{EI}\sum_{r=1}^{n}\frac{1}{\alpha_r^4-\alpha^4}\frac{1}{Q_r}\begin{bmatrix} W_r^2 & W_r \\ W_r & 1 \end{bmatrix}\begin{bmatrix} F \\ M \end{bmatrix}. \quad 8.2.13$$

Substituting for α_r , Q_r & W_r , the response amplitude vector is evaluated, thus

$$\begin{bmatrix} W_1 \\ \theta_1 \end{bmatrix} = \frac{L}{EI} \begin{bmatrix} \delta_{11} & \delta_{12} \\ \delta_{12} & \delta_{22} \end{bmatrix} \begin{bmatrix} F \\ M \end{bmatrix} \qquad 8.2.14$$

where
$$\delta_{11} = L^3 \left(\frac{0.527}{Q_1(\alpha_1^4-\alpha^4)} + \frac{0.0172}{Q_2(\alpha_2^4-\alpha^4)} \right)$$

$$\delta_{12} = -L^2 \left(\frac{0.726}{Q_1(\alpha_1^4-\alpha^4)} + \frac{0.131}{Q_2(\alpha_2^4-\alpha^4)} \right)$$

$$\delta_{13} = L \left(\frac{1.0}{Q_1(\alpha_1^4-\alpha^4)} + \frac{1.0}{Q_2(\alpha_2^4-\alpha^4)} \right)$$

& where $Q_1 = 0.129217$
$Q_2 = 0.002173$

If α=0.0, the static displacements at the free end are found to be the same as those obtained from eq.8.2.3. For the frequency at resonance, i.e.α=1.8796, infinity is expected in the response amplitude vector. However, for the exact frequency at resonance, i.e.α=1.8751, the response amplitude vector is obtained as shown in eq.8.2.4 .

Similar procedures can be performed with the exact function, but these are not duplicated here. It should be noted that whereas the response amplitude vector is obtained by superposition of two modes in the polynomial function, infinite modes are superposed in the exact function. However, the superpositions contributed from higher modes becomes insignificant, and the procedure may be truncated by discarding the higher frequencies. The degree of truncation is dependent on the value of $(\omega_r^4-\Omega^4)$ which is the denominator in eq.8.1.16 .

§8.2.3 Discussion on the methods

(a) Displacement functions

Considering the beam shown in fig.8.2 subjected to an excitation force of $F\sin\Omega t$ only, the vertical displacement is given by

(i) from eq.8.2.2 in the polynomial function

$$W_1 = \frac{3(1680-4\alpha^4)}{\alpha^8-1224\alpha^4+15120}\frac{FL^3}{EI} \qquad 8.2.15$$

(ii) from eq.8.2.6 in the exact function

$$W_1 = \frac{sch-csh}{\alpha^3(1+cch)}\frac{FL^3}{EI} \qquad 8.2.16$$

In fig.8.2.3a, the excitation displacements are plotted against the dimensionless frequency parameter (λL) according to eqs.8.2.15 & 8.2.16. The frequencies at resonance are given at points where the displacements are infinite.

(b) Computing time

In the frequency response method, the process requires repeated inversion if a range of frequencies is to be studied. In the normal mode method, the matrices are computed once only and the range of the frequencies is studied by simply substituting into $(\omega_r^2-\Omega^2)$. Therefore, as shown in fig.8.2.3b, the normal mode method is more economical in computation time if the number of frequencies to be obtained from the same vibrating system is more than 3.

§8.3 Examples on Structures of Tapered Section

§8.3.1 A free cantilever beam

(a) Analytical study

The presentation of the analytical study is typified by using the frequency response method in the polynomial function. Similar procedures for the normal mode method and in the quasi-exact function are not duplicated here. The wedged cantilever beam investigated is shown in fig.8.3.1a with a depth ratio of 4.0, the shallow end being free. The depth of the equivalent uniform section is 1.0 .

Substituting the boundary conditions and the depth ratio of the beam into the dynamic stiffness matrix (§5.2.3), the equation for the forced vibration is given as

$$\frac{EI}{840\,L^3}\begin{bmatrix} 259560-528\alpha_1^4 & (79128-86\alpha_1^4)L \\ \text{Sym.} & (32088-17\alpha_1^4)L^2 \end{bmatrix}\begin{bmatrix} W_1 \\ \theta_1 \end{bmatrix} = \begin{bmatrix} F \\ M \end{bmatrix} \qquad 8.3.1$$

If the dynamic stiffness matrix is referred to the equivalent uniform section (I,α) instead of the section at the shallow end (I_1, α_1) , a transformation is required. From eq.5.1.6 , this gives

$$p_1 = \frac{d_1}{d} = 0.4 \qquad 8.3.2$$

Again, from eq.5.1.10 & 5.1.16, the transformations are

$$\alpha_1 = \frac{\alpha}{\sqrt{p_1}} \qquad 8.3.3$$

$$\& \quad I_1 = p_1^3\, I \qquad 8.3.4$$

Substituting for α_1 & I_1 into eq.8.3.1 gives

$$\frac{EI}{13125L^3}\begin{bmatrix} 259560-3300\alpha^4 & L(79128-538\alpha^4) \\ \text{Sym.} & L^2(32088-106\alpha^4) \end{bmatrix}\begin{bmatrix} W_1 \\ \theta_1 \end{bmatrix} = \begin{bmatrix} F \\ M \end{bmatrix} \qquad 8.3.5$$

which is denoted in matrix notation as

$$[J]\{\delta\} = \{F\} \qquad 8.3.6$$

Premultiplying both sides of eq.8.3.5 by $[J]^{-1}$ gives

$$\begin{bmatrix} W_1 \\ \theta_1 \end{bmatrix} = Q \begin{bmatrix} (32088-106\alpha^4)L^2 & -(79128-538\alpha^4)L \\ \text{Sym.} & 259560-3300\alpha^4 \end{bmatrix}\begin{bmatrix} F \\ M \end{bmatrix} \qquad 8.3.7$$

where $Q = \dfrac{0.213L}{EI(\alpha^8-784\alpha^4+33499)}$

The frequency at resonance is obtained if

$$\alpha^8 - 784\alpha^4 + 33499 = 0 \qquad 8.3.8$$

which gives

$$\bar{\alpha}_1 = 2.5947 \qquad 8.3.9$$
$$\bar{\alpha}_2 = 5.2138$$

and these are compared with the exact solution,

$$\bar{\alpha}_1 = 2.5850 \qquad 8.3.10$$
$$\bar{\alpha}_2 = 5.0888$$

The static displacement vector is obtained by substituting $\alpha=0.0$ into eq.8.3.7, thus

$$\begin{bmatrix} W \\ \theta_1 \end{bmatrix} = L/EI \begin{bmatrix} 0.2037L^2 & -0.5023L \\ \text{sym.} & 1.6477 \end{bmatrix}\begin{bmatrix} F \\ M \end{bmatrix} \qquad 8.3.11$$

which is compared with the exact solution

$$\begin{bmatrix} W \\ \theta_1 \end{bmatrix} = L/EI \begin{bmatrix} 0.205L^2 & -0.488L \\ \text{sym.} & 2.440 \end{bmatrix}\begin{bmatrix} F \\ M \end{bmatrix} \qquad 8.3.12$$

For a range of frequencies, the response amplitudes are shown in fig.8.3.1b .

(b) Numerical study

The procedure of the analysis discussed in the last section is programmed so as to cater for a dynamic system with a large number of degrees of freedom. As it is necessary for the profiles of the deflected shapes to be precisely described by an adequate number of nodal points, each member is subdivided into a comprehensive number of elements. The assigned number of elements should be sufficient to give an almost exact solution.

Repeating the analysis of the beam shown in fig.8.3.1a, the response amplitudes at the free end obtained for a range of frequencies are shown in fig.8.3.1c. In the same diagram, the response amplitudes are also shown for members of prismatic and doubly tapered sections. The frequencies at resonance are indicated at the positions of infinite amplitude. When the driving frequency is about α=4.0574, the zero intersection in fig.8.3.1c indicates that the displacement at the free end is zero. (It is noted that α=4.0574 is the natural frequency of a propped cantilever.) The deflected curves with different driving frequencies are compared in fig.8.3.1d .

§8.3.2 Pitched portal

Harmonic excitation is acting horizontally at the eaves of the pitched frame (point B of fig.8.3.2a). The response amplitudes for a range of frequencies are shown in fig.8.3.2b. Two sets of curves respectively for horizontal response amplitudes at points B & D are compared. Natural frequencies of the frame are declared at the poles of singularity. The zero intersection at a frequency of about 94HZ indicates that there is no horizontal displacement at point B. The deflected shapes for the forcing frequencies before and after the zero intersection are shown in fig.8.3.2c .

If the horizontal force is considered with null forcing frequency, a static problem is observed. The computed horizontal displacement at point B is 5.892mm which is compared with 5.901mm from Ref.79 , the difference being only 0.1% . In this case the horizontal force is simply 1.0 KN .

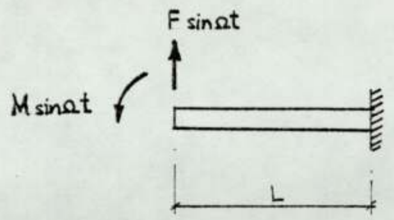

Fig.8.2 Free cantilever beam
undergoing harmonic forces

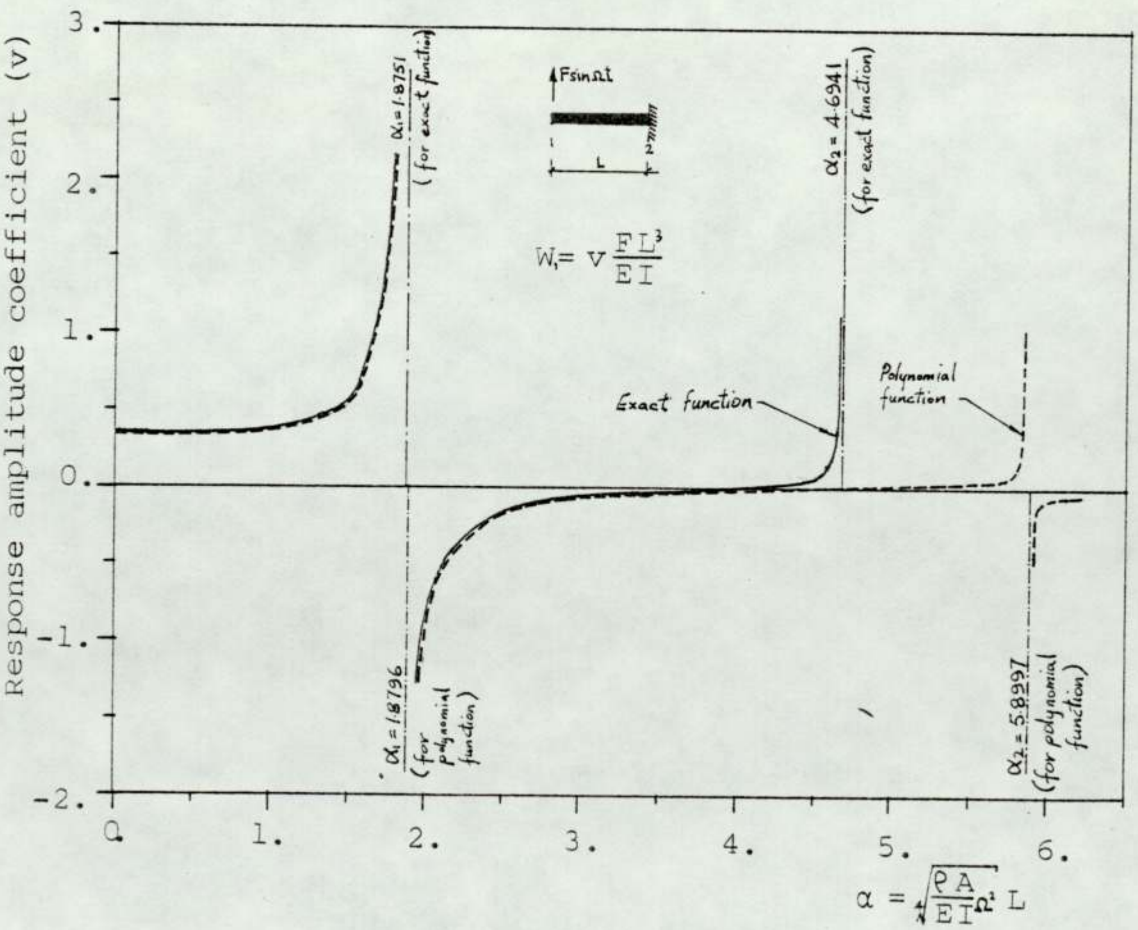

Fig.8.2.3a Frequency response of a prismatic beam

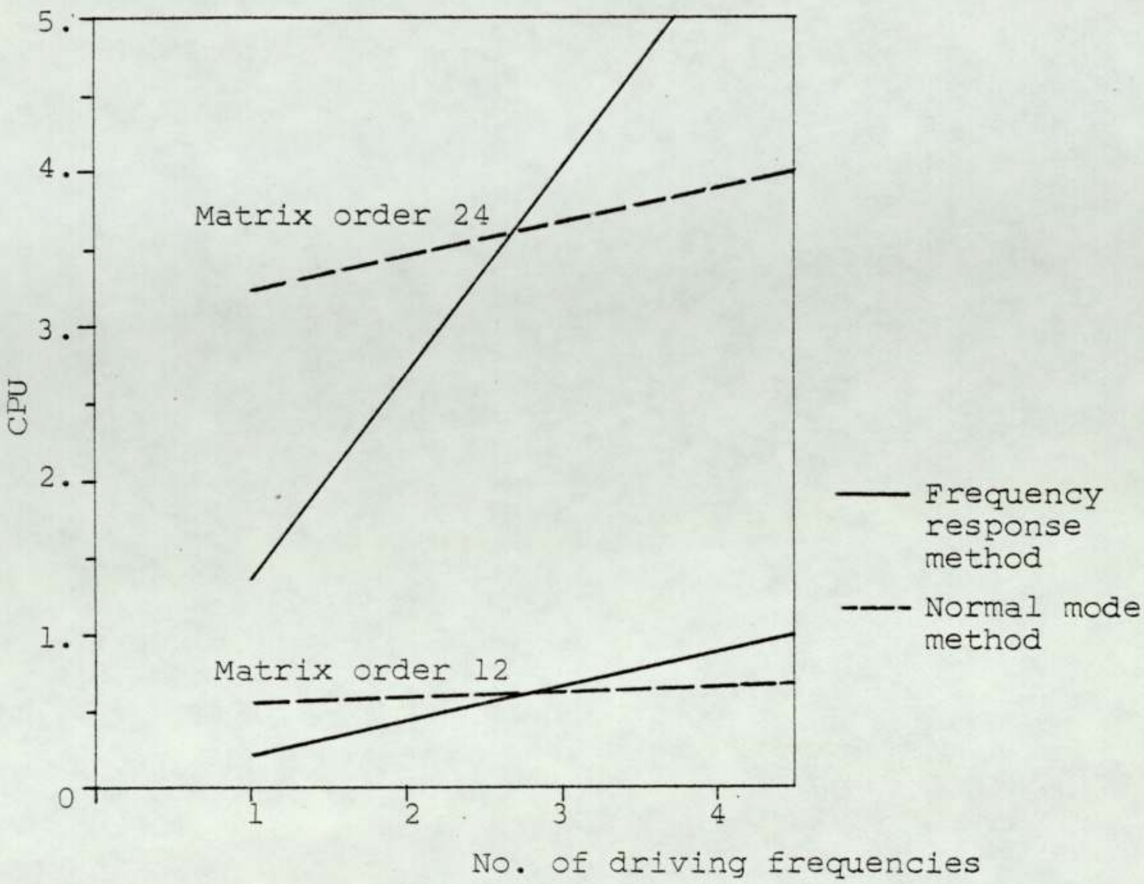

Fig.8.2.3b Computing time of the methods

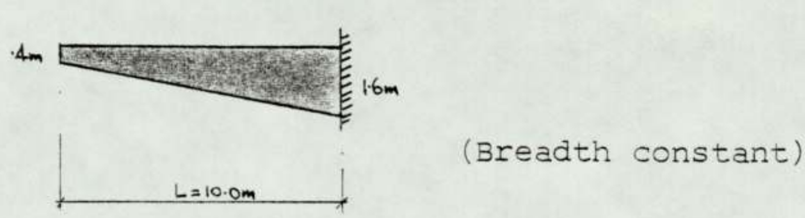

Fig.8.3.1a Free cantilever beam of wedged section

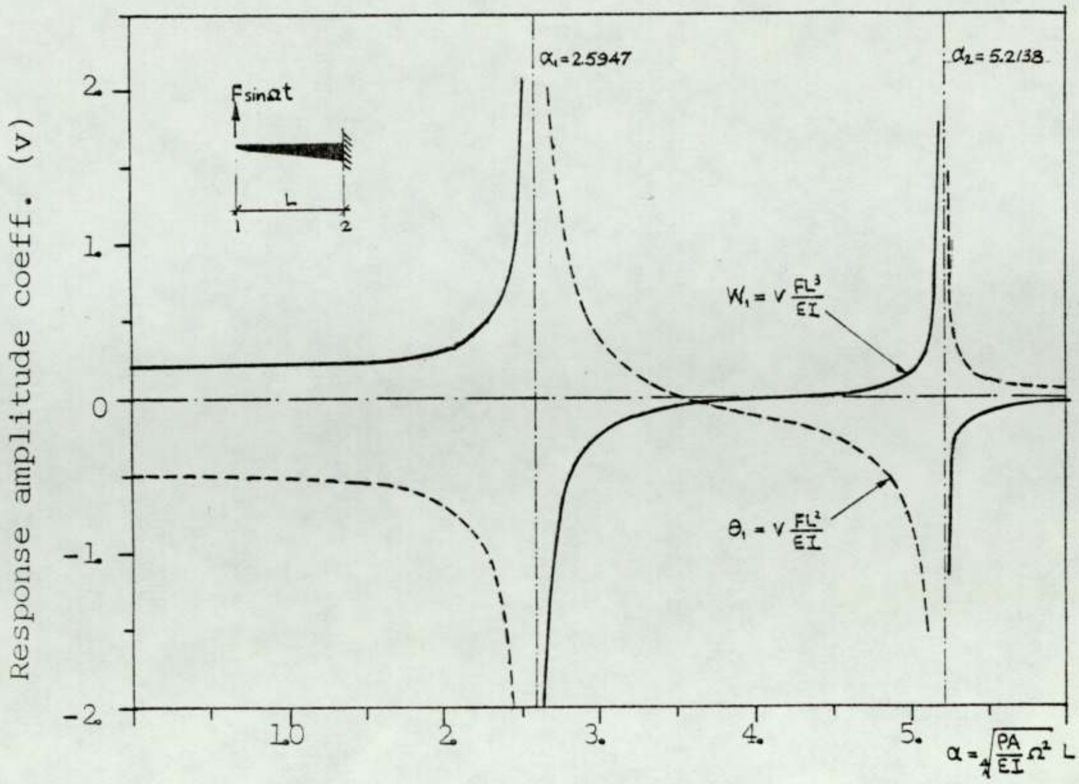

Fig.8.3.1b Frequency response of a wedged beam

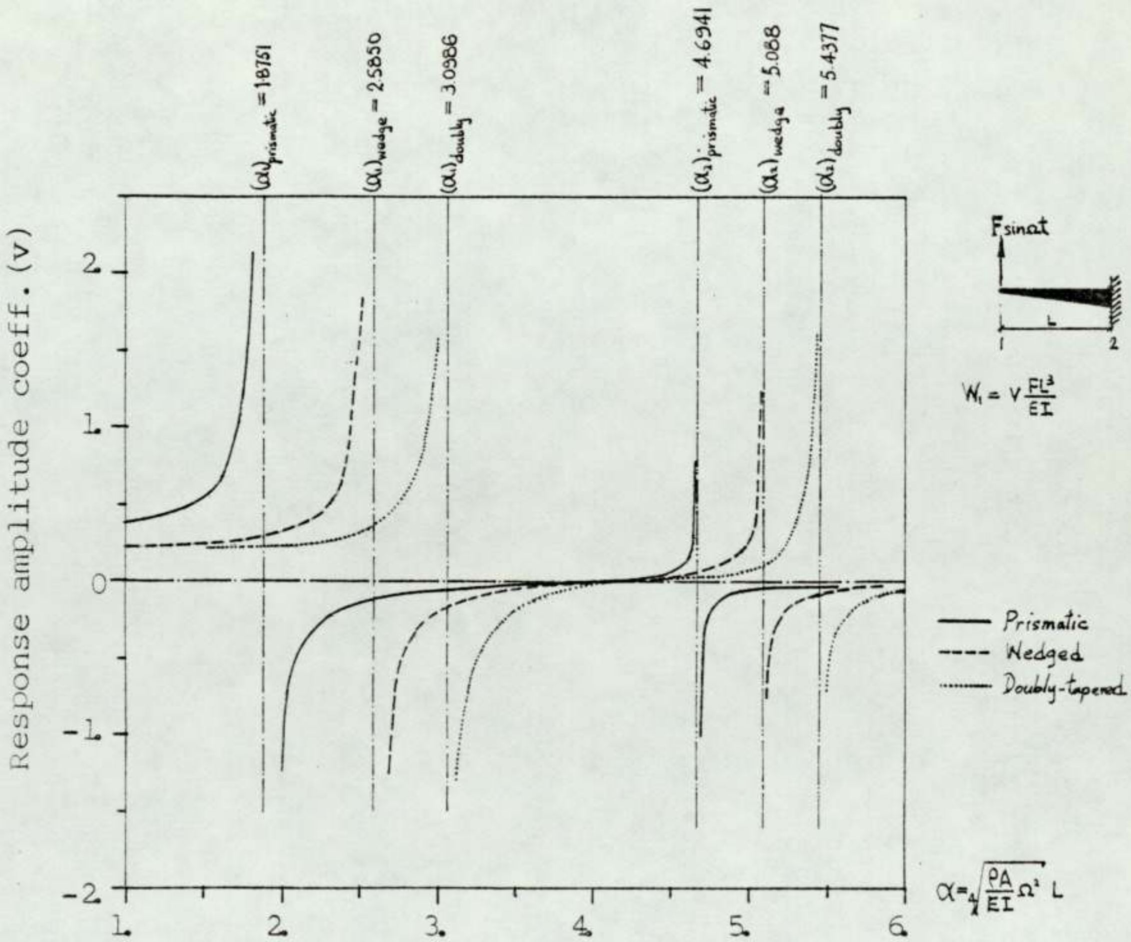

Fig.8.3.1c Response amplitude of Tapered section

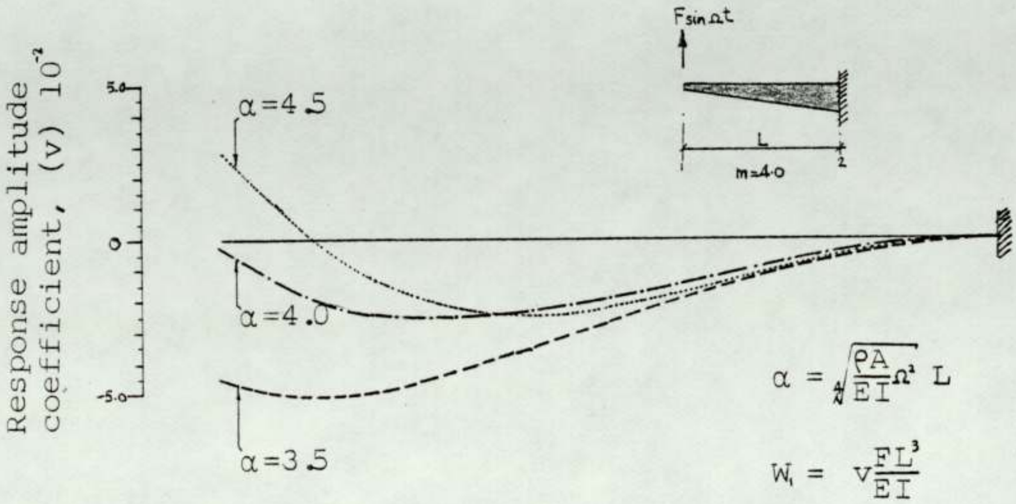

Fig.8.3.1d Deflected shapes of a wedged cantilever

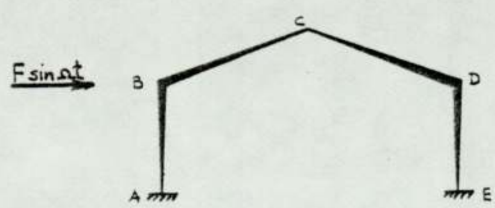

Dimension of the frame to be shown in fig.7.4.1

Fig.8.3.2a Pitched portal frame subjected to excitation force

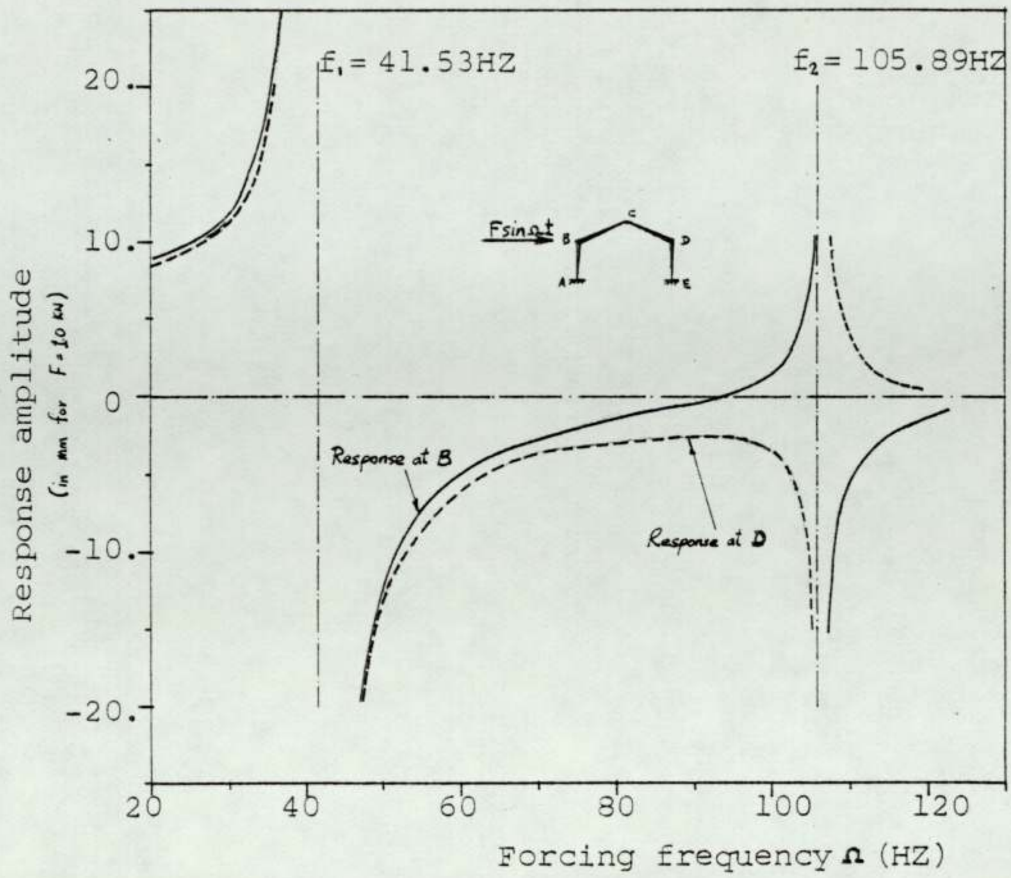

Fig.8.3.2b Response amplitude of the pitched frame

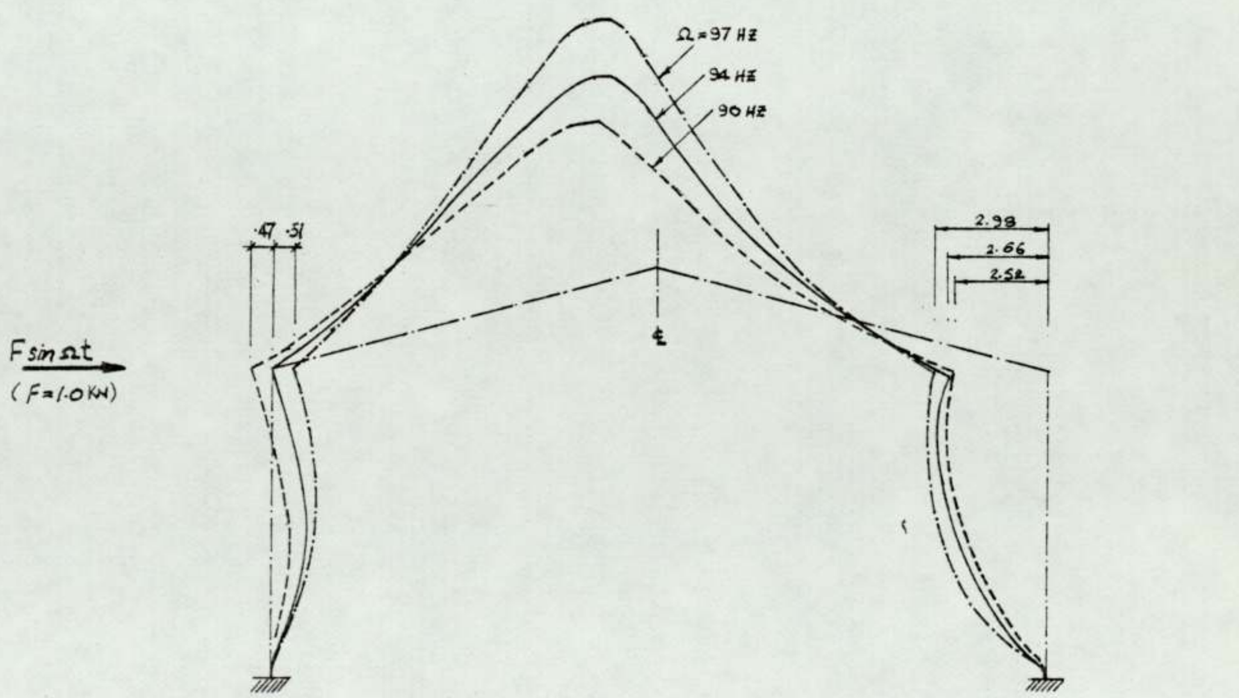

Fig.8.3.2c Deflected shapes of the pitched portal frame (mm)

Chapter 9

Techniques & Computer Aids

CHAPTER 9

TECHNIQUES & COMPUTER AIDS

§9.1 Evaluation of 1-cch

§9.1.1 The series expansion of 1-cch

By definition, 1-cch is the abbreviation for

$$1.0 - \cos\alpha\cosh\alpha \qquad 9.1.1$$

where α is the dimensionless frequency parameter. The evaluation of this expression may be critical especially in the prohibited range (§6.2). Its utmost significance is in the location of the asymptotic poles and is hence a crucial factor in the count algorithm (eq.6.1.4).

The series expansion of the trigonometrical and the hyperbolic functions are given in many textbooks,[103] thus

$$\cos\alpha = 1 - \frac{\alpha^2}{2!} + \frac{\alpha^4}{4!} - \frac{\alpha^6}{6!} + \cdots\cdots \qquad 9.1.2$$

$$\cosh\alpha = 1 + \frac{\alpha^2}{2!} + \frac{\alpha^4}{4!} + \frac{\alpha^6}{6!} + \cdots\cdots \qquad 9.1.3$$

Substituting into eq.9.1.1 gives

$$1\text{-cch} = \frac{4\alpha^4}{4!} - \frac{16\alpha^8}{8!} + \frac{64\alpha^{12}}{12!} - \frac{256\alpha^{16}}{16!} + \cdots\cdots \qquad 9.1.4$$

$$\cdots\cdots + (-1)^{n+1}\frac{2^{2n}\alpha^{4n}}{(4n)!}$$

The degree of accuracy in the evaluation of 1-cch is dependent on the computation of the number of terms in the right hand side of eq.9.1.4. It can be envisaged that more terms should be considered for larger values of α and even more when α is in the prohibited range.

§9.1.2 The application of the built-in standard functions

As the trigonometrical and the hyperbolic functions are commonly used in technological application, the evaluation of these functions are readily accessible in the digit processor system. These standard functions are designed for general mathematical purposes and a satisfactory accuracy is always achieved in an ordinary well conditioned application. The critical evaluation in the prohibited range is so ill-conditioned that the application of the standard evaluations is inaccurate.

In using the standard functions[107] of evaluation, the executive statement is written as

```
FDET = 1.0 - CØS(ALPHA)*CØSH(ALPHA)                  9.1.5
```

where ALPHA is a real variable for the dimensionless frequency parameter. The evaluations are compared in table 9.1.2a. To cater for the extreme cases, the comparison is focused on the evaluations in the prohibited range. It is also supplemented with the implementation of the double precision. In the single precision implementation, the accuracy of the evaluation can be achieved up to the 4th significant figure in the prohibited range of the first AP ($\alpha = 4.73004$), and up to the 3rd significant figure in that of the second ($\alpha = 7.85420$).

§9.1.3 Series expansion economiser

To facilitate the coding for the series expansion of 1-cch (APPENDIX E2c), eq.9.1.4 is rearranged in the form of

$$1\text{-cch}=H\frac{1}{4!}\left(1-H\frac{4!}{8!}\left(1-H\frac{8!}{12!}\left(\cdots\cdots\left(1-H\frac{(4n-4)!}{(4n)!}\left(\cdots\cdots\right)\right)\right)\right)\right) \qquad 9.1.6$$

where $H=\frac{4\alpha^4}{4!}$

The reliability of the evaluation depends on the number of terms being computed. It is shown in table 9.1.3a that, for $\alpha = 4.73004$, at least 7 terms are required to give an accurate 11-significant figure result in the single precision implementation, and 8 terms in the double precision implementation. More terms are required for higher values of α and the minimum number of terms required are tabulated in table 9.1.3b.

It is inevitable that the critical value of 1-cch deserves the privilege of being executed in double precision. If the results for the double precision implementation given in table 9.1.3b are presented graphically as shown in fig.9.1.3c, a linear relationship may be obtained for the required number of terms and the magnitude of α. The linearity is bounded by

$$NTT = 4.5 + 0.8\alpha \qquad 9.1.7$$

It is infallible if the required number of terms is over-rated by an additional term, and the rounding up gives

$$NTT = 6 + 0.8\alpha \qquad 9.1.8$$

NTT is automatically generated if the following statement is included in the coding, thus

```
NTT = 6 + INT (0.8*ALPHA)                                9.1.9
```

The coding of the economiser (NTT) can be found in APPENDIX E2c.

§9.2 Element Splitting

§9.2.1 The methods of element splitting

As far as this thesis is concerned, the subdivisions in the members are assumed to be of equal length. The equal length element splitting method (ELES), which has been assumed up till now, is based on the ground of its simplicity. It does not take any account of the geometrical properties of the member, i.e. the tapered ratio of a tapered member. Considering a tapered member, in the subdivisions, there is a decrease in the tapered ratio in every element as illustrated in fig.9.2.1a where the depth ratios of the two elements are 2.5 & 1.6.

If the subdivision is so devised that every element possesses the same tapered ratio, this decrease in the tapered ratio is eliminated and the prismatic form is adhered to as closely as possible throughout the structure. The equal taper element splitting method (ETES) hence gives an optimised tapered ratio in each element and is expected to produce a better convergence than the ELES method since the nearer each element is to the prismatic form the better suited is the quasi-exact function to the elements.

If a member is split into i number of regularised elements by the ETES method (fig.9.2.1c), the depth ratio of each element is equated to an optimised depth ratio (m'), thus

$$m' = \frac{d_2}{d_1} = \frac{d_3}{d_2} = \; \cdots\cdots \; = \frac{d_{k+1}}{d_k} = \; \cdots\cdots \; = \frac{d_j}{d_{j-1}} \qquad 9.2.1$$

Eliminating the intermediate depths in terms of the two extreme end depths gives

$$m' = \left(\frac{d_j}{d_1} \right)^{\frac{1}{i}} \qquad 9.2.2$$

Again, solving the equalities in eq.9.2.1, the depth at the kth node is given as

$$d_k = \left(d_1^{\,i-k+1} \; d_j^{\,k-1} \right)^{\frac{1}{i}} \qquad 9.2.3$$

Equating the depths in similar triangles, the distance from the 1st node to the kth node is

$$a_k = \frac{d_k - d_1}{d_j - d_1} \, L \qquad 9.2.4$$

Using the example shown in fig.9.2.1a, the application of these formulae in the ETES method is illustrated in fig.9.2.1b. Although it appears that the formulae for the ETES method are unwieldy the coding of the method in a computer program is similar to that of the ELES method (APPENDIX E1). There is no significant increase in computing time and no complication in the implementation.

§9.2.2 The comparison of element splitting methods

It is intended to show that a more rapid convergence is obtained from the new method (ETES) than the traditional method (ELES). Examples from beam structures and a frame structure are considered. For a consistent comparison, the test examples are analysed with the polynomial function. Comparisons using the quasi-exact function are expected to yield the same conclusion.

(a) Beam structures

Beams of wedged section are considered with classical boundaries. The members are split into 2,3,4&5 elements by the two methods. The results obtained are tabulated in table 9.2.1a. In the wedged cantilever beam, the results from the two methods give the same rate of convergence. In other beam structures, the results obtained from the ETES method give a better convergence.

(b) The pitched portal frame

The physical properties of the pitched portal are shown in fig.7.4.1. The fundamental mode results obtained from the two methods are tabulated in table 9.2.2b. It is again shown that the results obtained from the ETES method give a better convergence. The frame split into 15 elements of equal taper gives a better approximation than that with 24 elements of equal length.

§9.2.3 Limitation

The formulation of the optimised taper in every element of a wedged member can be extended to a dovetailed member by replacing the depths by the breadths. In a doubly tapered member, the split elements of equal taper in depths may not be of the same length as the split elements equal taper in breadths. A compromise, obtained by taking the average, will distort the optimisation and an improved convergence may not be observed. As the depth is more critical than the breadth of the section, the optimisation only in depth ratio may be the better alternative.

§9.3 The Symmetry of a Structure

§9.3.1 The analysis of structures exhibiting symmetry

If a structure is symmetric in geometry, only half of the structure about the plane of symmetry need be considered in the free vibrational analysis. Fig.9.3.1a & b shows two examples exhibiting symmetry. The geometry of the half structure of a single-bay frame is given by halving the span length only (fig. 9.3.1a), and symmetric & anti-symmetric constraints are then applied at the plane of symmetry. In a double-bay frame, the geometry of the half structure is a single-bay frame and the sectional properties of the members lying in the plane of symmetry are halved. (fig.9.3.1b)

In the half structures, fewer members (and hence fewer degrees of freedom) are considered. The most important advantage of symmetry is therefore the reduced computational time. The superposition of the natural frequencies which are obtained separately from both types of half structure gives all the natural modes (in order) of the whole structure . Each superposed mode can also indicate the type of vibrational mode, i.e. either symmetric or anti-symmetric. If half structures are not assigned, the designation on the type of the modes cannot be readily obtained until the mode shapes are available. The examples on the mode superposition for the frames in fig.9.3.1a & b are shown in table 9.3.1c & d respectively.

§9.3.2 The false mode in the plane of symmetry

The frequencies obtained in table 9.3.1c & d are roots obtained from the iteration process. These roots (with the order) are confirmed by the count algorithm. The biased roots (§6.2.2), which are identified by the count in the asymptotic pole algorithm, have been discarded. Table 9.3.2 shows the frequencies at the asymptotic poles for the member lying in the plane of symmetry of the frame in fig.9.3.1b.

Referring again to table 9.3.1d, the frequencies marked thus * in the half-structure analysis cannot be found in the analysis of the whole structure. Actually, these frequencies are frequencies at the asymptotic poles as given in table 9.3.2. In the half structure the asymptotic pole algorithm identities these as definite roots, and hence since they are non-existant, care must be taken in interpreting these results in half structure analyses. These modes, the false modes, are obtained as eigenvalues of a clamped-clamped member lying in the plane of symmetry — flexural eigenvalues in the symmetric half-frame and extensional eigenvalues in the anti-symmetric half-frame. Obviously, as there is no member lying in the plane of symmetry of the frame in fig.9.3.1a, no false mode is experienced.

§9.4 Notes on the Computer Programs

It is well recognised that the ultilisation of the finite element procedures is motivated by and pertains to the special characteristics of the computer. Throughout the examples in this thesis, the results are obtained with the aid of a computer. Different programs are prepared for the different requirements of the analysis. Due to the limited space in the thesis, only typical programs of the same kind are listed, with brief discussions and block diagrams as the media of introduction.

§9.4.1 Subroutine library maintenance

A library, in a sense of computer terminology, is a group of items in semicompiled format arranged in some logical order that permits easy access to the individual components of the library. If a subroutine is frequently used or common to several programs, it is advisable that it be compiled into a subroutine library. A consequential advantage is the saving in compilation time of the same subroutine when used in other steering programs. This particular feature is noticeable if a considerable number of modifications is necessary in the steering program.

(a) Library:JJTMC (Appendix E1)

This subroutine includes the following facilities:-

(i) It reads the information of a structure, e.g. the topology, sectional properties and the orientation of each member. It also reads the number of subdivisions in each member and the types of displacement at each joint.

(ii) It splits the members into elements. The topology, sectional properties and the orientation of each element are accordingly dealt with. Connections to connections of the split elements should be in the same format as the original structure.

(iii) It computes the total number of degrees of freedom for the whole structure and the equivalent uniform section to which the transformations of the sectional properties are referred.

It is noticed that if the subdivision is implemented with the computer execution, a huge amount of work in data preparation is saved, and also the tedious manual subdivision is eliminated. If the subdivision is manipulated with the ETES method, only a slight modification is required. The modification is included at the end of the listing of the subroutine.

(b) For the matrix formulation (Appendices E2a,b&c)

Three different groups of library subroutines are designed. The listings in Appendices E2a,b&c are respectively referred to as:-

(i) Library:KMPOLY —— subroutines KTWCU & MTWCU are used to formulate the static stiffness matrix and the mass matrix respectively, with the polynomial displacement function.

(ii) Library:JCUBIC —— for the formulation of the dynamic stiffness matrix, [J], with the polynomial displacement function.

(iii) Library:JEXACT —— for the formulation of the dynamic stiffness matrix, [J], with the quasi-exact displacement function.

In the libraries JCUBIC & JEXACT, independent subroutines JPRISM, JDOVET, JWEDGE & JDOUBL are provided for elements of prismatic, dovetailed, wedged and doubly-tapered sections respectively. Economical computation occurs with the appropriate choice of subroutine. The subroutine JDOUBL may be used for elements of any taper.

(c) Library:JSNGL (Appendix E3)

Two procedures are performed in this library:-

(i) The local coordinate of every element is transformed into a global system. An example of a transformed dynamic stiffness matrix is given in eq.2.4.4.

(ii) The transformed matrices are combined together forming an overall matrix.

(d) Library:ASYMPTOTE (Appendix E4)

It has been mentioned in §6.3.2 that since the evaluation is kept clear of the prohibited range in order to maintain a smooth iteration, it is therefore necessary to predict the positions of the asymptotic poles. These positions depend on the sectional properties of every element and the poles may be either flexural or extensional. This library gives the order of positioning of all these poles and their associated values. The prediction of these poles is particularly essential in the analysis of half-structures (§9.3).

(e) NAG Library (Numerical Algorithm Group)

This as a well-known library developed by the pioneer numerical mathematicians. The NAG library is a very important aid to the computer user in scientific computation. It provides excellent available routines for a variety of numerical subjects. The application of each routine is backed up with a full documentation which is up-dated annually. In the design of the source program, the numerical algorithm always employs the NAG Library whenever possible.

§9.4.2 Steering programs

With the facilities of the library subroutines, the programming of the steering programs for the analyses is much simplified. For different requirements in the analyses, programs of a wide variety can be designed. It is within this context that two typical steering programs are given as examples.

(a) Steering programs:LINEIG (Appendix F1)

It is understood that a system of linear simultaneous equations is obtained from the polynomial displacement function. The solutions of the linear eigenproblem may be performed with the matrix iteration methods which uses the standard routines in the NAG library. Frequencies (eigenvalues) and modal shapes (eigenvectors) are obtained from the same process of execution. The algorithm may be terminated at this stage (stage E in fig. 9.5.1) if dynamic response analysis is not required.

For the analysis of dynamic response, the algorithm continues with the concept of the normal mode method. The eigenvalues and the eigenvectors obtained in the previous stages are immediately used for the mode superposition. The block diagram showing the format of the whole program with the stages referenced to the listing of the program is shown in fig.9.5.1 (Appendix F1).

(b) Steering program:NONLIN (Appendix F2)

The program is based on the determinantal method (§3.3) and the stages for programming are shown in fig.9.5.2. The program uses the library:JEXACT which formulates the dynamic stiffness matrix for the quasi-exact function and hence a non-linear eigensystem results. With the facilities of the count algorithm, eigenvalues of the non-linear eigensystem are obtained.

Further extension to the program is the back substitution of the eigenvalues into the non-linear simultaneous equations, and to solve for the eigenvectors which give the modal shapes. Another program for the dynamic response analysis may be designed if the excitation forces are also considered in the setting up of the simultaneous equations. The solution routine, which solves the set of simultaneous equations to give the response amplitude, is based on the frequency response method.

Although the program is purposely designed for the solution of a non-linear eigensystem, a slight modification gives a program for a linear eigensystem. This is performed simply by replacing the use of library:JEXACT by library:JCUBIC which gives the dynamic stiffness matrix for the polynomial functions. As no asymptotic pole appears in the linear eigensystem, the asymptotic algorithm is suppressed. The count algorithm hence consists only of the sign count (eq.3.3.15).

Table 9.1.2 The accuracy of the evaluations

	α	1-cch		
		Standard function	Series expansion	Multiplier
Single precision	4.730040	4.294004	4.293769	10^{-5}
	4.730041	-1.470522	-1.470794	10^{-5}
	7.853204	-8.026654	-8.025566	10^{-4}
	7.853205	4.832914	4.835268	10^{-4}
Double precision	4.730040	4.293826	4.293826	10^{-5}
	4.730041	-1.470767	-1.470767	10^{-5}
	7.853204	-8.025222	-8.025222	10^{-4}
	7.853205	4.834719	4.834719	10^{-4}

Table 9.1.3a Series expansion of 1-cch (for α=4.73004)

No.of terms	single precision	double precision	Multiplier
1	-1.6002856254	-1.6002856255	10
2	7.5508913228	7.5508913183	10^{-1}
3	-1.3080945927	-1.3080945431	10^{-2}
4	1.4636667443	1.4636687950	10^{-4}
5	4.2516421333	4.2516090727	10^{-5}
6	4.2938902549	4.2939240286	10^{-5}
7	4.2937688522	4.2938258578	10^{-5}
8	4.2937688522	4.2938259968	10^{-5}
9	4.2937588522	4.2938259967	10^{-5}
10	4.2937588522	4.2938259967	10^{-5}

Table 9.1.3b Required number of terms (NTT) in series expansion

α	No. of terms required to give an accuracy of 10 sig. fig.	
	Single precision	Double precision
4.73004	7	8
7.85320	9	11
10.99560	11	14
14.13717	13	16
17.27875	16	19
20.42035	17	21
23.56194	19	23
26.70353	22	26
29.84513	24	28

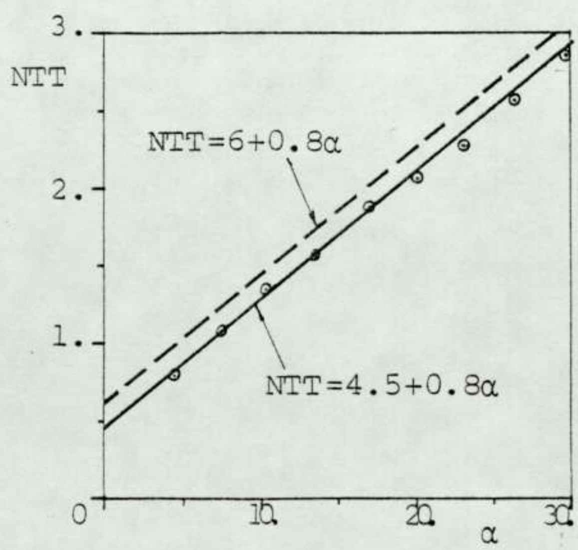

Fig.9.1.3c Series expansion economisation

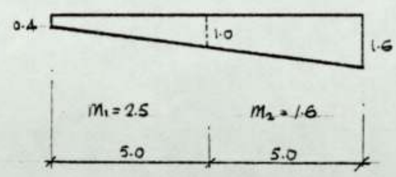

Fig.9.2.1a Example of ELES method

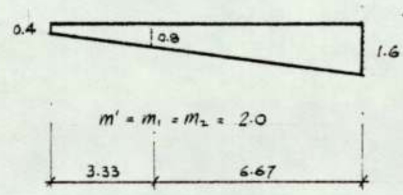

Fig.9.2.1b Example of ETES method

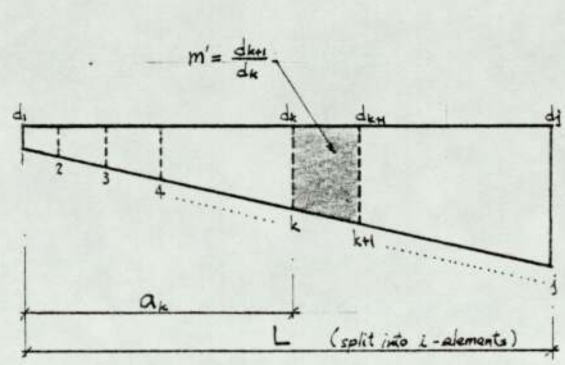

Fig.9.2.1c A member of i equal taper elements

Table 9.2.2a Element-splitting methods in beams

Beam structure	No. of elements	Dimensionless frequency parameter (α)	
		ELES method	ETES method
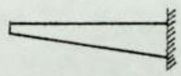	1	2.5947	
	2	2.5858	2.5858
	3	2.5851	2.5851
m = 4.0	4	2.5851	2.5851
Exact sol. = 2.5850	5	2.5850	2.5850
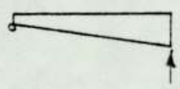	1	2.9551	
	2	2.9431	2.9443
	3	2.9345	2.9304
m = 4.0	4	2.9300	2.9272
Exact sol. = 2.9258	5	2.9279	2.9262
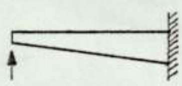	1	4.1687	
	2	4.0934	4.1172
	3	4.0749	4.0709
m = 4.0	4	4.0656	4.0616
Exact sol. = 4.0572	5	4.0615	4.0589
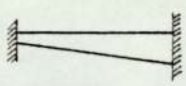	1	not applicable	
	2	4.9833	4.6975
	3	4.6570	4.5503
m = 4.0	4	4.5698	4.5204
Exact sol. = 4.5060	5	4.5372	4.5118

Table 9.2.2b Element-splitting methods in the pitched portal frame

No. of elements in each member	Total no. of elements	Size of matrix	Frequency (HZ)	
			ELES method	ETES method
1	3	6x6	53.84	
2	6	15x15	45.09	42.88
3	9	24x24	42.85	41.83
4	12	33x33	42.11	41.63
5	15	42x42	41.82	41.57
6	18	51x51	41.68	41.54
7	21	60x60	41.62	41.53
8	24	69x69	41.58	41.53

<u>Integer Representation</u>

Degrees of freedom (D.O.F.) in order :-

x - translation : y - translation : θ - rotation

'1' represents freedom

'0' represents suppression

e.g. 010 represents y - translation only .

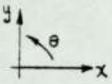

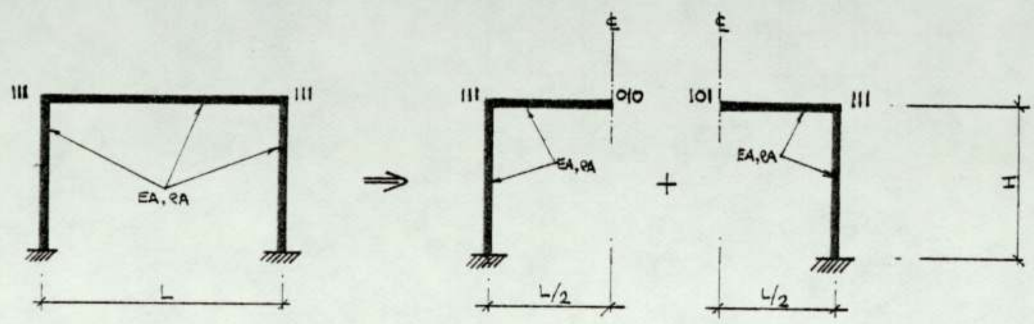

Whole frame
(6 DOF)

Symmetric
half-frame
(4 DOF)

Anti-symmetric
half-frame
(5 DOF)

Fig.9.3.1a Half-structuring of a single-bay frame

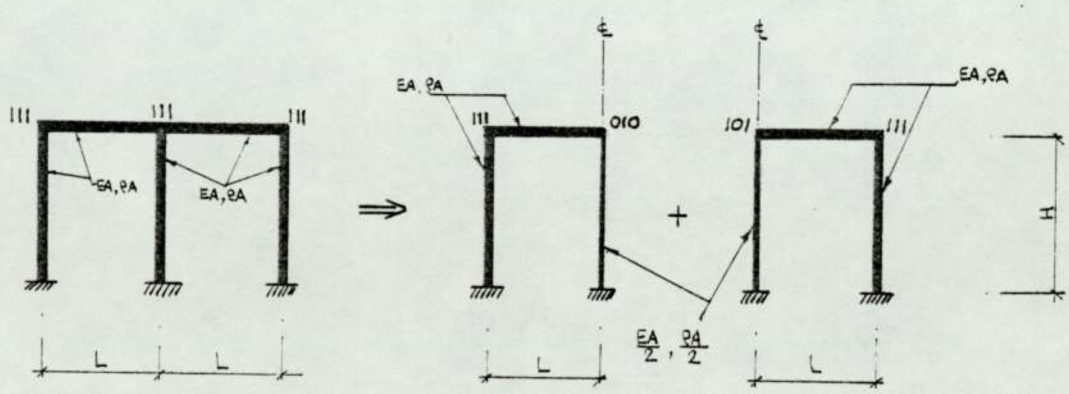

Whole frame
(9 DOF)

Symmetric
half-frame
(4 DOF)

Anti-symmetric
half-frame
(5 DOF)

Fig.9.3.1b Half structuring of a double-bay frame

Table 9.3.1c Frequencies of frame in fig.9.3.1a

	Half-frame		Whole frame	
	Symmetric	anti-symmetric	Frequency	Type
	66.6	15.1	15.1	A1
2	95.8	90.5	66.6	S1
3	174.6	123.2	90.5	A2
4	221.2	234.2	95.8	S2
5	335.0	338.5	123.2	A3
6	386.6	431.9	174.6	S3
7	507.7	521.2	221.2	S4
8	620.4	657.9	234.2	A4
9	761.5	678.9	335.0	S5
10	850.9	862.5	338.5	A5
11	⋮	⋮	386.6	S6
12			431.9	A6
13			507.7	S7
14			521.2	A7
15			620.4	S8
16			657.9	A8
⋮			⋮	

N.B.

(i) Dimension of the frame :- L=4m, H=6m, r_g=0.29m

(ii) Frequency in HZ

(iii) A3 to denote the third anti-symmetric mode & S5 the fifth symmetric mode, etc.

Table 9.3.1d Frequencies of frame in fig.9.3.1b

	Half-frame		Whole frame	
	Symmetric	anti-symmetric	Frequency	Type
1	69.0	14.3	14.3	A1
2	87.6	68.9	68.9	A2
3	92.2 *	91.0	69.0	S1
4	121.6 -	103.6	87.6	S2
5	163.3	159.5	91.0	A3
6	203.8	224.7	103.6	A4
7	254.0 *	237.6	121.6	S4
8	263.7	269.0 *	159.5	A5
9	327.4	343.5	163.3	S5
10	387.0	351.0	203.8	S6
11	443.8	427.9	224.7	A6
12	498.0 *	506.6	237.6	A7
13	529.9	514.0	263.7	S8
14	579.0	538.0 *	327.4	S9
15	608.3	644.4	343.5	A9
16	⋮	⋮	351.0	A10
17			387.0	S10
18			427.9	A11
19			443.8	S11
20			506.6	A12
⋮			⋮	

N.B.

(i) See notes above

(ii) Frequency marked by * to denote a false mode

order	1	2	3
Flexural	92.2	254.0	498.0
Extensional	269.0	537.9	806.9

L=6.0
r_s= 20.8

Table 9.3.2 Frequencies at the asymptotic poles

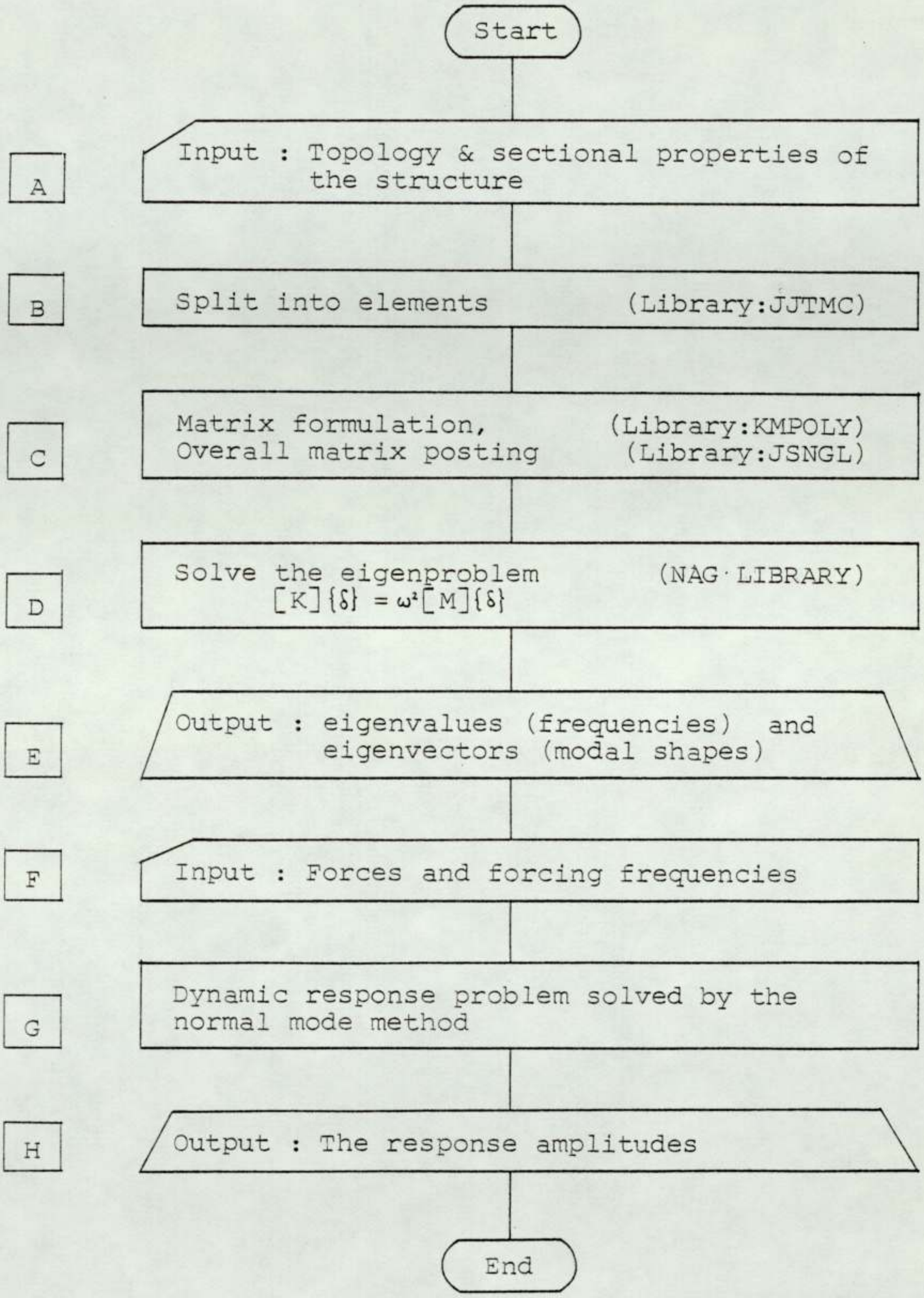

Fig.9.5.1 Block diagram showing the format of program LINEIG

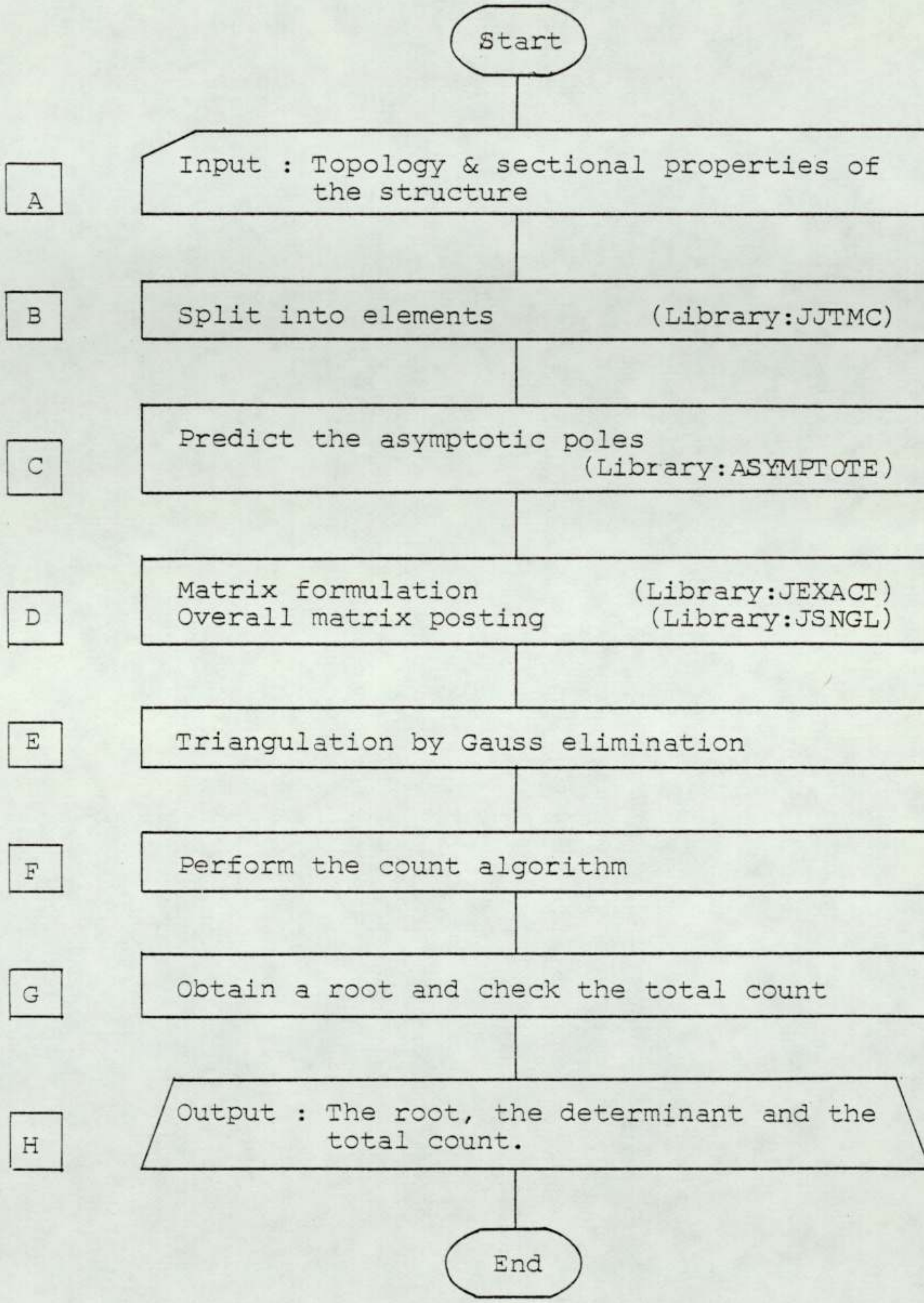

Fig.9.5.2 Block diagram showing the format of program NONLIN

Chapter 10

Discussion & Conclusion

§10.1 Discussion of structures with prismatic sections

§10.2 Discussion of structures with tapered sections

§10.3 Further general discussion

§10.4 Recommendations for further research

CHAPTER 10

DISCUSSION & CONCLUSION

§10.1 Discussion of Structures with Prismatic Sections

Although the static stiffness matrix is an important requirement, the production of the additional mass matrix is also an essential feature in the formulation of the dynamic problem. The mass matrix obtained by the lumped mass representation is inefficient in giving a reliable result, thus motivating the solution considering the mass distributed along the member. A true distribution of mass is an essential requirement in giving an exact solution. With the polynomial displacement function, the distributed mass solution gives a good representation of the mass matrix. With the exact displacement function, a true distribution of mass is represented in the mass matrix. As the static stiffness matrix is also formulated in the exact manner, the dynamic stiffness matrix is therefore exact. It is noted that the exact displacement function is obtained by solving the governing differential equation of motion.

The static stiffness matrix and the mass matrix are formulated by a similar procedure. The procedure involves the the triple multiplication and integration in the manipulation of the matrices. A considerable amount of arithmetical work always confines the procedure to the handling of simple expressions, e.g.polynomial functions. However, despite the heavy manipulation in the trigonometrical and hyperbolic functions, the static stiffness matrix and the mass matrix are formulated for the exact displacement function as well as those for the polynomial function.

In the formulation of the dynamic stiffness matrix for the exact displacement function, the tedious matrix manipulation is very much simplified since some of the element-terms are cancelled in the total matrix. Consequently, the dynamic stiffness matrix is expressed in simpler expressions than the static stiffness and the mass matrices. If the latter two matrices are available, the former matrix is directly formulated by obtaining the difference of the two given matrices taking account of the frequency parameter.

The requirements for the choice of a displacement function are accuracy and economy. The polynomial displacement function can give a very good approximated result with a coarse subdivision of the members. However, as an exact solution is possible and is also justified with the computational time, the choice is obviously in favour of using the exact displacement function.

The soultion methods are discussed under two main categories : matrix iteration and determinant evaluation. In the first category, eigenvalues and eigenvectors are obtained in the same process, but the methods are preferably used for the linear eigensystem, i.e. from the polynomial displacement function. The non-linear eigensystem, of which the frequency dependent matrix is derived from the exact displacement function, is more effectively solved by the determinantal method with the facility of the count algorithm. This algorithm consists of two counts, namely a sign count and an asymptotic pole count. A sign count is derived from the concept of the Sturm sequence, and the singularity evaluation from the exact displacement function is accounted for by the asymptotic pole count. The introduction of the count algorithm permits the identification of a definite mode without an actual evaluation of the determinant. It is an infallible method for finding any required number of roots of any specified order. If the asymptotic pole algorithm is suppressed, the method is also suitable for the solution of a linear eigensystem.

An advantage that occurs in the analysis of beam structures is the partitioning of the matrix so that pure flexural vibration and pure extensional vibration can be dealt with independently. Also the analysis of partitioned matrices always saves computational time. If the axial deformation is not suppressed, the order of a flexural mode may be affected by superimposing the extensional modes. In the analysis of frame structures, no matrix partitioning is possible. In these cases flexural vibration is coupled with the extensional vibration, and hence axial displacement should not be neglected.

A structure may contain prismatic members of different sectional properties. Different natural frequencies result from the variation in discontinuities, either at joints or by being abruptly stepped. The sectional properties may be so designed to give a structure where the natural frequency is a maximum.

§10.2 Discussion of Structures with Tapered Sections

A tapered member may be idealised into a member of stepped uniform sections, but the analysis using this stepwise idealisation always gives an unsatisfactory result. An exact solution is obtained only if the matrices are formulated from the exact displacement function of a tapered member. However, an exact solution does not appear to give a practical analysis due to the heavy computational procedures thus generated. An alternative is to obtain a close approximation by using assumed displacement functions and taking account of the continuous change in the sectional properties for the whole tapered member during the formulation of matrices. The matrices, which are written in simplified and uncomplicated form, are obtained for the polynomial displacement function. For the quasi-exact displacement function, as the complicated treatment in the trigonometrical and the hyperbolic expressions becomes intractable, the property matrices cannot be written in an elegant format. The dynamic stiffness matrix is hence obtained from the numerical execution of the triple matrix multiplication and the matrix integration which are readily formulated.

For coarse subdivision, the quasi-exact displacement function gives a better approximation. This function, which is also recommended in structures consisting of prismatic members, gives an exact solution for members of prismatic section. The most important deficiency in using this function is the disturbance of the asymptotic poles. Several approaches are suggested to diagnose the abnormalities. The count algorithm, which is originally developed for the identification of a root, provides an effective means for the remedial procedures.

For a better approximation, the members should be split into more elements. In a structure possessing fine subdivision, the results obtained from the polynomial displacement function are able to be justified with the computational time. This function also gives a linear eigensystem which is suitable for the matrix iteration methods, and the eigenvectors are readily obtained in the same process. Furthermore, the iteration in the polynomial function is steadier than the quasi-exact function due to the simpler execution in the polynomial expressions and the non-existence of the asymptotic poles.

Although the two assumed displacement functions described are different in nature , the obtained results are mutually agreeable. Also, for increasingly finer subdivision, they both give the same converged value which is taken as the exact solution. The reliability of the analyses is further confirmed by performing a dynamic test on a model pitched frame. (A similar test was repeated for a prismatic frame and agreeable results were obtained.)

In using the assumed displacement functions, by having the subdivision as fine as possible, the exact solution (for both natural frequencies and modal shapes) of a structure with different types of taper is obtained. In the same structure, different natural modes result from different arrangements of taper, and again optimisation of the structure to give a maximum natural frequency may be carried out using selected tapered sections. A guideline for such selection may be found in §7.2 which described an investigation into the variation of depth ratios.

§10.3 Further General Discussion

The dynamic analysis is further considered as a forced vibrating system by introducing excitation forces and forcing frequencies of harmonic motion. The frequency response method and the mode superposition method, which have been suggested in the response analysis of prismatic structures, are also suitable for structures of tapered sections. Both analytical and numerical results agree with each other. As a deflected shape is more accurately described by having more co-ordinates, more nodal points are required, these being formed by a finer subdivision of the structure. For a structure split into more elements than necessary to give a converged value, the rate of convergence is no longer a criterion in choosing a displacement function. Taking the advantage of its simplicity in the computation, the polynomial functions are always recommended. The same conclusion also applies to the analysis of modal shapes.

In the design of a frame structure, consideration should be given to the fixity of the supports. From the given example of a bridge, it is noticed that a lower natural frequency is given from the bridge with fixed supports. As supports are neither perfectly fixed nor pinned, a certain degree of judgement must be exercised in a design situation.

The most interesting feature in the quasi-exact displacement function is the existence of the asymptotic poles. A full investigation on the singularity of these poles was carried out unintentionally. The sensitivity of the evaluations near the vicinity of the poles becomes acute and steadier evaluations are observed if the necessary trigonometrical and hyperbolic functions are handled in series expansion with double precision implementation. It is, however, still advisable that such evaluation is avoided by introducing a prohibited range, and that the features within the range are predicted with the facilities of the count algorithm.

For a structure symmetrical in geometry, half-structuring at the plane of symmetry gives an economical analysis and the obtained results identify themselves as either symmetric or anti-symmetric mode. However, in the analysis of half-structures, false modes are obtained as well as the definite modes. These false modes are detected by observing the asymptotic poles of the members lying at the plane of symmetry.

A traditional method of subdivision is to achieve an equal length in every element. The subdivision is innovated by having an equal taper in every element. The new method, which gives an optimised tapered ratio, produces a better rate of convergence. No additional work in data preparation is necessary, and in fact the subdivision is processed automatically by the computer for both methods. The subdivision is accurately performed and the tedious manual procedure eliminated. The subroutines for processing the subdivisions together with other subroutines are maintained in a library system which is directly accessible by every steering program.

§10.4 Recommendations for Further Research

An immediate continuation of the work is the vibration of space structures. The matrices which have already been formulated are readily accessible for these analyses, although the number of degrees of freedom at each node must be increased from three to six . Another possible development is the consideration of non-harmonic forces in the dynamic response analysis, of which a knowledge of numerical integration is essential. It is also possible to study structures under vibration due to random excitation, moving loads and ground movement.

The analysis of non-prismatic structures has been commenced with members of linearly tapered section. By following a similar routine, non-prismatic members with non-linearly varying sections may be considered. Also, the dynamic analysis of a straight member may be extended to a curved member. Furthermore, for a comprehensive representation of an element, shear deformation and torsional effects are other aspects of displacement that should be included in the matrix formulation.

APPENDICES

(This page should be placed after the References)

REFERENCES & BIBLIOGRAPHY

1 TURNER, M.J. STIFFNESS AND DEFLECTION ANALYSIS OF COMPLEX STRUCTURES ;
JAS, SEPT, 1956
CO-AUTHORS : CLOUGH, MARTIN & TOPP

2 ARGYRIS, J.H. ENERGY THEOREMS AND STRUCTURAL ANALYSIS ;
AIRCRAFT ENGINEERING, VOL 26, 1955
CO-AUTHOR : KELSEY, S

3 CLOUGH, R.W. THE FINITE ELEMENT IN PLANE STRESS ANALYSIS ;
2ND ASCE CONFERENCE ON ELECTRONIC COMPUTATION, 1960

4 TIMOSHENKO, S.P. THEORY OF PLATES AND SHELLS ;
MCCRAW-HILL, 2ND ED, 1959
CO-AUTHOR: S.WOINOWSKY-KRIEGER

5 SZILARD, R. THEORY AND ANALYSIS OF PLATES, CLASSICAL AND NUMERICAL METHODS ;
PRENTICE-HALL, 1974

6 WARBURTON, G.B. THE DYNAMICAL BEHAVIOUR OF STRUCTURES;
PERGAMON, 2ND ED.,1976

7 CRANCH, E.T. BENDING VIBRATION OF VARIABLE SECTION BEAMS ;
JAM, MARCH, 1956
CO-AUTHOR : A.A.ADLER

8 GORMAN, D.J. FREE VIBRATION ANALYSIS OF BEAMS AND SHAFTS ;
WILEY, 1975

9 ROGERS, G.L. DYNAMICS OF STRUCTURES ;
WILEY, 1959

10 BISHOP, R.E.D. THE MECHANICS OF VIBRATIONS ;
CAMBRIDGE UNIVERSITY PRESS, 1960
CO-AUTHOR: D.C.JOHNSON

11 BIGGS, J.M. INTRODUCTION TO STRUCTURAL DYNAMICS ;
MCCRAW-HILL, 1964

12 HURTY, W.C. DYNAMICS OF STRUCTURES ;
PRENTICE-HALL, 1964
CO-AUTHOR : M.F.RUBINSTEIN

13 THOMSON, W.T. VIBRATION THEORY AND APPLICATION ;
PRENTICE-HALL, 1965

14 CLARK, S. DYNAMICS OF CONTINUOUS ELEMENTS ;
PRENTICE-HALL, 1972

15 KOLOUSEK, V. DYNAMICS IN ENGINEERING STRUCTURES, BUTTERWORTHS, 1973

16 CLOUGH, R.W. DYNAMICS OF STRUCTURES ; MCCRAW-HILL, 1975 CO-AUTHOR : J.PENZIEN

17 BLAKE, R.E. BASIC VIBRATION THEORY ; SHOCK & VIBRATION HANDBOOK, CH.2

* 18 STOKEY, W.F. VIBRATION OF SYSTEMS HAVING DISTRIBUTED MASS AND ELASTICITY ; SHOCK & VIBRATION HANDBOOK, CH.7

19 JENKINS, W.M. MATRIX AND DIGITAL COMPUTER METHODS IN STRUCTURAL ANALYSIS ; MCCRAW-HILL, 1969

20 BREBBIA, C.A. FUNDAMENTALS OF FINITE ELEMENT TECHNIQUE ; BUTTERWORTHS, 1973 CO-AUTHER : J.J.CONNOR

21 NATH, B. FUNDAMENTALS OF FINITE ELEMENTS FOR ENGINEERS ; ATHLONE PRESS, 1974

22 ZIENKIEWICZ, O.C. THE FINITE ELEMENT METHOD ; MCCRAW HILL, 3RD ED, 1977

23 COATES, R.C. STRUCTURAL ANALYSIS ; NELSON, 1972 CO AUTHORS : M.G.COUTIE & F.K.KONG

24 NEVILLE, A.M. STRUCTURAL ANALYSIS, A UNIFIED CLASSICAL AND MATRIX APPROACH ; CHAPMAN-HILL, 1978 CO-AUTHORS : A.GHALI & Y.K.CHEUNG

25 NEWMARK, N.M. A METHOD OF COMPUTATION FOR STRUCTURAL DYNAMICS ; ASCE-EM-3, JULY, 1959

26 WEBSTER, J.J. FREE VIBRATION ANALYSIS OF STRUCTURES USING RAYLEIGH-RITZ & FINITE-ELEMENT METHODS ; SYM. STRUCT. DYN.

27 CLOUGH, R.W. ANALYSIS OF STRUCTURAL VIBRATION AND DYNAMIC RESPONSE ; 1ST US-JAPAN SEMINAR, 1969

28 CLOUGH, R.W. FINITE ELEMENT ANALYSIS OF DYNAMIC RESPONSE ; 2ND US-JAPAN SEMINAR, 1972 CO-AUTHOR : K.L.BATHE

29 CHI, M. A NEW VARIATIONAL METHOD FOR SOLVING STATIC AND DYNAMIC RESPONSES OF STRUCTURES OF HIGH COMPLEXITY ;
VARIATIONAL METHODS IN ENGINEERING,
CO-AUTHORS : R.DAME & N.L.BASDEKAS

30 HATTER, D.J. MATRIX COMPUTER METHODS OF VIBRATION ANALYSIS ;
BUTTERWORTH, 1973

31 CRANDALL, S.H. NUMERICAL METHODS OF ANALYSIS ;
SHOCK & VIBRATION HANDBOOK, CH.28
CO-AUTHOR : R.B.MCCALLEY

32 BATHE, K.J. NUMERICAL METHODS IN FINITE ELEMENT ANALYSIS ;
PRENTICE-HALL, 1976
CO-AUTHOR : E.L.WILSON

33 JENNINGS, A. MATRIX COMPUTATION FOR ENGINEERS AND SCIENTISTS ;
WILEY, 1977

34 WILLIAMS, F.W. AN AUTOMATIC COMPUTATIONAL PROCEDURE FOR CALCULATING NATURAL FREQUENCIES OF SKELETAL STRUCTURES ;
IJMS, VOL.12, 1970, PP.781-791
CO-AUTHOR : W.H.WITTRICK

35 WITTRICK, W.H. A GENERAL ALGORITHM FOR COMPUTING NATURAL FREQUENCIES OF ELASTIC STRUCTURES ;
QJMAM, VOL.24, PART 3, 1971.
CO-AUTHOR : F.W.WILLIAMS

36 WILLIAMS, F.W. COMPACT COMPUTATION OF NATURAL FREQUENCIES AND BUCKLING LOADS FOR PLANE FRAMES ;
IJNME, VOL.11, 1977
CO-AUTHOR : W.P.HOWSON

37 BATHE, K.J. LARGE EIGENVALUE PROBLEMS IN DYNAMIC ANALYSIS ;
ASCE-EM-6, DEC.,1972.
CO-AUTHOR : E.L.WILSON

38 BATHE, K.J. EIGENSOLUTION OF LARGE STRUCTURAL SYSTEMS WITH SMALL BANDWIDTH ;
ASCE-EM-3, 1973
CO-AUTHOR : E.L.WILSON

39 WILLIAMS, F.W. NATURAL FREQUENCIES OF REPETITIVE STRUCTURES ;
QJMAM, VOL.24, PART 3, 1971

*40 BICKLEY, W.G. MATRICES, THEIR MEANING AND MANIPULATION ;
ENGLISH W.PRESS, 1964
CO-AUTHOR : R.S.H.G.THOMPSON

*41 PIPES, L.A. MATRIX - COMPUTER METHODS IN ENGINEERING ,
WILEY, 1969
CO-AUTHOR : S.A.HANDVANESSIAN

*42 NOBLE, B. APPLIED LINEAR ALGEBRA ;
PRENTICE-HALL, 1969

*43 HOHN, F.E. ELEMENTARY MATRIX ALGEBRA ;
MACMILLAN, 3RD ED., 1973

*44 GOURLAY, A.R. COMPUTATIONAL METHODS FOR MATRIX EIGENPROBLEMS ;
WILEY, 1973
CO-AUTHOR : G.A.WATSON

*45 STEINBERG, D.I. COMPUTATIONAL MATRIX ALGEBRA ;
MCCRAW-HILL, 1974

*46 BELL, W.W. MATRICES FOR SCIENTISTS AND ENGINEERS
VAN-NOSTRAND, 1976

47 HOUSEHOLDER, A.S. PRINCIPAL OF NUMERICAL ANALYSIS ;
MCCRAW-HILL, 1953

48 FOX, L. AN INTRODUCTION TO NUMERICAL LINEAR ALGEBRA ;
CLARENDON PRESS, 1964

49 WILKINSON, J.H. THE ALGEBRAIC EIGENVALUE PROBLEM ;
CLARENDON PRESS, 1965

50 MOURSUND, D.G. ELEMENTARY THEORY AND APPLICATION OF NUMERICAL ANALYSIS ;
MCCRAW-HILL, 1967
CO-AUTHOR : C.S.DURIS

51 SCHEID, F. THEORY AND PROBLEMS OF NUMERICAL ANALYSIS ;
MCCRAW-HILL, 1968, SCHAUM SERIES

52 FORSYTHE, G.E. COMPUTER METHODS FOR MATHEMATICAL COMPUTATION ;
PRENTICE-HALL, 1977
CO-AUTHORS : MALCOLM & MOLER

53 DODES, I.A. NUMERICAL ANALYSIS FOR COMPUTER SCIENCE ;
NORTH-HOLLAND, 1978

54 RALSTON, A. A FIRST COURSE IN NUMERICAL ANALYSIS ;
MCCRAW-HILL, 2ND ED, 1978
CO-AUTHOR: P.RABINOTWITZ

55 KELLER, J.B. BIFURCATION THEORY AND NON-LINEAR EIGENVALUE PROBLEMS ;
BENJAMIN INC., 1969
CO-AUTHOR: S.ANTMAN

56 TURNER, R.E.L. NONLINEAR EIGENVALUE PROBLEMS WITH APPLICATIONS TO ELLIPTIC EQUATIONS ; ARMA, VOL.42, 1971

57 RUHE, A. ALGORITHMS FOR THE NON-LINEAR EIGENVALUE PROBLEM ; SIAM-JNA, VOL.10, NO.4, SEPT.,1973

58 STEELE, C.R. APPLICATION OF THE WKB METHOD IN SOLID MECHANICS ; MECHANICS TODAY, VOL.3, 1976

59 HOLZE, G.H. FREE VIBRATION ANALYSIS USING SUBSTRUCTURING ; ASCE-ST-12, DEC., 1975 CO-AUTHOR :

60 JENNINGS, A. THE DEVELOPMENT AND APPLICATION OF SIMULTANEOUS ITERATION FOR EIGEN-VALUE PROBLEMS ; LECTURE NOTE IN MATHS, NO.228, SPRINGER-VERLAG, 1971

61 PETERS, G. AX=λBX AND THE GENERAL EIGENVALUE PROBLEMS ; SIAM-JNA, VOL.7, NO.4, DEC.,1971 CO-AUTHOR : J.H.WILKINSON

62 BATHE, K.J. SOLUTION METHODS FOR EIGENVALUE PROBLEMS IN STRUCTURAL MECHANICS ; IJNME, VOL.6, FEB.,1973. CO-AUTHOR : E.L.WILSON

63 GUPTA, K.K. RECENT ADVANCES IN NUMERICAL ANALYSIS OF EIGENVALUE PROBLEMS ; TPFESA, TOKYO, 1973

64 MOLER, C.B. AN ALGORITHM FOR GENERALISED MATRIX EIGENVALUE PROBLEMS ; SIAM-JNA, VOL.10 CO-AUTHOR : G.W.STEWART

65 GOLDSTINE, H.H. THE JACOBI METHOD FOR REAL SYMMETRIC MATRICES ; JACM, VOL.6, 1959 CO-AUTHORS : MURRAY & NEUMANN

*66 GIVENS, J.W. NUMERICAL COMPUTATION OF THE CHARACTERISTIC VALUES OF A REAL SYMMETRIC MATRIX ; OAK RIDGE NATIONAL LABORATORY REPORT, ORNL-1574, 1954

67 WILKINSON, J.H. HOUSEHOLDER METHOD FOR THE SOLUTION OF THE ALGEBRAIC EIGENPROBLEM ; COMPUTER J., VOL.3

68 RUTISHAUSER, H. ON JACOBI ROTATION PATTERNS ; PROC. AMS SYMP. IN APPL. MATH., VOL.15

69 FRANCIS, J.G.F. THE QR TRANSFORMATION, PART 1 & 2 ; COMPUTER J., VOL.4, 1961-2

*70 ORTEGA, J.M. THE LL^T AND QR METHODS FOR SYMMETRIC TRIDIAGONAL MATRICES ; COMPUTER J., VOL.6, 1963 CO-AUTHOR : H.F.KAISER

*71 GUPTA, K.K. SOLUTION OF EIGENVALUE PROBLEMS BY STURM SEQUENCE METHOD ; IJNME, VOL.4, 1972

72 WITTRICK, W.H. NEW PROCEDURES FOR STRUCTURAL EIGEN-VALUES CALCULATIONS MECHANICS OF STRUCTURES & MAT.,1973 CO-AUTHOR : F.W.WILLIAMS

73 WILLIAMS, F.W. RAPID ANALYSIS OF THE EFFECTS OF STRUCTURAL MODIFICATIONS ON INCON-VENIENTLY SITUATED EIGENVALUES ; JCS,VOL.3, 1973.

*74 DUNS, C.S. AN ECONOMIC METHOD FOR THE DYNAMIC ANALYSIS OF FRAMED STRUCTURES ; SYM. STRUCT. DYN.

75 MELOSH, R.J. BASIS OF DERIVATION OF MATRICES FOR THE DIRECT STIFFNESS METHOD ; AIAA, VOL.1, 1963.

76 TAYLOR, R.L. ON COMPLETNESS OF SHAPE FUNCTIONS FOR FINITE ELEMENT ANALYSIS ; IJNME, VOL.4, JAN.,1972

77 COHEN, E. IMPROVED DEFORMATION FUNCTIONS FOR FINITE ELEMENT ANALYSIS OF BEAM ; IJNME, VOL.1, JAN.,1969.

78 WARBURTON, G.B. THE DYNAMICAL BEHAVIOUR OF STRUCTURES; PERGAMON, 1ST ED.,1964

79 JUST, D.J. ANALYSIS OF PLAME FRAMES OF LINEARLY VARYING RECTANGULAR SECTION ; STRUCTURAL ENGINEER, VOL.53, JAN., 1975. (PAPER X51 FILED IN LIBRARY)

80 JONES, R.P.N. THE NATURAL FREQUENCIES OF FREE AND CONSTRAINED NON-UNIFORM BEAMS ; JRAS, NOV., 1960, VOL.64 CO-AUTHOR : S.MAHALINGAM

81 LINDBERG, G.M. VIBRATION OF NON-UNIFORM BEAMS ; AERONAUTICAL QUARTERLY, VOL.14, 1963

82 SANGER, D.J. TRANSVERSE VIBRATION OF A CLASS OF NON-UNIFORM BEAMS ;
JMES, VOL.10, NO.2, 1968

83 THOMAS, J. IMPROVED FINITE ELEMENTS FOR VIBRATION ANLAYSIS OF TAPERED BEAMS ;
AERONAUTICAL QUARTERLY, VOL.24, 1973
CO-AUTHOR : E.DOKUMACI

84 KLEN, L. TRANSVERSE VIBRATIONS OF NON-UNIFORM BEAMS ;
JSV, VOL.37, PT.4, 1974

85 RAJU, L.S. LARGE AMPLITUDE FREE VIBRATION OF TAPERED BEAMS ;
AIAA, VOL14, FEB.,1976
CO-AUTHORS : RAO & KANAKA

86 EASTEP, F.E. ESTIMATION OF THE FUNDAMENTAL FREQUENCY OF BEAMS & PLATES WITH VARYING THICKNESS ;
AIAA, VOL.14, NOV.,1976

87 PRATHAP, G. LARGE AMPLITUDE FREE VIBRATION OF TAPERED HINGED BEAMS ;
AIAA, VOL.16, JAN.,1978
CO-AUTHOR : T.K.VARADAN

88 TO, C.W.S. HIGHER ORDER TAPERED BEAM FINITE ELEMENTS FOR VIBRATION ANALYSIS
JSV, VOL.63, NO.1, 1979

89 IRIE, T. DETERMINATION OF THE STEADY STATE RESPONSE OF A TIMONSHENKO BEAM OF VARYING CROSS-SECTION BY USE OF THE SPLINE INTERPOLATION TECHNIQUE ;
JSV, VOL.63, PT.2, 1979
CO-AUTHORS : G.YAMADA & I.TAKAHASHI

*90 VELESOS, A.S. NATURAL FREQUENCY OF CONTINUUM FLEXURAL MEMBER ;
ASCE-PROC, VOL.81, 1955, PAPER735
CO-AUTHOR : N.W.NEWMARK

*91 SIDDALL, J.W. REPORT ON APPROXIMATE ANALYTICAL METHODS FOR DETERMINING NATURAL MODES AND FREQUENCIES OF VIBRATION ;
MASSACHUSETTS INSTITUTE OF TECHNOLOGY
CO-AUTHOR: G.ISAKSON

*92 ARCHER, J.S. CONSISTENT MASS MATRIX FOR DISTRIBUTED MASS SYSTEMS ;
ASCE-ST-4, VOL.89, 1963

*93 TURNER, M.J. DESIGN OF MINIMUM MASS STRUCTURES WITH SPECIFID NATURAL FREQUENCY ;
AIAA, VOL.5, 1967

*94 SWANNELL, P. THE AUTOMATIC COMPUTATION OF THE

NATURAL FREQUENCIES OF STRUCTURAL FRAMES USING AN EXACT MATRIX TECHNIQUE ; TPFESA, TOKYO, 1973

*95 FITZGEORGE, D. SOLUTION OF VIBRATION PROBLEM BY USE OF A SMALL DIGITAL COMPUTER ; JSV, VOL.43, 1975

96 WARBURTON, G.B. SOME RECENT ADVANCES IN STRUCTURAL DYNAMICS ; PROC. ICBSS, SEPT., 1977

*97 MIELE, A. NUMERICAL DETERMINATION OF MINIMUM MASS STRUCTURES WITH SPECIFID NATURAL FREQUENCIES ; IJNME, VOL.13, 1978 CO-AUTHORS : MANGIAVACCHI & WU

*98 PRAMILA, A. A PHYSICAL INTERPRETATION OF THE ARTIFICE USED IN FREQUENCY ANALYSIS OF UNSUPPORTED STRUCTURES IJNME, VOL.14, MARCH, 1979

*99 BASCI, M.I. IMPROVED METHOD OF FREE VIBRATION ANALYSIS OF FRAME STRUCTURS ; JCS, VOL.10, APR,79 CO-AUTHORS: TORID,KHOZEIMEN,ET.AL

*100 WILLIAMS, F.W. A WARNING ON THE USE OF SYMMETRY IN CLASSICAL EIGENVALUE ANALYSES ; IJNME, VOL.12, FEB.1978

*101 ELLER, E.E INTRODUCTION TO SHOCK AND VIBRATION MEASUREMENTS ; SHOCK & VIBRATION HANDBOOK, CH.12 CO-AUTHOR : R.W.CONRAD

*102 MCLACHLAN, N.W. BESSEL FUNCTIONS FOR ENGINEERS ; OXFORD , 1955

103 SPIEGEL, M.R. MATHEMATICAL HANDBOOK OF FORMULAS AND TABLES ; MCCRAW-HILL, 1968, SCHAUM SERIES

*104 GUTTMAN, A.J. PROGRAMMING AND ALGORITHMS ; HEINEMANN, 1977

*105 FOX, L. NAG LIBRARY MANUAL, MARK 6 ; NUMERICAL ALGORITHM GROUP CO-AUTHOR: J.H.WILKINSON

*106 ICL MANUAL, COMPILING SYSTEMS (TP4241) ; ICL, 2ND ED, 1976

107 ICL MANUAL, FORTRAN, COMPILER LIBRARIES (TP4428) ; ICL, 3RD ED, 1976

Bibliographical work denoted by *

ABBREVIATION IN THE REFERENCES

(A) JOURNAL

AIAA	AMERICAN INSTITUTE OF AERONAUTICS & ASTRONAUTICS
ARMA	ACHIEVE RATIONAL MECHANICS AND ANALYSIS
ASCE	PROCEEDING, AMERICAN SOCIETY OF CIVIL ENGINEER,
	-EM : ENGINEERING MECHANICS DIVISION
	-ST : STRUCTURAL DIVISION
EESD	EARTHQUAKE ENGINEERING & STRUCTURAL DYNAMICS
IJMS	INTERNATIONAL JOURNAL OF MECHANICAL SCIENCE
IJNME	INTER. JOURNAL OF NUMERICAL METHODS IN ENGINEERING
JACM	JOURNAL OF THE ASSOCIATION OF COMPUTING MECHANICS
JAM	JOURNAL OF APPLIED MECHANICS
JAS	JOURNAL OF AERONAUTICAL SCIENCE
JCS	JOURNAL OF COMPUTERS & STRUCTURES
JMES	JOURNAL OF MECHANICAL ENGINEERING SCIENCE
JRAS	JOURNAL OF THE ROYAL AERONAUTICAL SOCIETY
JSV	JOURNAL OF SOUND AND VIBRATION
QJMAM	QUARTERLY JOURNAL MECHANICS AND APPLIED MATHS.
SIAM	SOCIETY FOR INDUSTRIAL & APPLIED MATHS
	-JNA : JOURNAL OF NUMERICAL ANALYSIS

(B) CONFERENCE PROCEEDINGS & OTHERS

NUMERICAL METHODS FOR VIBRATION PROBLEM :
SYMPOSIUM PAPERS, JULY,1966, THE INSTITUTE OF SOUND AND VIBRATION IN UNIVERSITY OF SOUTHAMPTON

1ST US-JAPAN SEMINAR ; AUGUST,1969
RECENT ADVANCES IN MATRIX METHODS OF STRUCTURAL ANALYSIS AND DESIGN, ED.BY GALLAGHER,YAMADA & ODEN

SYM. STRUCT. DYN. :
SYMPOSIUM ON STRUCTURAL DYNAMICS, MARCH,1970 LOUGHBOROUGH UNIV. OF TECH., ED. BY D.J.JOHNS

2ND US-JAPAN SEMINAR ; AUGUST,1972
ADVANCES IN COMPUTATIONAL METHODS IN STRUCTURAL MECHANICS AND DESIGN, ED. BY ODEN, CLOUGH & YAMADA

VARIATIONAL METHODS IN ENGINEERINGS :
PROCEEDINGS, SEPT,1972, UNIV. OF SOUTHAMPTON

MECHANICS OF STRUCTURES & MATERIALS :
FOURTH AUSTRALASIAN CONFERENCE, BRISBANE, AUG.,1973

TPFESA : THEORY AND PRACTICE IN FINITE ELEMENT STRUCTURAL ANALYSIS , TOKYO, 1973

ICBSS : INTERNATIONAL CONFERENCE OF THE BEHAVIOUR OF SLENDER STRUCTURES, CITY UNIV., SEPT.,1977

SHOCK & VIBRATION HANDBOOK :
ED. BY HARRIS & CREDE, MCCRAW-HILL, 1976

APPENDIX A <u>The definite Integral</u> (for §5.3.2)

$\int_0^L h(x).x^n\,dx$	$f(x)=1$	$f(x)=x$	$f(x)=x^2$
$\int_0^L \sin^2\lambda x\ .f(x)dx$	$\alpha-sc$	$\alpha^2-2\alpha sc+s^2$	$2\alpha^3-6\alpha^2sc+6\alpha s^2-3\alpha+3sc$
$\int_0^L \sin\lambda x\cos\lambda x.f(x)dx$	s^2	$2\alpha s^2-\alpha+sc$	$6\alpha^2s^2-3\alpha^2+6\alpha sc-2s^2$
$\int_0^L \sin\lambda x.sh\lambda x.f(x)dx$	$sch-csh$	$2\alpha(sch-csh)+2cch-2$	$6\alpha^2(sch-csh)+12\alpha cch-6(sch+csh)$
$\int_0^L \sin\lambda x.ch\lambda x.f(x)dx$	$ssh-cch+1$	$2\alpha(ssh-cch)+2csh$	$6\alpha^2(ssh-cch)+12\alpha csh-6(ssh+cch)+6$
$\int_0^L \cos^2\lambda x\ .f(x)dx$	$\alpha+sc$	$\alpha^2+2\alpha sc-s^2$	$2\alpha^3+6\alpha^2sc-6\alpha s^2+3\alpha-3sc$
$\int_0^L \cos\lambda x.sh\lambda x.f(x)dx$	$ssh+cch-1$	$2\alpha(ssh+cch)-2sch$	$6\alpha^2(ssh+cch)-12\alpha sch+6(ssh-cch)+6$
$\int_0^L \cos\lambda x.ch\lambda x.f(x)dx$	$sch+csh$	$2\alpha(sch+csh)-2ssh$	$6\alpha^2(sch+csh)-12\alpha ssh+6(sch-csh)$
$\int_0^L sh^2\lambda x\ .f(x)dx$	$-\alpha+shch$	$-\alpha^2+2\alpha shch-sh^2$	$-2\alpha^3+6\alpha^2shch-3\alpha-6\alpha sh^2+3shch$
$\int_0^L sh\,\lambda x.ch\lambda x.f(x)dx$	sh^2	$2\alpha sh^2+\alpha-shch$	$6\alpha^2sh^2+3\alpha^2-6\alpha shch+3sh^2$
$\int_0^L ch^2\lambda x\ .f(x)dx$	$\alpha+shch$	$\alpha^2+2\alpha shch-sh^2$	$2\alpha^3+6\alpha^2shch+3\alpha-6\alpha sh^2+3shch$
Multipler	$1/2\lambda$	$(1/2\lambda)^2$	$2/3\cdot(1/2\lambda)^3$

$\int_0^L \sin^2\lambda x\ .f(x)dx = (1/2\lambda)^4.(\ 2\alpha^4-8\alpha^3sc+12\alpha^2s^2-6\alpha^2+12\alpha sc-6s^2\ )$ Where $f(x) = x^3$

$\int_0^L \sin\lambda x\cos\lambda x.f(x)dx = (1/2\lambda)^4.(\ 8\alpha^3s^2\ 4\alpha^3+12\alpha^2sc-12\alpha s^2+6\alpha-6sc\ )$

$\int_0^L \sin\lambda x.sh\lambda x.f(x)dx = (1/2\lambda)^4.(\ 8\alpha^3(sch-csh)+24\alpha^2cch-24\alpha(sch+csh)+24ssh\ )$

$\int_0^L \sin\lambda x.ch\lambda x.f(x)dx = (1/2\lambda)^4.(\ 8\alpha^3(ssh-cch)+24\alpha^2csh-24\alpha(ssh+cch)+24sch\ )$

$\int_0^L \cos^2\lambda x\ .f(x)dx = (1/2\lambda)^4.(\ 2\alpha^4+8\alpha^3sc-12\alpha^2s^2+6\alpha^2-12\alpha sc+6s^2\ )$

$\int_0^L \cos\lambda x.sh\lambda x.f(x)dx = (1/2\lambda)^4.(\ 8\alpha^3(ssh+cch)-24\alpha^2sch+24\alpha(ssh-cch)+24csh\ )$

$\int_0^L \cos\ x.ch\lambda x.f(x)dx = (1/2\lambda)^4.(\ 8\alpha^3(sch+csh)-24\alpha^2(ssh)+24\alpha(sch-csh)-24(1-cch)\ )$

$\int_0^L sh^2\lambda x\ \ x.f(x)dx = (1/2\lambda)^4.(-2\alpha^4+8\alpha^3shch-6\alpha^2-12\alpha^2sh^2+12\alpha shch-6sh^2\ )$

$\int_0^L sh\,\lambda x.ch\lambda x.f(x)dx = (1/2\lambda)^4.(\ 8\alpha^3sh^2+4\alpha^3-12\alpha^2shch+12\alpha sh^2+6\alpha-6shch\ )$

$\int_0^L ch^2\lambda x\ .f(x)dx = (1/2\lambda)^4.(\ 2\alpha^4+8\alpha^3shch-6\alpha^2-12\alpha^2sh+12\alpha shch-6sh^2\ )$

$\int_0^L \sin^2\lambda x\ .x^4dx = Q.(\ 4\alpha^5-20\alpha^4sc+20\alpha^3(2s^2-1)+60\alpha^2sc-30\alpha(2s^2-1)-30sc\ )$

$\int_0^L \sin\lambda x\cos\lambda x.\ x^4dx = Q.(\ 10\alpha^4(2s^2-1)+40\alpha^3sc-30\alpha^2(2s^2-1)-60\alpha sc+30s^2\ )$

$\int_0^L \sin\lambda x.sh\lambda x.\ x^4dx = Q.(\ 20\alpha^4(sch-csh)+80\alpha^3cch-120\alpha^2(sch+csh)+240\alpha ssh-120(sch-csh)\ )$

$\int_0^L \sin\lambda x.ch\lambda x.\ x^4dx = Q.(\ 20\alpha^4(ssh-cch)+80\alpha^3csh-120\alpha^2(ssh+cch)+240\alpha sch-120(ssh-cch+1)\ )$

$\int_0^L \cos^2\lambda x\ .x^4dx = Q.(\ 4\alpha^5+20\alpha^4sc-20\alpha^3(2s^2-1)-60\alpha^2sc+30\alpha(2s^2-1)+30sc\ )$

$\int_0^L \cos\lambda x.sh\lambda x.\ x^4dx = Q.(\ 20\alpha^4(ssh+cch)-80\alpha^3sch+120\alpha^2(ssh-cch)+240\alpha csh-120(ssh+csh-1)\ )$

$\int_0^L \cos\lambda x.ch\lambda x.\ x^4dx = Q.(\ 20\alpha^4(sch-csh)-80\alpha^3ssh+120\alpha^2(sch-csh)+240\alpha cch-120(sch+csh)\ )$

$\int_0^L sh^2\lambda x\ .x^4dx = Q.(\ -4\alpha^5+20\alpha^4shch-20\alpha^3(2sh^2+1)+60\alpha^2shch-30\alpha(2sh^2+1)+30shch\ )$

$\int_0^L sh\,\lambda x.ch\lambda x.\ x^4dx = Q.(\ 10\alpha^4(2sh^2+1)-40\alpha^3shch+30\alpha^2(2sh^2+1)-60\alpha shch+30sh^2\ )$

$\int_0^L ch^2\lambda x\ .x^4dx = Q.(\ 4\alpha^5+20\alpha^4shch-20\alpha^3(2sh^2+1)+60\alpha^2shch-30\alpha(2sh^2+1)+30shch\ )$

where $Q = 4/5\cdot(1/2\lambda)^5$

Notation : $\alpha=\lambda L$; $s=\sin\lambda L$; $c=\cos\lambda L$; $sh=\sinh\lambda L$; $ch=\cosh\lambda L$

Note : $\sinh\lambda x$ & $\cosh\lambda x$ have been abbreviated to $sh\lambda x$ & $ch\lambda x$ respectively.

APPENDIX B Matrix [X] of Exact Function

$$
[X] = \begin{bmatrix} X_{11} & X_{12} & X_{13} & X_{14} \\ & X_{22} & X_{23} & X_{24} \\ & \text{sym.} & X_{33} & X_{34} \\ & & & X_{44} \end{bmatrix}
$$

where

$$X_{11} = \tfrac{r}{16}\big(2\alpha^4(r+2)^2 - 8\alpha^3 sc(r+1)(r+2) + 4\alpha^2 s^2(3r^2+6r+2) - 6\alpha^2 r(r+2)$$
$$+12\alpha sc(r+1)r - 6s^2r^2\big)$$

$$X_{12} = \tfrac{r}{8}\big(4\alpha^3 s^2(r+1)(r+2) - 2\alpha^3(r+1)(r+2) + 2\alpha^2 sc(3r^2+6r+2)$$
$$-6\alpha s^2(r+1)r + 3\alpha r^2 - 3scr^2\big)$$

$$X_{13} = -\tfrac{1}{2}\big(\alpha^3(sch-csh)(r+1)(r^2+2r+2) - 4\alpha^2 r + \alpha^2 cch(3r^2+6r+4)r$$
$$-3\alpha(sch+csh)r^2(r+1) + 3sshr^3\big)$$

$$X_{14} = -\tfrac{1}{2}\big(\alpha^3(ssh-cch+1)(r+1)(r^2+2r+2) - \alpha^3 r(r^2+3r+4) + \alpha^2 csh(3r^2+6r+4)r$$
$$-3\alpha(ssh+cch-1)r^2(r+1) + 3schr^3 - 3\alpha r^3\big)$$

$$X_{22} = \tfrac{r}{16}\big(2\alpha^4(r+2)^2 + 8\alpha^3 sc(r+1)(r+2) - 4\alpha^2 s^2(3r^2+6r+2) + 6\alpha^2 r(r+2)$$
$$-12\alpha scr(r+1) + 6s^2r^2\big)$$

$$X_{23} = -\tfrac{1}{2}\big(\alpha^3(ssh+cch-1)(r+1)(r^2+2r+2) + \alpha^3 r(r^2+3r+4) - \alpha^2 sch(3r^2+6r+4)r$$
$$+3\alpha(ssh-cch+1)r^2(r+1) - 3\alpha r^3 + 3cshr^3\big)$$

$$X_{24} = -\tfrac{1}{2}\big(\alpha^3(sch+csh)(r+1)(r^2+2r+2) - \alpha^2 ssh(3r^2+6r+4)r$$
$$+3\alpha(sch-csh)r^2(r+1) - 3r^3 + 3cchr^3\big)$$

$$X_{33} = \tfrac{r}{16}\big(-2\alpha^4(r+2)^2 + 8\alpha^3 shch(r+1)(r+2) + 4\alpha^2 sh^2(3r^2+6r+2) - 6\alpha^2 r(r+2)$$
$$+12\alpha shch(r+1)r - 6sh^2r^2\big)$$

$$X_{34} = \tfrac{r}{8}\big(4\alpha^3 sh^2(r+1)(r+2) + 2\alpha^3(r+1)(r+2) - 2\alpha^2 shch(3r^2+6r+2)$$
$$+6\alpha sh^2 r(r+1) + 3\alpha r^2 - 3shchr^2\big)$$

$$X_{44} = \tfrac{r}{16}\big(2\alpha^4(r+2)^2 + 8\alpha^3 shch(r+1)(r+2) - 4\alpha^2 sh^2(3r^2+6r+2) - 6\alpha^2 r(r+2)$$
$$+12\alpha shchr(r+1) - 6sh^2r^2\big)$$

* Where $r = m-1$ $s = \sin\lambda_i L$ $sh = \sinh\lambda_i L$

$c = \cos\lambda_i L$ $ch = \cosh\lambda_i L$

APPENDIX C

$$X = \frac{r^2}{4\alpha_1^2}\varphi^2 \qquad \frac{d\varphi}{dX} = \frac{2\alpha_1^2}{(m-1)^2\varphi}$$

$$X = \frac{r^4}{16\alpha_1^4}\varphi^4 \qquad \frac{d^2\varphi}{dX^2} = -\frac{4\alpha_1^4}{(m-1)^4\varphi^3}$$

$$X = \frac{r^6}{64\alpha_1^6}\varphi^6 \qquad \frac{d^3\varphi}{dX^3} = \frac{24\alpha_1^6}{(m-1)^6\varphi^5}$$

$$\frac{d^4\varphi}{dX^4} = -\frac{240\alpha_1^8}{(m-1)^8\varphi^7}$$

$$\frac{dW}{d\varphi} = \frac{1}{\varphi}\frac{d\Psi}{d\varphi} - \frac{1}{\varphi^2}\Psi$$

$$\frac{d^2W}{d\varphi^2} = \frac{1}{\varphi}\frac{d^2\Psi}{d\varphi^2} - \frac{2}{\varphi^2}\frac{d\Psi}{d\varphi} + \frac{2}{\varphi^3}\Psi$$

$$\frac{d^3W}{d\varphi^3} = \frac{1}{\varphi}\frac{d^3\Psi}{d\varphi^3} - \frac{3}{\varphi^2}\frac{d^2\Psi}{d\varphi^2} + \frac{6}{\varphi^3}\frac{d\Psi}{d\varphi} + \frac{6}{\varphi^4}\Psi$$

$$\frac{d^4W}{d\varphi^4} = \frac{1}{\varphi}\frac{d^4\Psi}{d\varphi^4} - \frac{4}{\varphi^2}\frac{d^3\Psi}{d\varphi^3} + \frac{12}{\varphi^3}\frac{d^2\Psi}{d\varphi^2} - \frac{24}{\varphi^4}\frac{d\Psi}{d\varphi} + \frac{24}{\varphi^5}\Psi$$

$$\frac{dW}{dX} = \frac{d\varphi}{dX}\frac{dW}{d\varphi} = \frac{2\alpha_1^2}{r^2\varphi}\frac{dW}{d\varphi}$$

$$\frac{d^2W}{dX^2} = \frac{4\alpha_1^4}{r^4\varphi^2}\left(\frac{d^2W}{d\varphi^2} - \frac{1}{\varphi}\frac{dW}{d\varphi}\right)$$

$$\frac{d^3W}{dX^3} = \frac{8\alpha_1^6}{r^6\varphi^3}\left(\frac{d^3W}{d\varphi^3} - \frac{3}{\varphi}\frac{d^2W}{d\varphi^2} + \frac{3}{\varphi^2}\frac{dW}{d\varphi}\right)$$

$$\frac{d^4W}{dX^4} = \frac{16\alpha_1^8}{r^8\varphi^4}\left(\frac{d^4W}{d\varphi^4} - \frac{6}{\varphi}\frac{d^3W}{d\varphi^3} + \frac{15}{\varphi^2}\frac{d^2W}{d\varphi^2} - \frac{15}{\varphi^3}\frac{dW}{d\varphi}\right)$$

APPENDIX D **Series Expansion of Trigonometrical & Hyperbolic Functions**

$$\sin\alpha = \alpha - \frac{\alpha^3}{3!} + \frac{\alpha^5}{5!} \quad .....$$

$$\mathrm{sh}\,\alpha = \alpha + \frac{\alpha^3}{3!} + \frac{\alpha^5}{5!} \quad .....$$

$$\cos\alpha = 1 - \frac{\alpha^2}{2!} + \frac{\alpha^4}{4!} \quad .....$$

$$\mathrm{ch}\,\alpha = 1 + \frac{\alpha^2}{2!} + \frac{\alpha^4}{4!} \quad .....$$

$$\mathrm{ssh} = \sin\alpha\ \mathrm{sh}\,\alpha = \alpha^2 - \frac{\alpha^6}{90} - \frac{\alpha^8}{5040} \quad .....$$

$$\mathrm{cch} = \cos\alpha\ \mathrm{ch}\,\alpha = 1 + \frac{\alpha^4}{48} - \frac{\alpha^6}{720} \quad .....$$

$$\mathrm{sch} = \sin\alpha\ \mathrm{ch}\,\alpha = \alpha + \frac{\alpha^3}{3} - \frac{\alpha^5}{30} + \frac{\alpha^7}{336} \quad .....$$

$$\mathrm{csh} = \cos\alpha\ \mathrm{sh}\,\alpha = \alpha - \frac{\alpha^3}{3} + \frac{\alpha^5}{30} - \frac{\alpha^7}{336} \quad .....$$

$$\frac{\mathrm{sch-csh}}{\alpha^3} = \frac{2}{3} + \frac{\alpha^4}{168} \quad .....$$

$$\frac{\mathrm{sch+csh}}{\alpha} = 2 - \frac{\alpha^4}{15} \quad .....$$

$$\frac{\mathrm{ssh}}{\alpha^2} = 1 - \frac{\alpha^4}{90} \quad .....$$

$$1+\mathrm{cch} = 2 + \frac{\alpha^4}{48} \quad .....$$

If $\alpha = 0.0$

$$\frac{\mathrm{sch - csh}}{\alpha^3(1+\mathrm{cch})} = \frac{\frac{2}{3}}{2} = \frac{1}{3}$$

$$\frac{\mathrm{sch + csh}}{\alpha(1+\mathrm{cch})} = \frac{2}{2} = 1$$

$$\frac{\mathrm{ssh}}{\alpha^2(1+\mathrm{cch})} = \frac{1}{2}$$

Appendix E1 Library: JJTMC

(JTMBEQ) Statement No. (JTMBEQ)

```
      SEGMENTS (JJTMC)
      COMPRESS INTEGER AND LOGICAL
      COMPACT PROGRAM
      TRACE 0
      END

      SUBROUTINE JTMBEQ (MXX,MYY,NOJ,XC,YC,LR,LQ,JN,MSIZE,LOCAT,MEM,NOM,
     1 IPT,JPT,THI,THJ,HYP,ZM,CS,SN,WII,WIJ,ZN,EQU,EPU,THU,WIU,
     2 NWIPT,NWJPT,NWIST,NWJST,NSE,SETH,SEWI,NWRT,NWLR)
      DIMENSION JN(MYY),XC(MYY),YC(MYY),LR(MYY,3),LQ(MYY),EPU(MYY),
     1 EQU(MYY),MEM(MYY),IPT(MYY),JPT(MYY),THI(MYY),THJ(MYY),LOCAT(MYY),
     2 ZN(MYY),HYP(MYY),ZM(MYY),CS(MYY),SN(MYY),WII(MYY),WIJ(MYY),
     3 NWIPT(MYY),NWJPT(MYY),NWIST(MYY),NWJST(MYY),NSE(MYY),
     4 SETH(MXX,MYY),SEWI(MXX,MYY),NWRT(MYY),NWLR(MYY,3)
   11 FORMAT(I0,2F0.0,1X,3I1)
   12 FORMAT(3I0,4F0.0,I0)
   21 FORMAT(20X,I5,2F10.5,3X,3I1)
   22 FORMAT(20X,3I5,4F10.5,I5)
   23 FORMAT(1X,'JOINT   PARAMETERS :   JN,XC,YC,LR')
   24 FORMAT(1X,'MEMBER  PARAMETERS :   MEM,IPT,JPT,THIJ,WIIJ,NSE')
      WRITE(2,23)
      DO 231 JT=1,NOJ
      READ (1,11)  JN(JT),XC(JT),YC(JT),(LR(JT,KA),KA=1,3)
  231 WRITE(2,21)  JN(JT),XC(JT),YC(JT),(LR(JT,KA),KA=1,3)
      WRITE(2,24)
      DO 232 MB=1,NOM
      READ (1,12)  MEM(MB),IPT(MB),JPT(MB),THI(MB),THJ(MB),
     1             WII(MB),WIJ(MB),NSE(MB)
  232 WRITE(2,22)  MEM(MB),IPT(MB),JPT(MB),THI(MB),THJ(MB),
     1             WII(MB),WIJ(MB),NSE(MB)
      DO 331 MB=1,NOM
      CS(MB)=XC(JPT(MB))-XC(IPT(MB))
      SN(MB)=YC(JPT(MB))-YC(IPT(MB))
      HYP(MB)=SQRT(CS(MB)*CS(MB)+SN(MB)*SN(MB))
      CS(MB)=CS(MB)/HYP(MB)
  331 SN(MB)=SN(MB)/HYP(MB)
      SPAN=0.0
      VOLWI=0.0
      VOLTH=0.0
      DO 332 MB=1,NOM
      VOLWI=VOLWI+(WII(MB)+WIJ(MB))*HYP(MB)/2.0
      VOLTH=VOLTH+(THI(MB)+THJ(MB))*HYP(MB)/2.0
  332 SPAN=SPAN+HYP(MB)
      WIU=VOLWI/SPAN
      THU=VOLTH/SPAN
      DO 435 MB=1,NOM
      MSE=NSE(MB)
      SETH(     1,MB) = THI(MB)
      SEWI(MSE+1,MB) = WIJ(MB)
      SETHIJ = ( THJ(MB)-THI(MB) ) / FLOAT(MSE)
      SEWIIJ = ( WIJ(MB)-WII(MB) ) / FLOAT(MSE)
      IF( MSE.EQ.1 ) GOTO 433
      DO 434 KAA=2,MSE
      SETH(KAA,MB) = SETH(1,MB) + SETHIJ*FLOAT(KAA-1)
      SEWI(KAA,MB) = SEWI(1,MB) + SEWIIJ*FLOAT(KAA-1)
  434 CONTINUE
  433 CONTINUE
  435 CONTINUE
      DO 1031 MB=1,NOM
      IF(MEM(MB).NE.5)GOTO 1031
      MEM(MB)=1
      IF(NSE(MB).EQ.1)GOTO 1033
      DO 1032 KAA=1,NSE(MB)-1
      SETH(KAA,MB)=( SETH(KAA,MB) + SETH(KAA+1,MB) )/2.0
      SEWI(KAA,MB)=( SEWI(KAA,MB) + SEWI(KAA+1,MB) )/2.0
 1032 CONTINUE
      SETH(NSE(MB),MB) = (SETH(NSE(MB),MB)+THJ(MB))/2.0
      SEWI(NSE(MB),MB) = (SEWI(NSE(MB),MB)+WIJ(MB))/2.0
      GOTO 1031
 1033 SETH(1,MB)=( SETH(1,MB)+THJ(MB) )/2.0
      SEWI(1,MB)=( SEWI(1,MB)+WIJ(MB) )/2.0
 1031 CONTINUE
      DO 260 KAA=1,NOJ
  260 NWRT(KAA)=-99
      NNM=1
      NNJ=1
      NWIPT(1)=1
      NWIST(1)=1
      NWLR(1,1)=LR(1,1)
      NWLR(1,2)=LR(1,2)
      NWLR(1,3)=LR(1,3)
      IF(NSE(1).EQ.1)GOTO 261
      DO 262 KAA=2,NSE(1)
      NNM=NNM+1
      NNJ=NNJ+1
      NWJPT(NNM-1)=NNJ
      NWIPT(NNM   )=NNJ
      NWLR(NNJ,1)=1
      NWLR(NNJ,2)=1
      NWLR(NNJ,3)=1
  262 CONTINUE
  261 NWJPT(NNM)=NNJ+1
      NWJST(1)=NWJPT(NNM)
      NWLR(NNJ+1,1)=LR(JPT(1),1)
      NWLR(NNJ+1,2)=LR(JPT(1),2)
      NWLR(NNJ+1,3)=LR(JPT(1),3)
```

(JTMBEQ) Statment No. (JTMBEQ)

```
      IF(NOM.EQ.1)GOTO 263
      DO 271 KAA=2,NOM
      NNM=NNM+1
      NNJ=NNJ+1
      DO 273 KAB=1,KAA-1
      IF (JPT(KAB).NE.IPT(KAA))GOTO 273
      NWIPT(NNM)=NWJST(KAB)
      GOTO 274
  273 CONTINUE
      DO 275 KAB=1,KAA-1
      IF (IPT(KAB).NE.IPT(KAA))GOTO 275
      NWIPT(NNM)=NWIST(KAB)
      GOTO 274
  275 CONTINUE
  274 NWIST(KAA)=NWIPT(NNM)
      IF(NSE(KAA).EQ.1)GOTO 276
      DO 277 KAB=2,NSE(KAA)
      NNJ=NNJ+1
      NNM=NNM+1
      NWJPT(NNM-1)=NNJ
      NWIPT(NNM   )=NNJ
      NWLR(NNJ,1)=1
      NWLR(NNJ,2)=1
      NWLR(NNJ,3)=1
  277 CONTINUE
  276 IF(NWRT(JPT(KAA)).GT.1)GOTO 278
      NWJPT(NNM)=NNJ+1
      NWLR(NNJ+1,1)=LR(JPT(KAA),1)
      NWLR(NNJ+1,2)=LR(JPT(KAA),2)
      NWLR(NNJ+1,3)=LR(JPT(KAA),3)
      GOTO 279
  278 DO 280 KAB=1,KAA-1
      IF(JPT(KAB).NE.JPT(KAA))GOTO 280
      NWJPT(NNM)=NWJST(KAB)
      NNJ=NNJ-1
      GOTO 279
  280 CONTINUE
  279 NWJST(KAA)=NWJPT(NNM)
      NWRT(JPT(KAA))=99
  271 CONTINUE
  263 NNJ=NNJ+1
      DO 281 KAA=1,NNM
      IPT(KAA)=NWIPT(KAA)
  281 JPT(KAA)=NWJPT(KAA)
      DO 282 KAA=1,NNJ
      DO 282 KAB=1,3
  282 LR(KAA,KAB)=NWLR(KAA,KAB)
      NWA=0
```

```
      NWA=NWA+1
      ZM(NWA) =SETH(KAB+1,KAA)/SETH(KAB,KAA)
      ZN(NWA) =SEWI(KAB+1,KAA)/SEWI(KAB,KAA)
      EQU(NWA)=SETH(KAB,KAA)/THU
      EPU(NWA)=SEWI(KAB,KAA)/WIU
  532 CONTINUE
      NWA=0
      DO 631 KAA=1,NOM
      DO 631 KAB=1,NSE(KAA)
      NWA=NWA+1
      THI(NWA)=SETH(KAB  ,KAA)
      THJ(NWA)=SETH(KAB+1,KAA)
      WII(NWA)=SEWI(KAB  ,KAA)
      WIJ(NWA)=SEWI(KAB+1,KAA)
  631 CONTINUE
      DO 632 KAA=1,NOM
      SETH(1,KAA)=CS(KAA)
      SEWI(1,KAA)=SN(KAA)
  632 CONTINUE
      NWA=0
      DO 633 KAA=1,NOM
      DO 633 KAB=1,NSE(KAA)
      NWA=NWA+1
      CS(NWA)=SETH(1,KAA)
  633 SN(NWA)=SEWI(1,KAA)
      DO 634 KAA=1,NOM
      SETH (1,KAA)=HYP(KAA)/FLOAT(NSE(KAA))
  634 NWIST(KAA)=MEM(KAA)
      NWA=0
      DO 635 KAA=1,NOM
      DO 635 KAB=1,NSE(KAA)
      NWA=NWA+1
      HYP(NWA)=SETH(1,KAA)
  635 MEM(NWA)=NWIST(KAA)
      WRITE(2,620)
      DO 611 MB=1,NNM
  611 WRITE(2,621)MEM(MB),IPT(MB),JPT(MB),HYP(MB),
     1 CS(MB),THI(MB),THJ(MB),ZM(MB),EQU(MB),
     2 SN(MB),WII(MB),WIJ(MB),ZN(MB),EPU(MB)
      WRITE(2,622) ((LR(KAA,KAB),KAB=1,3),KAA=1,NNJ)
  620 FORMAT(1X,'ELEMENT PARAMETER :    MEM,IPT,JPT,HYP,CS,',
     1                 'THI,THJ,ZM,EQ')
  621 FORMAT(20X,3I5,F10.5,1PE15.5,0P4F10.5,
     1 /45X,1PE15.5,0P4F10.5)
  622 FORMAT(24X,10(19(3I1,2X),/24X))
      NOM=NNM
      NOJ=NNJ
      DO 736 JT=1,NOJ
```

(JTMBEQ) — Statment No.

```
      LOCAT(1)=0                         201
      LOCAT(2)=1                         202
      LN = 2                             203
      IF(NOJ.LT.3) GOTO 734              204
      GOTO 733                           205
  732 LOCAT(1)=1                         206
      LN = 1                             207
  733 MSIZE=0                            208
      DO 731 LM=LN,NOJ-1                 209
      LOCAT(LM+1)=LOCAT(LM)+LQ(LM)       210
      MSIZE=MSIZE+LQ(LM)                 211
  731 CONTINUE                           212
      MSIZE=MSIZE+LQ(NOJ)                213
      GOTO 735                           214
  734 MSIZE=LQ(2)                        215
  735 RETURN                             216
      END                                217
      FINISH                             218
```

Subroutine for the ETES method

The above subroutine is based on the ELES method. The following modifications give the subroutine for the ETES method :-

(i) Statement nos.52-57 inclusive are replaced by

```
052       IF( MSE.EQ.1 ) GOTO 433
053       DO 434 KAA=2,MSE
054       AAA=FLOAT(MSE-KAA+1) / FLOAT(MSE)
055       BBB=FLOAT(KAA-1) / FLOAT(MSE)
056       CAA=SETH(1,MB)**AAA
057       CBB=SETH(MSE+1,MB)**BBB
058       SETH(KAA,MB)=CAA*CBB
059       HANN=( (SETH(KAA,MB)-SETH(1,MB)) / (SETH(MSE+1,MB)-SETH(1,MB)))
060       SEWI(KAA,MB)=HANN*(SEWI(MSE+1,MB)-SEWI(1,MB))+SEWI(1,MB)
```

(ii) The following statement is inserted before Statement no.159.

```
162       XC(KAA)=SETH(1,KAA)
```

(iii) Statement nos.176-184 inclusive are relaced by

```
180       DO 641 MB=1,NOM
181       MSE=NSE(MB)
182       IF(NSE(MB).EQ.1)GOTO 641
183       DO 642 KAA=2,MSE
184       SEWI(KAA,MB)=(SETH(KAA,MB)-XC(MB))
185      1                       /(SETH(MSE+1,MB)-XC(MB))
186   642 CONTINUE
187       SEWI(1,MB)=0.0
188       SEWI(MSE+1,MB)=1.00
189       DO 645 KAA=1,NSE(MB)
190       SEWI(KAA,MB)=(SEWI(KAA+1,MB)-SEWI(KAA,MB))*HYP(MB)
191   645 CONTINUE
192   641 NWIST(MB)=MEM(MB)
193       NWA=0
194       DO 644 MB=1,NOM
195       DO 644 KAA=1,NSE(MB)
```

Appendix E2 (a) Library:KMPOLY

(KTWCU) Statement No. (MTWCU)

```
SEGMENTS (KMPOLY)
COMPRESS INTEGER AND LOGICAL
COMPACT PROGRAM
TRACE 0
END

SUBROUTINE KTWCU (HP,RM,RN,EP,EQ,EI,EA,R)
DIMENSION  R(6,6)
H2=HP*HP
H3=HP*H2
RMN  = RM*RN
RM2  = RM*RM
RM3  = RM*RM2
RM2N = RN*RM2
RM3N = RN*RM3
ZJJ = EI/H3*EP*EQ/35.0*EQ*EQ
R(1,1) = ( 132.0*RM3N + 15.0*RM3 + 45.0*RM2N + 18.0*RM2
*          + 18.0*RMN  + 45.0*RM  + 15.0*RN   + 132.0 )   *ZJJ
R(1,2) = (  38.0*RM3N +  4.0*RM3 + 12.0*RM2N +  9.0*RM2
*          +  9.0*RMN  + 33.0*RM  + 11.0*RN   + 94.0 )*HP*ZJJ
R(1,4) = (  94.0*RM3N + 11.0*RM3 + 33.0*RM2N +  9.0*RM2
*          +  9.0*RMN  + 12.0*RM  +  4.0*RN   + 38.0 )*HP*ZJJ
R(2,2) = (  12.0*RM3N +  2.0*RM3 +  6.0*RM2N +  8.0*RM2
*          +  8.0*RMN  + 27.0*RM  +  9.0*RN   + 68.0 )*H2*ZJJ
R(2,4) = (  26.0*RM3N +  2.0*RM3 +  6.0*RM2N +      RM2
*          +      RMN  +  6.0*RM  +  2.0*RN   + 26.0 )*H2*ZJJ
R(4,4) = (  68.0*RM3N +  9.0*RM3 + 27.0*RM2N +  8.0*RM2
*          +  8.0*RMN  +  6.0*RM  +  2.0*RN   + 12.0 )*H2*ZJJ
R(1,3) = -R(1,1)
R(2,3) = -R(1,2)
R(3,4) = -R(1,4)
R(3,3) =  R(1,1)
R(5,5) = EQ*EP*EA/HP/6.0*(2.0*RMN+RM+RN+2.0)
R(5,6) = -R(5,5)
R(6,6) = R(5,5)
RETURN
END

SUBROUTINE MTWCU (HP,RM,RN,EP,EQ,EI,PA,R)
DIMENSION  R(6,6)
H2=HP*HP
RMN  = RM*RN
RR=RM+RN
ZJB = EP*EQ/2520.0*PA*HP
R(1,1)= ZJB*( 76.0*RMN +140.0*RR +580.0)
R(1,2)= ZJB*( 17.0*RMN + 25.0*RR + 65.0) *HP
R(1,3)= ZJB*( 92.0*RMN +70.0*RR + 92.0)
R(1,4)=-ZJB*( 19.0*RMN + 17.0*RR + 25.0) *HP
```

```
R(2,4)=-ZJB*(  5.0*RMN +  4.0*RR +  5.0) *H2
R(3,3)= ZJB*(580.0*RMN +140.0*RR + 76.0)
R(3,4)=-ZJB*( 65.0*RMN + 25.0*RR + 17.0) *HP
R(4,4)= ZJB*( 10.0*RMN +  5.0*RR +  4.0) *H2
ZJB = PA*EP*EQ/60.0*HP
R(5,5) = ZJB*(2.0*RMN+3.0*RR+12.0)
R(5,6) = ZJB*(3.0*RMN+2.0*RR+ 3.0)
R(6,6) = ZJB*(12.0*RMN+3.0*RR+2.0)
RETURN
END

FINISH
```

(JPRISM) & (JDOVET) Statement No. (JWEDGE)

```
SEGMENTS (JCUBIC)
COMPRESS INTEGER AND LOGICAL
COMPACT PROGRAM
TRACE 0
END

SUBROUTINE JPRISM (GL,GC,HP,EP,EQ,EI,EA,R)
DIMENSION R(6,6)
P = (GL*HP)**4/EQ/EQ
H2=HP*HP
H3=HP*H2
SZM = EI/420.0/H3*EP*EQ*EQ*EQ
R(1,1) = SZM*(5040.0 - 156.0*P)
R(1,2) = SZM*(2520.0 -  22.0*P)*HP
R(1,3) =-SZM*(5040.0 +  54.0*P)
R(1,4) = SZM*(2520.0 +  13.0*P)*HP
R(2,2) = SZM*(1680.0 -   4.0*P)*H2
R(2,3) =-R(1,4)
R(2,4) = SZM*( 840.0 +   3.0*P)*H2
R(3,3) = R(1,1)
R(3,4) =-R(1,2)
R(4,4) = R(2,2)
B = GC*H2*GC
R(5,5) = EA/HP*(1.0-B/3.0)*EP*EQ
R(5,6) =-EA/HP*(1.0+B/6.0)*EP*EQ
R(6,6) = R(5,5)
RETURN
END

SUBROUTINE JDOVET (GL,GC,HP,RN,EP,EQ,EI,EA,R)
DIMENSION R(6,6)
P = (GL*HP)**4/EQ/EQ
H2 = HP*HP
SZM = EI/H2/HP/840.0*EP*EQ*EQ*EQ
R(1,1) = SZM*( 5040.0*( 1.0+RN)
*              - 24.0*P*(10.0+RN*3.0) )
R(1,2) = SZM*( 1680.0*(2.0+RN)
*              -  2.0*P*(15.0+RN*7.0) )*HP
R(1,3) =-SZM*( 5040.0*( 1.0+RN)
*              + 54.0*P*( 1.0+RN) )
R(1,4) = SZM*( 1680.0*( 1.0+RN*2.0)
*              +  2.0*P*( 7.0+RN*6.0) )*HP
R(2,2) = SZM*(  840.0*( 3.0+RN)
*              -       P*(5.0+RN*3.0) )*H2
R(2,3) =-SZM*( 1680.0*( 2.0+RN)
*              +  2.0*P*( 6.0+RN*7.0) )*HP
R(2,4) = SZM*(  840.0*( 1.0+RN)
*              +  3.0*P*( 1.0+RN) )*H2
```

```
      R(3,4) =-SZM*( 1680.0*(1.0+RN*2.0)
     *                    -    2.0*P*( 7.0+RN*15.0) )*HP
      R(4,4) = SZM*(  840.0*( 1.0+RN*3.0)
     *                    -          P*( 3.0+RN*5.0) )*H2
      SZM = EA/HP/12.0*EP*EQ
      B   = GC*H2*GC
      R(5,5) = SZM*(6.0*(RN+1.0)-B*(3.0+RN))
      R(5,6) =-SZM*(6.0*(RN+1.0)+B*(1.0+RN))
      R(6,6) = SZM*(6.0*(RN+1.0)-B*(1.0+RN*3.0))
      RETURN
      END

      SUBROUTINE JWEDGE (GL,GC,HP,RM,EP,EQ,EI,EA,R)
      DIMENSION R(6,6)
      HP2=HP*HP
      P = (GL*HP)**4/EQ/EQ
      R(1,1) = (504.0*(7.0*RM**3+3.0*RM**2+3.0*RM+7.0)
     1   -24.0*(3.0*RM+10.0)*P)
      R(1,2) = (504.0*(2.0*RM**3+RM**2+2.0*RM+5.0)
     1   -2.0*(7.0*RM+15.0)*P)*HP
      R(1,3) = (-504.0*(7.0*RM**3+3.0*RM**2+3.0*RM+7.0)
     1   -54.0*(RM+1.0)*P)
      R(1,4) = (504.0*(5.0*RM**3+2.0*RM**2+RM+2.0)
     1   +2.0*(6.0*RM+7.0)*P)*HP
      R(2,2) = (168.0*(2.0*RM**3+2.0*RM**2+5.0*RM+11.0)
     1   -(3.0*RM+5.0)*P)*HP2
      R(2,3) = (-504.0*(2.0*RM**3+RM**2+2.0*RM+5.0)
     1   -2.0*(7.0*RM+6.0)*P)*HP
      R(2,4) = (168.0*(4.0*RM**3+RM**2+RM+4.0)
     1   +3.0*(RM+1.0)*P)*HP2
      R(3,3) = (504.0*(7.0*RM**3+3.0*RM**2+3.0*RM+7.0)
     1   -24.0*(10.0*RM+3.0)*P)
      R(3,4) = (-504.0*(5.0*RM**3+2.0*RM**2+RM+2.0)
     1   +2.0*(15.0*RM+7.0)*P)*HP
      R(4,4) = (168.0*(11.0*RM**3+5.0*RM**2+2.0*RM+2.0)
     1   -(5.0*RM+3.0)*P)*HP2
      DO 31 II=1,4
      DO 31 JJ=II,4
   31 R(II,JJ)=R(II,JJ)/840.0*EI*EP*EQ*EQ*EQ/HP2/HP
      SRM=EA*EQ/HP*EP
      B = GC*HP2*GC
      R(5,5)=((RM+1.0)/2.0-(RM+3.0)/12.0*B)*SRM
      R(5,6)=(-(RM+1.0)/2.0-(RM+1.0)/12.0*B)*SRM
      R(6,6)=((RM+1.0)/2.0-(RM*3.0+1.0)/12.0*B)*SRM
      RETURN
      END

      SUBROUTINE JDOUBL (GL,GC,HP,RM,RN,EP,EQ,EI,EA,R)
```

(JDOUBL) Statement No.

```
      H3=HP*H2
      ZJB  = GL*HP*GL*GL*H3*GL
      RMN  = RM*RN
      RM2  = RM*RM
      RM3  = RM*RM2
      RM2N = RN*RM2
      RM3N = RN*RM3
      ZJJ = EI/H3*EP*EQ/35.0
      ZJA = ZJJ*EQ*EQ
      ZJB = ZJJ/72.0*ZJB
      R(1,1) = 132.0*RM3N + 15.0*RM3 + 45.0*RM2N + 18.0*RM2
     *        + 18.0*RMN  + 45.0*RM  + 15.0*RN   + 132.0
      R(1,2) =  38.0*RM3N +  4.0*RM3 + 12.0*RM2N +  9.0*RM2
     *        +  9.0*RMN  + 33.0*RM  + 11.0*RN   + 94.0
      R(1,4) =  94.0*RM3N + 11.0*RM3 + 33.0*RM2N +  9.0*RM2
     *        +  9.0*RMN  + 12.0*RM  +  4.0*RN   + 38.0
      R(2,2) =  12.0*RM3N +  2.0*RM3 +  6.0*RM2N +  8.0*RM2
     *        +  8.0*RMN  + 27.0*RM  +  9.0*RN   + 68.0
      R(2,4) =  26.0*RM3N +  2.0*RM3 +  6.0*RM2N +      RM2
     *        +      RMN  +  6.0*RM  +  2.0*RN   + 26.0
      R(4,4) =  68.0*RM3N +  9.0*RM3 + 27.0*RM2N +  8.0*RM2
     *        +  8.0*RMN  +  6.0*RM  +  2.0*RN   + 12.0
      R(1,3) = -R(1,1)
      R(2,3) = -R(1,2)
      R(3,4) = -R(1,4)
      R(3,3) =  R(1,1)
      RR=RM+RN
      R(1,1)= R(1,1)*ZJA - ZJB*( 76.0*RMN +140.0*RR +580.0)
      R(1,2)=(R(1,2)*ZJA - ZJB*( 17.0*RMN + 25.0*RR + 65.0))*HP
      R(1,3)= R(1,3)*ZJA - ZJB*( 92.0*RMN +70.0*RR + 92.0)
      R(1,4)=(R(1,4)*ZJA + ZJB*( 19.0*RMN + 17.0*RR + 25.0))*HP
      R(2,2)=(R(2,2)*ZJA - ZJB*(  4.0*RMN +  5.0*RR + 10.0))*H2
      R(2,3)=(R(2,3)*ZJA - ZJB*( 25.0*RMN + 17.0*RR + 19.0))*HP
      R(2,4)=(R(2,4)*ZJA + ZJB*(  5.0*RMN +  4.0*RR +  5.0))*H2
      R(3,3)= R(3,3)*ZJA - ZJB*(580.0*RMN +140.0*RR + 76.0)
      R(3,4)=(R(3,4)*ZJA + ZJB*( 65.0*RMN + 25.0*RR + 17.0))*HP
      R(4,4)=(R(4,4)*ZJA - ZJB*( 10.0*RMN +  5.0*RR +  4.0))*H2
      ZJJ = EA/HP*EP*EQ/60.0
      ZJA = 10.0*(2.0*RMN+RR+2.0)
      ZJB = GC*GC*H2
      R(5,5) = ZJJ*( ZJA - ZJB*(2.0*RMN+3.0*RR+12.0) )
      R(5,6) = ZJJ*(-ZJA - ZJB*(3.0*RMN+2.0*RR+ 3.0) )
      R(6,6) = ZJJ*( ZJA - ZJB*(12.0*RMN+3.0*RR+2.0) )
      RETURN
      END

      FINISH
```

Appendix E2 (c) Library:JEXACT

(JPRISM) Statement No. (JDOVET)

```
      SEGMENTS (JLXACT)
      COMPRESS INTEGER AND LOGICAL
      COMPACT PROGRAM
      TRACE 0
      END

      SUBROUTINE JPRISM (GL,GC,HP,EP,LQ,EI,EA,CDET,R)
      EXTERNAL CDETT
      DOUBLE PRECISION CDETT,DDETT
      DIMENSION R(6,6)
      H2=GL*GL
      GA=GL*HP
      GB=GC*HP
      S  = SIN(GA)
      C  = COS(GA)
      SH = SINH(GA)
      CH = COSH(GA)
      DDETT=CDETT(GA)
      CDET=SNGL(DDETT)
      SZM=EI*GL/CDET*EP*EQ*EQ*EQ
      R(1,1)= SZM*H2*(S*CH+C*SH)
      R(1,2)= SZM*GL*S*SH
      R(1,3)=-SZM*H2*(S+SH)
      R(1,4)=-SZM*GL*(C-CH)
      R(2,2)= SZM    *(S*CH-C*SH)
      R(2,3)=-R(1,4)
      R(2,4)=-SZM    *(S-SH)
      R(3,3)= R(1,1)
      R(3,4)=-R(1,2)
      R(4,4)= R(2,2)
      R(5,6)=-EA*GC/SIN(GB)*EP*EQ
      R(5,5)=-R(5,6)*COS(GB)
      R(6,6)= R(5,5)
      RETURN
      END

      SUBROUTINE JDOVET (GL,GC,HP,RN,EP,EQ,EI,EA,CDET,R)
      EXTERNAL CDETT
      DOUBLE PRECISION CDETT,DDETT
      DIMENSION R(6,6)
      GA=GL*HP
      GB=GC*HP
      RS=RN-1.0
      GL2 = GL*GL
      S   = SIN (GA)
      C   = COS (GA)
      SH  = SINH(GA)
      CH  = COSH(GA)
```

```
      CDET=SNGL(DDETT)
      SCH = S*CH
      CSH = C*SH
      AS = SCH+CSH
      BS = CDET+SSH
      CS = CDET-SSH
      DS = SCH-CSH
      ES = S+SH
      FS = C-CH
      GS = S-SH
      AC = RS*CDET -GA*(RN*DS)
      BC =-RS*CSH  + GA*(RS-RN*BS)
      CC = RS*SCH  - GA*(RS-RN*CS)
      DC = RS*SSH  - GA*RN*AS
      ZJ = EI/HP/4.0/CDET/CDET*EP*EQ*EQ*EQ
      R(1,1)=(-2.0*( AS*(AS*AC+CS*BC) - BS*(AS*CC+CS*DC) ))*GL2*ZJ
      R(1,2)=(AS*DS+CS*CS)*BC +(AS*DS+BS*BS)*CC -(BS-CS)*(AS*AC+DS*DC)
      R(1,2)=R(1,2)*GL*ZJ
      R(1,3)=( 2.0*AS*ES*AC + (CS*ES+AS*FS)*BC
     *          + (AS*FS-BS*ES)*CC - FS*(BS-CS)*DC )*GL2*ZJ
      R(1,4)=( 2.0*AS*FS*AC - (AS*GS-CS*FS)*BC
     *          - (AS*GS+BS*FS)*CC + GS*(BS-CS)*DC )*GL*ZJ
      R(2,2)=( 2.0*( CS*(BS*AC-DS*BC) + DS*(BS*CC-DS*DC) ) )*ZJ
      R(2,3)=( ES*(BS-CS)*AC - (CS*FS+DS*ES)*BC
     *        + (BS*FS-DS*ES)*CC - 2.0*DS*FS*DC )*GL*ZJ
      R(2,4)=( FS*(BS-CS)*AC + (CS*GS-DS*FS)*BC
     *        - (BS*GS+DS*FS)*CC + 2.0*DS*GS*DC )*ZJ
      R(3,3)=(-2.0*(ES*ES*AC + ES*FS*(BC+CC) + FS*FS*DC ))*GL2*ZJ
      R(3,4)=-ES*FS*AC*2.0 + (ES*GS-FS*FS)*(BC+CC) + 2.0*FS*GS*DC
      R(3,4)=R(3,4)*GL*ZJ
      R(4,4)=(-2.0*(FS*FS*AC - FS*GS*(BC+CC) + GS*GS*DC ))*ZJ
      S   = SIN(GB)
      C   = COS(GB)
      ZJ=EA*EP/HP*EQ
      R(5,5)= ZJ*(GB*C/S+RS/2.0)
      R(5,6)=-ZJ*(RN+1.0)/S*GB/2.0
      R(6,6)= ZJ*(GB*C/S*RN-RS/2.0)
      RETURN
      END

      SUBROUTINE JWEDGE (GL,GC,HP,RM,EP,EQ,EI,EA,CDET,RE)
      EXTERNAL CDETT
      DOUBLE PRECISION CDETT,DDETT,TZM
      DIMENSION RB(6,6),Q(4,4,4),T(4,4),PX(4),CC(4,4)
      P=GL*HP
      P2=P*P
      P3=P*P2
      P4=P*P3
```

(JWEDGE) Statement No. (JWEDGE)

```
      H3=H1*H2
      H4=H1*H3
      S=SIN(P)
      C=COS(P)
      SC=S*C
      SH=SINH(P)
      CH=COSH(P)
      SHCH=SH*CH
      SCH=S*CH
      CSH=C*SH
      SSH=S*SH
      CCH=C*CH
      S2=S**2
      SH2=SH**2
      DDETT=CDETT(P)
      CDET = SNGL(DDETT)
      HSC1=SCH-CSH
      HSC2=SCH+CSH
      HSC3=SSH-CCH
      HSC4=SSH+CCH
      Q(1,1,1)=(P-SC)/2.0/H1
      Q(1,1,2)=(P2-2.0*P*SC+S2)/4.0/H2
      Q(1,1,3)=(2.0*P3-6.0*P2*SC+6.0*P*S2-3.0*P+3.0*SC)/12.0/H3
      Q(1,1,4)=(2.0*P4-8.0*P3*SC+12.0*P2*S2-6.0*P2+12.0*P*SC
     1       -6.0*S2)/16.0/H4
      Q(1,2,1)=S2/2.0/H1
      Q(1,2,2)=(2.0*P*S2-P+SC)/4.0/H2
      Q(1,2,3)=(4.0*P2*S2-2.0*P2+4.0*P*SC-2.0*S2)/8.0/H3
      Q(1,2,4)=(4.0*P3*S2-2.0*P3+6.0*P2*SC-6.0*P*S2
     1       +3.0*P-3.0*SC)/8.0/H4
      Q(1,3,1)=(HSC1)/2.0/H1
      Q(1,3,2)=((HSC1)*P-CDET)/2.0/H2
      Q(1,3,3)=((HSC1)*P2+2.0*P*CCH-(HSC2))/2.0/H3
      Q(1,3,4)=((HSC1)*P3+3.0*P2*CCH-3.0*P*(HSC2)
     1       +3.0*SSH)/2.0/H4
      Q(1,4,1)=(HSC3+1.0)/2.0/H1
      Q(1,4,2)=((HSC3)*P+CSH)/2.0/H2
      Q(1,4,3)=((HSC3)*P2+2.0*P*CSH-(HSC4)+1.0)/2.0/H3
      Q(1,4,4)=((HSC3)*P3+3.0*P2*CSH-3.0*P*(HSC4)
     1       +3.0*SCH)/2.0/H4
      Q(2,2,1)=(P+SC)/2.0/H1
      Q(2,2,2)=(2.0*P2+4.0*P *SC-2.0*S2)/8.0/H2
      Q(2,2,3)=(2.0*P3+6.0*P2*SC-6.0*S2*P +3.0*P-3.0*SC)/12.0/H3
      Q(2,2,4)=(2.0*P4+8.0*P3*SC-12.0*S2*P2
     1       +6.0*P2-12.0*P*SC+6.0*S2)/16.0/H4
      Q(2,3,1)=((HSC4)-1.0)/2.0/H1
      Q(2,3,2)=((HSC4)*P -SCH)/2.0/H2
      Q(2,3,3)=((HSC4)*P2-SCH*P *2.0+(HSC3)+1.0)/2.0/H3
```

```
      Q(2,4,1)=((HSC2))/2.0/H1
      Q(2,4,2)=((HSC2)*P -SSH)/2.0/H2
      Q(2,4,3)=((HSC2)*P2-SSH*P *2.0+(HSC1))/2.0/H3
      Q(2,4,4)=((HSC2)*P3-SSH*P2*3.0+(HSC1)*P*3.0
     1       -3.0*CDET)/2.0/H4
      Q(3,3,1)=(-P        +SHCH)/2.0/H1
      Q(3,3,2)=(-P2       +SHCH*P *2.0-SH2)/4.0/H2
      Q(3,3,3)=(-P3*2.0+SHCH*P2*6.0-SH2*P *6.0-3.0*(P-SHCH))/12.0/H3
      Q(3,3,4)=(-P4       +SHCH*P3*4.0-SH2*P2*6.0-3.0*P2
     1       +6.0*P*SHCH-3.0*SH2)/8.0/H4
      Q(3,4,1)=(SH2)/2.0/H1
      Q(3,4,2)=(SH2*P *2.0+P        -SHCH)/4.0/H2
      Q(3,4,3)=(SH2*P2*4.0+P2*2.0-SHCH*P *4.0 +SH2*2.0)/8.0/H3
      Q(3,4,4)=(SH2*P3*8.0+P3*4.0-SHCH*P2*12.0+SH2*P*12.0
     1       +6.0*P-6.0*SHCH)/16.0/H4
      Q(4,4,1)=(P         +SHCH)/2.0/H1
      Q(4,4,2)=(P2        +SHCH*P *2.0-SH2)/4.0/H2
      Q(4,4,3)=(P3*2.0+SHCH*P2*6.0-SH2*P *6.0-3.0*(P-SHCH))/12.0/H3
      Q(4,4,4)=(P4        +SHCH*P3*4.0-SH2*P2*6.0-3.0*P2
     1       +6.0*P*SHCH-3.0*SH2)/8.0/H4
      Z1 = HP
      Z2 = HP*Z1
      Z3 = HP*Z2
      RR = RM -1.0
      EQ2=1.0
      PX(4)=RR*RR*RR*EQ2
      PX(3)=3.0*Z1*RR*RR*EQ2
      PX(2)=Z2*RR*(3.0*EQ2-1.0)
      PX(1)=Z3*(EQ2-1.0)
      DO 63 I=1,4
      DO 63 J=I,4
   63 T(I,J)=0.0
      DO 61 I=1,2
      DO 61 J=I,2
      DO 61 K=1,4
      T(I  ,J  ) = T(I  ,J  ) + Q(I  ,J  ,K)*PX(K)
   61 T(I+2,J+2) = T(I+2,J+2) + Q(I+2,J+2,K)*PX(K)
      PX(1)=-PX(1)-2.0*Z3
      PX(2)=-PX(2)-2.0*Z2*RR
      PX(3)=-PX(3)
      PX(4)=-PX(4)
      DO 62 I=1,2
      DO 62 J=3,4
      DO 62 K=1,4
   62 T(I,J) = T(I,J) + Q(I,J,K)*PX(K)
      DO 65 I=1,3
      DO 65 J=I+1,4
   65 T(J,I) = T(I,J)
```

(JDOUBL) Statment No. (JDOUBL)

```
      CC(3,1)=-CC(1,1)
      CC(4,1)=(1.0-HSC4)
      CC(1,2)=CC(4,1)/H1
      CC(2,2)=HSC1/H1
      CC(3,2)=CC(2,1)/H1
      CC(4,2)=-CC(2,2)
      CC(1,3)=(S+SH)
      CC(2,3)=(COS(P)-CH)
      CC(3,3)=-CC(1,3)
      CC(4,3)=-CC(2,3)
      CC(1,4)=CC(2,3)/H1
      CC(2,4)=-(S-SH)/H1
      CC(3,4)=-CC(1,4)
      CC(4,4)=-CC(2,4)
      TZM=EI*EG*EQ*EQ*H4/Z3/DDETT/DDETT/4.0*EP
      DO 66 I=1,4
      DO 66 J=I,4
      RB(I,J) = 0.0
      DO 66 K=1,4
      RB(I,J) = RB(I,J) + CC(K,I) * ( CC(1,J)*T(K,1)
     *                            +    CC(2,J)*T(K,2)
     *                            +    CC(3,J)*T(K,3)
     *                            +    CC(4,J)*T(K,4) )
   66 CONTINUE
      DO 67 I=1,4
      DO 67 J=I,4
   67 RB(I,J)=RB(I,J)*TZM
      GB = GC*Z1
      S  = SIN(GB)
      C  = COS(GB)
      SZM=EA*EG/Z1*EP
      RB(5,5)= SZM*(GB*C/S+RR/2.0)
      RB(5,6)=-SZM*(RM+1.0)/S*GB/2.0
      RB(6,6)= SZM*(GB*C/S*RM-RR/2.0)
      RETURN
      END

      SUBROUTINE JDOUBL (GL,GC,HP,RM,RN,EP,EQ,EI,EA,CDET,RB)
      EXTERNAL CDETT
      DOUBLE PRECISION CDETT,DDETT,TZM
      DIMENSION RB(6,6),Q(4,4,5),T(4,4),PX(5),CC(4,4)
      P=GL*HP
      P2=P*P
      P3=P*P2
      P4=P*P3
      P5=P*P4
      H1=GL
      H2=H1*H1
      H5=H1*H4
      S=SIN(P)
      C=COS(P)
      SC=S*C
      SH=SINH(P)
      CH=COSH(P)
      SHCH=SH*CH
      SCH=S*CH
      CSH=C*SH
      SSH=S*SH
      CCH=C*CH
      S2=S**2
      SH2=SH**2
      DDETT=CDETT(P)
      CDET = SNGL(DDETT)
      HSC1=SCH-CSH
      HSC2=SCH+CSH
      HSC3=SSH-CCH
      HSC4=SSH+CCH
      Q(1,1,1)=(P-SC)/2.0/H1
      Q(1,1,2)=(P2-2.0*P*SC+S2)/4.0/H2
      Q(1,1,3)=(2.0*P3-6.0*P2*SC+6.0*P*S2-3.0*P+3.0*SC)/12.0/H3
      Q(1,1,4)=(2.0*P4-8.0*P3*SC+12.0*P2*S2-6.0*P2+12.0*P*SC
     1          -6.0*S2)/16.0/H4
      Q(1,1,5)=(4.0*P5 - 20.0*P4*SC + 40.0*P3*S2 - 20.0*P3
     #                 + 60.0*P2*SC - 60.0*P *S2 + 30.0*P
     #                 -30.0*SC   )/40.0/H5
      Q(1,2,1)=S2/2.0/H1
      Q(1,2,2)=(2.0*P*S2-P+SC)/4.0/H2
      Q(1,2,3)=(4.0*P2*S2-2.0*P2+4.0*P*SC-2.0*S2)/8.0/H3
      Q(1,2,4)=(4.0*P3*S2-2.0*P3+6.0*P2*SC-6.0*P*S2
     1          +3.0*P-3.0*SC)/8.0/H4
      Q(1,2,5)=( 20.0*P4*S2 - 10.0*P4 + 40.0*P3*SC
     #          - 60.0*P2*S2 + 30.0*P2 - 60.0*P *SC
     #          + 30.0*S2     )/40.0/H5
      Q(1,3,1)=(SCH-CSH)/2.0/H1
      Q(1,3,2)=((SCH-CSH)*P+CCH-1.0)/2.0/H2
      Q(1,3,3)=((SCH-CSH)*P2+2.0*P*CCH-(SCH+CSH))/2.0/H3
      Q(1,3,4)=((SCH-CSH)*P3+3.0*P2*CCH-3.0*P*(SCH+CSH)
     1          +3.0*SSH)/2.0/H4
      Q(1,3,5)=( 20.0*P4*(SCH-CSH) + 80.0*P3*CCH - 120.0*P2*(SCH+CSH)
     #          + 240.0*P *SSH       - 120.0*(SCH-CSH) )/40.0/H5
      Q(1,4,1)=(SSH-CCH+1.0)/2.0/H1
      Q(1,4,2)=((SSH-CCH)*P+CSH)/2.0/H2
      Q(1,4,3)=((SSH-CCH)*P2+2.0*P*CSH-(SSH+CCH)+1.0)/2.0/H3
      Q(1,4,4)=((SSH-CCH)*P3+3.0*P2*CSH-3.0*P*(SSH+CCH)
     1          +3.0*SCH)/2.0/H4
      Q(1,4,5)=( 20.0*P4*(SSH-CCH) + 80.0*P3*CSH - 120.0*P2*(SSH+CCH)
```

(JDOUBL) Statement No. (JDOUBL)

```
      Q(2,2,2)=(2.0*P2+4.0*P *SC-2.0*S2)/8.0/H2
      Q(2,2,3)=(2.0*P3+6.0*P2*SC-6.0*S2*P +3.0*P-3.0*SC)/12.0/H3
      Q(2,2,4)=(2.0*P4+8.0*P3*SC-12.0*S2*P2
     1         +6.0*P2-12.0*P*SC+6.0*S2)/16.0/H4
      Q(2,2,5)=( 4.0*P5 + 20.0*P4*SC - 40.0*P3*S2
     #         +20.0*P3 - 60.0*P2*SC + 60.0*P *S2
     #         -30.0*P  + 30.0*SC  )/40.0/H5
      Q(2,3,1)=((SSH+CCH)-1.0)/2.0/H1
      Q(2,3,2)=((SSH+CCH)*P -SCH)/2.0/H2
      Q(2,3,3)=((SSH+CCH)*P2-SCH*P *2.0+(SSH-CCH)+1.0)/2.0/H3
      Q(2,3,4)=((SSH+CCH)*P3-SCH*P2*3.0+(SSH-CCH)*P*3.0
     1         +3.0*CSH)/2.0/H4
      Q(2,3,5)=( 20.0*P4*(SSH+CCH) - 60.0*P3*SCH + 120.0*P2*(SSH-CCH)
     #         + 240.0*P *CSH - 120.0*(SSH+CCH-1)  )/40.0/H5
      Q(2,4,1)=((SCH+CSH))/2.0/H1
      Q(2,4,2)=((SCH+CSH)*P -SSH)/2.0/H2
      Q(2,4,3)=((SCH+CSH)*P2-SSH*P *2.0+(SCH-CSH))/2.0/H3
      Q(2,4,4)=((SCH+CSH)*P3-SSH*P2*3.0+(SCH-CSH)*P*3.0
     1         -3.0*(1.0-CCH))/2.0/H4
      Q(2,4,5)=( 20.0*P4*(SCH+CSH) - 80.0*P3*SSH + 120.0*P2*(SCH-CSH)
     #         + 240.0*P *CCH - 120.0*(SCH+CSH)  )/40.0/H5
      Q(3,3,1)=(-P       +SHCH)/2.0/H1
      Q(3,3,2)=(-P2      +SHCH*P *2.0-SH2)/4.0/H2
      Q(3,3,3)=(-P3*2.0+SHCH*P2*6.0-SH2*P *6.0-3.0*(P-SHCH))/12.0/H3
      Q(3,3,4)=(-P4      +SHCH*P3*4.0-SH2*P2*6.0-3.0*P2
     1         +6.0*P*SHCH-3.0*SH2)/8.0/H4
      Q(3,3,5)=( - 4.0*P5 + 20.0*P4*SHCH - 40.0*P3*SH2 - 20.0*P3
     #                   + 60.0*P2*SHCH - 60.0*P *SH2 - 30.0*P
     #                   + 30.0*SHCH   )/40.0/H5
      Q(3,4,1)=(SH2)/2.0/H1
      Q(3,4,2)=(SH2*P *2.0+P       -SHCH)/4.0/H2
      Q(3,4,3)=(SH2*P2*4.0+P2*2.0-SHCH*P *4.0 +SH2*2.0)/8.0/H3
      Q(3,4,4)=(SH2*P3*8.0+P3*4.0-SHCH*P2*12.0+SH2*P*12.0
     1         +6.0*P-6.0*SHCH)/16.0/H4
      Q(3,4,5)=( 20.0*P4*SH2 + 10.0*P4 - 40.0*P3*SHCH + 60.0*P2*SH2
     #                      + 30.0*P2 - 60.0*P *SHCH
     #                      + 30.0*SH2 )/40.0/H5
      Q(4,4,1)=(P       +SHCH)/2.0/H1
      Q(4,4,2)=(P2      +SHCH*P *2.0-SH2)/4.0/H2
      Q(4,4,3)=(P3*2.0+SHCH*P2*6.0-SH2*P *6.0-3.0*(P-SHCH))/12.0/H3
      Q(4,4,4)=(P4      +SHCH*P3*4.0-SH2*P2*6.0-3.0*P2
     1         +6.0*P*SHCH-3.0*SH2)/8.0/H4
      Q(4,4,5)=( 4.0*P5 + 20.0*P4*SHCH - 40.0*P3*SH2 - 20.0*P3
     #                  + 60.0*P2*SHCH - 60.0*P *SH2 - 30.0*P
     #                  + 30.0*SHCH    )/40.0/H5
      Z1 = HP
      Z2 = HP*Z1
      Z3 = HP*Z2
```

```
      RS = RN -1.0
      EQ2=1.0
      PX(5)=EQ2*RR*RR*RR*RS
      PX(4)=EQ2*Z1*RR*RR*(RR+3.0*RS)
      PX(3)=Z2*RR*(3.0*EQ2*(RR+RS) - RS)
      PX(2)=Z3*(EQ2*(3.0*RR+RS) - (RR+RS))
      PX(1)=Z4*(EQ2 - 1.0)
      DO 63 I=1,4
      DO 63 J=1,4
   63 T(I,J)=0.0
      DO 61 I=1,2
      DO 61 J=1,2
      DO 61 K=1,5
      T(I  ,J  ) = T(I  ,J  ) + Q(I  ,J  ,K)*PX(K)
   61 T(I+2,J+2) = T(I+2,J+2) + Q(I+2,J+2,K)*PX(K)
      PX(1)=-PX(1)-2.0*Z4
      PX(2)=-PX(2)-2.0*Z3*(RR+RS)
      PX(3)=-PX(3)-2.0*Z2*RR*RS
      PX(4)=-PX(4)
      PX(5)=-PX(5)
      DO 62 I=1,2
      DO 62 J=3,4
      DO 62 K=1,5
   62 T(I,J) = T(I,J) + Q(I,J,K)*PX(K)
      DO 65 I=1,3
      DO 65 J=I+1,4
   65 T(J,I) = T(I,J)
      CC(1,1)=-(SCH+CSH)
      CC(2,1)=(1.0+SSH-CCH)
      CC(3,1)=-CC(1,1)
      CC(4,1)=(1.0-SSH-CCH)
      CC(1,2)=CC(4,1)/H1
      CC(2,2)=(SCH-CSH)/H1
      CC(3,2)=CC(2,1)/H1
      CC(4,2)=-CC(2,2)
      CC(1,3)=(S+SH)
      CC(2,3)=(COS(P)-CH)
      CC(3,3)=-CC(1,3)
      CC(4,3)=-CC(2,3)
      CC(1,4)=CC(2,3)/H1
      CC(2,4)=-(S-SH)/H1
      CC(3,4)=-CC(1,4)
      CC(4,4)=-CC(2,4)
      TZM=EI*EQ*EQ*EQ*H4/Z4/DDETT/DDETT/4.0*EP
      DO 66 I=1,4
      DO 66 J=I,4
      RB(I,J) = 0.0
      DO 66 K=1,4
```

(JDOUBL) Statement No.

```
 *                          +   CC(3,J)*T(K,3)
 *                          +   CC(4,J)*T(K,4) )
66 CONTINUE
   DO 67 I=1,4
   DO 67 J=1,4
67 RB(I,J)=RB(I,J)*TZM
   GB = GC*Z1
   S  = SIN(GB)
   C  = COS(GB)
   SZM = EA*EP*EQ/Z1/GB/S/S/2.0
   RMN = RR*RS* (GB-S*C)
   RB(5,5)=SZM*( RMN + 2.0*GB*GB*S*C + (RM+RN-2.0)*GB*S*S )
   RB(5,6)=SZM*(-RMN - (RM*RN+1.0)*GB*GB*S )
   RB(6,6)=SZM*( RMN + 2.0*GB*GB*S*C*RM*RN
  #               - (2.0*RM*RN-RM-RN)*GB*S*S )
   RETURN
   END

   FUNCTION CDETT (GA)
   DOUBLE PRECISION GAA,G2,W,U2,U1,CDETT
   NTT=6+INT(0.8*GA)
   GAA=DBLE(GA)
   G2=GAA*GAA
   W=4.0*G2*G2
   U2=1.0
   NT4=4*NTT+4
   DO 32 J=1,NTT
   U1=1.0
   DO 31 I=NT4-3,NT4
31 U1=U1*FLOAT(I)
   U2=1.0-U2/U1*W
   NT4=NT4-4
32 CONTINUE
   CDETT=W*U2/24.0
   RETURN
   END

   FINISH
```

(TRIRECT) Statement No. (TRIRECT)

```
      SEGMENTS (JSNGL)
      COMPRESS INTEGER AND LOGICAL
      COMPACT PROGRAM
      TRACE 0
      END

      SUBROUTINE TRIRECT (MYY,MZZ,LOCAT,LR,X,R,DS,DC,L1,L2)
      DIMENSION LOCAT(MYY),LR(MYY,3),X(MZZ,MZZ),AKA(6,6),R(6,6)
      AKA(1,1) = DS*DS*R(1,1) + DC*DC*R(5,5)
      AKA(1,2) = DS*DC*(R(5,5)-R(1,1))
      AKA(1,3) =-DS*R(1,2)
      AKA(1,4) = DS*DS*R(1,3)+DC*DC*R(5,6)
      AKA(1,5) = DS*DC*(R(5,6)-R(1,3))
      AKA(1,6) =-DS*R(1,4)
      AKA(2,2) = DS*DS*R(5,5)+DC*DC*R(1,1)
      AKA(2,3) = DC*R(1,2)
      AKA(2,4) = DS*DC*(R(5,6)-R(1,3))
      AKA(2,5) = DS*DS*R(5,6)+DC*DC*R(1,3)
      AKA(2,6) = DC*R(1,4)
      AKA(3,3) = R(2,2)
      AKA(3,4) =-DS*R(2,3)
      AKA(3,5) = DC*R(2,3)
      AKA(3,6) = R(2,4)
      AKA(4,4) = DS*DS*R(3,3)+DC*DC*R(6,6)
      AKA(4,5) = DS*DC*(R(6,6)-R(3,3))
      AKA(4,6) =-DS*R(3,4)
      AKA(5,5) = DS*DS*R(6,6)+DC*DC*R(3,3)
      AKA(5,6) = DC*R(3,4)
      AKA(6,6) = R(4,4)

      LC=LOCAT(L1)
      IF(LR(L1,1).NE.0)GOTO 141
151   IF(LR(L1,2).NE.0)GOTO 142
152   IF(LR(L1,3).NE.0)GOTO 143
      GOTO 301
141   X(LC,LC)=X(LC,LC)+AKA(1,1)
      LC=LC+1
      GOTO 151
142   IF(LR(L1,1).NE.0)X(LC-1,LC)=X(LC-1,LC)+AKA(1,2)
      X(LC,LC)=X(LC,LC)+AKA(2,2)
      LC=LC+1
      GOTO 152
143   IF(LR(L1,1).NE.0.AND.LR(L1,2).NE.0)
     *                 X(LC-2,LC)=X(LC-2,LC)+AKA(1,3)
      IF(LR(L1,1).NE.0.AND.LR(L1,2).EQ.0)
     *                 X(LC-1,LC)=X(LC-1,LC)+AKA(1,3)
      IF(LR(L1,2).NE.0)X(LC-1,LC)=X(LC-1,LC)+AKA(2,3)
      X(LC,LC)=X(LC,LC)+AKA(3,3)
```

```
      IF(LR(L2,1).NE.0)GOTO 241
251   IF(LR(L2,2).NE.0)GOTO 242
252   IF(LR(L2,3).NE.0)GOTO 243
      GOTO 302
241   X(LC,LC)=X(LC,LC)+AKA(4,4)
      LC=LC+1
      GOTO 251
242   IF(LR(L2,1).NE.0)X(LC-1,LC)=X(LC-1,LC)+AKA(4,5)
      X(LC,LC)=X(LC,LC)+AKA(5,5)
      LC=LC+1
      GOTO 252
243   IF(LR(L2,1).NE.0.AND.LR(L2,2).NE.0)
     *                 X(LC-2,LC)=X(LC-2,LC)+AKA(4,6)
      IF(LR(L2,1).NE.0.AND.LR(L2,2).EQ.0)
     *               . X(LC-1,LC)=X(LC-1,LC)+AKA(4,6)
      IF(LR(L2,2).NE.0)X(LC-1,LC)=X(LC-1,LC)+AKA(5,6)
      X(LC,LC)=X(LC,LC)+AKA(6,6)

302   LC1=LOCAT(L1)
      IF(LR(L1,1).NE.0.AND.LR(L2,1).NE.0)GOTO 41
51    IF(LR(L1,1).NE.0.AND.LR(L2,2).NE.0)GOTO 42
52    IF(LR(L1,1).NE.0.AND.LR(L2,3).NE.0)GOTO 43
53    IF(LR(L1,1).NE.1)LC=0
      IF(LR(L1,1).EQ.1)LC=1
      LC1=LOCAT(L1)+LC
      IF(LR(L1,2).NE.0.AND.LR(L2,1).NE.0)GOTO 44
54    IF(LR(L1,2).NE.0.AND.LR(L2,2).NE.0)GOTO 45
55    IF(LR(L1,2).NE.0.AND.LR(L2,3).NE.0)GOTO 46
56    IF(LR(L1,1).NE.1.AND.LR(L1,2).NE.1)LC=0
      IF(LR(L1,1).NE.1.AND.LR(L1,2).EQ.1)LC=1
      IF(LR(L1,1).EQ.1.AND.LR(L1,2).NE.1)LC=1
      IF(LR(L1,1).EQ.1.AND.LR(L1,2).EQ.1)LC=2
      LC1=LOCAT(L1)+LC
      IF(LR(L1,3).NE.0.AND.LR(L2,1).NE.0)GOTO 47
57    IF(LR(L1,3).NE.0.AND.LR(L2,2).NE.0)GOTO 48
58    IF(LR(L1,3).NE.0.AND.LR(L2,3).NE.0)GOTO 49
      RETURN
41    LC2=LOCAT(L2)
      X(LC1,LC2)=X(LC1,LC2)+AKA(1,4)
      GOTO 51
42    IF(LR(L2,1).NE.1)LC=0
      IF(LR(L2,1).EQ.1)LC=1
      LC2=LOCAT(L2)+LC
      X(LC1,LC2)=X(LC1,LC2)+AKA(1,5)
      GOTO 52
43    IF(LR(L2,1).NE.1.AND.LR(L2,2).NE.1)LC=0
      IF(LR(L2,1).NE.1.AND.LR(L2,2).EQ.1)LC=1
      IF(LR(L2,1).EQ.1.AND.LR(L2,2).NE.1)LC=1
```

(TRIRECT) Statement No.

```
      X(LC1,LC2)=X(LC1,LC2)+AKA(1,6)
      GOTO 53
   44 LC2=LOCAT(L2)
      X(LC1,LC2)=X(LC1,LC2)+AKA(2,4)
      GOTO 54
   45 IF(LR(L2,1).NE.1)LC=0
      IF(LR(L2,1).EQ.1)LC=1
      LC2=LOCAT(L2)+LC
      X(LC1,LC2)=X(LC1,LC2)+AKA(2,5)
      GOTO 55
   46 IF(LR(L2,1).NE.1.AND.LR(L2,2).NE.1)LC=0
      IF(LR(L2,1).NE.1.AND.LR(L2,2).EQ.1)LC=1
      IF(LR(L2,1).EQ.1.AND.LR(L2,2).NE.1)LC=1
      IF(LR(L2,1).EQ.1.AND.LR(L2,2).EQ.1)LC=2
      LC2=LOCAT(L2)+LC
      X(LC1,LC2)=X(LC1,LC2)+AKA(2,6)
      GOTO 56
   47 LC2=LOCAT(L2)
      X(LC1,LC2)=X(LC1,LC2)+AKA(3,4)
      GOTO 57
   48 IF(LR(L2,1).NE.1)LC=0
      IF(LR(L2,1).EQ.1)LC=1
      LC2=LOCAT(L2)+LC
      X(LC1,LC2)=X(LC1,LC2)+AKA(3,5)
      GOTO 58
   49 IF(LR(L2,1).NE.1.AND.LR(L2,2).NE.1)LC=0
      IF(LR(L2,1).NE.1.AND.LR(L2,2).EQ.1)LC=1
      IF(LR(L2,1).EQ.1.AND.LR(L2,2).NE.1)LC=1
      IF(LR(L2,1).EQ.1.AND.LR(L2,2).EQ.1)LC=2
      LC2=LOCAT(L2)+LC
      X(LC1,LC2)=X(LC1,LC2)+AKA(3,6)
      RETURN
      END
      FINISH
```

(ASPOLE) Statement No. (ORDER)

```
      SEGMENTS (ASYMPTOTE)
      COMPRESS INTEGER AND LOGICAL
      COMPACT PROGRAM
      TRACE 0
      END

      SUBROUTINE ASYPOLE (HYP,FF,ABCD,NOM,AHYP)
      DIMENSION HYP(NOM),AHYP(20),IHYP(20),CSY(320)
      AHYP(1)=HYP(1)
      IHYP(1)=1
      JASY=1
      IF(NOM.EQ.1)GOTO 538
      DO 531 KASY=2,NOM
      DO 532 IASY=1,JASY
      BHYP = ABS ( HYP(KASY)-AHYP(IASY) )
      IF ( BHYP.LT.1.0E-6 )GOTO 531
  532 CONTINUE
      JASY=JASY+1
      AHYP(JASY)=HYP(KASY)
      IHYP(JASY)=KASY
  531 CONTINUE
  538 MASY=JASY*2*8
      CALL ORDER (JASY,AHYP,MASY,CSY,IHYP,FF,ABCD)
      DO 539 I=1,20
  539 AHYP(I)=CSY(I)
      RETURN
      END

      SUBROUTINE ORDER (JASY,AHYP,MASY,CSY,IHYP,FF,ABCD)
      DIMENSION AHYP(JASY),CSY(MASY),IHYP(JASY),ASY(8),BSY(8)
      ASY(1)= 4.730040745
      ASY(2)= 7.853204624
      ASY(3)=10.995607838
      ASY(4)=14.137165491
      ASY(5)=17.278759658
      ASY(6)=20.420352246
      ASY(7)=23.561944902
      ASY(8)=26.703537556
      DO 530 I=1,8
  530 BSY(I)=ABCD*FLOAT(I)
      WRITE(2,520)
      DO 534 I=1,JASY
      LASY=(I-1)*8
      DO 535 J=1,8
  535 CSY(LASY+J)=ASY(J)/AHYP(I)
  534 WRITE(2,521)I,IHYP(I),AHYP(I),(CSY(K),K=LASY+1,LASY+3)
      DO 536 I=1,JASY
      LASY=(I-1+JASY)*8
      DO 537 J=1,8
  537 CSY(LASY+J)=SQRT( BSY(J)/AHYP(I) )*FF
  536 WRITE(2,521)I,IHYP(I),AHYP(I),(CSY(K),K=LASY+1,LASY+3)
      CALL M01ANF (CSY,1,MASY,IFAIL)
      WRITE(2,522)(CSY(I),I=1,10)
      DO 541 I=2,MASY
      IF( ABS(CSY(I)-CSY(I-1)) . GT. 1.0E-6 ) GOTO543
      DO 542 J=I,MASY-1
  542 CSY(J)=CSY(J+1)
      GOTO 541
  543 MMASY=MMASY+1
      IF(MMASY.EQ.10)GOTO 544
  541 CONTINUE
  544 WRITE(2,522)(CSY(I),I=1,10)
  520 FORMAT(1X,'ASYMPTC PARAMETER :')
  521 FORMAT(21X,2I4,5F10.5)
  522 FORMAT(24X,'ORDER',5F10.5,/29X,5F10.5)
      RETURN
      END

      FINISH
```

Appendix F1 Steering Program: LINEIG

(Stages A & B) Statement No. (Stages C & D)

```
      LIST (LP)
      PROGRAM (LINEIG)
      INPUT 1 = CRO
      OUTPUT 2 = LPO
      COMPRESS INTEGER AND LOGICAL
      COMPACT PROGRAM
      TRACE 0
      END

      MASTER LINEAR
      DIMENSION RK(6,6),RM(6,6),XMI(47,47),XM(47,47),XK(47,47),
     * VK(47),VM(47),ITG(47),XJ(47,47),WSC(47),IP(47),IST(47),
     *         JN(16),XC(16),YC(16),LQ(16),LR(16,3),
     #         LOCAT(16),IPT(16),JPT(16),THI(16),THJ(16),
     ?         HYP(16),ZM(16),CS(16),SN(16),EQU(16),
     %         MEM(16),WII(16),WIJ(16),EPU(16),ZN(16),
     3 NWIPT(16),NWJPT(16),NWIST(16),NWJST(16),NSE(16),
     4 SETH(10,16),SEWI(10,16),NWRT(16),NWLR(10,3)
      MXX=10
      MYY=16
      MZZ = 47
   10 FORMAT(10,2F0.0)
   11 FORMAT(7I0,2F0.0)
   12 FORMAT(F0.0,2I0)
   13 FORMAT(2I0,F0.0)
   20 FORMAT(/1X,'CONTROL PARAMETERS :',3X,'NFN,ITN,IR,JR,NMORE,',
     *         'NOJ,NOM,ZZ,XLIMIT')
   21 FORMAT(20X,7I5,2F10.5)
   22 FORMAT(21X,I4,6X,2F14.5)
   23 FORMAT(/4X,'NFN=',I2,3X,'NFC=',I2,11X,1P4E15.5)
   24 FORMAT(1X ,'SECTION PARAMETERS :',3X,'THU,WIU,YMS,DEN,EI,EA,PA')
   25 FORMAT(21X,1P5E14.5)
   26 FORMAT(I15,I7,I5,I3,1PE15.5)
   27 FORMAT(1X,'OUTPUT  PARAMETERS :')
    2 FORMAT(1X,'PROGRAM PARAMETERS :',3X,'LINEIG,  DATED 300479',/)
        WRITE(2,2)
      PI = 4.0*ATAN(1.0)
   88 READ(1,11)NFN,ITN,IR,JR,NMORE,NOJ,NOM,ZZ,XLIMIT
        WRITE(2,20)
        WRITE(2,21)NFN,ITN,IR,JR,NMORE,NOJ,NOM,ZZ,XLIMIT

      CALL JTMBEQ (MXX,MYY,NOJ,XC,YC,LR,LQ,JN,MSIZE,LOCAT,MEM,NOM,
     1 IPT,JPT,THI,THJ,HYP,ZM,CS,SN,WII,WIJ,ZN,EQU,EPU,THU,WIU,
     2 NWIPT,NWJPT,NWIST,NWJST,NSE,SETH,SEWI,NWRT,NWLR)
      MZ=MSIZE
      READ(1,10)MAT,YMS,DEN
      IF(MAT.NE.0)GOTO 198
      YMS=25.0
      DEN=2400.0
  198 YMS=YMS*1.0E9
```

```
      EA = YMS*WIU*THU
      EI = EA *THU*THU/12.0
      PA = DEN*WIU*THU
        WRITE(2,24)
        WRITE(2,22)MAT,THU,WIU
        WRITE(2,25)YMS,DEN,EI,EA,PA
        WRITE(2,199)MSIZE,MYY,MZZ
  199 FORMAT(24X,'MSIZE',I4,5X,'MYY,MZZ=',2I4,5X,
     *         'CUBIC, NORMAL MODE;   NAT FREQ, MODE SHAPE, RESPONSE')
        WRITE(2,27)

      DO 734 MB=1,NOM
      YM=ZM(MB)
      YN=ZN(MB)
      DC=CS(MB)
      DS=SN(MB)
      L1=IPT(MB)
      L2=JPT(MB)
      EP=EPU(MB)
      HP=HYP(MB)
      EQ=EQU(MB)
  744 CALL KTWCU (HP,YM,YN,EP,EQ,EI,EA,RK)
      CALL MTWCU (HP,YM,YN,EP,EQ,EI,PA,RM)
  740 CALL TRIRECT (MYY,MZZ,LOCAT,LR,XK,RK,DS,DC,L1,L2)
      CALL TRIRECT (MYY,MZZ,LOCAT,LR,XM,RM,DS,DC,L1,L2)
  734 CONTINUE

      DO 32 K=1,MZ-1
      DO 32 L=K+1,MZ
      XK(L,K)=XK(K,L)
   32 XM(L,K)=XM(K,L)
      CALL F01AAF (XK,MZZ,MZ,XMI,MZZ,WSC,IFAIL)
      DO 751 I=1,MZ
      VK(I) = 0.0
      DO 751 J=1,MZ
      XJ(I,J)=0.0
      DO 751 K=1,MZ
  751 XJ(I,J)=XJ(I,J)+XMI(I,K)*XM(K,J)
      DO 752 I=1,MZ
      DO 752 J=1,MZ
      XK(I,J)=0.0
  752 XMI(I,J)=0.0
      CALL F02AGF (XJ,MZZ,MZ,VK,VM,XK,MZZ,XMI,MZZ,ITG,IFAIL)
      CALL M01ABF (VK,1,MZ,IP,IST,IFAIL)

      DD1=PA/EI
      DD2=SQRT(DD1)
      DD3=SQRT(DD2)
      PI2 = PI*2.0
        WRITE(2,224)
```

(Stage E)

Statement No.

```
    DO 753 K=1,MZ
    IF(VK(K).LT.0.0) WRITE(2,220)K,ITG(K),VK(K),VM(K)
      IF(ABS(VM(K)).NE.0.0)      WRITE(2,220)K,ITG(K),VK(K),VM(K)
753 VM(K)=0.0
    DO 754 K=1,MZ
    DO 754 I=1,MZ
    QQ=0.0
    DO 755 J=1,MZ
755 QQ=QQ+XM(I,J)*XK(J,K)
754 VM(K)=VM(K)+XK(I,K)*QQ
    DO 784 K=1,MZ
    MZK=MZ+1
    IF(K.EQ.MZ)MZK=1
    WSC(K)=0.0
    DO 784 I=1,MZ
    QQ=0.0
    DO 785 J=1,MZ
785 QQ=QQ+XM(I,J)*XK(J,K)
784 WSC(K)=WSC(K)+XK(I,MZK)*QQ
      WRITE(2,226)
      WRITE(2,222)(WSC(I),I=1,MZ)
      WRITE(2,223)
    DO 750 I=1,MZ
    VK(I)=1.0/VK(I)
    YM=SQRT(VK(I))
    YN=YM/PI2
    DC=SQRT(YM)*DD3
    DS=DC*DC*THU/SQRT(12.0)
750 WRITE(2,225)I,VK(I),YN,IP(I),YM,DC,DS,IP(I),VM(I)
      WRITE(2,231)
    DO 781 I=1,MZ
    DO 781 J=1,MZ
781 XMI(I,IP(J))=XK(I,J)
    DO 630 I=1,MZ
    DO 630 J=1,MZ
630 XK(I,J)=XMI(I,J)
    DO 631 I=1,MZ
631 WSC(IP(I))=VK(I)
    DO 632 I=1,MZ
632 VK(I)=WSC(I)
    DO 633 I=1,MZ
633 WSC(IP(I))=VM(I)
    DO 634 I=1,MZ
634 VM(I)=WSC(I)
    JIP=MZ
    IF ( JIP.GT.10 ) JIP=10
    DO 601 I=1,JIP
    YM=SQRT(VK(I))
    YN=YM/PI2
    DC=SQRT(YM)*DD3
```

(Stage F)

```
    DS=DC*DC*THU/SQRT(12.0)
601   WRITE(2,232)I,YN,YM,DC,DS,IP(I)
      WRITE(2,224)
    JIP=MZ
    IF ( JIP.GT.ITN ) JIP=ITN
    DO 620 I=1,JIP
    YM=SQRT(VK(I))
    YN=YM/PI2
    DC=SQRT(YM)*DD3
    DS=DC*DC*THU/SQRT(12.0)
    WRITE(2,235)I,YN,YM,DC,DS,IP(I)
    III=0
    DO 621 K=1,NOJ
    DO 621 L=1,3
    XM(K,L)=0.0
    IF(LR(K,L).EQ.0)GOTO 621
    III=III+1
    XM(K,L)=XMI(III,I)
621 CONTINUE
    DO 622 K=1,NOJ
    WRITE(2,234)K,(XM(K,L),L=1,3)
622 CONTINUE
620 CONTINUE
      WRITE(2,224)
      WRITE(2,233)IR,JR
    III=0
    DO 794 K=1,NOJ
    DO 794 L=1,3
    IF(LR(K,L).EQ.0) GOTO 794
    III=III+1
    IF (IR.EQ.K) GOTO 793
    GOTO 794
793 IF (JR.EQ.L) GOTO 795
794 CONTINUE
795 DO 788 J=1,ITN
    XMU=XMI(III,J)
    IF(XMU.EQ.0.0)GOTO 788
    DO 783 I=1,MZ
783 XMI(I,J)=XMI(I,J)/XMU
788 CONTINUE
    DO 624 I=1,JIP
    WRITE(2,235)I
    III=0
    DO 625 K=1,NOJ
    DO 625 L=1,3
    XM(K,L)=0.0
    IF(LR(K,L).EQ.0)GOTO 625
    III=III+1
    XM(K,L)=XMI(III,I)
625 CONTINUE
```

(Stage G) Statement No. (Stage H)

```
    DO 626 K=1,NOJ
    WRITE(2,234)K,(XM(K,L),L=1,3)
626 CONTINUE
624 CONTINUE

    IF(NFN.LT.1)GOTO 737
    DO 771 NSSM=1,NFN
    READ(1,12)ZZ,NZZ,NFC
    IF(NZZ)81,82,83
 83 HZ = ZZ
    GW = ZZ*PI2
    GL = SQRT(GW)*DD3
    GOTO 84
 82 GW = ZZ
    HZ = GW/PI2
    GL = SQRT(GW)*DD3
    GOTO 84
 81 GL = ZZ
    GW = GL*GL/DD2
    HZ = GW/PI2
 84 GC=GL*GL*THU/SQRT(12.0)
      WRITE(2,23)NSSM,NFC,HZ,GW,GL,GC
    DO 53 K=1,NFC
 53 READ(1,13)IPT(K),JPT(K),XC(K)

    KL=1
    III=0
    DO 842 K=1,NOJ
    DO 842 L=1,3
    IF( LR(K,L).EQ.0.0 )GOTO 842
    III=III+1
    YC(III)=0.0
    IF( IPT(KL).EQ.K.AND.JPT(KL).EQ.L) GOTO 843
    GOTO 842
843 YC(III)=XC(KL)
    JN(KL)=III
    KL=KL+1
842 CONTINUE
      WRITE(2,224)
    DO 54 K=1,NFC
 54 WRITE(2,26)K,JN(K),IPT(K),JPT(K),YC(JN(K))

    DO 772 KR=1,MZ
    GW2=GW*GW
    GWD=GW2-VK(KR)
    DO 756 I=1,MZ
    DO 756 J=1,MZ
756 XMI(I,J) = XK(I,KR)*XK(J,KR)
    DO 757 I=1,MZ
    XC(I)=0.0
```

```
      DO 757 J=1,MZ
 757 XC(I) = XC(I) + XMI(I,J)*YC(J)
      DO 758 I=1,MZ
 758 XJ(KR,I) = XC(I)/GWD/VM(KR)
 772 CONTINUE

      DO 759 J=1,MZ
      WSC(J)=0.0
      DO 759 I=1,MZ
 759 WSC(J) = WSC(J) + XJ(I,J)
        WRITE(2,224)
      III=0
      DO 611 K=1,NOJ
      DO 611 L=1,3
      XM(K,L)=0.0
      IF(LR(K,L).EQ.0)GOTO 611
      III=III+1
      XM(K,L)=WSC(III)
 611 CONTINUE
      DO 612 K=1,NOJ
      WRITE(2,234)K,(XM(K,L),L=1,3)
 612 CONTINUE
        WRITE(2,224)
        WRITE(2,224)
 771 CONTINUE

 737 IF(NMORE.NE.8)GOTO 9999
1330 FORMAT(/1X,'#£%& NO ERROR &%£#')
 220 FORMAT(1X,'IMAGINERY ROOT GENERATED :  K,ITG(K),VK(K),VM(K)  ',
    *  2I5,1P2E16.5)
 222 FORMAT(1P8E15.5)
 223 FORMAT(15X,'K,VK,HZ,IP,GW,GL,GC,IP,VM')
 224 FORMAT(10X,'..')
 225 FORMAT(I15,1P2E15.5,I7,1P3E15.5,I7,1PE15.5)
 226 FORMAT(15X,'ORTHOGONALITY;  WSC(I),I=1,MZ' )
 227 FORMAT(I7,I6,2X,7(3X,1PE12.5) )
 228 FORMAT(4X,'JOINT  XYZ ',9X,'1ST',12X,'2ND',12X,'3RD',12X,
    *            '4TH',12X,'5TH',12X,'6TH',12X,'7TH')
 231 FORMAT(15X,'FIRST TEN MODES;  HZ,GW,GL,GC')
 232 FORMAT(I15,2F15.5,2F13.5,I10)
 233 FORMAT(15X,'NORMALISED AT ',I2,',',I1)
 234 FORMAT(I10,1P3E17.5)
 235 FORMAT(15X,'MODESHAPE FOR MODE ORDER NUMBER =',I3,
    1         2F15.5,2F13.5,I5)
9999 WRITE(2,1330)
      STOP
      END

      FINISH
```

Appendix F2 Steering Program: NONLIN

(Stage A & B) Statement No. (Stage C)

(Stage A & B)

```
      LIST (LP)
      PROGRAM (NONLIN)
      INPUT  1 = CR0
      OUTPUT 2 = LP0
      COMPRESS INTEGER AND LOGICAL
      COMPACT PROGRAM
      TRACE 0
      END

      MASTER NONLINEAR
      DIMENSION X(89,89),DET(2),R(6,6),E(2),JCCH(2),FCCH(2),
     *          JN(29),XC(29),YC(29),LQ(29),LR(29,3),
     #          LOCAT(29),IPT(29),JPT(29),THI(29),THJ(29),
     ?          HYP(29),ZM(29),CS(29),SN(29),EQU(29),
     %          MEM(29),WII(29),WIJ(29),EPU(29),ZN(29),MQ(29),
     *          JJ(3,3),INDEX(2),CSY(29),
     3 NWIPT(29),NWJPT(29),NWIST(29),NWJST(29),NSE(29),
     4 SETH(10,29),SEWI(10,29),NWRT(29),NWLR(29,3)
      MXX=10
      MYY=29
      MZZ=89
    1 FORMAT(1X,'PROGRAM PARAMETERS :',3X,'NONLIN,  DATED 300479',/)
    2 FORMAT(/1X,'CONTROL PARAMETERS :',3X,'NFN,ITN,IR,JR,NMORE,',
     *          'NOJ,NOM,ZZ,XLIMIT')
    3 FORMAT(1X ,'SECTION PARAMETERS :',3X,'MAT,KEI,THU,WIU,ACH,EYE;',
     *          ' YMS,DEN,EI,EA,PA')
    4 FORMAT(24X,'MSIZE ',I3,5X,3I5,10X,'TRIG, ',
     *        ' PR,WE,TA,TW,  UNCLASSIFIED MODE ',F7.4)
    5 FORMAT(1X,'OUTPUT  PARAMETERS :')
    6 FORMAT(/10X,'YOU KNOW WHAT I WANT')
   11 FORMAT(7I0,2F0.0)
   12 FORMAT(I0,2F0.0)
   13 FORMAT(F0.0)
   21 FORMAT(20X,7I5,2F10.5)
   22 FORMAT(21X,I4,5X,I6,F17.9,F18.9,4X,1P2E18.9,/21X,1P5E18.9)
   28 FORMAT(/1X,I2,3X,I2,'+',I2,'=',I2,F11.4,F11.6,
     *        F9.3,I1,1X,10(2X,3I3))
   19 FORMAT(14X,F11.4,F11.6,F9.3,I1,1X,10(2X,3I3))
       WRITE(2,1)
      ABCD = 4.0*ATAN(1.0)
   88  READ(1,11)NFN,ITN,IR,JR,NMORE,NOJ,NOM,ZZ,XLIMIT
      WRITE(2,2)
      WRITE(2,21)NFN,ITN,IR,JR,NMORE,NOJ,NOM,ZZ,XLIMIT

      CALL JTMBEQ (MXX,MYY,NOJ,XC,YC,LR,LQ,JN,MSIZE,LOCAT,MEM,NOM,
     1 IPT,JPT,THI,THJ,HYP,ZM,CS,SN,WII,WIJ,ZN,EQU,EPU,THU,WIU,
     2 NWIPT,NWJPT,NWIST,NWJST,NSE,SETH,SEWI,NWRT,NWLR)
        READ(1,12)MAT,YMS,DEN
      IF(MAT-1)196,197,198
  196 YMS=25.0
```

(Stage C)

```
      DEN=2400.0
      GOTO 198
  197 YMS=200.0
      DEN=7500.0
  198 YMS=YMS*1.0E9
      ACH=WIU*THU
      EYE=ACH*THU*THU/12.0
      EA = YMS*ACH
      EI = YMS*EYE
      PA = DEN*ACH
      MZ=MSIZE
      EIA=ALOG10(EI)
      JEI=INT(EIA)
      EIB=EXP10(FLOAT(JEI))
      KEI=JEI*MZ
      READ(1,13)EPS
      WRITE(2,3)
       WRITE(2,22)MAT,KEI,THU,WIU,ACH,EYE,YMS,DEN,EI,EA,PA
       WRITE(2,4)MSIZE,MXX,MYY,MZZ,EPS
      IF(MSIZE.GT.MZZ)GOTO 187
      IF(NOJ.GT.MYY)GOTO 187
      IF(NOM.GT.MYY)GOTO 187
      EI=EI/EIB
      EA=EA/EIB
      GOTO 188
  187 WRITE(2,6)
      GOTO 737
  188 FF=SQRT( SQRT(12.0)/THU )
      GGW=THU*SQRT(YMS/DEN/12.0)
      GG=GGW/2.0/ABCD

      NOMPOLE=NOM
      IF(NOM.GT.20)NOMPOLE=20
      CALL ASYPOLE (HYP,FF,ABCD,NOMPOLE,CSY)
       WRITE(2,5)
      THUSQRT=THU/SQRT(12.0)
      N=0
      ND=1
      IORDER=1
  762 IF(ZZ.LT.CSY(IORDER))GOTO 761
      IORDER=IORDER+1
      GOTO 762
  761 DO 731 NR=1,19
      POL=CSY(IORDER)-EPS
      IPOL=0
      NIN=-3
      YY=ZZ
      NIT=NFN
      FNN=1.0
      DO 50 I=1,NFN
```

(Stages D & E)

Statement No,

```
 50 FNN=FNN*10.0
752 N=N+1
    E(ND)=YY+FLOAT(N-1)/FNN
    IF( E(ND).LT.POL ) GOTO 763
    E(ND)=POL
    IPOL=1
763 GL = E(ND)
    GC = GL*GL*THUSQRT
    DO 54 K=1,5
 54 JN(K)=0
    DO 8001 I=1,MZ
    DO 8001 J=1,MZ
8001 X(I,J)=0.0

    DO 734 MB=1,NOM
    RM=ZM(MB)
    RN=ZN(MB)
    DC=CS(MB)
    DS=SN(MB)
    L1=IPT(MB)
    L2=JPT(MB)
    EP=EPU(MB)
    HP=HYP(MB)
    EQ=EQU(MB)
    GLL=GL/SQRT(EQ)
    IF(MEM(MB).NE.1)GOTO 741
    CALL JPRISM (GLL,GC,HP,EP,EQ,EI,EA,CDET,R)
    GOTO 740
741 IF(MEM(MB)-3)742,743,744
742 CALL JDOVET (GLL,GC,HP,RN,EP,EQ,EI,EA,CDET,R)
    GOTO 740
743 CALL JWEDGE (GLL,GC,HP,RM,EP,EQ,EI,EA,CDET,R)
    GOTO 740
744 CALL JDOUBL (GLL,GC,HP,RM,RN,EP,EQ,EI,EA,CDET,R)
740 DUMMY=0.0
    CALL TRIRECT (MYY,MZZ,LOCAT,LR,X,R,DS,DC,L1,L2)
    J1L=INT(GLL*HP/ABCD)
    J1C=INT(GC*HP/ABCD)
    J1K=1
    IF(CDET.LT.0.0)J1K=-1
    JN(1)=JN(1)+J1L+J1C-( 1-(-1)**J1L*J1K )/2
    JJ(1,ND)=JN(1)
734 CONTINUE

    DO 32 K=1,MZ-1
    DO 32 L=K+1,MZ
 32 X(L,K)=X(K,L)
    DO 51 LA=2,MZ
    PPPVOT=X(LA-1,LA-1)
    DO 51 K=LA,MZ
```

(stage F)

```
    EM=X(K,LA-1)/PPPVOT
    DO 51 L=LA,MZ
    X(K,L)=X(K,L)-EM*X(LA-1,L)
 51 CONTINUE

    XC(1)=ABS(X(1,1))
    XC(2)=ALOG10(XC(1))
    JN(4)=INT(XC(2))
    XC(3)=10.0**JN(4)
    K=1
    IF(XC(1).LT.1.0)K=-1
    JN(5)=JN(4)*MZ*K
    DET(ND)=1.0
    DO 52 K=1,MZ
 52 DET(ND)=DET(ND)/XC(3)*X(K,K)
    AK=1.0
    IF(DET(ND).LT.0.0)AK=-1.0
    DETA=ALOG10(ABS(DET(ND)))
    JDET=INT(DETA)
    DETB=DETA-FLOAT(JDET)
    DETA=EXP10(DETB)
    DET(ND)=DETA*AK
    JCCH(ND)=JN(5)+JDET
    IF( ABS(DET(ND)).GE.1.0 )GOTO 784
    JCCH(ND)=JCCH(ND)-1
    DET(ND)=DET(ND)*10.0
784 DO 53 K=1,MZ
 53 IF(X(K,K).LT.0.0)JN(2)=JN(2)+1
    JJ(2,ND)=JN(2)
    JJ(3,ND)=JJ(1,ND)+JJ(2,ND)
    IF(ND.GT.1)GOTO 751
    ND=2
    GOTO 752

751 IF(JJ(1,1).NE.JJ(1,2))GOTO 754
    IF(JJ(2,1).NE.JJ(2,2))GOTO 754
    JJ(1,1)=JJ(1,2)
    JJ(2,1)=JJ(2,2)
    JJ(3,1)=JJ(3,2)
    DET(1)=DET(2)
    E(1)=E(2)
    JCCH(1)=JCCH(2)
    IF(IPOL.GE.1)GOTO 764
    GOTO 752
764 IF(IPOL.EQ.2)GOTO 754
    E(2)=POL+EPS*2.0
    IPOL=2
    GOTO 763
754 NIN=NIN+3
    DO 772 K=1,3
```

(Stages G & H)

Statement No.

```
      LQ (NIN+K)-JJ(K,1)
  772 MQ(NIN+K)=JJ(K,2)
      IF(IPOL.EQ.2)GOTO 755
      IF(NIT.EQ.ITN)GOTO 755
      IPOL=0
      YY=E(1)
      N=1
      NIT=NIT+1
      FNN=FNN*10.0
      GOTO 752
  755 NTN=3*(NIT-NFN+1)
      IF(IPOL.NE.0)GOTO 765
      IF(ITN.NE.5)GOTO 757
      ISEC=JCCH(2)-JCCH(1)
      IF(ISEC.GT.70)GOTO 757
      BISE=DET(2)*EXP10(FLOAT(ISEC))
      BISE=DET(1)/(DET(1)-BISE)*0.000010
      GL=E(1)+BISE
      GOTO 781
  757 GL=E(1)
      GOTO 781
  765 GL=CSY(IORDER)

  781 GC=GL*GL*THUSGRT
      GW=GL*GL*GGW
      HZ=GW/2.0/ABCD
      DO 783 IDET=1,2
  783 INDEX(IDET)=JCCH(IDET)+KEI
        WRITE(2,28)NR,JJ(1,2),JJ(2,2),JJ(3,2),
     *             HZ,GL,DET(1),INDEX(1),(LQ(NEN),NEN=1,NTN)
       WRITE(2,19)GW,GC,DET(2),INDEX(2),(MQ(NEN),NEN=1,NTN)
      JJ(1,1)=JJ(1,2)
      JJ(2,1)=JJ(2,2)
      JJ(3,1)=JJ(3,2)
      ZZ=E(2)
      N=1
      E(1)=E(2)
      DET(1)=DET(2)
      JCCH(1)=JCCH(2)
      IF( JJ(3,2).GE.JR )GOTO 737
      IF(ZZ.GT.XLIMIT)GOTO 737
      IF(IPOL.NE.2)GOTO 731
      IPOL=0
      IORDER=IORDER+1
  731 CONTINUE
  737 IF(NMORE.NE.8)GOTO 9999
 1330 FORMAT(/1X,'#E%K      NO ERROR     K%E#')
      GOTO 88
 9999  WRITE(2,1330)
      STOP
      END

      FINISH
```

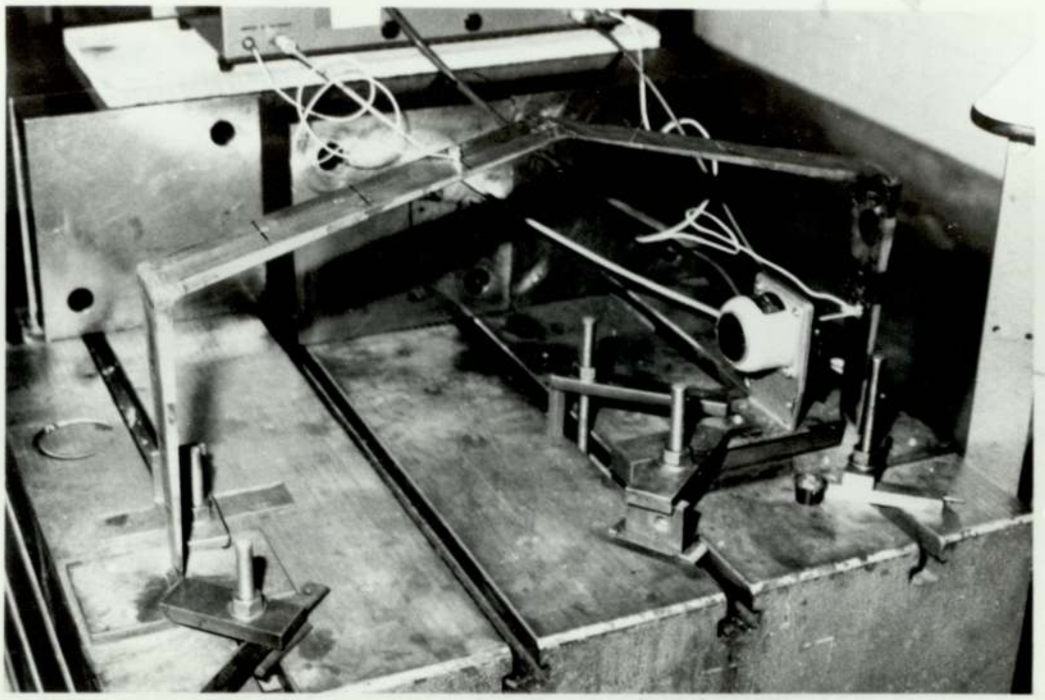

THE DYNAMIC TEST OF THE PITCHED FRAME

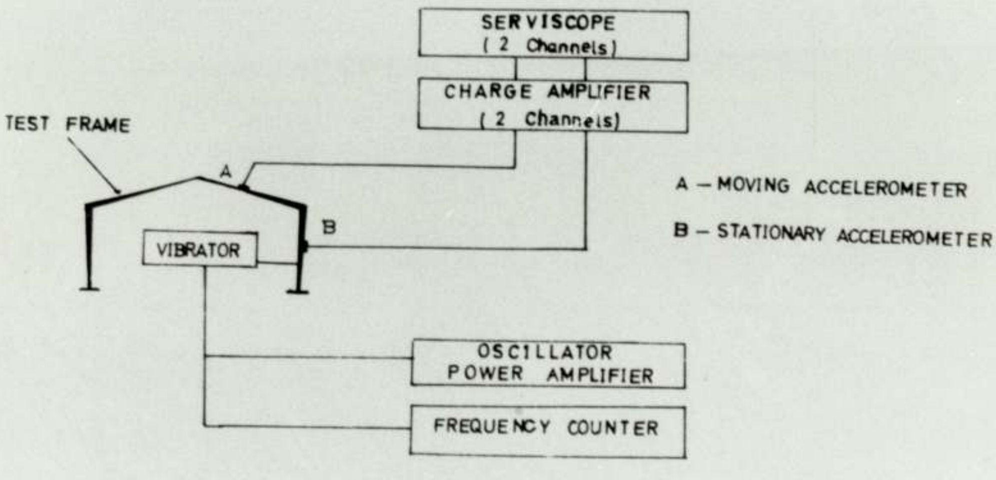

BLOCK DIAGRAM SHOWING THE SETTING UP OF THE APPARATUS